ICE NAVIGATION QUALITIES OF SHIPS

D. E. Kheisin, et al

Cold Regions Research and Engineering Laboratory
Hanover, New Hampshire

August 1973

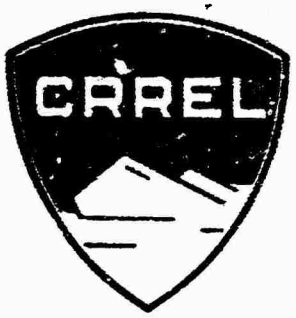

Draft Translation 417

ICE NAVIGATION QUALITIES OF SHIPS

D.Ie. Kheisin and Yu.N. Popov

August 1973

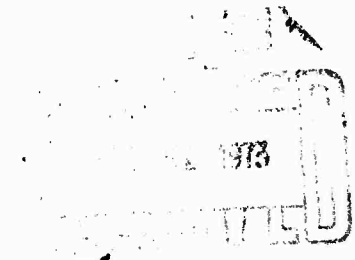

CORPS OF ENGINEERS, U.S. ARMY
COLD REGIONS RESEARCH AND ENGINEERING LABORATORY
HANOVER, NEW HAMPSHIRE

Unclassified
Security Classification

DOCUMENT CONTROL DATA - R & D

Security classification of title, body of abstract and indexing annotation must be entered when the overall report is classified)

1. ORIGINATING ACTIVITY (Corporate author)
U.S. Army Cold Regions Research and Engineering Laboratory
Hanover, New Hampshire

2a. REPORT SECURITY CLASSIFICATION
Unclassified

2b. GROUP

3. REPORT TITLE
ICE NAVIGATION QUALITIES OF SHIPS

4. DESCRIPTIVE NOTES (Type of report and inclusive dates)
Draft Translation

5. AUTHOR(S) (First name, middle initial, last name)
D.IE. Kheisin and IU.N. Popov

6. REPORT DATE	7a. TOTAL NO. OF PAGES	7b. NO. OF REFS
August 1973	287 288	110

8a. CONTRACT OR GRANT NO	9a. ORIGINATOR'S REPORT NUMBER(S)
b. PROJECT NO.	Draft Translation 417
c.	9b. OTHER REPORT NO(S) (Any other numbers that may be assigned this report)
d.	

10. DISTRIBUTION STATEMENT
Approved for public release; distribution unlimited.

11. SUPPLEMENTARY NOTES	12. SPONSORING MILITARY ACTIVITY

13. ABSTRACT

This collection is devoted to the results of theoretical and experimental investigations of the ice qualities of ships, conducted at the Arctic and Antarctic Scientific Research Institute in the past decade. The basic attention is given to problems directly associated with ice navigating capability and strength. Navigating capability and maneuvering characteristics of ships in motion in solid ice is investigated. Together with the traditional experimental-theoretical approach to these problems, theoretical-probability methods of estimating ice navigation speed and maneuvering qualities of ships are developed, based on data from full-scale tests. An analysis of the process of wedging of an ice breaker in ice is also given. Where ice strength is referred to, the effect of the slope of the hull on the parameters of direct and reflected impacts is investigated, and various schemes for the calculation of elements of the side framing and shell plating are considered. Description and analysis of strain-gauge tests of the ice resistance of hulls of transport vessels and ice breakers is reported. The successive application of the probability approach to the processing and interpretation of the results of the tests has found its reflection in articles where the strength of the side framing and ice vibration of hull structures are considered. Experimental data on the physical characteristics of full-scale and model ice are given, and also a description is given of improved measuring methods used in the tests.

DD FORM 1 NOV 1473 REPLACES DD FORM 1473, 1 JAN 66, WHICH IS OBSOLETE FOR ARMY USE.

Unclassified
Security Classification

14. KEY WORDS	LINK A		LINK B		LINK C	
	ROLE	WT	ROLE	WT	ROLE	WT
Displacement						
Ice breakers						
Ice resistance						
Ice strength						
Ice thickness						
Solid ice						
Strain-gauge (tensometer)						

DRAFT TRANSLATION 417

ENGLISH TITLE: ICE NAVIGATION QUALITIES OF SHIPS

FOREIGN TITLE: LEDOVY KACHESTVA SUDOV

AUTHOR: Kheisin, D.IE. and Popov, IU.N.

SOURCE: Arkticheskii i Antarkticheskii Nauchno-Issledovatel'stvo Institut, Trudy 309, 1973, 240 p.

Translated by U.S. Joint Publications Research Service for U.S. Army Cold Regions Research and Engineering Laboratory, 1973, 287 p.

UDC 629.124

ICE NAVIGATION QUALITIES OF SHIPS

[Edited by Doctor of Physical and Mathematical Sciences D.IE. Kheisin and Candidate of Engineering Sciences Yu. N. Popov; Leningrad, Trudy AANII, Russian, Volume 309, Leningrad, Gidrometeoizdat, 1973, 240 pages.]

TABLE OF CONTENTS

Table of Contents (con't)

PREFACE

This collection is devoted to the results of theoretical and experimental investigations of the ice qualities of ships, conducted at the Arctic and Antarctic Scientific Research Institute in the past decade. In this case the basic attention is devoted to problems directly associated with ice navigating capability and strength.

A considerable place in the collection is devoted to the investigation of the navigating capability and maneuvering characteristics of ships in motion in solid ice. Together with the traditional experimental-theoretical approach to these problems, in a number of articles theoretical-probability methods of estimating ice navigation speed and the maneuvering qualities of ships are developed, based on data from full-scale tests. An analysis of the process of the wedging of an ice breaker in ice is given.

In articles referring to ice strength (ice resistance), the effect of the shape of the hull on the parameters of direct and reflected impacts is investigated, various schemes for the calculation of elements of the side framing and shell plating are considered. Several articles are devoted to a description and analysis of strain-gauge (tensometer) tests of the ice resistance of hulls of transport vessels and ice breakers. The successive application of the probability approach to the processing and interpretation of the results of the tests has found its reflection in articles where the strength of the side framing and ice vibration of hull structures are considered.

In the conclusion of the collection, experimental data on the physical characteristics of full-scale and model ice are given, and also a description is given of improved measuring methods used in the tests.

The collection is of interest for engineers, technicians, and scientific workers engaged in problems in the designing and operation of ice breakers and transport vessels intended for ice navigation, and also may be useful to undergraduate and graduate students.

The compilation and scientific editing of the collection was performed by the senior scientific workers of the Laboratory of the Ice Qualities of Ships of the AANII (Arctic and Antarctic Scientific Research Institute) Yu. N. Popov and D. Ye. Kheysin. Great assistance was rendered in the preparation and formulation of the volume by O. V. Faddeyev, A. G. Sarri, and Ye. Ye. Yemel'yanova.

Arctic and Antarctic Scientific
Research Institute

METHODS OF ESTIMATING THE ICE NAVIGATING CAPABILITY OF A SHIP IN SOLID ICE

V. I. Kashtelyan pages 5-17

The first ship equipped with a mechanical power plant and specially intended for navigating in ice appeared more than a hundred years ago. However, the problem of the quantitative estimate of the capability of ships to overcome ice resistance was inadequately fully studied for a long time. The complexity of the process of the motion of a ship in ice and the diversity of factors affecting the ice resistance did not make it possible to develop a reliable method for calculation of ice navigating capability. Aside from this, comparatively little attention was devoted to the properties of the ice cover, which are distinguished for their great diversity.

The investigation of the processes of the reaction of a hull with ice demonstrate that the ice navigating capability must be considered in each particular case with reference to those ice conditions in which the basic features of the ice cover are manifested as a medium, causing the resistance to the motion, namely: in solid ice, fine broken ice, large broken ice, and bits of fields.

At the present time, several methods of estimating ice navigating capability have been developed. The majority of them refer to navigation in solid ice, which represents the greatest obstacle for ice breakers. This article is also devoted to an analysis of these methods and to the evaluation of the possibility of using them in designing ice breakers.

Methods of calculating ice navigating capability in solid ice may be divided into theoretical, semi-empirical and empirical methods.

Empirical methods, derived on the basis of the processing of full-scale data, associate the power (thrust) of an icebreaker with the speed of its motion and the parameters of the ice. They are applicable only to a ship

which has passed through its trials. Empirical methods of calculating ice navigating capability, as a rule, are not universal, and therefore in the future they are not considered.

The motion of a ship in solid ice may be accomplished either by continuous steaming or short runs. In the first case the icebreaker overcomes the ice resistance with a steady-state speed of motion, i.e., statically, as it were. The process of the operation of the icebreaker in short runs is particularly dynamic in nature. The breaking of the ice occurs basically by means of the kinetic energy of the ship accumulated in acceleration. Operation by short runs is used in such ice conditions where the icebreaker cannot move continuously, since the thrust developed by the screws turns out to be less than the ice resistance. In accordance with what was said above, we will also distinguish methods of evaluating ice navigating capability in solid ice in continuous steaming and in operation by short runs.

The motion of a ship in solid ice is a complex phenomenon, which does not yield to a strict analytical description. Therefore, in the theoretical solution of the problem of ice navigating capability, a number of assumptions are tolerated, making it possible to obtain comparatively simple calculation formulas for the ice resistance. The majority of existing theoretical methods are based on a single-contact scheme of the reaction of the icebreaker hull with the ice, which assumes that the ice resistance is caused by the breaking of the ice by the stem of the ship. In such an idealized scheme, for the parameter determining the icebreaking capability it is usually the vertical component of the pressure of the stem during the pressure of the icebreaker against the ice that is selected. For this vertical force a dependence connecting it with the elements of the ship is found. Although such a simplified scheme of icebreaking does not reflect the real picture of its breaking by the hull of the icebreaker, nevertheless it is applied even at the present time.

We will briefly discuss the theoretical method of determining the ice navigating capability, based on a single-contact scheme of the breaking of ice by an icebreaker. R. I. Runeberg [4] proposed for the first time a formula for estimating the icebreaking capability of a ship in continuous motion in solid ice. In analyzing the forces acting on an icebreaker in its static pressure against the ice, he established the following analytical dependence between the magnitude of the vertical force on the stem (P_{zf}) and the thrust pressure of the screw propellers (T):

$$P_{z\phi} = T\frac{\cos\varphi\cos\beta - f\sin\varphi}{\sin\varphi\cos\beta + f\cos\varphi}, \qquad (1)$$

where φ_1 is the angle of inclination of the stem; β is the angle between the normal to the side in the vicinity of the stem and the diametrical plane (center line); and f is the coefficient of friction of the ice against the hull [$P_{z\,\phi} = P_{z\,f} = P_{z\,stem}$].

The founder of the theoretical method of estimating the ice navigating capability in operating by short runs is I. V. Vinogradov [1]. In solving the equation of the energy balance, when the breaking of ice by the stem occurs from acceleration due to the work of the thrust of the screw propellers and the kinetic energy of the moving ship, he obtained the following expression for the vertical force on the stem:

$$P_{z\phi} = aT + \left\{a^2T^2 + \frac{b}{c}\frac{D^2}{gH}v^2\left[1-(1-e^2)\sin^2\varphi - v_1^2\right]\right\}^{1/2}. \qquad (2)$$

where

$$a = \frac{\cos\varphi\cos\beta - f\sin\varphi}{\sin\varphi\cos\beta + f\cos\varphi},$$

$$b = F_1(\varphi, \beta, f);$$

$$e = F_2(\delta, \alpha);$$

D is the displacement of the icebreaker; H is the longitudinal metacentric height; v is the speed at the moment that the stem meets the ice; d_1 is the speed at the moment that the stem breaks the ice; e is the righting factor during impact; α is the coefficient of fineness of the area of the water line; δ is the total coefficient of fineness.

We should note that, having assumed in equation (2) that $v = v_1 = 0$, we will obtain an expression differing from Runeberg's formula [4] in a multiplier of 2. The appearance of this multiplier is explained by the fact that in the derivation of dependence (2) the thrust pressure of the propellers in the process of pressing the hull against the ice was assumed to be variable, changing according to a linear law. Since the functional connection between the speed, the thrust pressure of the propellers and the displacement in the acceleration section of the icebreaker is not known, the dependence (2) proposed by I. V. Vinogradov may be used for calculation of the absolute value of the vertical force breaking the ice if the rate of impact is assumed. In the analysis of the effect of the ship's characteristics on the vertical force on the stem, the author has considered only a case when the acceleration of the icebreaker before impact occurs in clear water. Therefore, the conclusions of I. V. Vinogradov relative to the selection of optimum methods of

the operation of various icebreakers in short runs is especially particular in nature, which reduces the practical value of this method.

From foreign theoretical investigations of ice navigating capability, based on a single-contact scheme of the breaking of ice by an icebreaker, we should discuss the works of Milano [9] and White [12]. For estimating the ice navigating capability of an icebreaker in continuous motion, Milano used as expression (2) at $v = v_1 = 0$ and a dependence obtained by Nevel [10, 11] for the carrying capability of an ice plate on an elastic base.

Milano's formula has the form:

$$h = 2{,}177 T^{1/4} \left(\frac{\cos\varphi \cos\beta - f \sin\varphi}{\sin\varphi \cos\varphi + f \cos\varphi} \right)^{1/4} \sigma_p^{-1/4}, \qquad (3)$$

where h is the thickness of the ice being broken; σ_p is the ultimate bending strength of the ice [$\sigma_p = \sigma_r$]; and T is the thrust pressure of the screw propellers during dock trials.

White, solving the equations of equilibrium of forces acting on an icebreaker as it presses against the ice, obtained the following expressions for the vertical force originating in the stem in continuous motion:

$$P_{z\phi} = T \frac{\cos\varphi (\cos\beta + f \sin\beta) - f \sin\varphi}{\sin\varphi (\cos\beta + f \sin\beta) + f \cos\varphi}. \qquad (4)$$

Formula (4) differs from expression (3) in its additional term $f \sin\beta$, lying in the parentheses of the numerator and denominator. The appearance of this item is caused by the fact that simultaneously with the pressing of the icebreaker against the ice White tried to consider the cutting of the ice field by the stem. In connection with this, in addition to the friction forces acting along the tangential to the stem, the friction forces directed along the tantential to the shell plating of the hull and normal to the stem are considered. In this case the total magnitude of each of the groups of friction forces indicated is assumed to be equal to fN (where N is the normal pressure on the side, and f is the friction factor). Such an approach to the solution of the problem, apparently, is inadequately invalidated, since the resultant of all the friction forces cannot be greater than the magnitude of fN.

White also proposed a simplified analytical expression for the vertical force on the stem

$$P_{z\phi} = 6{,}64 A^{0{,}845} D^{0{,}845}, \qquad (5)$$

where v is the speed at the moment of the impact of the ship against the ice; D is the displacement of the icebreaker; $A = F(B/H, \alpha, \beta, \varphi, f)$ is the index of the operation of the icebreaker in short runs.

Lewis and Edwards [8], having used White's equation (5) and Nevel's solution [10] for the vertical force breaking the ice cover obtained the following formula for the determination of the thickness of the ice being broken by an icebreaker in operation by short runs, when the ice plate, in the effect of the stem, is divided into four wedges with a flare angle of 67.5° each:

$$h = \left(\frac{0{,}775\sigma A^{0{,}85} D^{0{,}85}}{\sigma_p}\right)^{0{,}5}. \qquad (6)$$

In order to answer the question as to what degree the theoretical dependences (1), (2), (3), and (4) may be applicable for estimation of the ice navigating capability of an icebreaker in solid ice in continuous motion, we will consider the picture of the breaking of ice by an icebreaker in more detail. In the process of the reaction of an icebreaker hull with the ice, both the stem and the sides participate, mainly in the forward part of the hull. In this case, the number of points of the hull simultaneously reacting with the ice plate is determined by the beam of the ship and the geometry of the breaking of the ice cover (by the dimensions and quantity of sectors), which depends upon the speed of the ship, and the thickness and strength characteristics of the ice.

The total resistance of solid ice may be conditionally divided into resistance referred to the stem and resistance referred to the sides of the icebreaker. These two components include the resistance caused by the breaking of the ice and other forms of resistance, such as, for example, the resistance of the broken ice to packing, upheaval (overturning) of ice floes, their separation, etc. Thus, if the capability of the ship to overcome the ice resistance is estimated by the thickness of the solid ice, determined from the condition of its breaking only by the stem, tolerates an error, the magnitude of which will depend upon the fraction of the total resistance falling to the stem.

Model tests in solid ice demonstrate that the resistance referred to the stem, $R_f \approx 0.3\ R$ (where R is the total ice resistance). Consequently, if we assume that such a ratio between R_f and R is observed also in full-scale conditions, we may make the conclusion that according to the theoretical method considered we cannot perform an adequately reliable quantitative estimation of the capability of the icebreaker to overcome solid ice by continuous steaming. They also do not make it possible to consider the effect of

various elements of the ship on its ice navigation speed with an adequate degree of accuracy for designing.

Comparative calculations according to the formulas of I. V. Vinogradov (2) and White (5) demonstrate that at one of the same values of the velocities of collision with the ice the divergences in the magnitude of the vertical force on the stem for various icebreakers does not exceed ~10%. This makes it possible to consider these methods as being equal in value from a quantitative standpoint.

During operation by short runs, just as in continuous steaming, it is not only the stem, but also the sides of the icebreaker, that usually participate in breaking the ice. The breakage of ice only by the stem may be observed in a case when the icebreaking stops until such time as the sections of the sides will enter into reaction with the ice cover.

Breakup of the field sets in as soon as the vertical force on the stem causes stresses in the ice that are equal to the limits of its bending strength. Actually, in the operation of an icebreaker in solid ice ahead of the stem, as a rule, no breakup of the ice cover as a consequence of bending is observed. A continuous cutting of the ice by the stem from the moment of its contact with the ice occurs, up to the breaking of sectors by the sections of the sides directly adjoining the stem. Thus, the thickness of the ice being broken only by the stem and determined from the condition of the breakage of the ice by bending by means of the methods of I. V. Vinogradov and White must be considered as a conditional quantity, which only approximately estimates the capability of the operation of the icebreaker in short runs. For the limiting thickness of the ice which the icebreaker can break from an acceleration, apparently it is more correct to assume the thickness of the ice broken by sections of the sides in the vicinity of the stem.

From other theoretical investigations of the estimation of the ice navigating capability of a ship, we should discuss the method of "conditional gauges" proposed by Yu. A. Shimanskiy [5]. In distinction from other methods, this one is based on a scheme assuming the reaction of the ship's hull with the ice simultaneously along the entire length of the bow section of the waterline, i.e., from the stem to the broadest section. Without dwelling on the assumptions which the author made in the derivation of the dependences for "conditional gauges", we will note that they are suitable only for a comparative estimate of ice navigating capability. However, in spite of the face that the "conditional gauges" have not found wide application in the designing of ice breakers, the scheme of the reaction of the hull of an icebreaker proposed by Yu. A. Shimanskiy is widely used in semi-empirical methods of calculating the ice navigating capability for consideration of the effect of the

lines of an icebreaker on its resistance during motion in ice.

In recent years in the USSR great amounts of theoretical and experimental works have been conducted on the study of the laws of resistance of solid ice to the motion of a ship. The first experiment in the history of icebreaker construction with a model ice field of reduced strength were accomplished in 1949-1950, and they confirmed the feasibility of model tests for the study of the laws of ice resistance. In connection with this, in 1955 in the Arctic Scientific Research Institute for the performance of systematic model tests in ice, the first ice basin in the world was constructed. The results of model experiments supplement theoretical conclusions and data from full-scale tests. Such a method of the solution of the problem made it possible to create semi-empirical calculation formulas associating the ice resistance with the characteristics of the ship and the parameters of the ice. In the derivation of these dependences, the following method was used.

On the basis of the accepted scheme of the reaction of a ship's hull with the ice [3], an expression was compiled for the ice resistance, in which correction factors were introduced, considering the conditional nature of the scheme accepted and other assumptions. The numerical values of the factors were found according to the results of a model experiment, conducted on the basis of the theory of modeling the motion of a ship in solid ice, and from data from full-scale tests. In 1958 in the ice basin of the AANII model tests of the icebreaker "Yermak" were accomplished in model ice of various thickness and strength, which made it possible for the first time to obtain a semi-empirical expression for the ice resistance in continuous motion in solid ice [3]:

$$R = R_1 + R_2 + R_3 + R_в = k_1 B^{3} \gamma_0 h^{2} \mu_0 + k_2 \gamma_{12} h^{2} \mu_0 + \\ + k_3 B^{1.65} h v^{1.5} \gamma_{12} + R_в, \tag{7}$$

where R_1 is the resistance of the ice to breaking; R_2 is resistance of a weight nature (packing, overturning, etc., and also the resistance of friction, not depending upon speed); R_3 is speed resistance (expansion, towing of ice, and also friction depending upon the speed of the ship); R_v is the resistance of the water to the motion of the ship in the ice [$R_в = R_v = R_{water}$]; $k_1 = 0.004$; $k_2 = 3.6$ and $k_3 = 0.25$ are coefficients whose numerical values are found according to the experimental data; μ_0 [$\mu_0 = \mu_0 = \mu_{line}$] and γ_{12} are coefficients characterizing the lines of the ship's hull; and γ_1 [$\gamma_1 = \gamma_1 = \gamma_{ice}$] is the density of the ice.

This equation may serve for the determination of the magnitude of the thrust of the screw propellers, necessary to overcome ice of given thickness and strength with a given speed, or for finding the limiting thickness of the ice which the icebreaker is capable of breaking at a given thrust and the speed attained by continuous steaming. A comparison of calculations according to formula (7) with full-scale data demonstrates that this expression may be used with success in the initial stage of the designing of icebreakers differing from the icebreaker "Yermak" in their principal dimensions and the shape of the hull. In the determination of the thickness of the limiting ice in which various icebreakers can move continuously, the error does not exceed ±10%. The differences in the comparisons of the speeds of the ships are more essential. Expression (7) is valid for continuous motion in level solid ice covered with snow, and inadequately strictly considers the different natural variations in the ice cover, which are primarily felt on the speeds of the ship. Therefore, in the use of formula (7) for the calculation of speed it is necessary to introduce corrections for the snow cover, degree of breakage, and hummocking of the ice cover according to data from full-scale tests of the icebreakers. One of the possible methods of the introduction of these corrections is explained in reference [2].

An example of one more semi-empirical method of determining the capability of an icebreaker to overcome the ice resistance is a method of M. S. Yakovlev, developed with reference to river icebreakers [6]. In considering the continuous motion in solid ice, the author presents the total resistance of the icebreaker in the form of the sum of two components: the resistance R_1, not depending upon speed (resistance to breakage and resistance of the friction of ice against the hull) and determined by the calculation method on the basis of the theoretical solution of the deformation of the semi-infinite beam-strip on an elastic base, and the resistance R_2 which depends upon speed and is determined according to data from tests of a model in broken ice. The scheme accepted for division of the total resistance into components is very highly simplified. However, the results of the calculations of the limiting thicknesses of ice according to M. S. Yakovlev's method agree well with full-scale data obtained during operation of icebreakers in ice conditions.

The semi-empirical approach in the development of calculation methods of ice navigating capability developed in the USSR is finding application at the present time also abroad, in particular in the USA. Thus, Edwards and Lewis in 1970 proposed the following semi-empirical expression for estimation of the ice resistance in continuous motion of an icebreaker in solid ice [8]:

$$R = c_0\sigma_u h^2 + c_1\rho g B h^2 + c_2\rho B h v^2, \qquad (8)$$

where R is the ice resistance; $c_0 \sigma_r h^2$ is the resistance of the ice to breakage, and the friction associated with it; $c_1 \rho g B h^2$ is the resistance caused by the buoyancy of the ice; and $c_2 \rho B h v^2$ is the inertial component of the forces of resistance.

A comparison of expressions (7) and (8) demonstrate that the items entering into them have the same physical sense. The structure of the second term (to which the greatest fraction of the total resistance falls) in these equations is identical. In formula (7) only the first two items are subordinate to conditions of strict modeling, and in expression (8) the speed component of the ice resistance also formally satisfies this condition. In other words, the method of Edwards and Lewis assumes a conversion to full scale of both each component of the resistance individually and of their sum. However, tests of a scale series of models in the basin of the AANII demonstrated that the speed component of the resistance cannot be converted to full scale, since actually this component is not subordinate to a quadratic law as was assumed by Edwards and Lewis. Aside from this, expression (8) does not consider in the explicit form the effect of the shape on the ice resistance. The characteristics of the shape enter into the coefficients c_0, c_1, and c_2, which in each particular case must be determined experimentally.

In Figure 1 the dependence of the ice resistance (thrust of the screw propellers) of an icebreaker of the "Wind" class upon the thickness of the ice is given, at a speed of continuous motion close to zero, $v \approx 0$. The curves were calculated with the use of the theoretical and semi-empirical methods considered.[1] In the drawing a curve of the resistance of this icebreaker obtained according to data from full scale tests is also drawn. An analysis of this curve demonstrates that the semi-empirical methods of calculating the ice navigating capability determined the limiting thickness of the ice more accurately than theoretical methods. This confirms the previously expressed considerations of the unsuitability of the use of purely theoretical methods based on a single-contact scheme of the breaking of the ice, for the estimates of the capability of the icebreaker to overcome ice by continuous steaming. In connection with this, at the present time for determination of ice navigating capability in the process of the designing of ice breakers we should recommend semi-empirical formulas.

In our opinion, a further development and improvement of methods of determining the ice navigating capability in solid ice must be based on semi-empirical methods assuming the use of the results of model and full-scale experiments. In this case, the continuous motion of the ship in ice

[1] Figure 1 is adapted from a work by Edwards [7].

must be considered as a random process, caused by the heterogeneity of the thickness and the physical-mechanical properties of the ice cover. Therefore, semi-empirical formulas must, with an adequate degree of accuracy, determine the average statistical value of the ice resistance corresponding to the so-called standard ice conditions, in which the heterogeneities of the medium are at the minimum. Solid ice, not covered with snow, with a zero degree of breakage and hummocking should be considered as such standard ice conditions.

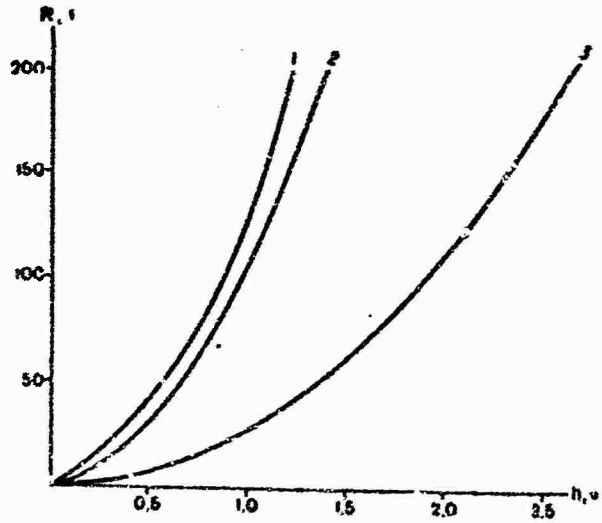

Figure 1. Comparison of methods of estimating the ice navigating capability of an icebreaker of the "Wind" class: 1) full-scale curve; 2) semi-empirical curve (Kashtelyan's method); 3) theoretical curve (the White-Milano method). a) R, tons; b) h, meters.

The development of a single method of calculating the ice resistance which would include all cases of the motion of an icebreaker in natural solid ice is not feasible. Apparently, we should develop semi-empirical methods of determining the navigating capability of icebreakers in ice for the most characteristic ice conditions (ice in the stage of growth, snow-covered ice field, etc.). Aside from this, in a further development of methods of estimating ice navigating capability it is necessary to consider more strictly the effects of the principal dimensions and the shape of the ship's lines on the ice resistance.

As the initial stage it is desirable to have criterion of the efficiency of operation of the icebreaker in ice (indices of ice navigating capability) which would make it possible, in approximation, to estimate the technical perfection of the ship being designed. It is also convenient to use such indices in conversions from a prototype.

We should note that the indices of ice navigating capability existing at the present time are not finding wide application in practice. In a majority of cases these indices, developed on a theoretical basis, consider the effect on ice resistance of the factors determining it inadequately completely. As an example, the measurement of icebreaking capability proposed by I. V. Vinogradov [1] and Yu. A. Shimanskiy [5] may serve. Among the unsuccessful indices we should also include the "energy ratio" (the ratio of the capacity of the power plant to the displacement), which, as experiences in operation has demonstrated, does not give any concept of the efficiency of an icebreaker either in continuous motion or during in operation in short run.

Indices of the ice navigating capability of icebreakers are proposed below, which were obtained with the use of the latest investigations in the field under consideration.

In the derivation of an operating index of an icebreaker running in continuous motion, we will use formula (7). With reference to motion in the ice of limiting thickness, i.e., at v = 0, this expression may be presented in the form

$$T = k_2 \gamma_1 B h_{\text{пр}}^2 \mu_0, \tag{9}$$

where T is the thrust of the screw propellers in dock trials; B is the beam of the hull; h_{pr} is the limiting thickness of the ice being broken [$h_{пр} = h_{pr} = h_{limiting}$]; γ_1 is the density of the ice [$\gamma_1 = \gamma_1 = \gamma_{ice}$].

For the index being sought it is feasible to accept the ratio $(T/B\mu_0)^{1/2}$ which, as is apparent from equation (9), is proportional to the limiting thickness of the ice, which is the basic criterion of the operation of an icebreaker in continuous motion.

The quantity μ_0, considering the effect of the hull shape on the ice resistance, is stable for different icebreakers. We will consider an approximation that T = kN (where k is a constant coefficient, and N is the capacity of the power plant). Then the index of the operating efficiency of the icebreaker running in continuous motion may be presented in the following form:

$$E_1 = \left(\frac{N}{B}\right)^{1/2} \sim h_{\text{пр}}. \tag{10}$$

With this index in the initial stage of designing we may in approximation estimate the capacity N of the power plant necessary for the icebreaker to overcome ice of a given thickness h in continuous motion, using an

acceptable prototype. By means of expression (10) we find

$$N = N_0 \frac{B}{B_0} \left(\frac{h}{h_0}\right)^2. \tag{11}$$

Formula (11) also makes it possible to find the limiting thickness of the ice which the icebreaker being designed can overcome at a given capacity of the power plant:

$$h = h_0 \left(\frac{N}{N_0}\right)\left(\frac{B_0}{B}\right)^{1/2}. \tag{12}$$

For estimation of the ice navigating capability of the icebreaker in operation by short runs we will introduce two indices, one of which characterizes the maximum capability of overcoming ice and the other gives an opportunity to compare the efficiency of the operation of icebreakers in one and the same conditions. As the first index, apparently, we may accept a quantity proportional to the limiting thickness of the ice in operation by short runs which is determined from the condition that the entire kinetic energy of the icebreaker is expended on breaking the ice, i.e., it is equal to the potential energy of breaking an infinite strip beam with a width B on an elastic base[1].

According to reference (3)

$$\frac{Mv^2}{2} = 0{,}27 B \sigma_p^2 h^4 a_0^3,$$

where

$$a_0 = \sqrt[4]{\frac{3}{Eh^3}};$$

M is the mass of the icebreaker; v is the speed at the moment that the ship encounters the ice; σ_r is the ultimate bending strength of the ice; and E is the modulus of elasticity of the ice.

---

1. Such a conditional scheme of the breaking of ice by an icebreaker was accepted in the derivation of the semi-empirical expression (7).

Assuming that E is proportional to σ_r, we obtain the following expression for the limiting thickness of the ice being broken by an icebreaker in operation by a short run:

$$h = k_4 \frac{D^{4/7} v^{2/7}}{B^{4/7} g^{2/7}}, \tag{13}$$

where k_4 is a proportionality factor.

Assuming that v = const, σ_r = const, we find the approximate index of the maximum capability of the icebreaker to break ice by short runs:

$$E_3 = \left(\frac{D}{B}\right)^{2/3} \approx \left(\frac{D}{B}\right)^{2/3}. \tag{14}$$

As the second index, which characterizes the operating efficiency of an icebreaker operating in short runs in one and the same ice conditions, we may accept the average speed of advance of an icebreaker, with consideration of the time expended on its start, acceleration in the channel, and advance in the solid ice in the braking section

$$v_{cp} = \frac{l}{t_1 + t_2 + t_3}, \tag{15}$$

where l is the length of the run in solid ice; t_1 is the time expended by the icebreaker in starting back (backing down); t_2 is the acceleration time in the channel; and t_3 is the time expended on running (coasting) into the solid ice.

Such an index makes it possible to estimate most completely the efficiency of an operation of an icebreaker in short runs, in breaking a channel in solid ice.

From equation (15) it is apparent that, other things being equal, v_{sr} [$v_{cp} = v_{sr} = v_{average}$] is proportional to the length of the run l. Therefore, l in the future will be accepted as the second index of the operation of an icebreaker in short runs. By expressing the ice resistance in solid ice by the approximate formula (9) we will determine the average length of a coasting run from conditions of equality of the kinetic energy of the ship to the work of the force of the ice resistance in the length l of a coasting run:

$$\frac{Dv^2}{2g} = Rl \approx k_2 \gamma_a B h^2 \mu_0 l,$$

from whence

$$l \approx \frac{Dv^2}{2g k_2 \gamma_a B h^2 \mu_0}. \tag{16}$$

The speed v of the ship at the moment it meets the ice is functionally connected with the thrust pressure of the propellers and the displacement. By using Milano's data [9], we find

$$v \sim \frac{S^{0.3} T^{0.5}}{D^{0.3}}, \tag{17}$$

where S is the length of the acceleration in the channel, filled with broken ice; T is the thrust of the screw propellers in dock trials.

By means of dependences (16) and (17), we finally obtain

$$l \sim \frac{D^{0.4} S^{0.6} T}{B h^2 \mu_0}. \tag{18}$$

Considering, as previously, that $T \sim N$ for the operating index of ice-breakers operating in short runs in ice of one and the same thickness and at the same lengths S of the acceleration section, we may assume the following ratio:

$$E_3 = \frac{D^{0.4} N}{B} \approx \frac{D^{1/3} N}{B}. \tag{19}$$

In comparing expressions (10), (14), and (19), we find

$$E_3 = E_1 E_2 N^{1/3}. \tag{20}$$

We may consider that the index E_3 as a whole characterizes the operating efficiency of an icebreaker both in continuous motion and in operation by short runs. In analyzing formula (19) we may become convinced that no optimum ratio between the capacity of the power plant of the icebreaker and its displacement exists. To increase the operating efficiency of the icebreaker in solid ice, it is more feasible to increase the ratio N/B, and not D/B, since such an increase has a favorable effect on the operating efficiency of the icebreaker both in continuous motion and in operating by short runs. The calculated values of E_1, E_2 and E_3 for different icebreakers are given in Table 1.

Table 1

Indices of the Operation of Modern Icebreakers in Solid Ice

(1) Ледокол	(2) N, л. с.	(3) D, т	(4) B, м	$E_1 = \left(\frac{N}{B}\right)^{1/3}$	$E_2 = \left(\frac{D}{B}\right)^{1/3}$	$E_3 10^4 = E_1 E_2 \times N^{1/3} 10^{-4}$
(5) „Москва"	22 000	13 300	23,5	30,6	23,7	10,7
(6) „Луи С. Сан-Лоран"	24 000	13 300	24,4	31,4	23,3	11,3
(7) „Гласье"	21 000	8 600	22,0	31,0	19,7	9.0
(8) „Макинау"	10 000	5 200	21,3	21,7	15,6	3,4
(9) „Сибирь"	10 300	11 000	21,7	22,0	22,5	5,0
(10) „Уинд"	10 000	5 400	18,9	23,0	17,0	3,9
(11) „К. Белоусов"	10 500	4 500	18,7	23,6	15,5	3,7
(12) „С. Челюскин"	5 400	2 700	17,5	17,6	12,4	1,6
(13) „Д. Макдональд"	15 000	9 700	21,0	26,8	21,5	7,0

Key: 1) icebreaker ; 2) N, horsepower ; 3) D, tons; 4) B, meters; 5) "Moskva"; 6) "Louis S.St. Laurent"; 7) "Glacier"; 8) "Mackinaw"; 9) "Sibir"; 10) "Wind"; 11) "K. Belousov"; 12) "S. Chelyuskin"; 13) "D. MacDonald".

BIBLIOGRAPHY

1. Vinogradov, I. V., Suda legovogo plavaniya (Ships for ice navigation), Moscow, "Oborongiz" 1946.

2. Kashtelyan, V. I., and Ryvlin, A. Ya., "Consideration of the natural characteristics of solid ice in the estimation of the possibility of an icebreaker passing through it, " in the collection: Problemy Arktiki i Antarktiki (Problems of the Arctic and Antarctic), Volume 22, Leningrad, Gidrometeoizdat, 1966.

3. Kashtelyan, V. I., Poznyak, I. I., and Ryvlin, A. Ya., Soprotivleniye l'da dvizheniyu sudna (Resistance of ice to the motion of a ship), Leningrad, "Sudostroyeniye", 1968.

4. Runeberg, R. I., O parokhodakh zimnego plavaniya i ledokolakh (On steam ships for winter navigation and icebreakers), St. Petersburg, 1890.

5. Shimanskiy, Yu. A., "Conditional gages of the ice qualities of ships," Tr. ANII (Transactions of the Arctic Scientific Research Institute), Volume 130, 1938.

6. Yakovlev, M. S., "Methodology of the determination of the ice navigation speed of river vessels," Tr. GPI (Transactions of Gor'kiy Polytechnical Institute), Volume XVII, No. 1, 1960.

7. Edwards, R. J., "Engineering research in Support of the development of Arctic sea transportation," Marketing and Transportation situation. Journal 1970, Volume 4, No. 5.

8. Lewis, J. W., Edwards. R. J., "Modelling the motion of ships through Polar Ice fields using unconstrained, selfpropelled models," Ice Symposium, 1970, Reikjavik.

9. Milano, V. R., "Notes on the Preliminary Design of Icebreakers," Webb Institute of Naval Architecture, 1961.

10. Nevel, D. E., "The Narrow Infinite Wedge on the Elastic Foundation," Webb Institute of Naval Architecture, 1961.

11. Nevel, D. E., "A Semi-Infinite Plate on ar Elastic Foundation," Research Report 136, Cold Regions Research and Engineering Laboratory, March 1965.

12. White, R. M., "Prediction of Icebreaker Capabilities," Royal Institute of Naval Architecture, 1961.

ON THE ICE NAVIGATION SPEED OF SHIPS IN EXTREMELY SOLID ICE

D. Ye. Kheysin pages 18-26

In motion in solid ice fields, a ship experiences a counter action composed of the forces of resistance of the water and the forces of the ice resistance. With an increase in the thickness of the ice the speed of the ship decreases, and the fraction of the ice resistance in the total resistance increases. The limiting thickness of the solid ice which a ship can pass through (overcome) by continuous steaming is one of the most important indices of the ice breaking qualities of a ship.

Practice demonstrates that the motion of a ship in solid ice with a thickness close to the limiting value is unstable: from time to time the ship stops, even in motion in what would appear to be ideally level ice. Thus, together with the determination of the maximum thickness of the ice being penetrated by the ship it is necessary to make an investigation of the stability of its motion in the given conditions.

Estimates of the forces of ice resistance to the motion of a ship in solid ice [3, 6, 12, 13], based mainly on the results of full-scale and model tests, are empirical in nature.

In this work a comparatively simple calculation scheme is proposed, which makes it possible to obtain an analytical solution of the problem. In this case probability methods of analysis are used, and the reaction of the hull of the ship with the ice is considered as a random process [11].

In motion in the ice at a low speed, the components of the resistance depending upon the speed are small. Resistance to the motion of the ship is basically determined by the so-called direct ice resistance, not depending upon the speed [3]. In the future, we will consider the dependence of the resistance upon the speed to be linear, with a constant proportionality

factor a, considering both the ice component and the resistance of the water. We will assume the disturbing force R(t), equal to the difference between the thrust of the propellers R_t [$R_T = R_t = R_{thrust}$] and the direct ice resistance R_v [$R_\beta = R_v = R_{water}$], will be assumed to be a random function of time with a determined component R_t and a random component R_v.

We may represent the force of the ice resistance R_v to the motion of a ship in ice as the result of shock impulses successively applied to the hull, thus counteracting the motion. For steady-state regimes of the motion of the ship, this random process is both steady-state and ergodic.

A counted set of discrete external effect forms a well-ordered time series. Such a series may be obtained, by having divided in a random manner the infinite time axis of an infinite series of points t_j into intervals of random length

$$\Delta t_j = t_{j+1} - t_j$$

If we take an arbitrary interval of time (-T, T), then the number of points N, which fell into this interval, will be a random quantity. As experiments [5] demonstrated, the number N, i.e., the quantity of impacts is subordinate to the Poisson law of distribution

$$P_N = \frac{(2\lambda T)^N}{N!} e^{-2\lambda T}. \tag{1}$$

For steady-state regimes the average distribution density of impact pulses in time, λ, is constant. This quantity was also experimentally determined [5]. It is clear that for an adequately large interval of time $N \approx 2\lambda T$.

Let $\{{}^k R(t)\}$ be a set of possible values of the external disturbance. The speed of a ship caused by the random force ${}^k R(t)$ also will be a random function of time ${}^k v(t)$. Then the differential equation of motion of a ship with a displacement D along a straight course is written thus [7]:

$$\frac{D}{g}\frac{d[{}^k v(t)]}{dt} + a[{}^k v(t)] = {}^k R(t), \tag{2}$$

where the superscript k corresponds to the k-th realization of the random process.

The right part of equation (2) in a steady-state regime of the motion of the ship is a steady-state random function of time. In the first approximation, it may be represented in the following manner:

$$^kR(t) = {}^kR_j \text{ at } \quad t_j \leqslant t < t_{j+1} \quad (j = 0, \pm 1 \ldots). \tag{3}$$

The random quantities $\left\{{}^kR_j\right\}$ are statistically independent and have identical mathematical expectations and dispersions, not depending upon time t, i.e., for arbitrary indices j we have

$$E_k[{}^kR_j] = \overline{R} = R_\tau - \overline{R}_s.$$

The intervals Δt_j are also independent random variables, having a probability distribution function not depending upon the subscript j.

Random process (3) describes the magnitude of the random impulse of force acting on the ship in motion along a straight line in statistically homogeneous ice conditions. As we have already noted, the process under consideration is a Poisson process. The spectral density of such a process is determined according to the formula [2, 9]

(4)

$$S_R(\omega) = \frac{2}{\pi}\frac{\sigma_R^2\lambda}{\omega^2+\lambda^2} + (\overline{R})^2\delta(\omega),$$

where

$$\sigma_R^2 = \overline{R}_s^2 - (\overline{R}_s)^2.$$

The correlation function for R(t) will have the form

$$K_R(\tau) = \sigma_R^2 e^{-\lambda|\tau|} + (\overline{R})^2. \tag{5}$$

The function of the spectral density at the beginning of the coordinates has a characteristic corresponding to the constant average value of the external effect $\overline{R}$.

According to the known ratio between the spectral densities of the input

and output, for the spectral density of the random process $\{^k v(t)\}$ being sought we find

$$S_v(\omega) = S_R(\omega)|Y(i\omega)|^2,$$

where $Y(i\omega)$ is the frequency characteristics of the system, described by differential equation (2). Having divided both parts of this equation by D/g, we obtain

$$Y(i\omega) = \frac{1}{\beta + i\omega}, \text{ where } \beta = \frac{ag}{D}.$$

Then

$$S_v(\omega) = \left(\frac{g}{D}\right)^2 \left\{ \frac{2}{\pi} \frac{\lambda \sigma_R^2}{(\lambda^2 + \omega^2)(\beta^2 + \omega^2)} + \frac{(\bar{R})^2}{\beta^2 + \omega^2} \delta(\omega) \right\}. \quad (6)$$

The mathematical expectation of the speed of the ship is determined according to the formula [8]

$$E_k[^k v(t)] = v_{cp} = \frac{R_t - \bar{R}_v}{a}.$$

[$v_{cp} = v_{sr} = v_{average}$].

At $R_t = \bar{R}_v$ the average speed is equal to zero. Thus, the motion occurs only at $R_t > \bar{R}_v$. However, in this case stoppages of the ship are possible if the random deviations R_v from the average value exceeds the magnitude $R_t - \bar{R}_v$.

We will establish the sense which here may be given to the term "stability of motion". By stable, we will understand a continuous motion of the ship, without stoppages, during quite long intervals of time with a given degree of guarantee. In other words, the probability that the speed will be equal to zero after the passage of a definite interval of time t must be limited, i.e.,

$$P(v_{cp}/0, t) \leq A,$$

where A and t should be determined according to the data from operation of the ship in ice conditions.

The mathematical expectation of a random speed v(t) is not equal to

zero. Therefore, for the determination of the probability $P(v_{sr}/0, t)$ we should decenter the process. For this purpose, we will consider it as a random oscillation of speed in space (t, v) relative to the average value v_{sr} when we arrive at the moment of time t = 0 from the point $v = v_{sr}$. We are interested in the probability of falling at the boundary $v = 0$. Since the motion of the ship is not renewed by itself after stopping, we are dealing with an absorbing boundary. In the model of the reaction of the ship with the ice accepted, when the pulses following each other are statistically independent, the asymptotic solution for the probability of stoppage (absorption) is written [1] thus

$$P(v_{cp}/0, t) = \exp\left(-\frac{2v_{cp}^2}{\sigma_v^2 t}\right),$$

where

$$\sigma_v^2 = \int_{-\infty}^{+\infty} (v - v_{cp})^2 p(v - v_{cp}, t)\, dv = D[v] - v_{cp}^2. \qquad (7)$$

The dispersion of the random quantity v(t) in expression (7) is determined according to the formula

$$D[v] = \int_0^{\infty} S_v(\omega)\, d\omega.$$

By using equality (6), we obtain

$$\sigma_v^2 = \frac{g}{aD} \frac{\sigma_R^2}{\beta + \lambda}.$$

Thus, we will finally find the probability of the stoppage of the ship in a time t

$$P(v_{cp}/0, t) = \exp\left[-\frac{2aD(\beta + \lambda) v_{cp}^2}{gt\sigma_R^2}\right]. \qquad (8)$$

By performing the replacement according to $l_0 = tv_{sr}$ in this formula, we will determine the probability of the stoppage of the ship in a section of track with a length l_0.

For estimation of the duration of continuous motion of a ship, without stoppages, we will find the probability density of the time that the boundary is reached [1]:

$$g(t) = \frac{v_{cp}}{\sqrt{2\pi\sigma_R^2 t^3}} \exp\left(-\frac{v_{cp}^2}{2\sigma_R^2 t}\right). \tag{9}$$

As is apparent from expression (8), for a ship of infinite mass the probability of stoppage is equal to zero. We have the same $t \to 0$ or $l_0 \to 0$, i.e., if the ship was moving at a given moment with an average speed v_{sr}, in the nearest following moment of time the probability of its stoppage is negligible.

The probability of stoppage of a ship decreases with an increase of the average speed v_{sr} of the ship and the number λ of its collisions with the ice. The probability of stoppage increases with an increase of the dispersion of the disturbing force, i.e., with an increase in the irregularity of the process of the reaction of the hull with the ice. Thus, the motion of a ship of large displacement in conditions that are not too close to limiting will be stable if the dispersion of the ice resistance is not excessively great.

The dispersion of the force of direct ice resistance σ_R^2 is not equal to zero even in ideally homogeneous solid ice, since the breaking of ice occurs along the length of the side in random sections having a different inclination. In this case the contact sources will depend upon the random coordinates of the point of reaction. The dispersion σ_R^2 here may be estimated by using a three-point static scheme of the breaking of the ice.

In this case such a reaction of the ship with the ice is considered when contact and breaking of the ice at three points is accomplished simultaneously. This triangle determines the equilibrium statically determined position of the ship. Point 1 (Figure 1) is the point of contact of the stem. Points 2 and 3 are located along the sides of the ship symmetrically to its center line. At these points, contact forces R_n act, directed along the normal to the side of the ship, and also the friction forces proportional to it, directed along the tangential to the side.

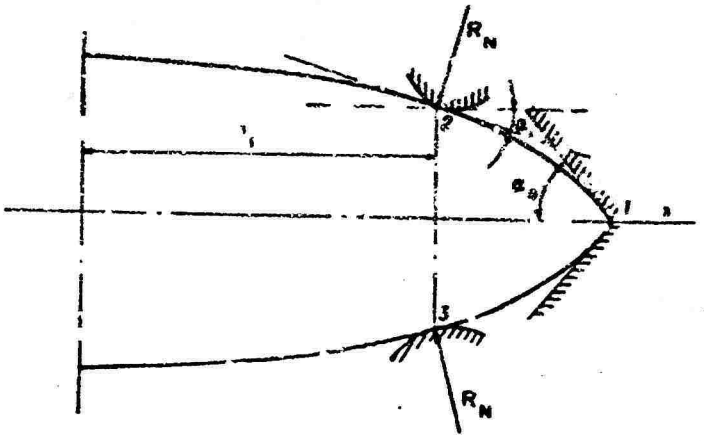

Figure 1. Three Point Scheme of Icebreaking

We will find the projection of the contact forces from both sides onto the axis x with consideration of the forces of friction.

$$R_x = 2R_N(l + f_\tau \cos\alpha),$$

where l is the guiding cosine of the normal to the side of the ship; α is the angle of inclination of the tangential to the water line to the center line (see Figure 1); and f_t is the coefficient of friction of the side of the ship against the ice [$f_\tau = f_t = f_{friction}$].

Under the effect of the vertical component of the contact force, $R_z = R_N \sin\beta$, the ice breaks. Here β is the angle of inclination of the side to the vertical at the point of contact. We will assume that semi-infinite ice plates enter into contact with the side at points 2 and 3. For breaking of such plates, the following force is required [4]:

$$R_z = 0{,}52\sigma_r h^2,$$

where h is the thickness of the ice; and σ_r is the ultimate bending strength of the ice.

At point 1 of the contact of the stem with the ice, a force R'_N that is normal to the stem acts, and a friction force $R'_t = f'_t R'_N$ proportional to it (Figure 2). The given friction factor f'_t is determined according to the following formula [10]:

$$f'_\tau = f_\tau \sqrt{1 + \frac{\sin^2\varphi}{\operatorname{tg}^2\alpha_0}},$$

where φ is the angle of inclination of the stem to the horizon; and α_0 is the angle of "entry" of the bow branch of the waterline.

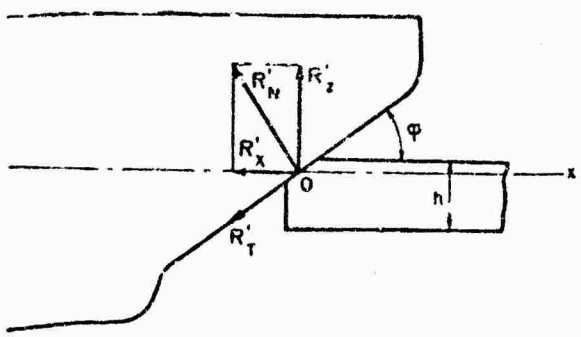

Figure 2. Contact of the stem with the ice.

The projection of these forces onto the axis x will be

$$R_x' = R_z'(\operatorname{tg}\varphi + f_\tau').$$

For determination of the vertical component of the contact force R_z' we will consider the breaking of an infinite plate with a wedge-shaped cut, having an angle $2\alpha_0$. In this case [4]

$$R_z' = 1{,}04\sigma_y h^2 \frac{\pi - \alpha_0}{\pi}.$$

We will compile the equation of static equilibrium of the ship in the projection on the axis x. Assuming the contact forces to be equal to the ice that is breaking, we will determine the magnitude of the force of the direct ice resistance according to the formula

$$R_v = 1{,}04\sigma_y k^2 k_f(x), \tag{10}$$

where

$$k_f(x) = \frac{1 + f_\tau \cos\alpha}{\sin\beta'} + \frac{\pi - \alpha_0}{\pi}(\operatorname{tg}\varphi + f_\tau') \tag{11}$$

is a dimensionless coefficient characterizing the shape of the ship's hull.

The quantity R_v will be random, since the coordinates of the points of contact with the ice, 2 and 3, are random. For determination of the average value of the force of ice resistance $\overline{R}_v$ we should introduce the function of the probability density t(x) of falling at a point of the side with a random coordinate x. This function was found according to data from strain-gauge tests of ships [5].

Then

$$\overline{R}_v = 1{,}04\sigma_y h^2 \overline{k}_f, \tag{12}$$

where

$$\overline{k}_f = \frac{\pi - \alpha_0}{\pi}(\operatorname{tg}\varphi + f_\tau') + \int_a \frac{1 + f_\tau \cos\alpha}{\sin\beta'} p(x)\, dx.$$

Here the integration is performed along one of the sides of the ship in sections where p(x) 0. The approximation for t(x) may be quite rough, since the possible errors are smoothed in integration. For numerical calculations, approximations similar to those given in Figure 3 were assumed. The quantity t_0 was determined from the standardization condition

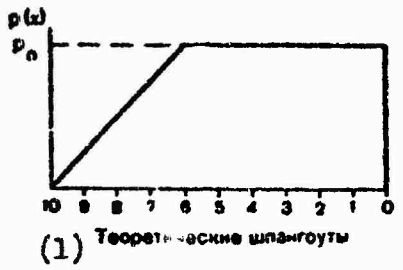

Figure 3. Probability density p(x) (of the average ice resistance falling at a point on the side) assumed in the calculation of ice breakers. 1) theoretical frames.

$$\int_0^{\infty} p(x)\,dx = 1.$$

In motion in limiting ice, the speed component of resistance may be ignored. Then instead of R_v in equation (10) we substitute the thrust R_t of the propellers and determine the thickness of the ice being broken in continuous steaming. Having arranged the side points of contact at different distances from the stem, we will construct a curve of the limiting thicknesses of the ice being broken, h(x), along the length of the ship. The nature of this curve gives a concept of the rationality of the designing of hull lines from the standpoint of their ice breaking qualities.

In calculations of the limiting thicknesses h of the ice being broken (Table 1) it was assumed that $f_t = 0.1$ and $\sigma_r = 100$ tons per square meter, which corresponds to other Arctic ice. From the table it is apparent that the quantity h is in constant along the length of the ship's hull, its least value is noted in the vicinity of the 4-th to 5-th theoretical frames, i. e., at the "bilge" of the waterline. The minimum thickness h_{min} of the ice, found according to curve h(x) is the guaranteed limiting thickness broken by the ship in continuous steaming.

As an integral parameter, determining the ice breaking capabilities of the ship, we may assume the average value of $\bar{h}$:

Table 1

Calculated Thicknesses of Ice Broken for Various Ships (in meters)

(1) Судно	(2) Теоретические шпангоуты						
	1	2	3	4	5	6	7
(3) Ледоколы:							
„Москва" (4)	1,36	1,36	1,36	1,34	1,31	1,34	1,40
„Сибирь" (5)	0,92	0,91	0,89	0,88	0,89	0,92	0,96
„Капитан Белоусов" (6)	0,92	0,91	0,90	0,89	0,90	0,92	0,96
„Ерофей Хабаров" (7)	0,61	0,60	0,60	0,59	0,59	0,60	0,63
(8) Дизель-электроходы:							
„Лена" (9)	0,58	0,53	0,50	0,51	0,55	0,58	—
„Пенжина" (10)	0,70	0,71	0,70	0,63	0,61	0,62	—

Key: 1) ship; 2) theoretical frames; 3) icebreakers; 4) "Moskva"; 5) "Sibir"; 6) "K. Belousov"; 7) "Yerofey Khabarov"; 8) diesel-electric icebreaking cargo vessels; 9) "Lena"; 10) "Penzhina".

$$\bar{h} = \int_{\Omega} h(x)\, p(x)\, dx.$$

For a complete estimate of the icebreaking qualities of a ship, it is also necessary to consider the indices characterizing the stability of its motion in limiting ice. As follows from equality (8), one of such parameters, depending upon the shape of the hull lines, is the dispersion σ^2_R of the force of direct ice resistance. Its magnitude is determined according to the formula

$$\sigma_R^2 = (1{,}04\sigma_\gamma h^2)^2 k_\alpha,$$

where

$$k_\alpha = \int_{\Omega} \left(\frac{l + f_T \cos\alpha}{\sin\beta'}\right)^2 p(x)\, dx - \left[\int_{\Omega} \frac{l + f_T \cos\alpha}{\sin\beta'} p(x)\, dx\right]^2$$

is a coefficient depending only upon the shape of the hull lines of the vessel.

From expression (8) it also follows that with a decrease in σ^2_R the probability of a stoppage of a ship moving in limiting ice will decrease. For the possibility of comparing the shape of the hulls of various ships, we will introduce the dimensionless magnitudes of the dispersion of the force of direct ice resistance and the average thickness of the ice being broken:

$$(\sigma_R^2)^* = \frac{\sigma_R^2}{(1{,}04 z_p k^2)^2} \text{ и } (\bar{h})^* = \bar{h} \sqrt[3]{\frac{1{,}04 z_p}{R_T}}.$$

The results of the calculation of these parameters for different vessels intended for ice navigation and icebreakers are given in Table 2. The values of the thicknesses of the ice being broken, as given in the table, are quite close to the averaged magnitudes obtained according to data from full-scale tests. The relative mean square deviations of the force of direct ice resistance σ^*_R are not great: 8--10% for icebreakers and 19--20% for transport vessels. This testifies to the high degree of perfection of the shape of the hull lines of modern icebreakers. Such calculations for ships of the same type make it possible to compare their ice qualities (see Table 2).

Table 2

Relative Characteristics of Ice Navigation Speed (ice navigating capability) of Various Vessels

(1) Судно	(2) R_T, т	h_{min}, м (3)	$\bar{h}$, м (4)	$(\bar{h})^*$	σ^*_R
(5) Ледоколы:					
„Москва" (6)	230	1,31	1,35	0,907	0,081
„Сибирь" (7)	100	0,88	0,90	0,922	0,094
„Капитан Белоусов" (8)	100	0,89	0,91	0,930	0,086
„Ерофей Хабаров" (9)	52	0,59	0,60	0,851	0,100
(10) Дизель-электроходы:					
„Лена" (11)	60	0,50	0,54	0,712	0,202
„Пенжина" (12)	63	0,61	0,66	0,847	0,188

Key: 1) ship; 2) R_t, tons; 3) h_{min}, meters; 4) $\bar{h}$, meters; 5) icebreakers; 6) Moskva"; 7) "Sibir'"; 8) "K. Belousov"; 9) "Yerofey Khabarov"; 10) diesel-electric icebreaking cargo vessels; 11) "Lena"; 12) "Penzhina".

BIBLIOGRAPHY

1. Bartlett, M. S., Vvedeniye v teorii sluchaynykh protsessov (Introduction to the theory of random processes) (Russian translation), Moscow, Izd-vo inostr. lit-ry, 1958.

2. Bendat, G., Osnovy teorii sluchaynykh shumov i yeye primeneniya (Bases of the theory of random noises and its applications), Moscow, "Nauka", 1965.

3. Kashtelyan, V. I., Poznyak, I. I., and Ryvlin, A. Ya., Soprotivleniye l'da dvizheniyu sudna (Resistance of ice to the motion of a ship), Leningrad, "Sudostroyeniye", 1968.

4. Kashtelyan, V. I., "Approximate determination of forces breaking the ice cover," in the collection: Problemy Arktiki i Antarktiki (Problems of the Arctic and Antarctic), No. 5, Leningrad, "Morskoy transport", 1960.

5. Likhomanov, V. A., "The strength of icebreakers and transport vessels (according to data from strain gauge tests)", in this collection.

6. Nogind, L. M., "Modelling the motion of a ship in a solid ice field and in broken ice," Tr. Leningr. Korablestr. in-ta, No. XXVIII, 1959.

7. Petrov, Ye. Yu., and Kheysin, D. Ye., "Calculation of the inertial characteristics of ships floating in ice," Dokl. XIV nauchn.-tekhn. konfer. korablestr. f-ta GPI (Papers of the XIVth Scientific and Engineering Conference of the Faculty of Naval Architecture of Gor'kiy Polytechnical Institute), Gor'kiy, 1967.

8. Sveshnikov, A. A., Prikladnyye metody teorii sluchaynykh funktsiy (Applied methods of the theory of random functions), Moscow, "Nauka", 1968.

9. Solodovnikov, V. V., Vvedeniye v statisticheskomu dinamiku sistem avtomaticheskogo upravleniya (Introduction to the Statistical dynamics of automatic control systems), Gostekhizdat, Moscow-Leningrad, 1952.

10. Kheysin, D. Ye., "Determination of contact forces in the impact of a ship's stem against the ice," in the collection: Problemy Arktiki i Antarktiki, No. 8, Leningrad, "Morskoy transport", 1961.

11. Kheysin, D. Ye., "General vibration of a ship's hull in motion in solid ice," Sudostroyeniye (Shipbuilding), 1970, No. 9.

12. Shimanskiy, Yu. A., "Conditional measurements of the ice qualities of a ship," Tr. Arkt. in-ta (Transactions of the Arctic Institute), volume 130, Leningrad, 1938.

13. Yakovlev, M. S., "Methodology of the determination of the ice navigating capability of river vessels," Tr. Gor'k. politekhn. in-ta (Transactions of Gor'kiy Polytechnical Institute), Volume XVII, No. 1, 1961.

RESISTANCE TO THE MOTION OF TRANSPORT VESSELS IN SOLID ICE

D. D. Maksutov

pages 27-34

At the present time, when special transport vessels for active ice navigation have appeared in the composition of the domestic maritime fleet, the necessity has arisen for the development of a method of at least approximate estimation of the ice navigating capability[1] of these ships in motion in solid ice fields. The ice navigating capability of ships is one of the most important elements of their ice qualities, and it depends upon many factors, primarily upon the shape of the hull lines, its strength, the capacity of the power plant, the features of the propulsion complex, and also the ice conditions of navigation.

Calculations of the ice navigating capability are necessary for the solution of certain problems originating both as the initial stage of the designing of ships and in the process of their operation. Ships intended for active ice navigation quite frequently must advance in solid ice independently, without the aid of icebreakers or force their way through individual ice fields and dikes of large broken ice with fragments of fields, and not infrequently even through fast ice of considerable thickness. For example, in Antarctica transport vessels sometimes break a channel with a length of dozens of miles in fast ice at an average thickness of the ice of 160--180 centimeters, which can be broken through only by impacts from an accelerated run. Such methods of the operation of transport vessels are noted in the approach to certain islands or to the coast, where polar stations or port points are located, to which cargos must be delivered.

---

1. By the term "ice navigating capability" we mean the safely possible speed which the ship develops in given ice conditions at full capacity of the power plant without damaging the hull.

Transport vessels for active ice navigation, capable of moving independently in solid ice, can provide for a winter navigation season in freezing non-Arctic seas without the assistance of icebreakers. Therefore, the provision of ice navigating capability of such vessels in solid ice is extraordinarily important. However, until recent times adequate attention was not devoted to problems of the study of the motion of transport vessels in solid ice fields.

In this article we have made an attempt to determine the total ice resistance to the motion of transport vessels in solid ice according to the formula obtained for icebreakers:

$$F_x = 0{,}004B\gamma_1 h_1 + 3{,}6\gamma_1 Bh^2 v + 0{,}25B^{1.5}\gamma_0 \frac{1}{v_0} + R_v. \qquad (1)$$

However, analysis of the results of calculations according to formula (1) and data from full-scale and model tests demonstrated that the calculation of the ice resistance to the motion of transport vessels according to this formula leads to considerable errors (sometimes more than 30%). It was necessary to find a dependence according to which we could calculate the ice resistance to the motion of transport vessels intended for active ice navigation with a different shape of the hull lines. For this the results of numerous full-scale and model tests of ships of the types of the diesel-electric icebreaking cargo vessels "Lena" and "Amguyema" were processed, and also tests of models of a hydrographic vessel for the Arctic.

We will divide the total ice resistance of a vessel into a number of components:

$$R_x = R_1 + R_2 + R_3 + R_v,$$

[$R_1 = R_1 = R_{ice}$] where R_1 is the resistance not depending upon the speed of the ship and representing the resistance of the ice to being broken by the bow of the hull; R_2 is the resistance to packing and overturning of ice floes and the resistance caused by the friction of the ice against the hull of the ship, which do not depend upon speed; R_3 is the resistance depending upon the speed of the ship and caused by the opening of the ice floes and the friction of the ice against the water, depending upon the speed; and R_v is the resistance of the water to the motion of the ship [$R_\theta = R_v = R_v$] is the resistance of the water to the motion of the ship.

To obtain analytical dependences of individual components, according to the theory of dimensionalities [2], we will present them in the form of power monomials.

Component R_1. In the motion of the ship in solid ice, the ice may be broken under the effect of both the vertical forces (bending) and the horizontal forces (compression). It is known that the potential energy in the breakage of ice by bending is considerably less than by breaking of it by compression, and therefore the shape of the lines of the bow end of the ship must be designed in such a manner that the basic breakage of the ice occurs as a result of bending.

We will represent the breaking of ice by the hull of a ship as the breaking of an ice plate lying on an elastic base. It is known that the force necessary for breaking such a plate is proportional to the time resistance of the material of the plate, σ_r, and the square of the thickness of the ice (h^2).

The resistance of the ice to breaking depends not only upon the physico-mechanical characteristics of the ice but also upon the principal dimensions of the ship and the shape of its lines. Investigations performed demonstrated that the most essential effect on the ice resistance is shown by the beam B of the ship. We will assume that the component R_1 is proportional to the beam of the hull to a power of 1 [1]. Consideration of the effect of the shape of the hull lines on the resistance of the ice to breaking can feasibly be performed by means of the conditional measurements proposed by Yu. A. Shimanskiy [4], and in particular by the conditional measurement η_1, which is the ratio of the total vertical force P_z to the total horizontal force P_x, acting on the bow of the ice waterline

$$\eta_1 = \frac{\Sigma P_z}{\Sigma P_x}.$$

At $P_z = 0$, i.e., with a total lack of vertical forces, which corresponds to a vertical side, no breaking of the ice occurs, since the resistance of the ice to breaking in this case is infinitely great ($\eta_1 = 0$). At $P_x = 0$, i.e., in the absence of horizontal forces (in practice this cannot occur), the resistance of the ice to breaking by bending is, as it were, equal to zero.

In order to consider the effect of the shape of the hull lines, we will introduce the co-multiplier $1/\eta_1$ into the expression for the resistance of the ice to breaking by the hull of a transport vessel. Then

$$R_1 = k_1' B \sigma_p h^2 \frac{1}{\eta_1}, \qquad (2)$$

where k'_1 is an empirical coefficient, considering the assumptions and conditions, which were made in the derivation of this expression.

Component R_2. We will use the dependence proposed by Yu. A. Shimanskiy [4], who considered this resistance to be proportional to the beam of the ship (B) and the square of the thickness of the ice (h^2). The effect of the shape of the hull lines on the magnitude of this component will be considered by means of the comultiplier $1/\eta_1$, since the packing and overturning of ice floes, just like the breaking of ice, occurs under the effect of vertical forces. Thus,

$$R_2 = k'_2 B h^2 \frac{1}{\eta_1}, \tag{3}$$

where k'_2 is an empirical coefficient.

The work of a transport vessel in motion in solid ice, just like the work of an icebreaker [1], is not merely expended in overcoming the forces of resistance to breaking, packing and overturning of the ice, but also in overcoming the forces of friction between the hull and the ice and the ice against the ice. We should distinguish the forces of "dry" friction and the forces of friction caused by the viscosity of the liquid. The magnitude of the forces of "dry" friction may be considered as proportional to the magnitude of the corresponding pressures which occur in the breaking of the ice, its packing and its overturning. Therefore, we may consider that the expressions obtained for the components of the resistance of the ice to breaking, packing, and overturning of ice floes consider the effect of the forces of dry friction which accompany these phenomena are proportional to the pressure and do not depend upon the speed of the ship. As for the forces of friction caused by the viscosity of the liquid, according to physical essence they represent the forces of friction of the ship against the water and the ice against the water. These forces must be considered in the derivation of expressions for the components of the total ice resistance depending upon speed.

Component R_3. The resistance caused by the opening of the broken ice depends basically upon its mass, the speed of the ship and the shape of the hull lines. We will consider the mass of ice to be proportional to the beam of the ship. Also assuming a linear dependence to this component of resistance upon the speed and the thickness of the ice, we find

$$R_3 = k'_3 B h v \frac{1}{\eta_1}, \tag{4}$$

where k'_3 is an empirical coefficient considering the conditional nature of the assumptions made above.

Component R_v. The resistance of the water to the motion of a ship is determined by a conventional method, accepted in the practice of model tests of ships in clear water.

Thus, the total resistance to the motion of a transport vessel in solid ice may be determined in the following manner:

$$R_л = k_1' B \sigma_р h^2 \frac{1}{\eta_1} + k_2' B h^2 \frac{1}{\eta_1} + k_3' B h \frac{1}{\eta_1} v + R_в. \quad (5)$$

In view of the complexity of the determination of the numerical values of coefficients k'_1 and k'_2, it is advisable to combine the components R_1 and R_2 and present them in the form of one power monomial:

$$R = kB\sigma_р h^2 \frac{1}{\eta_1}. \quad (6)$$

The coefficient k_1 considers all the assumptions which were made in the derivation of expression (6), and in particular the assumption of the applicability of the theory of the bending of a semi-infinite plate to the phenomenon of the breaking of an ice cover by a ship. Consequently, formula (5) will have the final form

$$R_л = k_1 B \sigma_р h^2 \frac{1}{\eta_1} + k_2 B h v \frac{1}{\eta_1} + R_в, \quad (7)$$

where R_1 is the total ice resistance, in tons; σ_r is the time resistance of the ice to bending, in tons per square meter; B is the beam of the ship, in meters; h is the thickness of the ice, in meters; v is the speed of the ship, in meters per day; R_v is the resistance of the water to the motion of the ship, in tons; η_1 is a conditional measurement[1]; k_1 and k_2 are coefficients determined by the means of model and full-scale experiments.

The dependence proposed, like any semi-empirical formula, has a certain error. It most accurately determines the ice resistance of ships having a hull shape close to ships of the type of the diesel-electric icebreaking cargo vessels "Lena" and "Amguyema".

Formula (7) may be used both for determination of the necessary

1. The methodology of the determination of this measurement is explained in reference [4].

thrust of the propellers at which the ship will be able to break through the solid ice of given thickness and strength with a definite speed, and for determination of the thickness of the ice which the ship can break through at a given thrust of the propellers with a given speed. Usually in the designing of new ships, the thickness of the ice which the ship must break through by continuous steaming with a definite speed is assigned, and therefore formula (7) is more convenient to use in the form previously proposed, i.e., to find the required thrust of the propellers.

The coefficient η_1 entirely satisfactorily considers the effect of the shape of the lines of the ship, because of which by means of formula (7) we may determine the ice resistance of transport vessels intended for ice navigation having a different hull shape. We should find this coefficient according to the table given in reference [1].

As we have already noted, the coefficients k_1 and k_2, entering into formula (7), may be determined according to data from model and full-scale experiments. Thus, as a result of the processing of materials from model and full-scale tests of ships of the type of the diesel-electric vessels "Lena" and "Amguyema" in solid ice of various thickness and strength, the numerical values of these coefficients were found: the coefficient $k_1 \approx 0.2$ and the coefficient $k_2 \approx 1.68$. Thus, formula (7) obtains the final form

$$R_x = 0{,}2\sigma_p B h^2 \frac{1}{\gamma_{ii}} + 1{,}68 B h \frac{v}{\gamma_{ii}} + R_w. \qquad (8)$$

In the future, as the result of full-scale tests of transport vessels intended for active ice navigation with lines differing from the lines of ships of the same type as the diesel-electric vessels "Lena" or "Amguyema" in solid ice are accumulated, we may be able to correct the values of the coefficient k_1 and k_2 and the exponents of the speed v and the thickness h of the ice.

According to formula (8), calculations of the total ice resistance were performed for ice of various thickness (Figures 1 and 2) at σ_r = 80 tons per square meter, for ships of two types, of category ULA, with a different shape of the hull lines (the coefficients η_1 differ considerably) (Figure 1).

The dependences of the speed of the ships upon the thickness of the solid ice obtained are plotted on curves of v = f(h) for comparison with data from full-scale tests (see Figure 2). As is apparent from the drawing, calculations according to the proposed formula provide an adequate degree of accuracy. The results of the calculation of the ice resistance according to

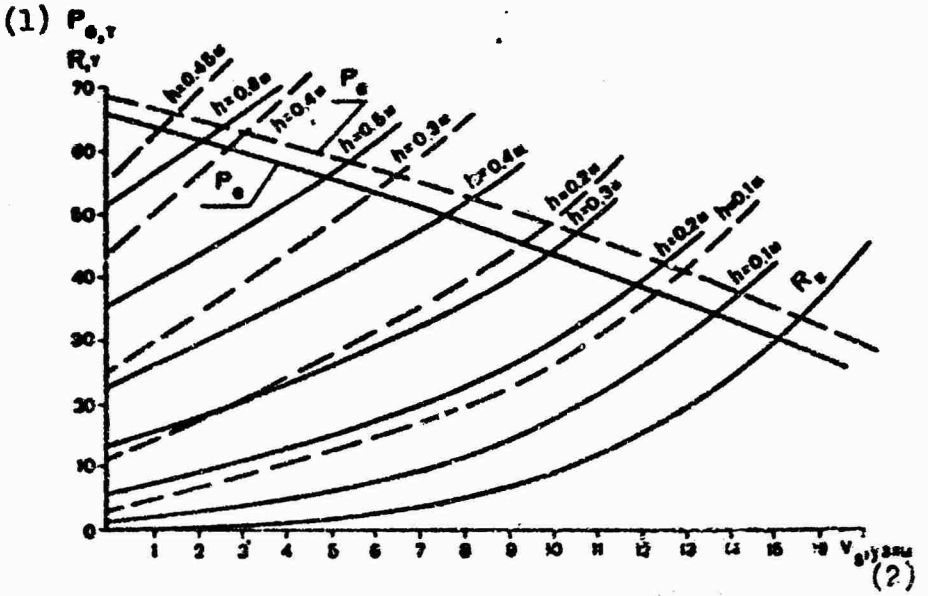

Figure 1. Dependence of the total ice resistance upon the speed at various thicknesses of the ice for ships of category ULA (according to calculation data): ---N_p = 7,000 horsepower; —N_p = 6,300 horsepower; (with improved hull lines). 1) P_e, tons; R, tons; 2) v_s, knots; M = meters.

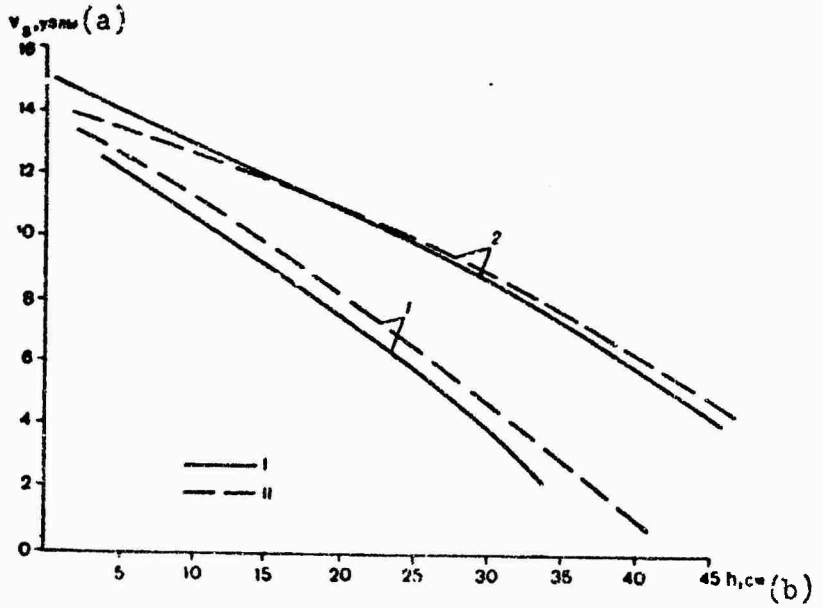

Figure 2. Dependence of the speed of ships of the category ULA upon the thickness of the solid ice in motion in young level ice: 1) N_p = 7,000 horsepower; 2) N_p = 6,300 horsepower; I) according to data from full-scale tests; II) according to calculation data. a) v_s, knots; b) h, centimeters.

formula (8) were analogously compared with data from a model experiment of a hydrographic vessel, performed in solid ice in the test basin of the AANII. The hull shape of this ship differs from the shape of the lines of ships of the same type as the diesel-electric vessels "Lena" and "Amguyema" but, however, the results of the tests in the basin and calculations according to the formula practically coincide. Consequently, formula (8) may be used in the process of designing of transport vessels for active ice navigation for an estimation of their ice navigating capability in solid ice.

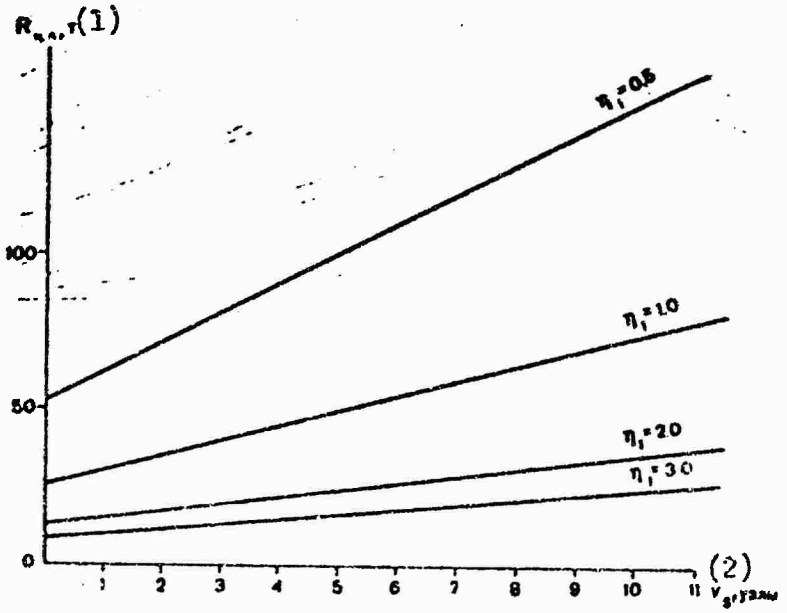

Figure 3. Dependence of the net ice resistance ($R_{ch.l}$) upon the ice breaking factor (η_1) at various speeds for ice breaking transport vessels. [$R_{ч.л}$ = $=R_{ch.l}=R_{net\ ice\ resistance}$] 1) $R_{ch.l}$, tons; 2) v_s, knots.

From an analysis of Figure 3 it follows that the resistance to the motion of a ship in solid ice noticeably increases with a decrease in the coefficient η_1 (η_1 is a function of the angles α° and β°, characterizing the shape of the bow end of the ship). The low value of the coefficient ($\eta_1 < 1.0$) corresponds to transport vessels with a highly developed cylindrical insert, a small angle of inclination of the stem to the vertical, and U-shaped frames in the bow end. In this case, resistance increases especially sharply with an increase in the speed of the ship. This conclusion makes it possible for designers to select the optimum angles of inclination of the frames, β°, and the waterlines α°, in the development of the drawing, in order to provide the minimum value of the magnitude of ice resistance.

BIBLIOGRAPHY

1. Kashtelyan, V. I., Poznyak, I. I., and Ryvlin, A. Ya., Soprotivleniya l'da dvizheniyu sudna (Resistance of the ice to the motion of a ship), Leningrad, "Sudostroyeniye", 1968.

2. Nogid, L. M., Teoriya podobiya i razmernostey (Theory of similarity and Dimensionalities), Leningrad, Sudpromgiz, 1959.

3. Popov, Yu. N., and Ryvlin, A. Ya., "On the problem of the shape of the lines of the bow ends of icebreaking transport vessels," in the collection: Problemy Arktiki i Antarktiki (Problems of the Arctic and Antarctic), No. 26, Leningrad, Gidrometeoizdat, 1967.

4. Shimanskiy, Yu. A., "Conventional measurement of the ice qualities of a ship," Tr. ANII (Transactions of the Arctic Scientific Research Institute), Volume 130, Leningrad, izd-vo Glavsevmorputi, 1938.

USE OF PROBABILITY METHODS IN ESTIMATING THE MANEUVERING QUALITIES OF SHIPS IN ICE

D. Ye. Kheysin

pages 35-49

The maneuvering qualities of ships intended for ice navigation and icebreakers are characterized by their capability of moving and making evolutions in various ice conditions. In this case, the maneuvering characteristics of ships are determined mainly by the process of the reaction of the ship's hull with the ice. The basic feature of this process is its random nature, associated with the hetergeneity of the natural ice cover and the random nature of the force contact of the side with the ice. Here the external force effect on the ship appear as random quantities, the deviation of which on the average values may be quite large.

The random nature of the external effects up to this time was only implicitly considered, in the selection of calculation schemes, the determination of experimental dependences, calculation of empirical coefficients, etc. Calculations of ice navigating capability and maneuvering characteristics of ships are performed according to ordinary schemes for calculations in mechanics, without consideration of the probability nature of the external loads.

In practice, in such an approach only the average values are determined: the average speed, average thickness of the ice being broken, etc. For a finer analysis, the idealized deterministic calculation schemes must obtain a statistical interpretation and must be complemented by probability ratios. This has special value for problems of ice navigating capability and maneuverability, the solutions of which depend not only upon the average values, but also upon the mean square deviations of the external effects, i.e., their dispersions.

In this work a model of the reaction of a ship's hull with the ice is considered, making it possible to apply probability methods of analysis.

As an example, two problems that are of importance in practice are investigated, in the estimation of the maneuvering qualities of ships in ice: the first is devoted to an investigation of the stability of motion of the ship along a straight course in solid ice, and the second to the determination of the scattering of the coasting runs of the ship in motion from an acceleration run in solid ice.

Model of the Reaction of a Ship's Hull with the Ice

Full-scale strain-gauge tests of ships intended for ice navigation and ice breakers have demonstrated that the reaction of the ship's hull with the ice should be considered as a discrete random process. In this case the impact pulses a_j acting in the zone of contact with the ice are imposed at arbitrary moments of time t_j upon the sections of the side with random coordinates $x = x_j$ (Figure 1). In a general case the quantities k_j, t_j, and x_j are statistically independent.

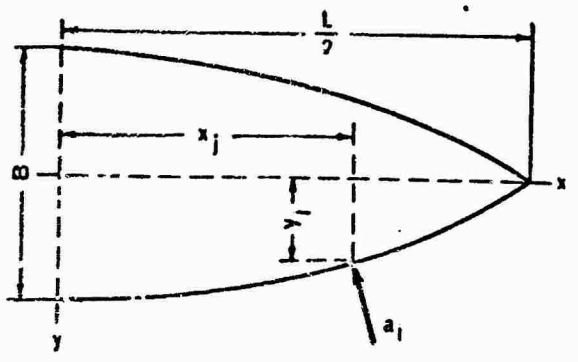

Figure 1. Diagram of the reaction of a ship's hull with the ice.

Ignoring the forces of friction, the impact pulse may be considered as directed along the normal to the side of the ship at the point of impact. Let $l(x)$, $m(x)$ and $n(x)$ be the guiding cosines of this normal. Then we will write the vector of the impact pulse in the following manner:

$$\begin{pmatrix} a_{jx} \\ a_{jy} \\ a_{jz} \end{pmatrix} = a_j \begin{pmatrix} l(x_j) \\ m(x_j) \\ n(x_j) \end{pmatrix}.$$

Here the amplitude of the impact pulse a_j is a random quantity, characterized by the probability density $t_a(a)$. We will designate the set of possible values of the amplitude of the impact pulse as $\{a_{jk}\}$. We will

determine the mathematical expectation for various components of the impact pulse by performing the averaging according to the k realization. For the x-component of the pulse we have

$$E_k[{}^k a_{jx}] = E_k[{}^k a_j] E[l(x_j)] = \bar{a} \int_{\Omega} l(x) p(x) dx, \tag{1}$$

where $\bar{a}$ is the average value of the amplitude of the impact pulse; p(x) is the probability density of an impact falling at a point of the side with the coordinate x; and Ω is the integration region.

The integral is taken every where along both sides of the ship, where $p(x) \neq 0$ and $l(x) \neq 0$. It is apparent that the average value of the y-component of the impact pulse is equal to zero as a consequence of the statistical equivalency and symmetry of both sides, and we find the z-component according to the expression analogous to formula (1).

We determine the second-order moments in the following manner:

$$E_k[{}^k a_{lx} {}^k a_{jx}] = \begin{cases} (\bar{a})^2 \left[\int_{\Omega} l(x) p(x) dx\right]^2 \text{ at } l \neq j, \\ \bar{a}^2 \int_{\Omega} l^2(x) p(x) dx \text{ at } l = j. \end{cases} \tag{2}$$

In motion in broken ice, when the breaking of the ice by denting does not occur, the magnitude of the impact pulse a_j may be considered as depending upon the random coordinate x_j of the point of its application. In accordance with references [7] and [8]

$$a_j = Mv \frac{l(x_j)}{C'(x_j)},$$

where v is the speed of the ship; m is its mass; $c'(x_j)$ is the given mass coefficient of the ship in the impact against the ice.

In this case formulas (1) and (2) must be changed. We will determine the mathematical expectation of the x-component of the impact pulse and the dispersion

$$\bar{a}_x = Mv \int_{\Omega} \frac{l^2(x)}{C'(x)} p(x) dx, \tag{3}$$

$$\sigma_a^2 = M^2 v^2 \int_{\Omega} \frac{l^4(x)}{C'(x)^2} p(x) dx - (\bar{a}_x)^2.$$

In a steady-state regime of motion, the random sequence of pulses a_j is a steady-state random process, at which the pulses act at independent moments of time. It was experimentally demonstrated that this process is a Poisson process, with a constant average distribution density of the impact pulses in time, λ.

The impact pulses, as a rule, have a bell-shaped form. In the first approximation the shape and duration τ_0 of each pulse will be considered as constant, excepting only the amplitude as a random parameter. By considering the short duration of the pulses we may, for example, describe them by means of the delta-function $\delta(t-t_j)$, equal to zero every where, except for $t = t_j$.

With a consideration of the local nature of the application of the impact pulse, we will represent a typical realization of such a random process in the following manner:

$$^{k}f(t, x) = \sum_{j=1}^{N} {}^{k}a_j \delta(t - t_i)\,\delta(x - x_j),$$

where N is the number of pulses falling in the interval of time under consideration.

Such a model of the reaction of a ship's hull with the ice was applied for the first time in the investigation of the general vibration during motion in solid ice [11]. Examples of the use of an analogous model in the solution of various problems with respect to the estimation of the maneuvering qualities of ships in ice are discussed below.

The impact pulses a_j, acting on the ship's hull in motion in ice, cause movements corresponding to six degrees of freedom of a solid body. The movements in the direction of the axis y and the rotations relative to the axis z determine the side drift and yawing of the ship; the movements in the direction of the axis z determine the heaving; rotations relative to the axes x and y determine, respectively, the rolling and pitching; the x-components of the impact pulses determine the magnitude of the ice resistance.

If the righting forces or moments enter into the equations of motion, the corresponding movements of the ship will be of the nature of force random oscillations. The right-hand parts of these equations in this case should be represented in the form of a random sequence of impact pulses a_j.

In motion in the ice, the amplitudes of the movements of the ship are small, which makes it possible to use a linear approximation. Therefore,

in the future we may consider each form of movement individually.

Estimation of the Stability of Motion of a Ship along a Straight Course in Solid Ice

The yawing of a ship and side drift from the course in motion in the ice are caused by the horizontal components a_{ix} and a_{iy} of the impact pulses acting on the ship's hull. We will investigate the plane motion of a ship along a straight course in the direction of the axis x. The rotation of the ship as a solid body relative to the axis z in this case is determined by the differential equation [10]:

$$(J_z+\lambda_{66})\frac{d\dot{\psi}}{dt}+\lambda_{26}\frac{du_2}{dt}+\lambda_{26}u_1\dot{\psi}=-(\lambda_{22}-\lambda_{11})u_1u_2+M_z. \qquad (4)$$

where $\dot{\psi}$ is the angular velocity of rotation relative to the axis z; u_1, u_2 are the projections of the linear velocity of the ship onto the axes x and y; J_z is the moment of inertia of the mass of the ship relative to the axis z; M_z is the moment of external forces; λ_{11}, λ_{22}, λ_{26}, λ_{66} are the bound masses.

In a steady-state regime of motion and comparatively small amount of yawing, the lateral drift of the ship is small, and we may consider the speed of its straight-line motion is constant, i.e., $u_1 = v = \text{const}$ and $u_2 = 0$. Then instead of expression (4) we obtain a linear differential equation for the yawing caused by the random sequence of impacts against the ice,

$$(J_z+\lambda_{66})\frac{d\dot{\psi}}{dt}+\lambda_{26}v\dot{\psi}=M_z. \qquad (5)$$

The bound masses λ_{26} and λ_{66} are usually determined in approximation, representing the lines of the ship's hull by a three-axis ellipsoid of the same dimensions as the ship [9, 10]. For the bound moment of inertia relative to the axis z we have

$$J_z+\lambda_{66}=J_z(1+n),$$

where the coefficient n is found according to the curves in reference [10], as a function of the ratios (L/B_1) and $(2T/B)$ (T is the draft).

The static moment of the transverse bound mass relative to the axis z may be calculated, in approximation, according to the formula

$$\lambda_{26}=\int_L \lambda_{22}(x)\,x\,dx,$$

where the value of $\lambda_{22}(x)$ is determined according to the curves in reference [4], as a function of the ratio (2T/B) and the coefficient β of fineness of the frame.

The moment a_j from a single pulse, applied at the point $x = x_j$, $y = y_j$ (see Figure 1) is written in the following manner:

$$M_{zj} = a_j [l(x_j) y_j - m(x_j) x_j]. \tag{6}$$

We will consider the steady-state regime of motion of the ship in a quite long interval of time (-T, T). Since the reaction of the ship's hull with the ice is a Poisson process, then in the interval of time 2T, $N \approx 2\lambda T$ pulses act on the ship. The differential equation (5) then takes the form

$$J_z(1+n)\frac{d\dot{\psi}}{dt} + \lambda_{26} v \dot{\psi} = \sum_{j=1}^{N} a_j(t)(l_j y_j - m_j x_j). \tag{7}$$

From the statistical independence of impact and the symmetry of both sides of the ship it follows that the mathematical expectation of the right-hand part of equation (7) is equal to zero ($\overline{M}_z = 0$). Assuming that the shape and duration of each pulse a(t) is constant, we will find the spectrum of the power of such a decentered process [5]:

$$S(\omega) = \frac{\sigma_M^2 \tau_0^2}{\pi \tau_a} |g(\omega\tau_0)|^2, \tag{8}$$

where σ^2_m is the dispersion of the amplitude of the moment M_z [$\sigma_M = \sigma_m = \sigma_{moment}$]; $\tau_a \approx \lambda^{-1}$ is the average duration of an interval of time between pulses; $g(\omega\tau_0)$ is a dimensionless Fourier spectrum of a single pulse of a single amplitude.

By approximating the real form of the pulse by a rectangle, we obtain

$$g(\omega\tau_0) = \frac{\sin\frac{\omega\tau_0}{2}}{\frac{\omega\tau_0}{2}}. \tag{9}$$

By introducing the probability density of an impact falling at a point of the side with the coordinate x, we determine the dispersion

$$\sigma_M^2 = \bar{a}^2 \int_{\Omega} (ly - mx)^2 p(x)\, dx. \tag{10}$$

In equation (10) the integral is taken only along one of the sides.

Thus, the problem is reduced to the analysis of the linear system (5), to the input of which a discrete signal is fed, having a power spectrum (8). According to the well-known theorem concerning the ratio between input and output spectra [1], we find

$$S_\psi(\omega) = |Y(i\omega)|^2 S(\omega).$$

Here $Y_{i\omega}$ is the frequency characteristic of homogeneous equation (5)

$$Y(i\omega) = \frac{1}{\beta_{26} - i\omega}, \text{ где } \beta_{26} = \frac{\lambda_{26}\rho}{J_z(1+n)}.$$

We finally determine the spectrum S_ψ

$$S_\psi = \frac{\lambda\sigma_M^2\tau_0^2 |g\,i\omega\tau_0|^2}{\pi J_z^2(1+n)^2(\omega^2+\beta_{26}^2)}. \tag{11}$$

We may obtain the dispersion of the angular velocities of the random deviations from a straight course if we integrate the spectrum of the output process (11) according to the entire range of frequencies. Assuming that the pulses are rectangular (square), we find

$$\sigma_\psi^2 = \frac{\lambda\sigma_M^2}{v^2\lambda_{23}^2}\left[\tau_0 - \frac{1}{\beta_{26}}\left(1 - e^{-\tau_0\beta_{26}}\right)\right].$$

usually $\tau_0\beta_{26} \ll 1$, from whence

$$\sigma_\psi^2 = \frac{\lambda\sigma_M^2\tau_0^2}{2v\lambda_{26}J_z(1+n)}. \tag{12}$$

As is apparent from formula (12), the dispersion of the angular velocities essentially depends upon the shape of the ship's hull lines and the parameters of the impact against the ice: their durations, amplitudes, the probability of falling at a given point of the side, etc. It was proven experimentally that a random process describing deviations from a straight course is Gaussian. Therefore, the assignment of the dispersion entirely determines all its parameters.

One of the important characteristics of stability of motion along a straight course is the average number of yawing motions per unit of time.

This quantity may be determined according to the general formula of the mathematical expectation of the number of nulls of a normal process

$$N_0 = \frac{1}{\pi}\left[\frac{\int_0^\infty \omega^2 S_\psi(\omega)\,d\omega}{\sigma_\psi^2}\right]^{1/2}.$$

Having substituted expressions (11) and (12) into this formula, after integration we obtain

$$N_0 = \frac{1}{\pi}\sqrt{\frac{2\lambda_{20}v}{J_z(1+n)\tau_0}}. \qquad (13)$$

For the possibility of a comparison of the characteristics of various ships, we will reduce equation (13) to a dimensionless form, having multiplied it by the fraction (L/v). Then we will obtain the dimensionless criterion of stability

$$K_N = \frac{N_0 L}{v} = \frac{L}{\pi}\sqrt{\frac{2\lambda_{20}}{J_z(1+n)\tau_0 v}}. \qquad (14)$$

It is clear that the large values of the quantity K_n corresponds to less stability on course. The collision time τ_0 is quite stable and depends only weakly upon the ice conditions. Therefore, stability on course in ice in motion with an adequate speed differs but little from stability in clear water. At low speeds the motion will be unstable.

Estimation of the Scattering of Coasting Runs of Ships with Respect to Inertia in Randomly Heterogeneous Ice

The length of a coasting run is an important tactical characteristic, determining the maneuvering qualities of ships to a considerable degree, and also the safety of navigation in ice. Calculation of the length of a coasting run has special significance in analysis of the motion of ships in a convoy, for determination of rational speeds and selection of a safe distance when ice-breakers are freeing ships from the ice, etc. In this case, coasting runs by inertia (thrust of propellers $R_t = 0$) and coasting runs in reversing, when the ship is actively being braked by the propellers ($R_t = R_{z.kh}$) are of the greatest practical interest [$R_T = R_t = R_{thrust}$; $R_{3.X} = R_{z.kh} = R_{engines\ backing}$].

For an idealized case of the motion of a ship in regular homogeneous ice (solid and broken) the calculation of the coasting run is performed by means of numerical integration of the differential equation of motion of the ship in the ice [6]

$$M\frac{dv}{dt} + R(v) = R_t(v, n), \tag{15}$$

or, having excluded differentiation with respect to time,

$$Mv\frac{dv}{dx} + R(v) = R_t(v, n). \tag{16}$$

In these expressions M is the mass of the ship, with consideration of the bound mass of water; R(v) is the total resistanee to the motion of the ship, composed of purely ice resistance and the resistance of the water; $R_t(v, n)$ is the total thrust of the propellers; and n is the number of revolutions of the screw propeller.

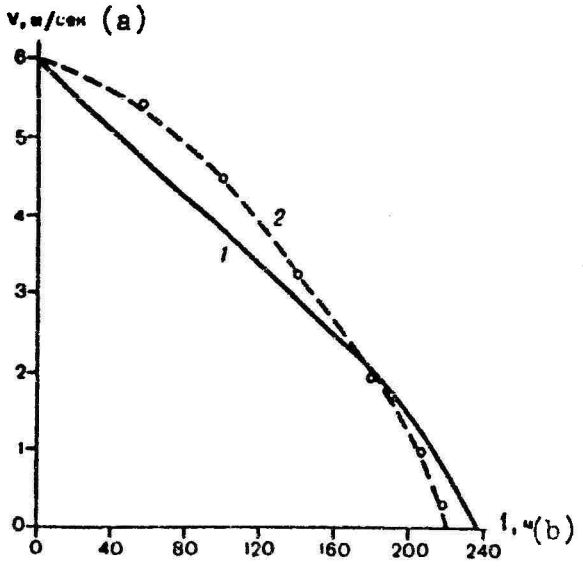

Figure 2. Dependence of the speed of the ship during a coasting run upon the length of the track passed over: 1) calculated curve; 2) experimental curve. a) v, meters per second; b) l, meters.

Integration of differential equations (15) and (16) turned out to be possible, since the empirical dependences for the forces of resistance R(v) were obtained [3].

In a general case

$$R(v) = R_{пр} + \alpha v + \beta v^2,$$

where $R_{пр}$ is the so-called direct ice resistance, not depending upon the speed [$R_{пр} = R_{pr} = R_{direct}$]; α and β are the empirical resistance factors.

The quantities R_{pr}, α and β depend upon the hull shape and the principal dimensions of the ship, and also upon the strength and thickness of the ice in motion in solid ice, or upon the length, thickness, and solidity of ice floes in motion in broken ice.

The results of calculations according to the methodology in [6] agree satisfactorily with data from full-scale tests (Figure 2).

Other things being equal, the length of a coasting run in solid ice depends upon the initial speed v_0 of the ship and the thickness h of the ice (Figure 3). As is apparent from Figure 3, even in level ice there is a considerable scattering of the magnitude of the coasting runs.

In heterogeneous ice the scattering of the coasting runs is very great (Figure 4). The abscissa in Figure 4 represents the ratio of the length $\underline{l}$ of the coasting run to the length L of the ship, and the ordinate of the ratio of the number of coasting runs n, corresponding to a given interval ($\underline{l}$/L) to their common number N.

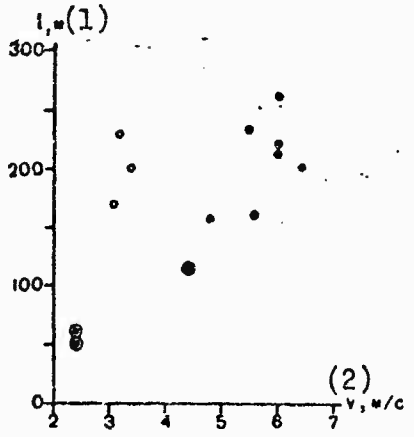

Figure 3. Coasting runs of a port ice breaker with respect to inertia in solid ice with a thickness of 25--30 centimeters (●); 17--29 centimeters (o); and 37--38 centimeters (⊙). 1) $\underline{l}$, meters; 2) v, m/s.

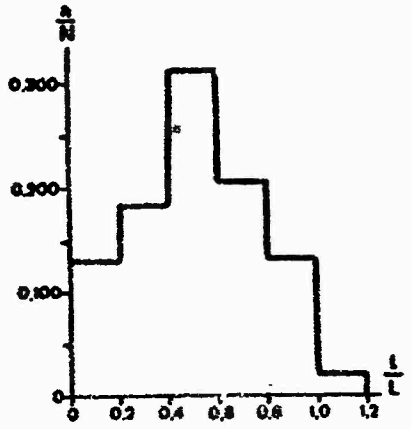

Figure 4. Histogram of coasting runs of a powerful ice breaker, by inertia, in operation in short runs in heavy two-year ice.

The scattering of the magnitude of coasting runs of the ship in full-scale conditions, obviously, is associated with the random nature of the process of reaction of the hull with the ice. The ice resistance to the motion of the ship varies in a random nature relative to a certain average value, which is caused both by the heterogeneity of the ice and by the instability of the power contact of the ship with the ice. The average value of the force of the ice resistance corresponds to the average ice conditions and the smoothed process of the reaction of the ship with the ice. Therefore, the coasting runs determined according to the equations of motion (15) with determined components should be considered as the average throughout the set of their possible values.

In ice that is randomly heterogeneous with respect to strength and thickness, the coefficients α, β and the direct ice resistance R_{pr} will be random functions of the track, i.e., the coordinate x. The speed v of the ship and the length $\underline{l}$ of the coasting run being sought also will be random functions.

We will consider a coasting run of the ship by inertia ($R_t = 0$) in motion with low speeds, when we may ignore the quadratic components of the resistance

$$Mv\frac{dv}{dx} + av = -R_{np}(x). \tag{17}$$

The right-hand part of equation (17) is a random function of the track. We will consider the coefficient α to be constant, since at the present time there are no data of any kind concerning its statistics.

If we assume the average value $\overline{R}_{pr}$ of the force of direct ice resistance in the right-hand part of equation (17), then, by separating the variables, we find the following integral:

$$l_0 = \int_0^{v_0} \frac{M v\, dv}{\overline{R}_{np} + av}.$$

After integration

$$l_0 = \frac{M}{a}\left[v_0 - \frac{\overline{R}_{np}}{a} \ln\left(1 + \frac{av_0}{\overline{R}_{np}}\right)\right]. \tag{18}$$

We will consider that $av_0 \ll R_{pr}$, which occurs in motion at low speeds in solid and continuous broken ice. Ignoring all the terms beginning with the third in the expansion of the logarithm into a series, we will obtain

$$l_0 = \frac{Mv_0^2}{2\overline{R}_{np}}. \tag{19}$$

This same expression may be obtained for a coasting run if we ignore at once all the velocity components of the resistance. Then

$$Mv\frac{dv}{dx} = -R_{np}(x).$$

By integrating this equation from the initial position ($x = 0$; $v = v_0$) to a stop ($x = l$; $p = 0$), we find

$$\frac{Mv_0^2}{2} = \int_0^l R_{np}(x)\, dx. \tag{20}$$

The initial speed v_0 is considered to be assigned. Equality (20), expressing the law of conservation of energy, may be considered as a functional equation with a random argument, the root of which has a certain distribution. Its properties are such that the integral of the random function $R_{pr}(x)$, taken in the interval of random length $\underline{l}$, remains unchanged.

The average value of a length of a coasting run, $\overline{l} = l_0$, is found according to formula (19). For estimation of the scattering of coasting runs

it is necessary to determine their dispersion, considering the statistical characteristics of the force of ice resistance to be assigned. By working from the discrete nature of the process of the reaction of the ship's hull with the ice, we will assume that the ice resistance changes suddenly, remaining constant in a certain small interval of track $\Delta x_j = x_{j+1}$, i.e.,

$$^{k}R_{np}(x) = {}^{k}R_{npj} \text{ at } x_j \leqslant x < x_{j+1}.$$

We will assume the ice cover to be stastically homogeneous and isotropic. Then it is natural also to consider the process $^{k}R_{pr}(x)$ to be statistically homogeneous and ergodic. In this case averaging according to the k-realizations does not depend upon the subscript j. In other words, the average value is

$$E_k\{{}^{k}R_{np}(x_j)\} = \overline{R}_{np}$$

for any interval out of Δx_j.

As a consequence of the independence of the random quantities R_{prj} the second-order moments are calculated in the following manner:

$$E_k\{{}^{k}R_{npi}, {}^{k}R_{npj}\} = \begin{cases} (\overline{R}_{np})^2 \text{ at } i \neq j, \\ \overline{R}^2_{np} \text{ at } i = j. \end{cases}$$

According to the determination of dispersion,

$$\sigma^2_R = \overline{R}^2_{np} - (\overline{R}_{np})^2.$$

The average value $\overline{R}_{pr}$ and the dispersion σ^2_R of direct ice resistance are the input parameters of the problem and must be assigned by some method or other.

In motion in statistically homogeneous ice the probability of a change of the force R_{pr} in the interval $\bar{l}$, i.e., the probability of some number or other of discontinuities falling in the interval $\bar{l}$ depends only on the length of this interval. In other words, a random distribution of discontinuities has an identical average density λ per unit of length. Aside from this, the discon-

tinuities are distributed along the axis x independently of each other and in practice do not coincide. In this case, the quantity of discontinuities in the interval $\underline{l}$ is distributed according to a Poisson law with the parameter λl [2]. The probability of ν discontinuities falling in a segment $\underline{l}$ is determined according to the formula

$$P_\nu = \frac{(\lambda l)^\nu}{\nu!} e^{-\lambda l}.$$

The length of the section Δx between adjacent discontinuities are distributed according to an exponential law, with a probability density [2]

$$P(\Delta x) = \lambda e^{-\lambda \Delta x}.$$

We find the mathematical expectation and the dispersion Δx

$$E(\Delta x_j) = \lambda^{-1}; \quad D(\Delta x_j) = \lambda^{-2}.$$

We will further designate

$$\Delta R = R_{np}(x) - \overline{R}_{np}; \quad \Delta l = l - l_0. \tag{21}$$

It is apparent that $\overline{\Delta R} = 0$ and $D(\Delta R) = \sigma^2 R$. The average value of the deviation Δl is equal to zero and the dispersion Δl^2 is the quantity being sought.

By using formula (19) and considering the symbols (21), we convert equation (20):

$$-\overline{R}_{np}\Delta l = \int_0^{l_0+\Delta l} \Delta R dx. \tag{22}$$

We find the dispersion of both parts of equality (22), considering the integral in the right-hand part as a finite sum of a random number of random quantities

$$(\overline{R}_{np})^2 D(\Delta l) = D\left\{\sum_{j=1}^{\nu} \Delta R_j \Delta x_j\right\}.$$

Here for a quite large interval l the number $\nu \approx \lambda l$.

For the dispersion of the sum of the random number ν of the random quantities ΔR_j Δx_j, not depending upon the number ν, we obtain [5]:

$$D\left\{\sum_{j=1}^{\nu} \Delta R_j \Delta x_j\right\} = D\{\Delta R\}\, D\{\Delta x\}\, E\{\nu\} + D\{\nu\}\,(E\{\Delta R_j \Delta x_j\})^2.$$

The second item in this expression is equal to zero, since the quantities ΔR_j and Δx_j are statistically independent, and $\overline{\Delta R} = 0$. In the first item, obviously,

$$E\{\nu\} = E\{\lambda(l_0 + \Delta l)\} = \lambda l_0.$$

Then we find the mean square deviation of the average coasting run

$$\sigma_{\Delta l}^2 = \overline{\Delta l^2} = \frac{l_0}{\lambda} \frac{\sigma_R^2}{(\overline{R}_{np})^2}. \tag{23}$$

The amplitudes of external ice conditions determining the direct ice resistance frequently may be considered as distributed according to a Rayleigh law. In this case, the mathematical expectation and dispersion are associated by the following dependence:

$$\overline{R}_{np} = \sigma_R \sqrt{\frac{\pi}{2}},$$

which is confirmed to some degree in statistical analysis of data from strain-gauge tests.

Then

$$\sigma_{\Delta l} = \sqrt{\frac{2}{\pi} \frac{l_0}{\lambda}}. \tag{24}$$

The form of the law of distribution of the length l of a coasting run may be estimated, by considering that

$$l = \sum_{j=1}^{\nu} \Delta x_j.$$

Since the increments Δx_j are independent, then with an increase in the number of intervals j the law of distribution of $\underline{l}$, on the basis of the central limiting theorem, tends to a normal law. In this case, the probability of the deviation of the length of a coasting run from the average value by the magnitude Δl to both sides is determined according to the formula

$$P(|l - l_0| < \Delta l) = 2\Phi^*\left(\frac{\Delta l}{\sigma_{\Delta l}}\right) - 1,$$

where the function Φ^* is a normal distribution functio . [2]. The probability of an excess of the given level Δl amounts to

$$P(|l - l_0|) \geqslant \Delta l) = 2\left[1 - \Phi^*\left(\frac{\Delta l}{\sigma_{\Delta l}}\right)\right].$$

For a normally distributed random quantity, all the scattering is, in practice, set in the section

$$l_0 \pm 3\sigma_{\Delta l} = l_0 \pm 3\sqrt{\frac{2}{\pi}\frac{l_0}{\lambda}}. \qquad (25)$$

In this case

$$P(|l - l_0| \geqslant 3\sigma_{\Delta l}) = 0{,}0028,$$

i. e., the probability of an excess of the level $\Delta l = 3\sigma_{\Delta}$ is small (~0. 3%). The probability of an excess of the level $\Delta l = 2\sigma_{\Delta l}$ is also not great (4. 56%).

By standardizing the random deviation $\varepsilon = (\Delta l / l_0)$, we obtain

$$\sigma_\varepsilon = \sqrt{\frac{2}{\pi \lambda l_0}}. \qquad (26)$$

In comparing formulas (24) and (26), we note that the absolute magnitude of the scattering of coasting runs increases with an increase in the average length l_0 of a coasting run, and the relative magnitude decreases. The absolute and relative scattering of coasting runs will decrease with an increase in the number λ. We may estimate this quantity in motion in solid ice, by working from the dimensions of the first series of sectors, broken by the bow end of the ship. The length of these sectors depends upon the thickness of the ice, and the shape of the stem, and it usually amounts to 3--5 meters. From

thence, $\lambda \sim 0.2 - 0.3$ meters^{-1}. In broken ice the average density λ is inversely proportional to the average dimension of an ice floe, r. In fine broken ice $r \sim 10$ meters, so that $\lambda \sim 0.1$ meters^{-1}. Thus, the scattering of coasting runs in broken ice is greater than in solid ice.

We will estimate the magnitude of the scattering of coasting runs for a case $l_0 = 200$ meters^{-1}, $\lambda = 0.3$. According to formula (25), we obtain

$$l_0 \pm 3\sigma_{\Delta l} = (200 \pm 60) \text{ meters},$$

i.e., the coasting runs are distributed in quite wide limits: from 140 to 260 meters. Such a large scattering of coasting runs is also noted in full-scale conditions, even in motion in level young ice (see Figure 3).

If we consider a coasting run with braking, then the thrust $R_{z.kh}$ of the propellers, which is constant during the coasting run, must enter into the right-hand part of equation (17):

$$Mv\frac{dv}{dx} + av = -R_{з.х} - R_{пр}(x).$$

The course of the solution of the problem in this case does not change in principle, but we should introduce correction factors into the final formulas. For example, the average coasting run l_0 of a ship will be equal to

$$l_0 = \frac{Mv_0^2}{(2\bar{R}_{пр} + R_{з.х})},$$

and the mean square deviation from the average coasting run

$$\sigma_{\Delta l}^2 = \frac{l_0}{\lambda}\frac{2}{\pi}\frac{(\bar{R}_{пр})^2}{(\bar{R}_{пр} + R_{з.х})^2},$$

i.e., the presence of thrust in backing down essentially decreases both the magnitude of the average coasting run and its scattering.

In the practical use of the dependences obtained we should remember that they are valid only for quite large values of the length l_0 of a coasting

run (either with a small thickness of the ice, or at large initial speeds of the coasting run). In the latter case, the velocity components of resistance will be commensurable with the direct ice resistance.

For an example, we will consider the motion of a port icebreaker with a displacement above 2700 tons in solid ice with a thickness of 20 centimeters. In motion with a speed v_0 = 5 knots, its direct ice resistance R_{pr} will be equal to 4.45 tons, and the velocity components R_v, including the resistance of the water, 12 tons. The average coasting run l_0 of the icebreaker, determined according to formula (19), amounts to 220 meters, and the coasting run l_γ, determined by means of graphic integration of equation (15), 90 meters $[l_\beta = l_v = l_{coasting}]$. In practice, by assuming the average thickness of the ice, we may determine the magnitude of the average coasting run with a consideration of all the components of resistance, and then according to formula (24), its mean square deviation, assuming that λ = 0.2--0.3.

Thus, finally we may make the following conclusions:

1. In the proposed probability model the process of the reaction of a ship's hull with the ice is considered as a discrete random sequence of statistically independent impact pulses, acting in the zone of contact with the ice.

2. The use of this model in the analysis in the stability of motion of a ship along a straight course in ice makes it possible to estimate the dispersion of deviations from the course and to determine the average number of yawings per unit of time.

3. The application of the probability approach for estimation of the scattering of coasting runs of a ship in randomly heterogeneous ice gives the opportunity of determining the probability of the deviation of the length of a coasting run upon its average value.

BIBLIOGRAPHY

1. Bendat, D. T., Osnovy teorii sluchaynykh shumov i yeye primeneniye (Bases of the theory of random noises and its application), Moscow, "Nauka", 1965.

2. Venttsel', Ye. S., Teoriya veroyatnostey, Moscow, "Nauka", 1969.

3. Kakhtelyan, V. I., Poznyak, I. I., and Ryvlin, A. Ya., Soprotivleniye l'da dvizheniyu sudov (Resistance of ice to the motion of ships), Leningrad, "Sudostroyeniye", 1968.

4. Kudryavtseva, N. A., "Forces and moments of an inertial nature acting on the cross-section of the underwater part of a listed ship," Tr. VNITOS (Transactions of the All-Union Scientific Engineering and Technical Society of Shipbuilding), Volume VII, No. 2, 1957.

5. Levin, V. R., Teoreticheskiye osnovy statisticheskoy radiotekhniki (Theoretical foundations of statistical radio engineering), Book 1, Moscow, "Sovetskoye radio", 1969.

6. Petrov, Ye. Yu., and Kheysin, D. Ye., "Calculation of the inertial characteristics of ships floating in ice," Dokl. XIV nauchn.-tekhn. konfer. Gor'k. politekhn. in-ta im. Zhdanova (Korablestr. fakul'tet) (Papers of the XIVth Scientific and Engineering Conference of Gor'kiy Polytechnical Institute imeni Zhdanov (Shipbuilding Faculty), 1967.

7. Popov, Yu. N., "On the problem of the impact of a ship against an ice floe," Tr. Leningr. Korablestr. in-ta (Transactions of the Leningrad Shipbuilding Institute), No. XV, 1955.

8. Popov, Yu. N., Faddeyev, O. D., Kheysin, D. Ye., and Yakovlev, A. A., Prochnost' sudov plavayushchikh vo l'dakh (Strength of ships floating in ice), Leningrad, "Sudostroyeniye", 1967.

9. Riman, I. S., and Kreps, R. L., "Bound masses of bodies of various shapes," Tr. TsAGI, No. 639, 1947.

10. Fedyayevskiy, K. K., and Sobolev, G. V., Upravlyayemost' korablya (Controlability of a ship), Leningrad, Sudpromgiz, 1963.

11. Kheysin, D. Ye., "General vibration of a ship's hull in motion in solid ice," Sudostroyenive (Shipbuilding), No. 9, 1970.

INVESTIGATION OF THE INERTIAL CHARACTERISTICS OF UNSTEADY-STATE MOTION OF AN ICEBREAKER IN ICE

A. Ya. Ryvlin and T. Kh. Tegkayeva pages 50-56

The determination of the parameters characterizing the operation of an icebreaker in unsteady-state motion is of important practical significance, since in ice an icebreaker frequently must change its speed or the direction of its motion, stop, etc. Such maneuvers are most frequently used in operation in short runs and in breaking out ships that have become stuck in the ice.

We will consider only changes in speed and the direction of straight-line motion of the ship. For this we will use characteristics analogous to those which are applied in the estimation of the inertia of ships in clear water: the length of the track and the time required for the run passed over by the ship in the performance of a number of standard maneuvers, such as: "stop" (i. e., when the operating regime of the propulsion plant changes from full ahead to stop), "braking" (from full ahead to full astern) and "acceleration" (stop to full ahead). The motion of the icebreaker after speeding up in ice, the thickness of which exceeds the limiting value that can be broken by continuous steaming, is of special interest. This process may be estimated by the length of the track and the time required for the run, passed over by the icebreaker with full power of the power plant, beginning from the moment of entry into the ice to full stop.

The methodology of calculation of the characteristics of unsteady-state motion of a ship in ice, developed by D. Ye. Kheysin and Ye. Yu. Petrov [1], based on an analysis of the differential equation of motion of the ship, is

$$\frac{\Delta}{g}(1+\lambda)\frac{dv}{dt} = \overline{T}(v) - R_x(v). \qquad (1)$$

In the transition to the relative coordinates $\zeta = (x/L)$ and speeds $F_n = (v/\sqrt{gL})$ this expression takes the form

$$\Delta(1+\lambda)F_n\frac{dF_n}{d\zeta} = \bar{T}(F_n) - R_1(F_n). \qquad (2)$$

where Δ is the weight displacement of the ship; L is the length of the ship; λ is the bound mass coefficient; v is the speed of the ship; R_1 is the total ice resistance to the motion of the ship [$R = R_1 = R_{ice}$]; $\bar{T}$ is the total thrust of the screw propellers; and g is the acceleration of gravity.

Admitting the quasi-steady-state nature of the processes under consideration, the resistance R_1, entering into the right-hand part of equations (1) and (2), may be determined by means of well-known methods referring to steady-state motion (analytical or experimental) and the thrust of the propellers is assumed to be constant, equal to the thrust when moored, $\bar{T}_{shv}$ [$T_{w\,s} = T_{shv} = T_{moored}$]. Such an assumption means the identity of the nature of the reaction of the hull with the ice in continuous motion of the ice breaker and operation by short runs. With a consideration of a quasi-steady-state nature, the right-hand part of equations (1) and (2) in a general form may be represented in the following manner:

$$\bar{T}(F_n) - R_1(F_n) = \bar{T}_{ws} - R_{np} - c_1F_n - c_2F_n^2, \qquad (3)$$

where R_{np} is the direct ice resistance, practically independent of speed [$R_{np} = R_{pr}^{pr} = R_{direct}$]; c_1 and c_2 are constants.

In this case expressions (1) or (2) are reduced to non-linear differential first-order equations, with separating variables. These equations may be solved by any of several well-known methods, in particular by Euler's graphic method [1].

It is not difficult to obtain the final calculation dependences for determination of the characteristics of the unsteady-state processes indicated. By subordinating the general solutions of equation (1) and (2) to the appropriate initial conditions, we find the formula for calculation of the length of the run in stopping of the icebreaker:

$$\frac{dF_n}{d\zeta} = -\frac{R_1(F_n)}{\Delta(1+\lambda)F_n}. \qquad (4)$$

The length of the run in the acceleration of the ice breaker and in motion in the ice with an acceleration run may be determined according to the following formula (with consideration of the sign before $\overline{T}_{shv}$):

$$\frac{dF_a}{dt} = \frac{R_s(F_a) \pm \overline{T}_{шв}}{\Delta(1+\lambda)F_a}. \qquad (5)$$

The basic part of the length of the run in braking, corresponding to the time during which the screw propellers operate when going astern, is determined from the expression

$$\frac{dF_a}{dt} = -\frac{R_s(F_a) + \overline{T}_{з.х}}{\Delta(1+\lambda)F_a}. \qquad (6)$$

To the basic part we must add the section of the run corresponding to the time during which reversing of the screw propeller is performed; it is considered separately according to formula (4). The comparatively rough assumptions used in the derivation of the formulas did not make it possible to recommend them for practical use without a thorough experimental check. The material accumulated in full-scale tests of icebreakers in various ice conditions, and the calculations performed, make it possible to perform such a check (Table 1).

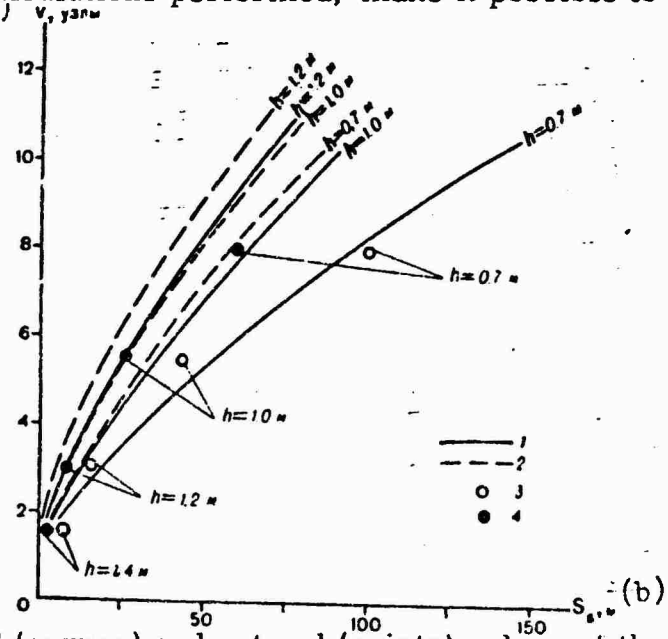

Figure 1. Calculated (curves) and natural (points) values of the length of runs of a powerful ice breaker in solid ice in stopping (13) and reversing (24). a) v, knots; b) S_s, meters; M = meters.

Table 1

Calculated Length of Run of Icebreakers in Ice

(1) Характеристика льда v_0, узлы	(2) «Москва»														(3) «Василий Прончищев»											
	(4) останов					(5) торможение				(6) движение с разбега				(7) разгон		(4) останов				(5) торможение				(6) движение с разбега			(7) разгон	
	2	5	8	10	14	2	5	8	10	5	8	10	14	0	0	2	5	8	10	2	5	8	10	5	8	10	0	0
(8) Сплошной лед																												
(9) Толщина, м																												
0,20																37	89	158	197	10	30	61	85					
0,30																20	55	95	130	6	25	48	68					220
0,40																10	31	50		5	18	36						
0,50																7	22			4	14						80	
0,60																6				3								
0,70	9	45	95	133		7	28	59	84															42	76	100		
0,80														495										25	50	67		
0,90																								17	37	50		
1,00	6	31	63			5	22	44						391				23	31									
1,20	4	22				2	17						196											7	16	23		
1,40																		13	19									
1,50			36	55	95	1,3				49	97	126	180															
2,00			22	33	59					14	34	49	86															
2,50			14	22	41					8	19	28	51															
(10) Природный мелкобитый лед																												
(11) Сплоченность, баллы																												
6	310	760	1060	1240		15	67	110	160							56	171	260	290	10	36	69	91					
8	70	210	390	510		13	48	99	138							16	60	104	135	8	26	52	68					
10	23	100	225	310		10	37	87	125							8	34	65	84	6	20	39	52					
(12) Мелкобитый лед в канале																												
(13) 8 баллов	13	69	158	240		8	37	78	116							8	42	88	123	6	22	49	68					

Key: 1) characteristics of ice v_0, knots; 2) "Moskva"; 3) "Vasiliy Pronchishchev"; 4) stop; 5) braking; 6) motion from acceleration; 7) acceleration run; 8) solid ice; 9) thickness, meters; 10) natural fine broken ice; 11) sea cover, balls; 12) fine broken ice in channel; 13) eight balls.

Full-scale observations demonstrated that the nature of the motion of an icebreaker and the picture of the reaction of the hull with the ice in the performance of maneuvers considered above by an icebreaker does not differ, in principal, from those occurring in continuous motion of icebreakers in ice with a constant speed [2]. This indirectly confirms the validity of the hypothesis of the quasi-steady-state nature of the maneuvers under consideration. The results of full-scale tests of icebreakers of the "Moskva", "Vasiliy Pronchishchev" and "Volga" types agree well (Figure 1) with data from calculations made for stop, braking, acceleration, and operations from acceleration.

Both the parameters of the ice cover and the elements of the ship have an effect on the characteristics of unsteady-state motion. In this case the following have the greatest significance: the form of the ice cover (solid, fine broken, etc.), the thickness of the ice, coverage and compression. As a rule, the absolute magnitude of the length of the run of the ship in stopping, braking, and acceleration into the ice is considerably less than in clear water (Figure 2).

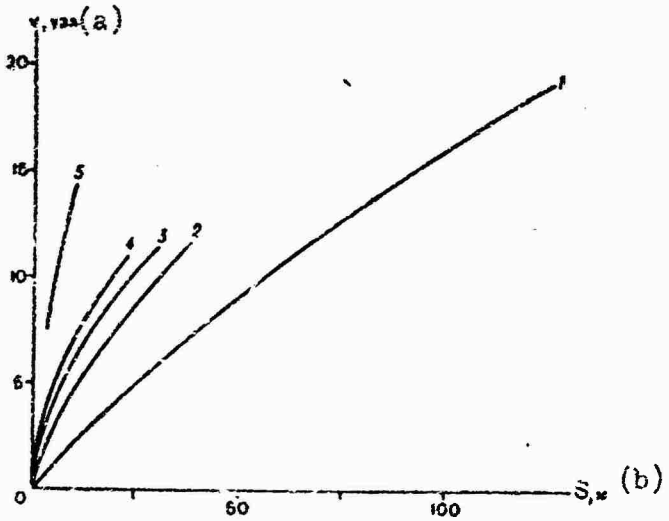

Figure 2. Calculated length of run of a powerful icebreaker in stopping:
1) clear water; 2) fine broken natural ice with a coverage of 10 balls;
3) fine broken ice in a channel behind an ice breaker (h = 1.5 meters);
4) fine broken ice in a channel broken by an ice breaker of the same type in a compression of 2 balls; 5) solid ice with a thickness of 1.5 meters.
a) v, knots, b) S, meters.

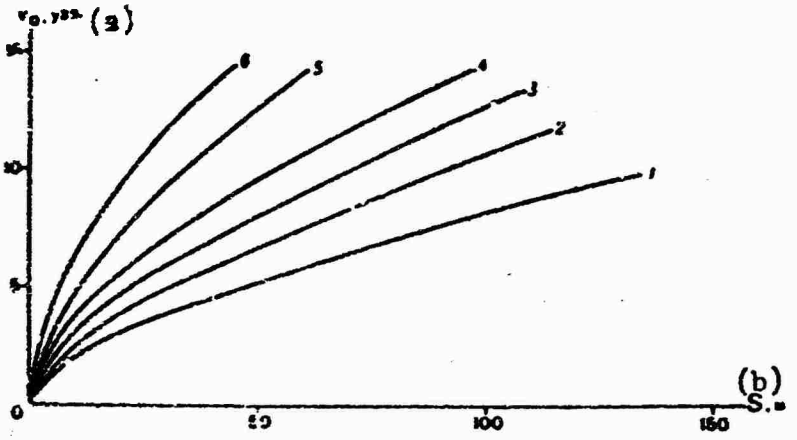

Figure 3. Dependence of the length of run of a powerful icebreaker upon initial speed in stopping in solid ice with a thickness of 0.7 meter (1); 1.0 meter (2); 1.2 meters (3); 1.5 meters (4); 2.0 meters (5); and 2.5 meters (6). a) v_0, knots; b) S, meters.

The initial speed v_0 (Figure 3) and the displacement Δ (Figure 4), which enter into the calculation dependences, have an essential effect on the characteristics of unsteady-state motion, as well as to the principal dimensions, coefficients of shape of the hull lines, etc., and they, in their turn, enter into the expressions for the determination of the ice resistance [2].

In acceleration, braking and advance into the ice from an acceleration run, the magnitude of the thrust of the screw propellers has great significance.

Analysis of formulas (4) and (6) and the results of the calculation demonstrate that on the average the length of the run of the icebreaker in level solid ice in stopping and in braking is proportional to its displacement to a power somewhat less than one.

In conclusion we should note that the calculations of the characteristics of unsteady-state motion of an icebreaker in ice by means of the given methodology are quite reliable and may find wide application. For a more accurate analytical description of the processes indicated, a detailed study of the nature of the variation of the ice resistance and the thrust of the propellers in the period of the reversing of the propulsion plant is necessary, and also at the moment preceeding the stopping (or the beginning of motion in acceleration) of the icebreaker.

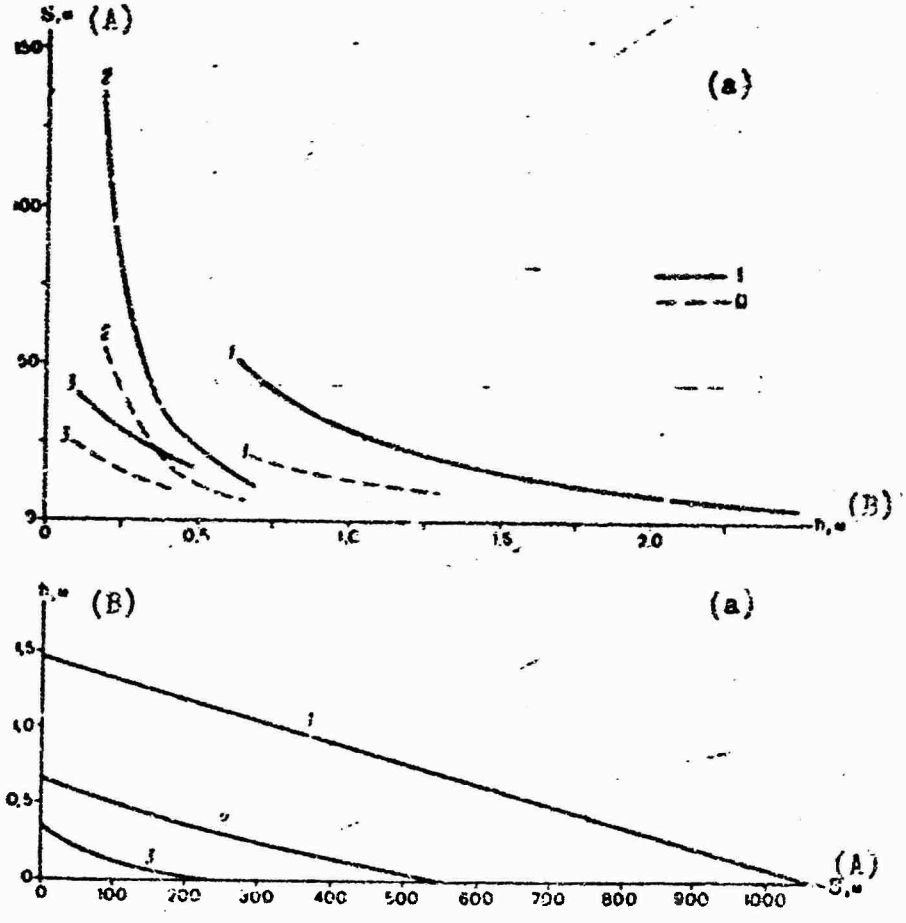

Figure 4. Length of run of icebreakers of various types in level solid ice at a stop (a) and acceleration (b): 1) icebreaker of the "Moskva" type, Δ = 13,300 tons; 2) icebreaker of the "Vasiliy Prunchishchev" type, Δ = 2,700 tons; 3) icebreaker of the "Volga" type, Δ = 770 tons, v_0 = 5 knots (I), v_0 = 3 knots (2). A) S, meters; B) h, meters.

BIBLIOGRAPHY

1. Petrov. Ye. Yu., and Kheysin, D. Ye., "Calculation of the inertial characteristics of ships floating in the ice," Dokl. XIV nauch.-tekhn. konfer. Gor'k. politekhn. in-ta im. Zhdanova (Korablestr. fakul'tet) (Papers of the XIVth Scientific and Engineering Conference of Gor'kiy Polytechnical Institute imeni Zhdanov (Shipbuilding Faculty)), 1967.

2. Kashtelyan, V. I., Poznyak, I. I., and Ryvlin, A. Ya., Soprotivleniye l'da dvizheniyu sudov (Resistance of ice to the motion of a ship), Leningrad, "Sudostroyeniye", 1968.

WEDGING OF ICEBREAKERS IN ICE

Yu. N. Popov and V. I. Pashtelyan Pages 57-73

The wedging of icebreakers is usually observed during their motion in fast ice and especially in operation by short runs in thick hummocky sections of ice fields. Wedging of an icebreaker causes delay of transport vessels under its escort and consequently also unproductive expenditures of fuel and wear of the power plant (during attempt to renew motion by means of multiple reversings of the screw propellers).

Up to the present time, inadequate attention has been devoted to the theoretical and experimental study of the wedging of icebreakers in ice. In Soviet literature concerning experience of the operations of ships in ice [1, 3, 5], only general information with respect to the arrangement and use of various devices applied for freeing an icebreakers from wedging in the ice are given. Investigation of the forced oscillations of a ship wedged in the ice [4] is of definite interest. Abroad [6--8], great significance is assigned to the given problem. However, even there as yet there are still no adequately complete publications.

In the wedging of icebreakers in ice, usually a floating of the hull occurs. Observations demonstrated that wedging of the center part of the hull is the most serious (somewhat forward of the waist), with the formation of two zones of contact with the ice (one along each side). Three zones of contact are formed comparatively more rarely: two in the midship part of the ice breaker and one in the vicinity of the stem. Wedging of the stem and the sections of the sides adjoining it only is also possible. In wedging of the ship in broken ice, some times no floating of the hull is noted.

In order for the wedged icebreaker to begin motion, it is necessary to overcome the forces of static friction originating in the zone of contact with the ice.

The forces of static friction may be decreased by the pumping out ballast, i. e., by means of reducing the normal reactions or by creation of conditions favorable for the transition of static friction to dynamic friction. Such conditions may arise as a result of transferring ballast, i. e., applying a healing or trimming moment, which leads to the rotation of the hull of the ice breaker relative to the ice field. Chipping and pressing down the ice, which also may lead to freeing the ship, sometimes can be achieved as a result of taking on ballast water or transferring it from tank to tank.

For freeing a ship from wedging, the following basic devices are used: a) operation of the screw propellers going astern; b) a heeling system; c) moving the rudder and operating the side propellers toward opposite sides; and d) a trimming system.

The problem of the study of the wedging of an icebreaker in ice is far from simple, in view of the diversity of factors causing this complex phenomenon which do not yield to strict consideration. In recent years in the Arctic and Antarctic Scientific Research Institute, broad theoretical investigations have been conducted: diagrams of forces acting on the hull of a wedged icebreaker were analyzed, an attempt was made to make a quantitative analysis of the efficiency of the application of various means of dealing with this phenomenon. In the development of the given problem, M. A. Ignat'yev, Ye. I. Petrov, D. Ye. Kheysin, V. I. Kashtelyan, and Yu. N. Popov participated.

In this article the theoretical works of the AANII are generalized, problems associated with the investigation of conditions of wedging and the forces originating in this case are considered, the results of theoretical investigations of the efficiency of the application of various devices for freeing an icebreaker from wedging are given.

Conditions of the Wedging of an Icebreaker in the Ice

During operation by short runs in thick ice an icebreaker, performing several operations of breaking the ice field, loses part of its kinetic energy and decreases its speed. Later the sides of the icebreaker, entering into contact with the unbroken ice cover, cannot break it by bending. An intensive fragmentation and warping of the ice begins, on which a considerable part of the energy of the moving icebreaker is expended. The floating of the hull noticeably increases, and the forces of friction also increase. Finally the icebreaker stops, since the thrusts of the screw propellers are inadequate to overcome the ice resistance. In this case, two variations are possible: a) the longitudinal components of the reactive normal forces acting from the ice side on the hull exceed the forces of friction

and no wedging of the icebreaker occurs; b) the reactive forces cannot overcome the forces of friction, and the icebreaker is wedged. In order to back down, it is necessary to use the operation of the screw propellers moving astern, and if this is inadequate, to apply some other means.

In wedging, usually floating of the hull occurs (i.e., a decrease in the average draft), and a trim down by the stern increases. The magnitude of floating depends mainly upon the shape of the lines of the icebreaker and its speed before wedging, and it may reach 1 meter. The trim rarely exceeds 2--2.5 degrees, so that it may be ignored in the theoretical solution of the problem.

We will consider two cases at which wedging originates: 1) with one section of contact of the hull with the ice, in the region directly adjacent to the stem; 2) with two symmetrical sections of contact of the hull with the ice (one on each side).

We will introduce the symbols: Q the lost force of buoyancy, which originates as a result of floating; N the reaction of the ice, normal to the hull, acting from each side; F is the force of friction, directed along the tangential to the shell plating; f is the coefficient of static friction of the ice along the shell plating; α is the angle between the tangential to the waterline in the zone of contact and the center line; β' is the angle of list of the side to the vertical in the zone of contact; β is the angle of list of the frame to the vertical[1]; γ is the angle between the tangential to the buttocks in the vicinity of the contact and the horizon[2]; φ is the angle of inclination of the stem to the horizontal; l; m; n; are the angles between the direction of the normal and the axes of the coordinates x; y; z.

The coordinates were selected in the following manner: the axis x is located on the waterline in the center line and is directed toward the bow, the axis y lies on the plane of the midship section and is directed toward the starboard side; and the axis z is vertically upward. By projecting the forces acting on the hull in wedging with the stem (Figure 1), in the direction of the stem and perpendicular to it, we obtain

$$2F - Q\sin\varphi = 0,$$

$$2N\sin m - Q\cos\varphi = 0.$$

1. The angles β and β' are associated by the ratio $(\mathrm{tg}\beta'/\mathrm{tg}\beta) = \cos\alpha$.

2. The angles α, β, and γ are associated by the dependence $\mathrm{tg}\alpha = \mathrm{tg}\gamma\ \mathrm{tg}\beta$.

From thence we may find the following condition for wedging by the stem

$$f \geqslant \sin m \operatorname{tg} \gamma = \operatorname{tg} \gamma \cos \alpha \frac{\sqrt{\operatorname{tg}^2 \alpha + \operatorname{tg}^2 \beta}}{\sqrt{1 - \cos^2 \alpha \operatorname{tg}^2 \beta}}. \quad (1)$$

We will determine the condition at which wedging occurs by two sections of the side. For this we will consider the equilibrium of an icebreaker under the effect of the force Q of buoyancy lost, directed vertically downward, the two normal reactive forces N, and the two forces of friction, F. The direction of the forces of friction may be determined by considering the motion of the icebreaker when going astern. Certain specialists consider that the forces of friction are directed along the tangential to the buttocks in the region of contact of the hull with the ice, and the others along the tangential to the waterline. By projecting the forces applied to an icebreaker on the axis x, we obtain the following conditions necessary for wedging:

in the first case

$$F \cos \gamma \geqslant N \cos l.$$

in the second case

$$F \cos \alpha \geqslant N \cos l.$$

By noting that N = (Q/2sin β') and assuming that F = fN, we find

$$f \geqslant \frac{\sin \alpha}{\operatorname{tg} \beta} \sqrt{\frac{\operatorname{tg}^2 \alpha + \operatorname{tg}^2 \beta}{1 + \operatorname{tg}^2 \alpha \operatorname{tg}^2 \beta}}, \quad (2)$$

$$f \geqslant \frac{\operatorname{tg} \alpha}{\sqrt{1 + \operatorname{tg}^2 \beta \cos^2 \alpha}}. \quad (3)$$

Condition (2) determines the cases at which the forces of friction are parallel to the buttocks, and condition (3), when they are directed along the tangential to the waterline. We note that in wedging by the vertical sides ($\beta = 0$), condition (3) makes the transition to a conventional solution or a wedge or inclined plane, i.e., $f \geq \operatorname{tg}\alpha$, while the right-hand part of condition (2) at $\beta = 0$ tends toward infinity.

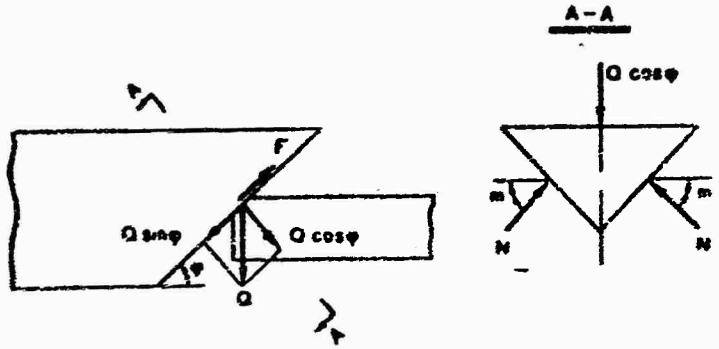

Figure 1. Diagram of the forces acting in wedging by the stem.

By designating as k the ratio of the right-hand part of expression (2) to the right-hand part of ratio (3), we obtain

$$k = \cos\alpha \sqrt{1 + \left(\frac{\operatorname{tg}\alpha}{\operatorname{tg}\beta}\right)^2}.$$

For icebreakers, the value of k amounts to 1.0--1.1. Consequently, condition (3) causes a large wedging zone. If the coefficient of static friction could be assumed to be equal to 0.25 in Arctic ice, then, according to condition (3) the wedging of icebreakers is possible from the waist to 4--5 theoretical frames. We will determine the magnitude of the thrust of the screw propellers when going astern, necessary in order to move a wedged icebreaker from its place, when there are two zones of contact. Having added the thrust of the propellers $P_{e.kh}$ to the forces F and N (we will assume that it is applied horizontally), and having compiled an equation of equilibrium, we obtain [$P_{3.x} = P_{z.kh} = P_{\text{backing down}}$]:

a) the forces of friction are directed along the tangential to the buttocks

$$P_{3.x} \geqslant Q \frac{f\dfrac{\operatorname{tg}\beta}{\sqrt{\operatorname{tg}^2\alpha + \operatorname{tg}^2\beta}} - \dfrac{\sin\alpha}{\sqrt{1 + \operatorname{tg}^2\beta\cos^2\alpha}}}{f\dfrac{\operatorname{tg}\alpha}{\sqrt{\operatorname{tg}^2\alpha + \operatorname{tg}^2\beta}} + \dfrac{\cos\alpha\operatorname{tg}\beta}{\sqrt{1 + \operatorname{tg}^2\beta\cos^2\alpha}}}. \qquad (4)$$

b) the forces of friction are directed along the tangential to the waterline

$$P_{3.x} \geqslant Q \frac{f\sqrt{1 + \cos^2\alpha\operatorname{tg}^2\beta} - \operatorname{tg}\alpha}{\operatorname{tg}\beta}. \qquad (5)$$

If the wedging occurred near the waist (the most serious case) where $\alpha \approx 0$, then conditions (4) and (5) are identical, so that

$$P_{z.x} > Q\frac{f}{\sin\beta} = \Delta T \gamma S \frac{f}{\sin\beta}. \qquad (6)$$

where ΔT is the average floating of the icebreaker; S is the area of the waterline and γ is the density of the water.

Calculations according to formula (6) demonstrate that an icebreaker can free itself from wedging by means of screw propellers only in a case if its floating ΔT turns out to be less than 0.1 meter.

Estimate of the Efficiency of the Application of Various Devices to free an Icebreaker from Wedging

Different specialists argue differently the problem of the efficiency of the application of some devices or other for controlling wedging (a heeling system, operation of screw propellers to different sides, shifting the rudder and a trimming system). For example, the feasibility of the instalation of a heeling system aboard powerful icebreakers is argued, since it requires comparatively large volumes for its location, is expensive, and does not always justify its purpose. Different opinions also exist concerning the efficiency of the use of trimming systems and replacement of them by heeling systems. With the great potential capability of trimming systems, they also have an essential shortcoming: for filling or pumping out (ballast) and transferring it from tank to tank, much time is required (in distinction from a heeling system).

The application of the devices listed is based on the fact that a torque acts on a wedged icebreaker, which causes a redistribution of reactive pressures from the ice side, and tries to turn the hull to the plane of action of the moment or to break up the ice field.

Preliminarily, we will introduce the following assumptions:

a) wedging occurred near the waist, symmetrically, on both sides;

b) the angle α is so small that $\cos\alpha = 1$;

c) the angle β is assumed to be constant in the entire wedging section;

d) the list and the trim after wedging are insignificant, and they may be ignored;

e) after completion of the process of dynamic floating of the icebreaker on the ice and its stopping, the static specific pressures acting on the hull (before the application of devices for freeing it from wedging), in a general

case are less than the limit of strength of the ice to warping and are uniformly distributed throughout the area of contact.

Heeling System

We will determine the minimum torque (or the quantity of heeling ballast transferred from side to side), which a heeling system must create, in order to convert the static friction to dynamic friction after warping, and so that the icebreaker will be able to free itself from wedging, by operating with screw propellers going astern. In this case we assume that as a result of the effect of the torque the ice field is not broken, but that this leads to a redistribution of the reactive normal pressures acting on the hull from the ice side. We will consider the appearance of specific pressures equal to the ultimate strength σ_s of the ice to warping [$\sigma_c = \sigma_s = \sigma_{warping}$] a condition of the rotation of the hull on a transverse plane. As a result of wedging, let us assume that the icebreaker floated by the magnitude ΔT and the resultant of the buoyancy force is equal to Q. This force is balanced by the normal pressures the equivalent of which from each side amounts to

$$N_0 = \frac{Q}{2\sin\beta}. \tag{7}$$

As a result of the effect of the heeling moment M_k [$M_k = M_k = M_{heeling}$], a redistribution of normal pressures occurs, and a shift of the points of application of their resultants, N_1 and N_2 (Figure 2, a), and $N_1 \neq N_2 \neq 0$. Between the shell plating of the ice, the friction forces $F_1 = fN_1$ and $F_2 = fN_2$ originate. The normal reactions and the forces of friction will hamper the rotation of the icebreaker. Assuming that the rotation of the hull may be accomplished around a longitudinal axis passing through the point "0", we will determine the magnitude M_k that is necessary in order to make the specific pressures at points a and b reach the limit of warping. According to Figure 2, a, we write the following equation of equilibrium

$$\left.\begin{aligned} \Sigma y &= N_1(\cos\beta - f\sin\beta) + N_2(\cos\beta + f\sin\beta) = 0 \\ \Sigma z &= N_1(\sin\beta + f\cos\beta) + N_2(\sin\beta - f\cos\beta) - Q = 0 \\ \Sigma M_0 &= N_1\left(x_1 + \frac{B}{2}\sin\beta\right) - N_2\left(\frac{B}{2}\sin\beta - x_2\right) + \\ &\quad + f\frac{B}{2}\cos\beta\,(N_1 + N_2) - M_k = 0 \end{aligned}\right| \tag{8}$$

From the first two equations of system (8) we find

$$N_1 = \frac{Q(\cos\frac{\beta}{2} + f\sin\frac{\beta}{2})}{2\sin\frac{\beta}{2}\cos\frac{\beta}{2}(1+f^2)}, \tag{9}$$

$$N_2 = \frac{Q(\cos\frac{\beta}{2} - f\sin\frac{\beta}{2})}{2\sin\frac{\beta}{2}\cos\frac{\beta}{2}(1+f^2)}. \tag{10}$$

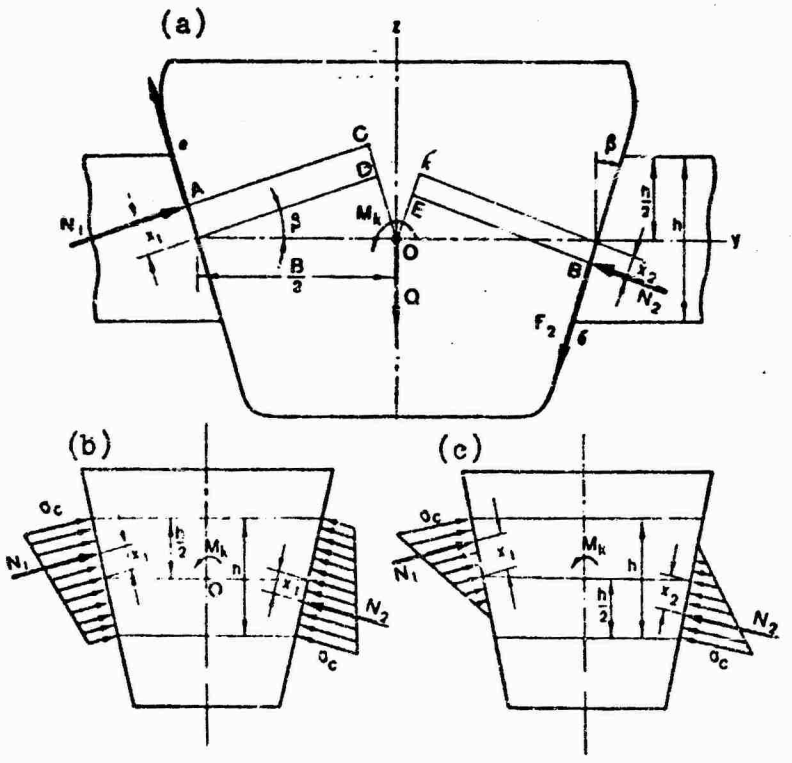

Figure 2. Freeing of an icebreaker by means of a heeling system: a) diagram of forces acting on the hull of the ship; b) curve of the normal pressures with respect to a trapezium; c) curve of the normal pressures with respect to a triangle.

If we assume that f = 0.25, and in the waist in icebreakers β = 15--20 degrees, then f cos β will be considerably greater than the product f sin β. Thus, the reactions N_1 and N_2 differ but little from each other.

In the redistribution of pressures throughout the molded depth and the appearance of stresses at points a and b, equal to σ_s, it is necessary to consider two cases: a) the curve of the pressures has the form of a trapezium

(Figure 2, b);

b) the curve of pressures has the shape of a triangle (Figure 2, c).

We will assume that $x_1 = x_2$ and the quantity f^2 is small in comparison with one. Then we may obtain a condition in the observation of which the curve of the pressures has the form of a trapezium (trapezoid)

$$\frac{hrx_c}{Q} \leqslant \left(\frac{1}{\operatorname{tg}\beta} - f\right); \tag{11}$$

where r is the length of the zone of contact; and h is the thickness of the ice.

The magnitude of M_k is determined in this case according to the formula

$$M_k \geqslant \frac{1}{3\sin 2\beta}[Q(3Bf - h) + 2h^2 r x_c \operatorname{tg}\beta]. \tag{12}$$

If $\frac{hrx_c}{Q} \geqslant \left(\frac{1}{\operatorname{tg}\beta} - f\right)$, , i.e., the curve of pressures has the form of a triangle, the heeling moment should be calculated according to the expression

$$M_k' = \frac{Q}{3\sin 2\beta}\left[3(Bf + h) - 2\frac{Q}{x_c r \operatorname{tg}\beta}\right]. \tag{13}$$

We will consider a case, when, simultaneously with the heeling system, the operation of the screw propellers going astern is used. Assuming that $N_1 = N_2 = N_0 = \frac{Q}{2\sin\beta}$, , we may obtain

$$F = \frac{Qf}{2\sin\beta}\sqrt{1 - \left(\frac{P_{3.x}}{Q}\right)^2\left(\frac{\sin\beta}{f}\right)^2} = kfN_0,$$

where

$$k = \sqrt{1 - \left(\frac{P_{3.x}}{Q}\right)^2\left(\frac{\sin\beta}{f}\right)^2}. \tag{14}$$

Thus, for consideration of the operation of screw propellers in expressions (12) and (13), instead of f we should substitute the quantity kf. The thickness h of the ice and the length r of the zone of contact enter into

formulas (12) and (13), although this length, generally speaking, is an indefinite parameter and, as full-scale observations demonstrate, may reach 25 meters. However, if the following condition is satisfied,

$$\frac{hr_c}{Q} = \frac{1}{\operatorname{tg}\beta} - f, \tag{15}$$

then in the region where the trapezoidal curve makes a transition to a triangular curve, M_k does not depend upon r. Having substituted expression (15) into formulas (12) and (13), we obtain

$$M_k \geqslant \frac{QB}{3\sin 2\beta}\left[3f + \frac{h}{B}(1 - 2f\operatorname{tg}\beta)\right]. \tag{16}$$

$$M'_k \geqslant \frac{QB}{3\sin 2\beta}\left[3f + \frac{h}{B}\frac{1 - 3f\operatorname{tg}\beta}{1 - f\operatorname{tg}\beta}\right]. \tag{17}$$

The expressions given above, although they do differ with respect to structure, give a practically identical result. Actually at f = 0.25 and β = 20 degrees, $M_k/M'_k \approx 1.004$, i.e., it is close to one.

By simplifying the problem under consideration, i.e., ignoring the redistribution of normal pressures, we find

$$M_k \geqslant \frac{fBQ}{2\operatorname{tg}\beta}. \tag{18}$$

If the screw propellers are operating simultaneously, then

$$M_k \geqslant \frac{fkBQ}{2\operatorname{tg}\beta}. \tag{19}$$

Having compared formulas (16) and (18), it is not difficult to become convinced that at h/B = 0.2, f = 0.25, β = 20 degrees the simplification of the solution leads to an understatement of M_k by 20% in comparison with the result which is obtained in the use of expression (16). By means of dependence (16) we may write the following expression for the minimum necessary volume of the heeling tanks of one side:

$$V_0 = \frac{0,8}{\gamma}\frac{Q}{\sin 2\beta}\left[3fk + \frac{h}{B}(1 - 2fk\operatorname{tg}\beta)\right]. \tag{20}$$

Calculations demonstrate that assuming that for powerful icebreakers V_0 = 500 cubic meters, they may free themselves from wedging with simultaneous use of the operation of screw propellers going astern and a heeling system if the magnitude $\Delta T \approx 0.22$ meters.

We will now consider the possibility of freeing an icebreaker from wedging when after transferring the heeling ballast from side to side a formation of cracks occurs due to the bending of the ice in the zone that has contact with the hull.

A force equal to $\left(\frac{Q}{2} + \gamma\frac{V_0}{2}\right)(1 - f\cos\beta)$ and directed downward acts on each of the edges of the ice field. By equalizing this force to the vertical force necessary for the formation of cracks in the ice plate [2], we obtain

$$\frac{1}{2}(Q + \gamma V_0)(1 - f\cos\beta) = 0{,}7\sigma_p h^2,$$

where σ_r is the temporary resistance of the ice to bending, which may be assumed to be equal to 80 tons per square meter.

Assuming that f = 0.25 and β = 20 degrees, we find

$$h = \frac{\sqrt{Q + \gamma V_0}}{12}. \qquad (21)$$

Calculations according to formula (21) demonstrate that without the assistance of a heeling system ($\gamma V_0 = 0$), powerful icebreakers can break ice with a thickness of 1.75 and 3.75 meters by bending, with the hull floating by 0.2 and 0.8 meters, respectively.

The application of a heeling system with a volume of 500 tons makes it possible to increase the thickness of the ice indicated by 45% at ΔT = 0.2 meter and by 20% at ΔT = 0.8 meter.

In practice, however, cases are observed when after the formation of bending cracks in the ice the icebreaker cannot pack the broken ice floes. This occurs because the shape of the hull in the midship section does not always provide for free packing of ice floes, but it is possible if the lower edge of the ice floe preliminarily begins to be broken due to warping (Figure 3). By using the diagram of the forces given in Figure 3, we may obtain the following expression for the compression stresses at point A:

$$\sigma_A = \frac{6N_z b}{lh^2} + \frac{N_y}{lh} - \frac{6N_y a}{lh^2} + \frac{Nf\sin\beta}{hl} - \frac{6Nfa\sin\beta}{lh^2} - \frac{6Nfb\cos\beta}{lh^2},$$

where b is the width of the sector being packed; and l is the additional length of the sector.

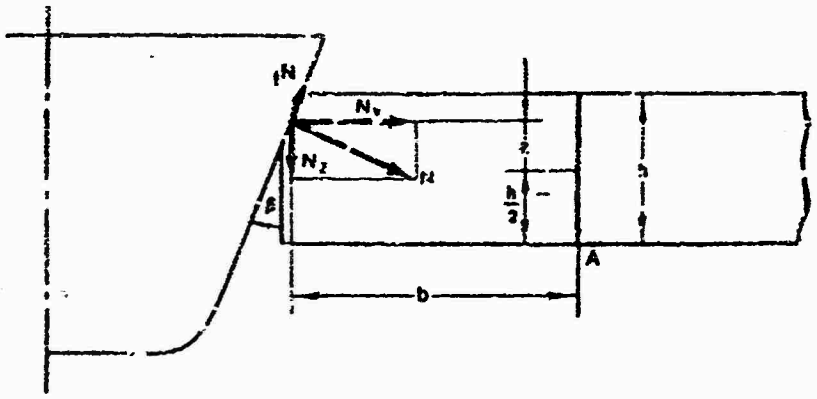

Figure 3. Diagram of forces during packing of an ice floe.

The magnitude of a is determined from the following conditions: at $\beta = 0$, $a = 0$ and at $\beta = 90^\circ$, $a = (h/2)$, i.e., $a = h(\sin \beta / 2)$.

Having assumed that $\sigma_A = \sigma_s$; $f = 0.25$; $\beta = 20^\circ$ and having assumed that with the heeling system operating $N = \frac{Q + \gamma V_0}{2 \sin \beta}$, $N_z = \frac{Q + \gamma V_0}{2}$, $N_y = \frac{Q + \gamma V_0}{2 \operatorname{tg} \beta}$, we obtain $\sigma_c = 0{,}94 \frac{Q + \gamma V_0}{h^2} \frac{b}{l}$.

The ratio b/l should be considered as a conditional parameter. The data from tests of powerful icebreakers demonstrate that with reference to spring-summer ice with a thickness of 1.5--2.0 meters, with an ultimate warping strength of $\sigma_s = 250$ tons per square meter, the ratio $b/l = 0.5$. Then

$$h = \frac{\sqrt{Q + \gamma V_0}}{23}. \qquad (22)$$

From expression (22) it follows that powerful icebreakers can pack ice with a thickness of 1.2 meter when floating by 0.2 meter and with a thickness of 2 meters when floating by 0.8 meter. From an analysis of the calculations performed according to formulas (21) and (22), it follows that it is easier to break ice than to pack it.

If after wedging we start the screws going astern and pump out ballast to the volume of 500 cubic meters from the heeling tanks, then due to the corresponding decrease in the normal reactions (and, consequently, the

forces of friction), powerful icebreakers will be able to free themselves from wedging if the hull is floating by approximately 0.3--0.35 meter.

Simultaneous use of Shifting of the Rudder and Operation of the Side Screws in Opposite Directions

Let us assume that an icebreaker equipped with three stern propellers has wedged the midship section of its hull in the ice and to free it shifting of the rudder is being used. In this case the side propellers operate in opposite directions to increase the torque, and the midship screw is going ahead, in order to create a force on the rudder (Figure 4).

We will introduce the following symbols: P_s, P_{pr} are the thrust of the midship and starboard side screw when going ahead [$P_c = P_s = P_{\text{center line}}$; $P_{nr} = P_{pr} = P_{\text{starboard}}$]; P'_1 is the thrust of the port side screw when going astern [$P'_n = P'_1 = P'_{\text{port}}$]; c is the distance between the side screws; R is the force on the rudder; and γ_0 is the rudder angle.

We will determine the minimum torque M_γ which the rudder and the side screws must create in order to rotate the hull on a horizontal plane and simultaneously have it move in a longitudinal direction. As in the consideration of the heeling system, we will consider that the rotation of the hull is possible in a case when the pressure at point A reaches the warping strength of the ice, and the greater of the forces of friction reaches its maximum value, i.e., $F_2 = fN_2$.

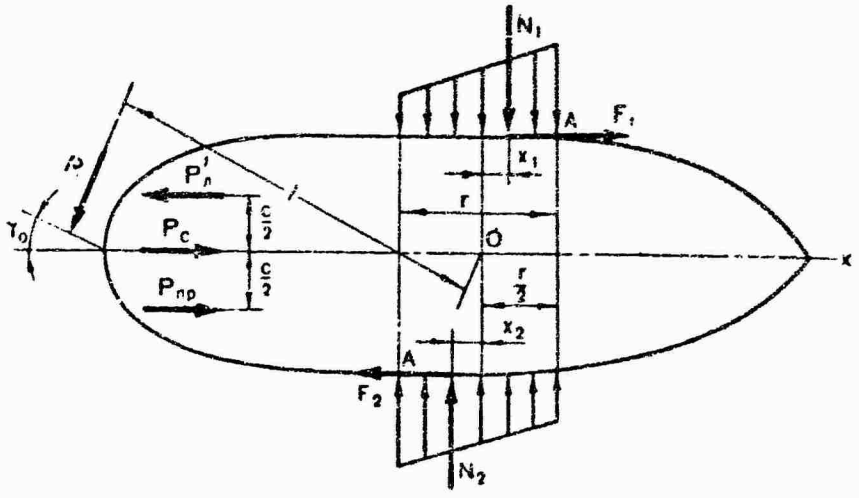

Figure 4. Diagram of forces in the freeing of an icebreaker by means of the rudder and the screw propellers.

We will write the equations of equilibrium

$$\left.\begin{aligned}
\Sigma x &= P_c + P_{ep} - P_s' + F_1 - F_2 - R\sin\gamma_0 = 0,\\
\Sigma y &= N_1\cos\beta - N_2\cos\beta + R\cos\gamma_0 = 0,\\
\Sigma z &= N_1\sin\beta + N_2\sin\beta - Q = 0,\\
\Sigma M_0 &= Rl + (P_s + P_s')\frac{c}{2} - (F_1 + F_2)\frac{B}{2} -\\
&\quad - N_1x_1\cos\beta - N_2x_2\cos\beta = 0,
\end{aligned}\right\} \qquad (23)$$

where x_1 and x_2 are the distances from the points of application of the resultant normal pressures N_1 and N_2 to the transverse axis passing through point O. Assuming that $x_1 = x_2 = x$, we obtain

$$\begin{aligned}
M_0 = Rl + (P_{ep} + P_s')\frac{c}{2} = \frac{Q}{\sin\beta}\left(f\frac{B}{2} + x\cos\beta\right) +\\
+ \frac{B}{2}\left[P_s' - P_c - P_{ep} + R\left(f\frac{\cos\gamma_0}{\cos\beta} + \sin\beta\right)\right].
\end{aligned} \qquad (24)$$

We will determine, in approximation, the force on the rudder

$$R = \frac{\rho(v\sin\gamma_0)^2}{2}s_0,$$

where v is the average velocity of the downward flow of water discharged by the propeller to the rudder, for powerful icebreakers it may be assumed to be equal to 10 meters per second; s_0 is the area of the rudder blade; ρ =0.102 tons (force) per meter^4 is the mass density of the water.

The quantity x entering into expression (24) is determined from the conditions that the normal pressures at points A reach the warping strength. With observation of the condition

$$\frac{rh}{Q} \leqslant \frac{1}{\sigma_c\,\mathrm{tg}\,\beta}$$

the curve of the pressures has the form of a trapezium. Then

$$x = r\frac{2\sigma_c rh\,\mathrm{tg}\,\beta - Q}{6Q}.$$

If $\frac{rh}{Q} \geq \frac{1}{\varepsilon_c \operatorname{tg} \frac{\gamma}{2}}$,

then the curve of the pressures has the shape of a triangle. Then

$$x = \frac{3\varepsilon_c hr \operatorname{tg} \frac{\gamma}{2} - 2Q}{6h\varepsilon_c \operatorname{tg} \frac{\gamma}{2}}.$$

At $\frac{rh}{Q} = \frac{1}{\varepsilon_c \operatorname{tg} \frac{\gamma}{2}}$ and in the first and in the second case, $x = r/6$. The quantity M_v does not depend upon the thickness of the ice, and, other things being equal, it is a function of the length r of the zone of contact. In simplifying the problem, we may consider that no redistribution of the normal pressures along the length of the hull occurs[1]. Then for the determination of M_v we should assume in formula (24) that $x = 0$.

If the rudder is amidship, the side screws are operating in different directions (toward different sides), and the midships screw is going astern, then expression (24) is reduced to the form:

$$M_s = (P_{np} + P'_s)\frac{c}{2} = \frac{Q}{\sin \frac{\gamma}{2}} f \frac{B}{2} + \frac{B}{2}(P'_s - P'_c - P_{np}). \qquad (25)$$

where P'_s is the thrust of the amidships screw when going astern.

Calculations according to formulas (24) and (25) demonstrate that the methods of freeing a ship from wedging under consideration are not very effective. Thus, by using the shifting of the rudder and operating with the screw propellers, we may free ourselves from wedging if the magnitude of the floating of the hull does not exceed 0.15 meter.

Trimming System

For freeing an icebreaker from wedging, a trimming system, having both a bow and a stern group of tanks, may be used in the following manner: a) water may be transferred from one group of tanks into another (or one may be filled and simultaneously the other pumped dry), as a result of which a trimming moment will act on the icebreaker, and the vertical force Q which originated due to floating, does not change; b) by filling (or draining) the after or forward group of tanks, and in this case the vertical force changes

1. This assumption is all the more valid if the quantity r is less in magnitude.

and a trimming moment appears; c) by filling (or draining) the trimming tanks of both groups simultaneously. In this case the vertical force Q which appeared after the wedging of the icebreaker changes.

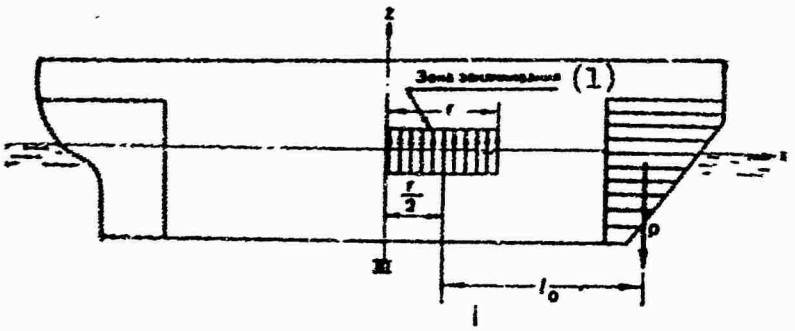

Figure 5. Diagram of the operation of a trimming system. 1) wedging zone.

The possibility of the application of one method or other in practice depends upon the quantity of the ballast water in the trimming tanks before wedging or upon the degree of their use as additional capacities for taking on fresh water.

In the use of a trimming system, freeing a ship from wedging may occur in the rotation of the icebreaker due to the warping of the ice, and also the breaking and subsequent packing of it in the zone of contact with the hull or after trimming tanks are drained as a consequence of the decrease in normal pressures and, consequently, the forces of friction.

We will consider each of the possible cases.

We will determine the minimum quantity of water, $P = \gamma V$, which must be taken into the forward trimming tank in order to warp the ice and so that the icebreaker will be able to free itself from wedging, by operating the screw propellers, going astern. We will consider that the warping of the ice occurs as a result of the rotation of the icebreaker relative to its transverse axis, passing through the center of the zone of wedging (Figure 5). By preserving all the assumptions made previously in the consideration of a heeling system, we may obtain the following expressions:

1. If the curve of normal pressures has the form of a trapezium,

$$P = \frac{\sigma_c r h (2\operatorname{tg}^2\beta - 1{,}5f^2) + (1{,}5f - \operatorname{tg}\beta) Q}{6\left(\operatorname{tg}\beta - \frac{f}{2}\right)\frac{l_0}{r} - (1{,}5f - \operatorname{tg}\beta)} \approx \frac{\sigma_c r h (2\operatorname{tg}^2\beta - 1{,}5f^2)}{6\frac{l_0}{r}\left(\operatorname{tg}\beta - \frac{f}{2}\right)}, \qquad (26)$$

where l_0 is the distance from the center of gravity of the tank to the axis of rotation. Formula (26) is valid with observation of the condition

$$Q+P\geqslant a_c rh\left(\operatorname{tg}\beta+\frac{f}{2}\right). \tag{27}$$

2. If the curve of normal pressures has the shape of a triangle with a base $x \geqslant (r/2)$,

$$P=\frac{rhz_c}{24\frac{l_0}{r}}\cdot\frac{4x-r}{x}(\operatorname{tg}\beta+f), \tag{28}$$

where x is determined from the equation

$$x=\frac{(\operatorname{tg}\beta+f)r^2hz_c}{4\{(\operatorname{tg}\beta+f)rhz_c-(P+Q)\}}. \tag{29}$$

3. If the curve of normal pressures has the form of a triangle with a height $x \leqslant (r/2)$,

$$P=\frac{(Q+P)[2z_crh(\operatorname{tg}\beta+f)-(Q+P)]}{6l_0z_ch(\operatorname{tg}\beta+f)}. \tag{30}$$

Expressions (28) and (30), which may be used at

are quadratic relative to the unknown quantity P, and for its determination we may use the method of successive approximation. The formulas given may be used in a case if for freeing the ship from wedging the drainage of a ballast tank or the transfer of water from one tank to another tank is performed. For this, it is necessary to assume in equations (26), (27), (29), and (30) that P = -P (if the tank is being drained) or P = 0 and $\underline{l} = 2l_0$ (transferring ballast).

By ignoring the redistribution of normal pressures in the process of the operation of the trimming system, we obtain the following expression:

$$Pl_0=\frac{rf}{2\sin\beta}(P+Q), \tag{31}$$

from whence

$$P=\frac{Qf}{2\frac{l_0}{r}\sin\beta-f}. \tag{32}$$

If the freeing of the ship from wedging occurs only due to a decrease in the forces of friction after drainage of the tanks or in the breaking of the ice with its subsequent packing as a result of taking on ballast water, in the given case all the considerations given above and the consideration of a heeling system are valid. The calculations demonstrate that at the assumptions made the trimming system is the most effective means of freeing a

ship from wedging. Thus, if the floating of a powerful icebreaker amounted to 0.8 meter, the quantity of water taken in or pumped out that is sufficient to free the ship from wedging, amounts to $\approx$ 600 tons (or 300 tons if water is pumped from tanks of the forward group to the after tanks). However, experience in the use of trimming tanks aboard powerful icebreakers has demonstrated that a single rotation of the hull around the transverse axis is not an adequate condition for freeing an ice breaker from wedging.

In practice, the icebreaker is freed from wedging only by multiple transferring of the ballast, which requires a long period of time. In the use of trimming tanks, the greatest effect may be obtained if they are completely drained.

BIBLIOGRAPHY

1. Gotskiy, V. M., Opyt ledovogo plavaniya (Experience in ice navigation), Leningrad, "Morskoy transport", 1957.

2. Kashtelyan, V. I., "Approximate determination of forces breaking the ice cover," in the collection: Problemy Arktiki i Antarktiki (Problems of the Arctic and Antarctic), No. 5, Leningrad, Gidrometeoizdat, 1960.

3. Petrov, M. K., Plavaniye vo l'dakh (Navigating in ice), Leningrad, "Morskoy transport", 1955.

4. Petrov, Ye. Yu., and Kheysin, D. Ye., "Loosening of a ship in wedging in ice," Dokl. no XIV nauchn.-tekhn. konfer. (Papers read at the XIVth Scientific and Engineering Conference), izd. Gor'k. politekhn. in-ta, 1967.

5. Stepanovich, A. N., Ledokoly (Icebreakers), Leningrad, "Morskoy transport", 1958.

6. Johnson, H. F., "Development of Icebreaking Vessels for U. S. Coast Guard," Transactions of the Society of Naval Architects and Marine Engineers, 1946, Vol. 54.

7. Thiele, E. H., "Technical Aspects of Icebreaker Operation," Transactions of the Society of Naval Architects and Marine Engineers, 1959, Vol. 67.

8. Watson, A., "The Design and Building of Icebreakers," Transactions of the Society of Naval Architects and Marine Engineers, Feb. 1959.

FEATURES OF THE OPERATION OF ICE-BREAKING TRANSPORT VESSELS IN THE ANTARCTIC

D. D. Maksutov

pages 73-78

Every year a whole flotilla of various vessels belonging to countries, which in accordance with the International Treaty, are investigating the nature of the sixth continent, are sent to the shores of Antarctica. Among these ships are icebreakers, transport vessels equipped for active and passive ice navigation, passenger vessels, scientific-research vessels, and fishing vessels. However, the specifics of navigation in seas washing the shores of Antarctica impose special requirements upon ships, and therefore far from all ships can successfully perform their mission in this region.

Conditions of the formation of sea ice in the seas washing the Antarctic continent essentially differ from those in Arctic seas. As is well known, the primary forms of ice--ice crystals and slush ice--usually make the transition to ice crust, pancake ice, or slobice, depending upon the state of the weather and the sea. But because of the frequent storms, ocean swell, and the transfer of enormous amounts of snow accompanied by winds of hurricane force, the slush and ice crusts are rarely formed, only near the shores.

The basic primary forms of ice in the Antarctic are snow sludge, sludge ice, and pancake ice. In the period of intense ice formation pancake ice (not infrequently of considerable thickness) may be observed in enormous spaces [1]. Young ice is covered by snow, submerged in the water under its weight, and obtains a stratified structure: layers of hard crystalline ice are intermixed with layers of ice formed from the snow and friable ice inside the water [4]. The thickness of the crystalline ice, as a rule, is considerably less than the thickness of the other layers, representing the friable ice, permeated by water. For the greater part of Antarctic ice, the value of the

"crystallinity factor"[1] varies within considerable limits (from 0.15 to 0.87).

In the Antarctic, just as in the Arctic, compression and hummocking of ice occurs. The hummocked ice rapidly freezes, abundant snowfalls and snow storms level out its surface and thus are formed fields rising 100--150 centimeters above the surface of the water with a snow layer of 100 centimeters or more. Such ice resembles pack ice, and it is difficult to force a way through it even for icebreakers, and for transport vessels equipped for active ice navigation such ice is not penetrable.

The Antarctic fast ice is formed primarily in the bays and gulfs of the continent, and also along the shoreline of islands and in places where icebergs accumulate. The width of the fast ice amounts to several dozen miles, and the thickness of the ice towards the end of winter reaches 150--200 centimeters or more. Melting of fast ice is almost unobserved, and the ice is frequently preserved almost in its winter state up to the moment of breaking up. The high degree of snow cover of the fast ice is a specific feature of Antarctica.

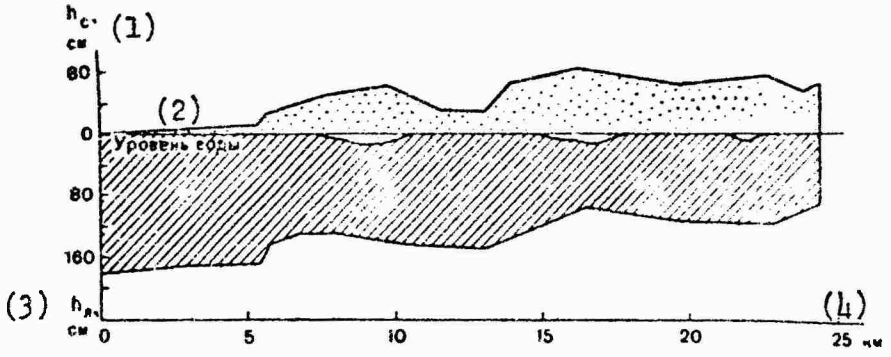

Figure 1. Thickness of fast ice and snow in the profile at Cape Mabus, northern edge (14 January 1966). 1) h_s, centimeters [$h_c = h_s = h_{snow}$]; 2) water level; 3) h_l, centimeters [$h_л = h_l = h_{ice}$]; 4) kilometers.

The greatest masses of snow are deposited on the sea ice in winter during the hurricanes, and also during gravity winds, and the thickness of the snow is irregularly distributed. At a distance of approximately one kilometer from the shore barrier, there is almost no snow on the ice. As the distance from the shoreline increases, the thickness of the snow cover also increases. On the leeward side of islands and icebergs, the quantity

1. By the "crystallinity factor" [3] we mean the ratio of the thickness of the layer of crystalline ice to the entire thickness of the ice.

of snow reaches the maximum magnitude, which presents a serious obstacle both for ships and for ground transport [2].

As we have already noted, the fast ice, under the weight of the snow, is somewhat packed, the surface of the ice goes under the water, and the salt sea water permeates the lower layers of snow. Such sections of fast ice are exceptionally difficult for ships to force their way through. In Figure 1 a section of the fast ice in the vicinity of the Mirnyy observatory, over a length of almost 25 kilometers, is shown. Some times, operating in short runs, ships equipped for active ice navigation of the class of the diesel-electric vessel "Lena" during a watch of continuous operation advance not more than a hull length. With comparatively the same strength characteristics, Antarctic ice, because of the features of its structure and the great amount of snow cover, have greater resistance to ice-breaking vessels than Arctic ice.

A. F. Treshnikov [4], investigating the physico-mechanical properties of Antarctic ice, noted the very high values of the temporary resistance to compression (60 kilograms per square centimeter or more). In summer the temporary resistance of the center layers of ice to bending reaches approximately 10 kilograms per square centimeter, and that of the edge layers 6--7 kilograms per square centimeter.

As was already indicated, the "crystallinity factor" of Antarctic ice is considerably less than one, while the "crystallinity factor" of Arctic ice amounts to 0.9--1.0. In this also lies the basic difference between the ice of the Arctic and the Antarctic. The predominating layers of friable ice, permeated with water, noticeably hampers the cleavage of fast ice in the motion of a ship. Aside from this, the "pillow" of wet ice and snow formed ahead of the stem also creates an additional resistance. Even in operation in short runs during an attempt to force a way through the fast ice a ship advances ahead only insignificantly, since the Antarctic ice, being more "viscous", breaks with considerably more difficulty than the dry crystalline ice of the Arctic.

The enormous quantity of icebergs in the seas of Antarctica extraordinarily hampers the navigation of ships and presents a serious hazard for them. Ships must have good maneuverability and the necessary reserve of power in order to be able to maneuver rapidly if a hazard of collision with an iceberg appears.

The regions of Antarctica differ essentially between themselves with respect to the degree of ice cover, which depends upon the latitude of the locality, the configuration of the coast, the relief of the adjoining part of the

continent, the features of the circulation of water and air masses in the surrounding region, and many other factors. In this article the ice cover and conditions for navigation of ships only in those regions of the Antarctic where Soviet vessels mainly navigate are considered.

Davis Sea. The most favorable ice conditions for navigation of ships are observed from the beginning of January to the beginning of March. At this time, the fast ice, with a width from 15 to 25 miles, presents a serious obstacle for the approach of ships to the shore. The thickness of the fast ice reaches 150--200 centimeters, and the snow cover on the average up to 100 centimeters. Before an approach to the fast ice, ships must get through a belt of drifting ice with a width of 60--80 miles. It consists of large and small broken ice, with a cover varying from 5-6 to 10 balls, and also of fragments of fields and a large quantity of icebergs. Then ships must force their way through the fast ice in order to reach a point that is convenient for unloading. It is possible to break through the fast ice with a thickness of 160--180 centimeters only by impact with an acceleration run, and therefore transport vessels must have high ice navigating qualities. The breakup of the fast ice in the vicinity of the Mirnyy observatory usually occurs in the second half of January, but sometimes may extend up to the beginning of March.

In a case of arrival of ships after the fast ice breaks up and is carried away, communications with the shore are very difficult. The height of the ice barrier in the vicinity of the observatory amounts to 20--25 meters. Mooring alongside such a high barrier is a great hazard. There is no anchorage on the roadstead of the Mirnyy observatory because of the great depth and the rocky bottom of the sea. Therefore, the only variation of mooring is to push the stem of the ship against the barrier with the screw turning over at a low speed and to fasten the caprone mooring lines to mooring posts, embedded in the ice at a certain distance from the edge of the barrier [2]. In this case unloading operations can be performed only by boats or by means of a "ropeway", which is a cable stretched between the ship on the shore along which a net holding the cargo moves. The capacity of such a "ropeway" does not exceed one ton. In this case the ship must have a strong upper part of the stem, since with prolonged mooring in such a position the ship experiences strong impacts against the barrier in the approach of the ocean swell. Navigation safety in the coastal zone of the Davis Sea depends upon the maneuverability of the propulsion plant of the ship: rapid reversing and smooth change in the number of revolutions. The large quantity of rocky islands, submerged rock, icebergs, and the sharp changes of the weather (when the wind force increases to a hurricane level in a very short interval of time) present a serious hazard for ships. Consequently, ships must also have good controlability and unsinkability if any

any two watertight compartments are flooded.

New ice formation usually begins in the first days of March. Near the shores ice is formed (primary form), which does not present any obstacle for a ship. Further to the north enormous masses of solid year-old large broken ice and fine broken ice are located, held together by young ice. Towards the middle of March this massif presents a serious obstacle for ships. At moments of compression of the ice, the ship's hull experiences considerable loads.

Enderby Land Region. The western part of Enderby Land, and, in particular, Alasheyeva Gulf, where the Molodezhnaya observatory is located, is difficult to reach for ships even in years that are favorable from the standpoint of ice conditions. In order to approach the shore, ships are obliged to get through a comparatively broad belt (100--150 miles) of drifting ice entirely covering the sea, among which ice extensive fields are encountered, covered by hummocks and with a large quantity of snow. In motion in broken ice, ships are frequently pinched, during which even with the use of full power they cannot advance. In the belt of drifting ice, large accumulations of icebergs are observed.

In the vicinity of the Molodezhnaya station the fast ice with a thickness of 120--150 centimeters extends for several dozen kilometers. In recent years ships have not been forcing their way entirely through the fast ice to the shore, but only have been penetrating by 3--4 hull-lengths into it, in order to provide safety in unloading. But sometimes it is necessary to approach the shore, when the fast ice has still not been broken. Thus, for example, in 1962 the diesel-electric vessel "Ob'" expended almost thirty days in forcing its way in the fast ice in Alasheyeva Gulf. Consequently, transport vessels not only must open the ice, but also force it open.

After the fast ice breaks up and is carried away, ships can moor near the station, directly to the barrier, the height of which amounts to 6--8 meters. Mooring is accomplished alongside, the ends of the ship fastened to ice anchors frozen into the ice on the barrier. However, the almost continuous swell coming from the north, from the open ocean, causes strong impact of the side of the ship against the ice barrier, as a result of which the side plating may receive considerable damages. Such mooring requires the installation of thick fenders on the side of the ship.

Aside from this, mooring a ship alongside a low barrier presents a hazard at the moment of a sharp intensification of the wind. Thus, in February 1965 a strong gust of wind broke five steel and five caprone mooring lines aboard the diesel-electric vessel "Ob'", and the stern of the ship

was thrown away from the barrier. As a result, the ship was forced to depart from the barrier and go out to drift into a safe region. Such a circumstance requires good and reliable mooring gear on board ship, and additional quantities of mooring lines (preferably caprone lines), which take up the shock of transverse oscillations caused by the wind and swell, and also an adequately strong capstan at the stern, in order to make it possible to pull the stern in when mooring during wind.

Leningradskiy Zaliv (Gulf). (The region where the Novolazarevskaya station is located.) In this gulf the fast ice has little snow cover, is very strong, and a way can be forced through it only with great difficulty. The thickness of the year-old fast ice, depending upon the time it is established, varies from 1.7 to 2.5 meters. A specific feature of the region is the frequent recurrence and extraordinary strength of winds of storm and hurricane force at the end of summer and in autumn, which leads to partial breakup of the fast ice, and sometimes complete breakup. Thus, for example, during the operation of the eleventh Expedition in February 1966, a wind of hurricane force that began unexpectedly continued (almost without interruption) for ten days. As a result, an intensive breakup of the fast ice occurred, which made the situation of the ship and the unloading of cargo very complicated [2]. In the approach to Leningradskiy Zaliv, ships must pass through a wide belt of 7--9 ball drifting ice.

Ice conditions are analogous also in the vicinity of the new Leningradskaya station. The degree of ice cover of one region or other plays an important part in the determination of the dates when it is accessible for ships of various classes. At the same time, the dates when navigation begins and ends in the seas of the Antarctic greatly depend upon the ice qualities of the ships: the hull lines, ice strength, capacity of the propulsion plant, and the features of the propeller and rudder complex. Ships equipped for active ice navigation, having high ice qualities, may arrive in Antarctic earlier, enter into the ice with greater confidence, commence performing their functions earlier, conduct scientific research operations in regions with increased ice cover, and leave Antarctica earlier.

As Captain A. I. Dubinin notes [1], in Antarctic operations it is desirable that two or more ships equipped for active ice navigation participate. In this case, we may considerably extend the dates of the beginning and ending of the navigation season and increase the results obtained from the operation of each ship in connection with the more decisive actions of ships in calculations for insurance and assistance.

The difficult conditions of navigation in Antarctic waters, the necessity of intensive force operation in the ice, prolonged ocean passages

in periods of strong storms and winds of hurricane force impose extraordinarily high requirements upon ships voyaging to Antarctica: the high ice qualities must be combined with excellent seaworthiness, stability, and unsinkability.

Some Antarctic expeditions send icebreakers to Antarctica. Thus, for example, the United States of America use their best icebreakers there, of the "Glacier" and "Wind" classes, which provide for the escorting of transport vessels, and for scientific research operations the icebreaker transport vessel "Eltanin" is used. Japan built the icebreaker "Fuji" for navigation in the waters of Antarctica and Argentina the icebreaker "General San Martin". Australia, France, Belgium, and Britain charter icebreaking transport vessels of Danish construction of the "Dan" type for this purpose, as these ships have good ice navigating capability and adequate strength. The Soviet Union sends ships equipped for active ice navigation to the Antarctic, of the types of the diesel-electric vessels "Lena" and "Amguyema", which successfully cope with problems in the supplying of Soviet Antarctic stations. The flagship of the Soviet Antarctic Expedition, the diesel-electric vessel "Ob'", by this time has made eighteen voyages to the Antarctic, and on each voyage the ship has navigated for 2--2.5 thousand miles in ice of various degrees of sea cover, operating as an icebreaker, and it has repeatedly rendered assistance to ships of other expeditions held in the ice. Soviet vessels arrive in the waters of Antarctica earliest of all and depart later than all others, and therefore the Soviet Antarctic Expedition is extremely interested in a systematic and thorough study of the features of the ice regime of the seas of the Southern Ocean and the operating conditions of transport vessels intended for ice navigation there.

BIBLIOGRAPHY

1. Dubinin, A. I., Plavaniye v Antarktiku (A voyage to Antarctica), Leningrad, "Transport", 1966.

2. Maksutov, D. D., "Eleventh seasonal expedition, 1965/66," Tr. SAE (Transactions of the Soviet Antarctic Expedition), Volume 50, Leningrad, Gidrometeoizdat, 1969.

3. Peschanskiy, I. S., "Arctic and Antarctic sea ice," in the collection: Problemy Arktiki i Antarktiki (Problems of the Arctic and Antarctic), No. 4, Leningrad, "Morskoy Transport", 1960.

4. Treshnikov, A. F., "Features of the ice regime of the Antarctic Ocean", Tr. SAE, Volume 21, Leningrad, "Morskoy Transport", 1963.

EFFECT OF THE LINES OF AN ICEBREAKER ON THE MAGNITUDE OF ICE LOADS

Yu. N. Popov, T. Kh. Tegkayeva, and C. V. Faddeyev pages 79-87

The theoretical and experimental investigations indicate that among the basic parameters which affect the magnitude of impact loads acting on the hull of an icebreaker in motion in the ice are the angle β of inclination of the frames to the vertical and the shape of the bow branch of the waterline. The shape of the bow branch of the waterline is characterized at a given point by the angle α of inclination between a tangential to the waterline and the center line. In turn, the angle α may be considered as depending upon the ratio L/B and the coefficient α_n of fineness of the area of the bow part of the waterline [$\alpha_n = \alpha_{bow}$].

For the analysis of the effect of the parameters indicated (β, L/B, α_n) on impact ice loads, we use the results of investigations which have been published [2]. In this case we will consider the impact of the icebreaker against an infinite ice field, without consideration of the bending of the latter. In this case the ice load in the transverse section of the icebreaker are determined according to the expressions:

on the side framing
$$q_н = 0{,}084\left(\frac{D}{C'}\right)^{3/4}\frac{v_s^{1/4}\sigma_1^{1/4}\sigma_c^{3/4}}{\sin^{3/4}\beta\cos^{3/4}\beta}, \quad (1)$$

on the side plating
$$p_н = 10^{-2}k\alpha^{1/4}L^{1/4}\frac{m^{1/4}}{(C')^{3/4}}. \quad (2)$$

In formulas (1) and (2) the following are designated: q_{load} is the running load on the framing [$q_н = q_{load}$]; p_{load} is the load on the shell plating, uniformly distributed throughout the area; D is the displacement of the icebreaker; L is the length of the icebreaker; v_s is the speed at the beginning of the impact; σ_s is the temporary resistance of the ice to warping [$\sigma_c = \sigma_s = \sigma_{warping}$]; C' is a coefficient considering the given mass of

the icebreaker; k is a coefficient depending upon the ice class of the icebreaker[1] [1]; β is the angle of inclination between the tangential tc the frame at the point of impact and the vertical; α is the angle between the tangential to the waterline at the point of impact and the center line.

The quantities $\underline{l}_1$ and $\underline{m}$ are found according to the formulas:

$$l_1 = 0{,}01\alpha m, \quad (3)$$

$$m = 1{,}6\cos\beta + 0{,}11. \quad (4)$$

The coefficient C', entering into formulas (1) and (2), strictly speaking, is expressed as a complex dependence upon the hull shape, the ratios of the principal dimensions and the coordinates of the point of impact. However, specially conducted calculations demonstrated that the coefficient C' is basically a function of the angle β and the coordinates of the point of impact and it depends only weakly upon the other parameters determining the shape of the lines (the ratios of the principal dimensions L/B, B/T, L/H, the coefficients of fineness, coefficient of fineness of the water line, etc.). Therefore, for the point under consideration we may assume that C' is only a function of the angle β, i.e.,

The values of $C' = \varphi(\beta)$ for various theoretical frames are given in Figure 5, a, of the work mentioned above.

By means of formulas (3) and (4), we convert expressions (1) and (2)

$$q_н = k_q f(\alpha) f_1(\beta), \quad (5)$$

$$p_н = k_p f(\alpha) f_2(\beta), \quad (6)$$

where

$$k_q = 0{,}084\,(0{,}01)^{4/3} \cdot D^{5/3} v_s^{4/3} \sigma_c^{2/3}; \quad (7)$$

$$k_p = 10^{-2} k L^{4/3}; \quad (8)$$

$$f(\alpha) = \alpha^{4/3}; \quad (9)$$

1. For powerful icebreakers (class I) k = 30.5; for intermediate icebreakers (class II) k = 24; for auxiliary or small icebreakers (class III) k = 18.

$$f_1(\beta) = \frac{(1.6\cos\beta + 0.11)^{4/3}}{(C')^{5/3}\sin^{5/3}\beta\cos^{1/3}\beta}; \tag{10}$$

$$f_2(\beta) = \frac{(1.6\cos\beta + 0.11)^{4/3}}{(C')^{2/3}} = f_1(\beta)\sin^{2/3}\beta\cos^{2/3}\beta. \tag{11}$$

For investigation of the effect of the lines on the ice loads of the icebreaker, we will assign the bow branch of the waterline by the equation

$$y = F(x) = 0{,}5B\left[1 - \left(\frac{x}{0{,}5L}\right)^2\right]\left[1 - b\left(\frac{x}{0{,}5L}\right)^2\right], \tag{12}$$

where B is the beam of the icebreaker; L is the length of the icebreaker; and b is a parameter determining the fineness of the area of the bow part of the waterline.

For a real ship's surface, equation (13) must satisfy two conditions:

$$\begin{aligned} &\frac{\partial y}{\partial x} \leqslant 0 \text{ at } \quad x = 0{,}5L, \\ &\frac{\partial^2 y}{\partial x^2} \leqslant 0 \text{ at } \quad x = 0. \end{aligned} \tag{13}$$

The first condition signifies that the curve y = F(x) must not intersect the axis x in the interval $0 < x < 0.5$ L, the second condition requires the presence of a maximum of the function F(x) at point x = 0, i.e., at the midship section.

Conditions (13) impose limitations on the magnitude of the parameter b, which must lie within limits

$$-1 \leqslant b \leqslant +1. \tag{14}$$

The coefficient of fineness of the bow part (forward part) of the waterline is determined in the following manner:

$$\alpha_н = \frac{\int_0^{0,5L} F(x)\,dx}{0{,}5L0{,}5B}.$$

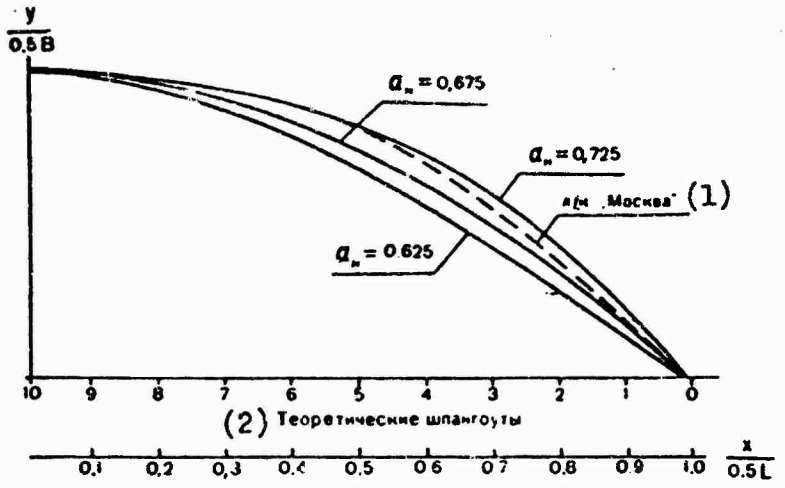

Figure 1. Shapes of the bow branch of the waterlines of various icebreakers. 1) icebreaker "Moskva"; 2) theoretical frames.

After integration we obtain

$$\alpha_n = \frac{2}{15}(5 - b). \tag{15}$$

With a consideration of condition (14), we find the possible limits of the variation of α_n

$$0{,}533 \leqslant \alpha_n \leqslant 0{,}800.$$

In Figure 1 waterlines are represented as assigned by equation (12), and the waterline of the icebreaker "Moscow", reduced to the dimensionless form with respect to beam and length. We should note that expression (12) embraces the entire range of shapes of the waterlines of existing icebreakers.

For determination of the magnitude of the angle α we differentiate equation (12) with respect to x. We find

$$\frac{\partial y}{\partial x} = \operatorname{tg}\alpha = \frac{B}{L}\left[-(1+b)\frac{2x}{0{,}5L} + 4b\left(\frac{x}{0{,}5L}\right)^3\right], \tag{16}$$

from whence

$$\alpha = \operatorname{arctg}\frac{2B}{L}\frac{x}{0{,}5L}\left[-(1+b) + 2b\left(\frac{x}{0{,}5L}\right)^2\right] \tag{17}$$

or, with consideration of expression (15)

$$\alpha = \operatorname{arctg} \frac{2B}{L} \frac{x}{0{,}5L} \left[-\frac{3}{2}(4 - 5\alpha_n) + 5(2 - 3\alpha_n)\left(\frac{x}{0{,}5L}\right)^2 \right]. \tag{18}$$

We note that in the selected analytical method of assignment of the waterline by means of equation (12), a value of the relative coordinate x/0.5L exists (except x/0.5L = 0), at which the angle α (or tgα) does not depend upon the coefficient of fineness of the forward branch of the waterline, α_n (or upon the parameter b). Actually, having differentiated expression (16) with respect to the parameter b and having equalized it to zero, we obtain

$$\frac{\partial}{\partial b}\left(\frac{\partial y}{\partial x}\right) = \frac{B}{L}\left[-\frac{2x}{0{,}5L} + 4\left(\frac{x}{0{,}5L}\right)^3 \right] = 0.$$

From this we find that at x/0.5L = 0.707 the angle α does not depend upon the parameter b.

In the analysis of the effect of the hull lines on the ice loads we will consider that for the selected range of the variation of the parameters L/B and α_n the angles β of inclination of the frames do not depend upon the shape of the waterline. We will also assume that the effect of each parameter being investigated on the ice load does not depend upon the other parameters. As a standard we will assume an icebreaker in which $(L/B)_0 = 4.5$; $\alpha_n = (\alpha_n)_0 = 0.675$, and the angles β are assigned as the average of the three curves $\beta_0 = \psi_0(x/0.5L)$, which are graphically presented in Figure 2 (also see Table 1).

Then the ratio of the ice loads on the side framing and shell plating for the icebreaker being investigated and the standard icebreaker may be written in the following manner:

$$\frac{q_н}{(q_н)_0} = \frac{k_q f(\alpha) f_1(\beta)}{(k_q)_0 f(\alpha_0) f_1(\beta_0)}, \tag{19}$$

$$\frac{p_н}{(p_н)_0} = \frac{k_p f(\alpha) f_2(\beta)}{(k_p)_0 f(\alpha_0) f_2(\beta_0)}. \tag{20}$$

The quantities entering into these expressions are determined according to formulas (7)--(11).

Table 1

Values of Angles of Inclination of Theoretical Frames

(1) Углы наклона (градусы)	(2) Теоретические шпангоуты									
	1	2	3	4	5	6	7	8	9	10
(3) β_1 (форма 1)	50	48	44	38	32,5	27	23	20,5	20	20
(4) β_0 (форма 0)	40	37	32	27	22	18	16	15	15	15
(5) β_2 (форма 2)	30	25	20	16	12,5	10,5	9	8	8	8

Key: 1) angles of inclination (degrees); 2) theoretical frames; 3) β_1 (shape 1); 4) β_0 (shape 0); 5) β_2 (shape 2).

The effect of the coefficient of fineness of the area of the forward part of the waterline was investigated for values of α_n = 0.625; 0.650; 0.675; 0.700; 0.725; and 0.750 at L/B and $\beta = \psi(x/0.5L)$, accepted for the standard icebreaker (see Figure 2, center curve), i.e.,

$$\frac{L}{B} = \left(\frac{L}{B}\right)_0 = 4{,}5;$$

$$\beta = \beta_0 = \psi_0\left(\frac{x}{0{,}5L}\right).$$

The effect of the ratio of the beam of the icebreaker to its length was determined for L/B = 3.5; 4.0; 4.5; and 5.0 at $\alpha_n = (\alpha_n)_0 = 0.675$ and $\beta = \beta_0 = \psi_0(x/0.5L)$.

In turn, the effect of the variation of angles of inclination of the side to the vertical was investigated for three hull shapes, differing in angles β of inclination of the side at $L/B = (L/B)_0 = 4.5$ and $\alpha_n = (\alpha_n)_0 = 0.675$. The values of the functions $\beta = \psi(x/0.5L)$ are given in Figure 2 and Table 1.

The curves β_1 and β_0 characterize icebreakers having, respectively, large and moderate inclinations of the frames from the center line. The curve β_2 may, to a certain degree, determine the shape of the frames of certain icebreaking tugs (class UL and L) with small angles of inclination of the frames to the vertical. The range of variation of the parameters α_n, L/B and $\beta = \psi(x/0.5L)$ accepted for analysis entirely embraces the existing shapes of the lines of icebreakers in the region of the design waterline.

Assuming that the displacement D, the length L, the ice class, the speed v_s and the ice conditions for navigation of the given icebreaker and the standard icebreaker are identical, we will obtain the following calculation formulas for calculation of the coefficients of the effect of the parameters of shape being investigated on ice loads.

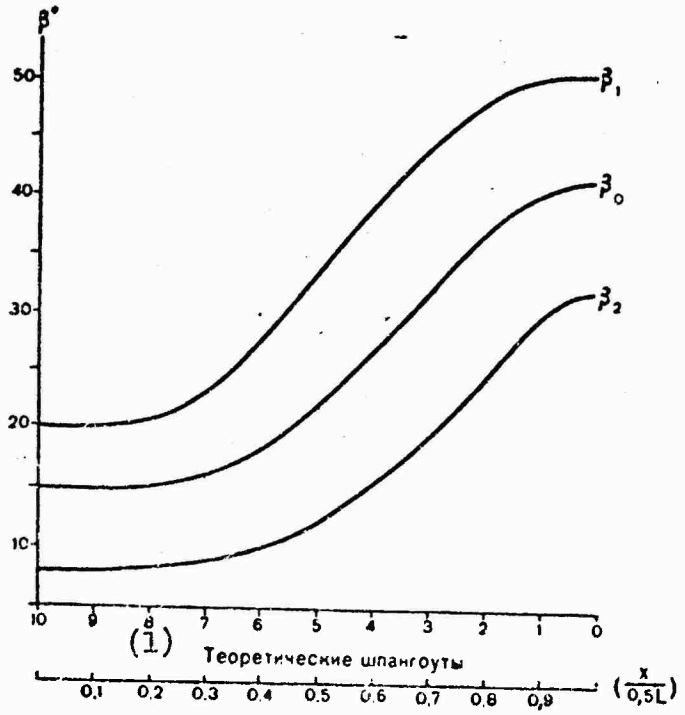

Figure 2. Values of the function $\beta = \psi(x/0.5L)$ for the lines of the standard icebreaker (β_0); icebreaker lines (β_1) and semi-icebreaker lines (β_2).
1) theoretical frames.

For the side framing:

the coefficient considering the effect of α_n is

$$a_{\alpha_н} = \frac{q_н}{(q_н)_0} = \frac{f(\alpha)}{f(\alpha_0)} =$$

$$= \left\{ \frac{\operatorname{arctg} \frac{2B_0}{L_0} \frac{x}{0,5L} \left[-\frac{3}{2}(4 - 5\alpha_н) + 5(2 - 3\alpha_н)\left(\frac{x}{0,5L}\right)^2 \right]}{\operatorname{arctg} \frac{2B_0}{L_0} \frac{x}{0,5L} \left\{ -\frac{3}{2}[4 - 5(\alpha_н)_0] + 5[2 - 3(\alpha_н)_0]\left(\frac{x}{0,5L}\right)^2 \right\}} \right\}^{n_1} \qquad (21)$$

the coefficient considering the effect of L/B, is

$$a_{L/B} = \frac{q_н}{(q_н)_0} = \left\{ \frac{\operatorname{arctg}\frac{2B}{L}\frac{x}{0{,}5L}\left\{-\frac{3}{2}[4-5(\alpha_н)_0]+5[2-3(\alpha_н)_0]\left(\frac{x}{0{,}5L}\right)^2\right\}}{\operatorname{arctg}\frac{2B_0}{L_0}\frac{x}{0{,}5L}\left\{-\frac{3}{2}[4-5(\alpha_н)_0]+5[2-3(\alpha_н)_0]\left(\frac{x}{0{,}5L}\right)^2\right\}} \right\}^{n}, \quad (22)$$

the coefficient considering the effect of the angles β of inclination is

$$a_\beta = \frac{q_н}{(q_н)_0} = \frac{f_1(\beta)}{f_1(\beta_0)} = \left(\frac{1{,}6\cos\beta + 0{,}11}{1{,}6\cos\beta_0 + 0{,}11}\right)^{1/3}\left(\frac{C_0'}{C'}\right)^{2/3}\left(\frac{\sin\beta_0}{\sin\beta}\right)^{2/3}\left(\frac{\cos\beta_0}{\cos\beta}\right)^{2/3}. \quad (23)$$

From the structure of formulas (5) and (6) it is apparent that the effect of the parameters α_n and L/B on the ice load for the outer-shell plating and side framing is identical, i.e.,

$$a_\alpha' = \frac{p_н}{(p_н)_0} = a_\alpha, \quad (24)$$

$$a_{L/B}' = \frac{p_н}{(p_н)_0} = a_{L/B}. \quad (25)$$

The effect of the angles β of inclination on the magnitude of the ice load for the external shell plating is determined by the coefficient

$$a_\beta' = \frac{p_н}{(p_н)_0} = \left(\frac{1{,}6\cos\beta + 0{,}11}{1{,}6\cos\beta_0 + 0{,}11}\right)^{1/3}\left(\frac{C_0'}{C'}\right)^{2/3}. \quad (26)$$

In formulas (21)--(26)

$$\left(\frac{L}{B}\right)_0 = 4{,}5;$$

$$(\alpha_н)_0 = 0{,}675;$$

$\beta_0 = \psi_0(x/0.5L)$ is determined according to the curve given in Figure 2 (center curve).

The values of the coefficients $a_\alpha = a_\alpha'$; a_β and a'_β , depending upon the relative coordinate, are given in Figures 3 and 4.

The values of the coefficients $a_{L/B} = a'_{L/B}$ are given below:

L/B	3,50	3,75	4,00	4,25	4,50	4,75	5,00	5,25	5,50
$a_{L/B}$	1,220	1,155	1,100	1,045	1,000	0,955	0,920	0,885	0,855

As is apparent from Figure 3, the coefficients of fineness of the forward part of the waterline essentially affect the magnitude of the ice load, acting on the side framing and the outer shell plating, with the exception of a small section near the third theoretical frame. In the region located toward the bow from the third theoretical frame, a decrease in α_n leads to a decrease in the ice load (the coefficient a_α is decreased). Such a decrease in the ice loads is especially noticeable in the vicinity of the first theoretical frame. With a change of α_n from 0.725 to 0.625, i.e., by 16%, the ice load at the first theoretical frame decreases by more than 30%.

For the region located aft of the third theoretical frame, a decrease in α_n leads to an increase in the ice load (the coefficient a_α increases). This increase enlarges as we approach the midship section. Thus, for example, with a change of α_n from 0.725 to 0.625, the ice load at the fifth frame increases by approximately 30%, and at the seventh frame by 50%. Such a dependence of the ice load upon α_n is explained by the corresponding change of the angles α between the tangential to the waterline and the center line.

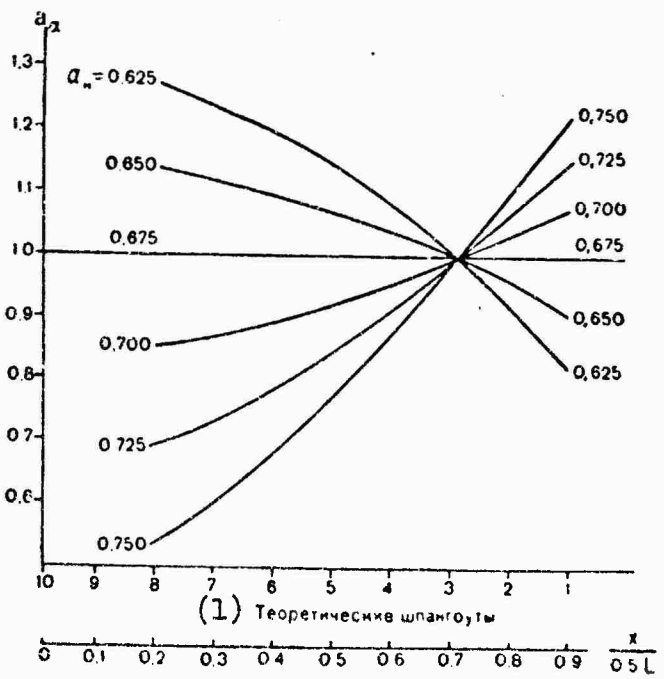

Figure 3. Values of the coefficients a_α. 1) theoretical frames.

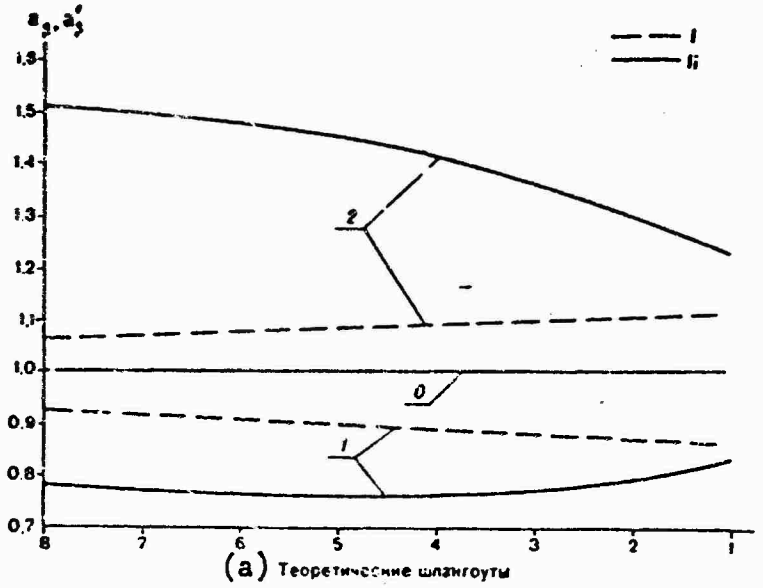

Figure 4. Dependence of the coefficient a_β and a'_β for the side shell plating (I) and the side framing (II) upon the semi-icebreaker shape of the lines (2), the standard icebreaker (0) and the icebreaker shape (1). a) theoretical frames.

An increase in the L/B ratio leads to a monotonous decrease in the ice loads and, as the calculations demonstrated, the effect of L/B is practically independent of the relative coordinate x/0.5L (i.e., upon the number of the theoretical frame). A change in the L/B ratio has a somewhat weaker effect on the ice load than α_n. Thus, with an increase in L/B from 3.5 to 5.5, i.e., by a factor of almost 1.6, the coefficient $a_{L/B}$ (or, in other words, the ice load) decreases by 35%.

In Figure 4 curves of the coefficients a_β and a'_β are presented, illustrating the effect of the inclination of the side (the angle β) upon the ice loads, which decrease with an increase of this angle. A change in the angles of inclination of the frames essentially effects the loads for the side framing and weakly affects the load for the side shell plating. Thus, in the transition from an icebreaker shape to a semi-icebreaker shape (the two extreme shapes) the loads on the shell plating increase by an average of 20%, and the load on the side framing by 40% (at the bow end) and by 70% (in the vicinity of the seventh and eighth theoretical frames).

The comparatively weak dependence of the load on the shell plating upon the angles β of inclination of the frames is explained by the assumption made in the derivation of formula (2) that the intensity of the ice stresses applied to the shell plating depends upon the shape of the hull only to the de-

gree to which it affects the force of the impact, i.e., that it affects the bound mass of the ship and the given speed. The geometry of the warping of the edge of the ice at the point of impact, which is a function of β, has no noticeable effect on the magnitude of the ice load on the shell plating.

Thus, the results of the given theoretical investigations demonstrate that the hull lines have an essential effect on the magnitude of the impact loads originating in the forward part of the hull. The dependences obtained may be used in the process of designing the hull lines of icebreakers and in the determination of ice loads.

BIBLIOGRAPHY

1. Kashtelyan, V. I., Ryvlin, A. Ya., Faddayev, O. V., and Yagodkin, V. Ya., Ledokoly (Icebreakers), Leningrad,"Sudostroyeniye", 1972.

2. Popov, Yu. N., Faddayev, O. V., Kheysin, D. Ye., and Yakovlev, A. A., Prochnost' sudov plavayushchikh vo l'dakh (Strength of ships floating in ice), Leningrad, "Sudostroyeniye", 1967.

DETERMINATION OF THE ICE LOADS ON AN ICEBREAKER'S HULL WITH CONSIDERATION OF REFLECTED IMPACT

Yu. N. Popov, T. Kh. Tegl.areva, and O. V. Faddayev pages 88-99

The theoretical method of the determination of ice loads acting on a hull in the impact of a ship against ice, and also a practical method of the calculation of these loads, were explained in reference [2]. On the basis of this method, at the Arctic and Antarctic Scientific Research Institute, special requirements have been developed for the classification and construction of icebreakers and ships intended for ice navigation [3], regulating the magnitude of the calculated forces acting on the side framing and shell plating. In this case, the loads at the forward end were determined with a consideration of the impact of the hull by various sections of the side against the ice field, the mass of which was assumed to be much greater than the mass of the ship.

In practice of navigation in ice, cases are possible when a ship, having first struck one side against the ice field and received an impulse, is deflected to the side, and then strikes against the ice with the other side. The so-called "reflected" impact occurs. It may turn out that the projection on the normal of the velocity of a point of the side at which the second, "reflected" impact falls, i.e., the given speed, will be greater than in an ordinary impact by the same point of the side. In connection with this, the contact forces which may be the cause of damage to the hull essentially increase. We will note that, other things being equal, the intensity of the ice load in a reflected impact will be greater if the interval of time between the first and second impacts is shorter. Damages to hull structures as a result of reflected impacts most frequently fall in a region located between the third and sixth theoretical frame, although damages are also possible at other places on the hull.

A reflected impact was theoretically investigated in reference [2]. For practical calculations in this work a simplified formula is proposed,

obtained on the basis of the assumption that the effect of the rate of floatation and the angular velocities corresponding to the list and trim, which originate as the result of the first impact, on the magnitude of the given velocity of the reflected impact is insignificant. However, the use of this formula leads to noticeable errors (up to 25%) in certain cases and, in particular, to an exaggeration of the reduced velocities in the vicinity of the first to third theoretical frames and an understatement of them in the section arranged aft of this region.

In this article, a general formula is proposed for determination of the given velocity of the reflected impact and the corresponding ice loads.

Since the calculation of the given velocity is associated with quite cumbersome calculations, in the future it is advisable to consider the reflected impact by means of the introduction of corrections into the ice loads, which are determined for an ordinary impact of the ship against an ice field. These corrections were obtained on the basis of an analysis of the results of the calculation of the given velocities of the reflected impact for Soviet-built icebreakers and ships of the ULA category. We will recollect that in the derivation of the formula for the given velocity of the reflected impact all the assumptions accepted for solution of the problem of the collision of a ship's hull with an ice floe in Section 2, Chapter II of reference [2] were used. It was also assumed that the interval of time and the displacement of the ship between the first and second impact are insignificant[1]. In this case we need not consider the resistance forces and the righting forces acting on the ship in the interval between the impacts. Thus, the velocities of the ship obtained after the first impact are assumed as the initial quantities for determination of the given velocity of the reflected impact.

We will arrange the coordinate axes connected with the ship so that the beginning of the coordinate coincides with the center O of gravity of the ship, the axis x is directed toward the bow, the axis y toward the starboard side, and the axis z vertically upward. We will assume that the center O of gravity lies on the plane of the load line. Up to the first impact, the ship was moving in a translational manner, with a speed (velocity) v_0 in the direction of the axis x. Let us assume that the first time the ship struck the ice with its starboard side at a point with coordinates x_1, y_1, and z_1 ($z_1 = 0$), as a result of which the effect of the impulse S, the ship began to move, having all six degrees of freedom. We will designate the projection of the velocity of the center of gravity as v_1, u_1, w_1 and the projections of the angular velocity of the ship on the coordinate axes after impact as p_1, q_1, and r_1. By using

1. It is assumed that this interval of time is considerably less than the period of the rolling, pitching, and heaving of the ship.

the results given in Section 5 of Chapter II in reference [2], we may obtain the following expressions for the velocity components of the ship:

$$\left.\begin{aligned} v_1 &= v_0\left[1-\frac{l_1^2}{C'(1+\lambda_{11})}\right], \\ u_1 &= -\frac{v_0 l_1 m_1}{C'(1+\lambda_{22})}, \\ w_1 &= -\frac{v_0 l_1 n_1}{C'(1+\lambda_{33})}, \\ p_1 &= -\frac{v_0 l_1 \lambda_1}{C'\frac{I_x}{M}(1+\lambda_{23})}, \\ q_1 &= -\frac{v_0 l_1 \mu_1}{C'\frac{I_y}{M}(1+\lambda_{13})}, \\ r_1 &= -\frac{v_0 l_1 \nu_1}{C'\frac{I_z}{M}(1+\lambda_{12})}. \end{aligned}\right\} \qquad (1)$$

In system of equations (1) the following symbols are used: l_1; m_1; and n_1 are the cosines of the angles between the normal to the surface of the side at the point of impact (x_1, y_1, $z_1 = 0$) and the coordinate axes;

$$\left.\begin{aligned} \lambda_1 &= y_1 n_1 \\ \mu_1 &= -x_1 n_1 \\ \nu_1 &= x_1 m_1 - y_1 l_1 \end{aligned}\right\}$$ are the arms of the impact pulse;

M is the mass of the ship; I_x; I_y; and I_z are the moments of inertia of the mass relative to the coordinate axes; λ_{ij} are the coefficients of the bound masses and the moments of the bound masses of water; C' is a coefficient considering the given mass of the ship during the impact.

The coefficient C' is determined according to the well-known formula

$$C' = \frac{l_1^2}{1+\lambda_{11}} + \frac{m_1^2}{1+\lambda_{22}} + \frac{n_1^2}{1+\lambda_{33}} + \left[\frac{\lambda_1^2}{I_x(1+\lambda_{23})} + \frac{\mu_1^2}{I_y(1+\lambda_{13})} + \frac{\nu_1^2}{I_z(1+\lambda_{12})}\right] M. \qquad (2)$$

Let us assume that the reflected impact occurs with the port side and falls at a point with coordinates x_2, y_2 and $z_2 = 0$, where the cosines of the angles between the external normal and the axes of the coordinates will be:

l_2, m_2 and n_2. Then the projection of the velocity of point (x_2, y_2, z_2) onto the direction of the external normal, i. e., the given velocity of the reflected impact, is found according to the formula[1]

$$v_{отр} = v_1 l_2 + u_1 m_2 + w_1 n_2 + p_1 \lambda_2 + q_1 \mu_2 + r_1 \nu_2. \tag{3}$$

[$v_{отр} = v_{otr} = v_{reflected}$]

Having substituted the value of the velocities determined by the dependences (1), after transformation we obtain

$$v_{отр} = v_0 l_{отр}, \tag{4}$$

where l_{otr} is the coefficient of the given velocity in a reflected impact, which is found according to the expression

$$l_{отр} = l_2\left[1 - \frac{l_1^2}{C'(1+\lambda_{11})}\right] - \frac{l_1}{C'}\left(\frac{m_1 m_2}{1+\lambda_{22}} + \frac{n_1 n_2}{1+\lambda_{33}}\right) - \tag{5}$$
$$- \frac{l_1}{C'}\left[\frac{y_1 y_2 n_1 n_2}{I_x(1+\lambda_{23})} + \frac{x_1 x_2 n_1 n_2}{I_y(1+\lambda_{13})} + \frac{(x_1 m_1 - y_1 l_1)(x_2 m_2 - y_2 l_2)}{I_z(1+\lambda_{12})}\right] M.$$

The cosines of the angles between the normals to the surface of the hull at the points of impact entering into formula (5) may be determined for the system of coordinates accepted, according to the following formulas obtained from geometrical considerations

$$\left.\begin{aligned} l_1 &= l_2 = \sin\alpha\cos\beta', \\ m_1 &= -m_2 = \cos\alpha\cos\beta', \\ n_1 &= n_2 = -\sin\beta', \end{aligned}\right\} \text{ at } \quad x_1 = x_2, \tag{6}$$

where α is the angle between the tangential to the waterline at the point of impact and the center line; $\beta' = \operatorname{arctg}(\operatorname{tg}\beta\cos\alpha)$ is the angle of inclination of the side to the vertical (on a plane normal to the side); and β is the angle between the tangential to the frame at the point of impact and the axis z.

The angles α and β for various points are taken from the design. We note that for the system of axes accepted, the coordinate y_2 in formula (5) must be assumed with a minus sign. To find the ice loads, with consideration of the reflected impact, it is necessary to calculate the maximum values

1. The subscript "1" refers to the first impact, and the subscript "2" to the second impact.

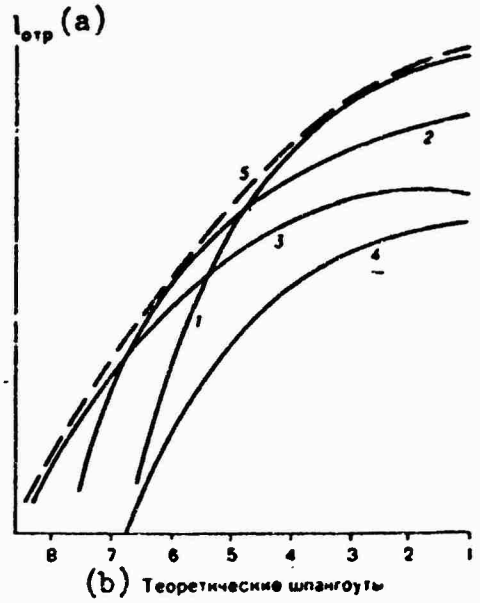

Figure 1. Determination of $(l_{отр})_{max}$ in the first impact at various theoretical frames: at the first (1), at the second (2), at the third (3), at the fourth (4), and (5), the value of $(l_{отр})_{max}$. a) $l_{отр}$; b) theoretical frames.

of $l_{отр}$. For this, in sequence, the values of $l_{отр}$ are determined at impact by various points of the starboard side (first impact), and a series of curves of $l_{отр} = f(x_2)$ at various values of x_1 is constructed (Figure 1). The maximum values of $(l_{отр})_{max}$ are taken from the envelope of these curves (--- in Figure 1).

Ice loads, with a consideration of reflected impact, are determined according to the dependences in Chapter III of reference [2], if into them we substitute the magnitude of $(l_{отр})_{max}$ instead of l_1. The (running) load on the side framing is

$$q_н = 0{,}084 \frac{D^{2/3}}{(C')^{2/3}} \frac{v_s^{4/3} v_c^{2/3} (l_{отр})_{max}^{1/3}}{\sin^{2/3}\beta \cos^{2/3}\beta}. \quad (7)$$

The load on the side shell plating (uniformly distributed throughout the area) is

$$p_н = \frac{L^{2/3}}{(C')^{2/3}} (l_{отр})_{max}^{1/3} \frac{100^{4/3}}{10^2} k. \quad (8)$$

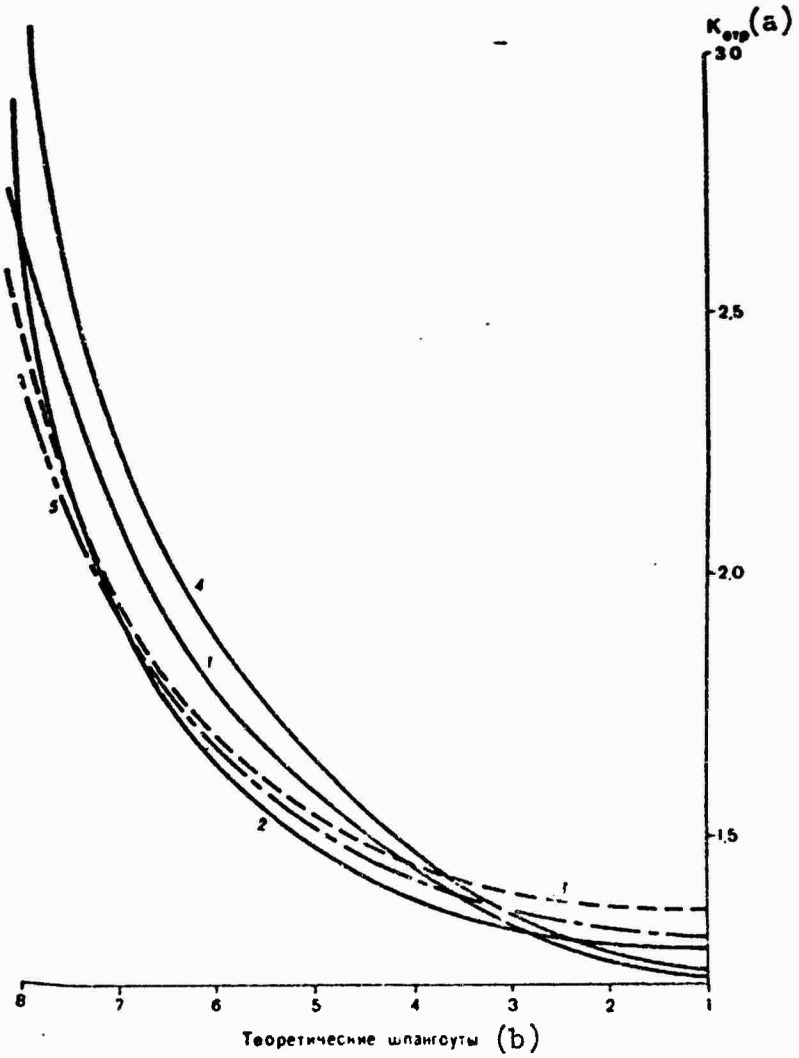

Figure 2. Values of $k_{отр} = \frac{(l_{отр})^{4/3}_{max}}{l^{4/3}_{1}}$ for icebreakers with stern screws: 1) "Moskva"; 2) "Sibir'"; 3) "Krasin"; 4) "Sibiryakov"; and 5) "Yermak". a) k_{otr}; b) theoretical frames.

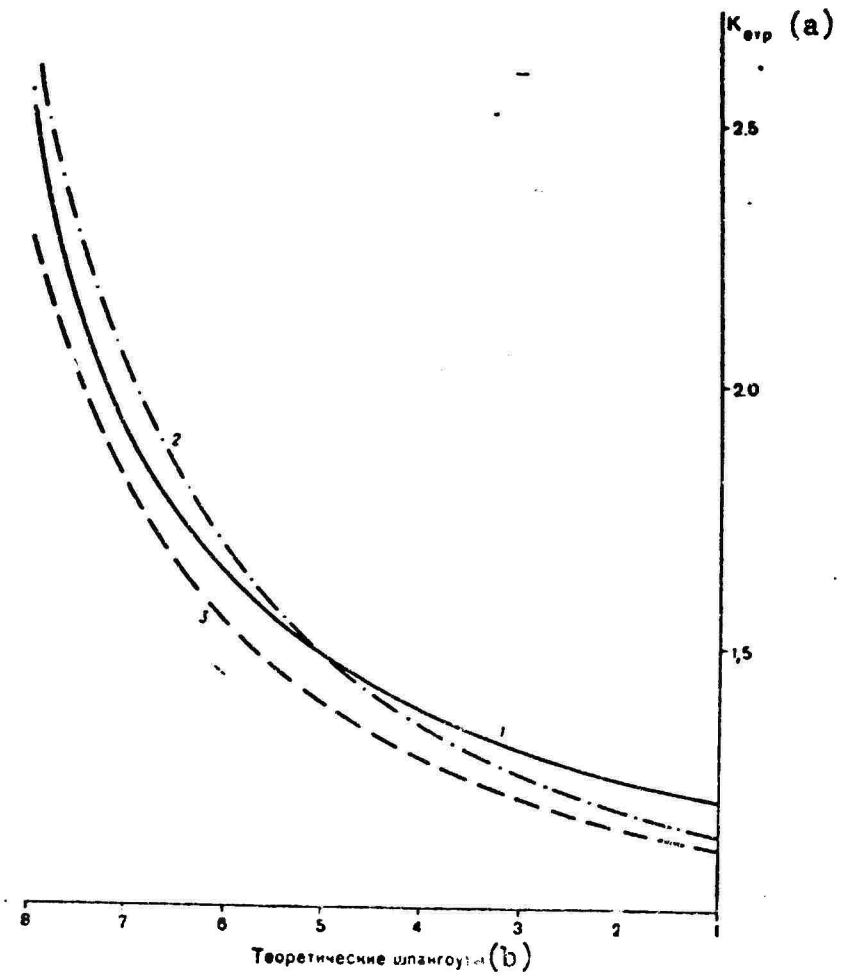

Figure 3. Values of $k_{отр} = \frac{(l_{отр})^{4/3}_{max}}{l_1^{4/3}}$ for icebreakers with bow and stern screws: 1) "Kapitan Belousov"; 2) "Vasiliy Pronchishchev"; and 3) "Il'ya Muromets". a) k_{otr}; b) theoretical frames.

In formulas (1) and (2) the following symbols are used: D is the displacement of the icebreaker, in tons; L is the length of the icebreaker, in meters; v_s is the speed at the beginning of the first impact, in knots; σ_s is the temporary resistance of the ice to warping, tons per square meter; and k is a coefficient depending upon the ice class of the icebreaker or transport vessel.

We will present formulas (7) and (8) in the form

$$q_n = \frac{0{,}094 D^{2/3} v_s^{4/3} \sigma_c^{2/3} l_1^{4/3}}{\sin^{2/3}\beta \cos^{2/3}\beta} \frac{k_{отр}}{(C')^{2/3}}, \tag{9}$$

$$p_n = 10^{-2} k L^{2/3} l_1^{4/3} \frac{k_{отр}}{(C')^{2/3}} 100^{4/3}, \tag{10}$$

where $k_{отр} = \frac{(l_{отр})_{max}^{4/3}}{l_1^{4/3}}$ is a coefficient considering the reflected impact of the icebreaker.

The coefficient l_1 of the given velocity of the first impact is determined according to formula (6) or, with an adequate degree of accuracy, according to the expression

$$l_1 = \frac{a^\circ}{100}(1{,}6\cos\beta + 0{,}11). \tag{11}$$

Dependences (9) and (10) differ from conventional formulas for determination of the ice loads only in the presence of the coefficient k_{otr}.

For finding k_{otr} according to formula (5), the values of $(l_{otr})_{max}$ were preliminarily calculated for a number of Soviet icebreakers, the principal elements and characteristics of which are given in Tables 1 and 2.

The results of calculations of $k_{отр} = \frac{(l_{отр})_{max}^{4/3}}{l_1^{4/3}}$ are presented in Table 3 and in Figures 2 and 3 (in the range from the first to the eighth theoretical frames). From these curves it is apparent that for various icebreakers the coefficients k_{otr} are close in magnitude and depend only upon the number of the theoretical frame, i.e., upon the coordinate x. The curve k_{otr} (see Figures 2 and 3) may be approximated with an adequate degree of accuracy by the following dependences:

$$k_{отр} = \frac{1{,}25}{\sqrt[3]{\frac{x_s}{0{,}5L}}} \tag{12}$$

Table 1

Ratios of Principal Dimensions and Coefficients of Fineness of Various Icebreakers

(1) Ледокол	L/B	B/T	L/H	δ	α	β
(2) „Москва"	4,78	2,47	8,03	0,511	0,742	0,853
(3) „Сибирь"	4,51	2,51	8,10	0,504	0,720	0,845
(4) „Красин"	4,42	2,93	7,33	0,525	0,721	0,855
(5) „Ермак"	4,44	2,90	7,36	0,530	0,700	0,860
(6) „Сибиряков" . . .	4,08	2,88	7,72	0,520	0,735	0,820
(7) „Капитан Белоусов"	4,14	3,02	8,16	0,490	0,700	0,820
(8) „Василий Прончищев"	3,54	3,18	7,47	0,447	0,687	0,780
(9) „Илья Муромец"	4,30	2,36	6,16	0,412	0,714	0,714
(10) д/э „Амгуема" . . .	6,65	2,43	10,60	0,643	0,880	0,949

Key: 1) icebreaker; 2) "Moskva"; 3) "Sibir'"; 4) "Krasin"; 5) "Yermak"; 6) "Sibiryakov"; 7) "Kapitan Belousov"; 8) "Vasiliy Pronchishchev"; 9) "Il'ya Muromets"; 10) diesel-electric icebreaking cargo vessel "Amguyema".

Table 2

Characteristics of the Hull Lines of Various Icebreakers

(1) Ледокол	(2) Углы	(3) Теоретические шпангоуты 1	2	3	4	5	6	7	8	9	10
(4) „Сибирь"	α	22	20,5	18	16	13	9	5,5	2,5	0,5	0
	β	39,5	37	33,5	29	24,5	21	19	18	18	18
(5) „Красин"	α	22	21	19	16,5	13,5	10	6,5	3,5	0,5	0
	β	40	39	34	27	21	18	16,5	15,5	15	15
(6) „Ермак"	α	22	20	17,5	15,5	13,0	10,5	6,0	3,5	0,5	0
	β	43	39,5	33	24	18	15	14	14	14	14
(7) „Сибиряков"	α	27,5	26	32	17	11,5	8	5	2,5	0,5	0
	β	38	36,5	20	27	23	20	19	18	18	18
(8) „Василий Прончищев"	α	29	29	26	26	14,5	10	6,0	3,5	1,0	0
	β	47,5	47	43	35	28,5	23	21	20	20	20
(9) „Илья Муромец"	α	28,5	29,5	25	20	15,5	11	7	4	1	0
	β	40,5	40,5	38,5	34,5	30	26	23	21	20	20
(10) д/э „Амгуема"	α	22	20	15,5	10	5	2	1	—	—	—
	β	42	38	29	15	10,5	8	8	—	—	—

Key: 1) icebreaker; 2) angles; 3) theoretical frames; 4) "Sibir'"; 5) "Krasin"; 6) "Yermak"; 7) "Sibiryakov"; 8) "Vasiliy Pronchishchev"; 9) "Il'ya Muromets"; 10) diesel-electric icebreaking cargo vessel "Amguyema".

for powerful and medium icebreakers (Class I and II) with stern screws [1],

$$k_{отр} = \frac{1{,}16}{\sqrt[3]{\frac{x_2}{0{,}5L}}} \qquad (13)$$

for medium and port icebreakers (Class II and III), having bow and stern screws.

Table 3

Values of k_{otr} for Various Icebreakers

(1) Теоретические шпангоуты	(2) „Москва"	(3) „Сибирь"	(4) „Красин"	(5) „Ермак"	(6) „Сибиряков"	(7) „Капитан Белоусов"	(8) „Василий Прончищев"	(9) „Илья Муромец"	(10) д/э „Амгуема"
1	1,22	1,26	1,35	1,28	1,24	1,20	1,14	1,13	1,28
2	1,25	1,27	1,36	1,33	1,27	1,26	1,17	1,13	1,33
3	1,34	1,35	1,40	1,40	1,34	1,32	1,22	1,19	1,41
4	1,46	1,41	1,47	1,45	1,45	1,38	1,34	1,30	1,63
5	1,58	1,46	1,54	1,52	1,66	1,49	1,48	1,39	2,16
6	1,79	1,67	1,68	1,59	1,87	1,64	1,68	1,54	3,32
7	2,11	1,92	1,97	1,94	2,27	1,88	2,06	1,81	4,97
8	2,74	2,92	2,55	2,41	3,36	2,55	2,62	2,29	—

Key: 1) theoretical frames; 2) "Moskva"; 3) "Sibir'"; 4) "Krasin"; 5) "Yermak"; 6) "Sibiryakov"; 7) "Kapitan Belousov"; 8) "Vasiliy Pronchishchev"; 9) "Il'ya Muromets"; 10) diesel-electric cargo vessel "Amguyema".

As was already noted[1], the coefficient C' is practically independent of the ratios of the principal dimensions and coefficients of fineness of icebreakers. Additional calculations demonstrate that the magnitude of $(C')^{2/5}$, entering into formulas (9) and (10) depends comparatively weakly upon the angle for the given coordinate x. Since in icebreakers the angles β for the given theoretical frame vary within comparatively small limits, we may assume that $(C')^{2/5}$ is a function of x only. In this case the quantity $(C')^{2/5}$ is well approximated by the formula

$$(C')^{2/5} = 0{,}74\left(1{,}05 + \frac{x_2}{0{,}5L}\right). \qquad (14)$$

1. See the article by Yu. N. Popov, T. Kh. Tegkayeva, and O. V. Faddeyev, "Effect of the lines of an icebreaker on the magnitude of ice loads," in this collection.

Considering expressions (11), (12) and (13), we may write:

for icebreakers of class I and II

$$\frac{k_{отр}}{(C')^{2/3}} = \frac{1,25}{0,74\left(1,05 + \frac{x_2}{0,5L}\right)\sqrt[3]{\frac{x_2}{0,5L}}}, \tag{15}$$

for icebreakers of class II and III (with bow screws)

$$\frac{k_{отр}}{(C')^{2/3}} = \frac{1,16}{0,74\left(1,05 + \frac{x_2}{0,5L}\right)\sqrt[3]{\frac{x_2}{0,5L}}}. \tag{16}$$

For the regions between the first and eighth theoretical frames, i.e., in the interval $0,2 \leq (x_2/0,5L) \leq 0,9$ formulas (15) and (16) may be presented adequately accurately in the following form:

for icebreakers of class I and II

$$f\left(\frac{x_2}{0,5L}\right) = \frac{k_{отр}}{(C')^{2/3}} = \frac{1,025}{0,24 + \frac{x_2}{0,5L}}, \tag{17}$$

for icebreakers of class II and III (with bow screws)

$$f\left(\frac{x_2}{0,5L}\right) = \frac{k_{отр}}{(C')^{2/3}} = \frac{0,952}{0,24 + \frac{x_2}{0,5L}}. \tag{18}$$

By using expressions (9), (10), and (11), and omitting the subscript 2 at x, we obtain the following formulas for determination of the impact ice load, with a consideration of reflected impact:

for the load on the side framing

$$q_н = 0,084D^{2/3}v_s^{4/3}\sigma_c^{2/3}(0,01\alpha^\circ)^{4/3}f\left(\frac{x}{0,5L}\right)f_q(\beta), \tag{19}$$

for the load on the side shell plating

$$p_н = 10^{-2}kL^{4/3}(\alpha^\circ)^{4/3}f\left(\frac{x}{0,5L}\right)f_p(\beta), \tag{20}$$

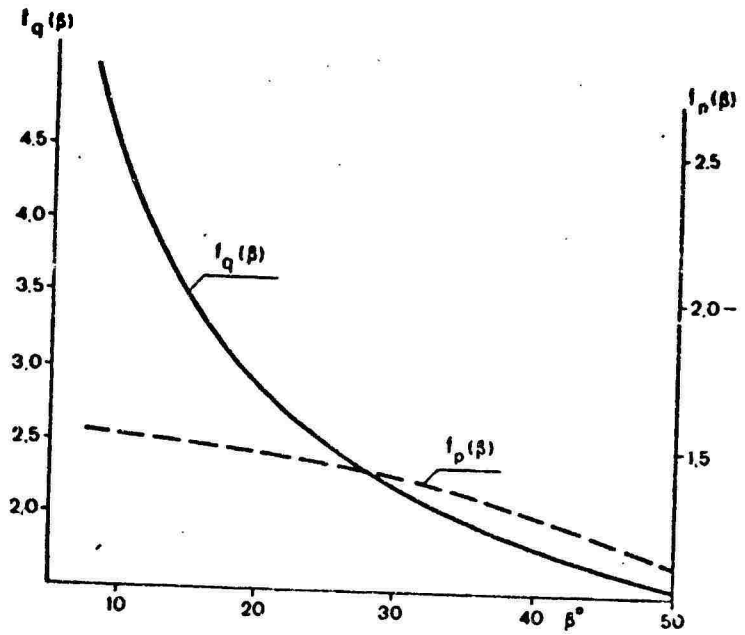

Figure 4. Functions $f_q(\beta)$ and $f_p(\beta)$.

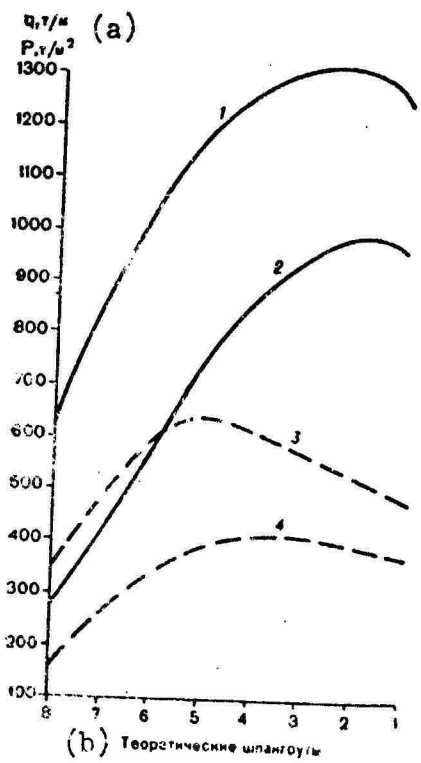

Figure 5. Values of ice loads on the side shell plating in reflected impact (1); in ordinary impact (2); on the side framing in reflected impact (3); and in ordinary impact (4). a) q, tons per meter; p, tons per square meter; b) theoretical frames.

where

$$f_q(\beta) = \frac{(1{,}6\cos\beta + 0{,}11)^{4/3}}{\sin^{5/3}\beta\cos^{1/3}\beta}; \quad (21)$$

$$f_p(\beta) = (1{,}6\cos\beta + 0{,}11)^{4/3}. \quad (22)$$

The quantity f(x/0.5L) is determined according to equation (17) or (18). For convenience in calculations, the functions $f_q(\beta)$ and $f_p(\beta)$ are given in Figure 4.

The ice loads of transport vessels of category ULA, having icebreaker lines, may be determined according to formulas obtained for icebreakers of classes II and III.

Analysis of formulas (20) and (21) demonstrates that in reflected impact the ice loads noticeably increase (by $\sim$ 40% for the shell plating and by $\sim$60% for the framing) in distinction from an ordinary impact, and the region where the impact loads have an effect has a greater length.

Example. Determine the ice loads on the side framing and outer shell plating of an icebreaker of class I for ordinary impact and reflected impact.

Initial data: D = 15,000 tons; L = 115 meters; v_s = 10 knots; σ_s = = 500 tons per square meter; k = 30.5.

The values of the angles α and β for various theoretical frames are given in Table 4.

Table 4

Angles α and β of Icebreaker being Calculated

(1) Угол, град	(2) Теоретические шпангоуты							
	1	2	3	4	5	6	7	8
α	23	21,5	18	14	10,5	7	4,5	2,5
β	40,5	39	35	28	21,5	18,5	18	18

Key: 1) angle, degrees; 2) theoretical frame.

We will find the magnitudes of the constants in formulas (19) and (20)

$$0{,}084\,(0{,}01)^{0{,}3}D^{0{,}6}v_c^{1{,}2}\gamma_c^{0{,}8} = 0{,}084\,(0{,}01)^{0{,}3}\cdot 15000^{0{,}6}\cdot 10^{0{,}24}\cdot 500^{0{,}8} \approx 26{,}1;$$
$$10^{-2}kL^{0{,}6} = 10^{-2}\cdot 30{,}5\cdot 115^{0{,}6} \approx 90{,}5.$$

We will perform further calculations by means of the data in Table 5, and also in this table for comparison the values of q_n and p_n in conventional impact are given. Curves of the ice loads on the framing and the shell plating are shown in Figure 5.

Table 5

Ice Loads in Direct and Reflected Impact for the Icebreaker Being Considered

(1) Характеристика	(2) Теоретические шпангоуты							
	1	2	3	4	5	6	7	8
$\frac{x_2}{0{,}5L}$	0,9	0,8	0,7	0,6	0,9	0,4	0,3	0,2
$(\alpha^c)^{0{,}6}$	12,3	11,7	10,1	8,3	6,6	4,8	3,3	2
$f\left(\frac{x}{0{,}5L}\right)$	0,900	0,986	1,089	1,218	1,381	1,583	1,882	2,300
$f_q(\beta)$	1,70	1,86	2,00	2,32	2,74	3,00	3,05	3,05
$f_p(\beta)$	1,25	1,28	1,32	1,40	1,46	1,48	1,48	1,48
$(q_н)_{отр}$	492	549	574	612	650	595	494	366
$(p_н)_{отр}$	1252	1336	1314	1281	1204	1017	881	616
$q_н$	380	410	415	405	395	352	262	170
$p_н$	980	990	935	860	760	600	442	289

Key: 1) characteristics; 2) theoretical frames.

The data obtained demonstrates that the magnitudes of the ice loads in reflected impact increase by ~40% for the side shell plating and by 60% for the side framing.

BIBLIOGRAPHY

1. Kashtelyan, V. I., Ryvlin, A. Ya., Faddayev, O. V., and Yagodkin, V. Ya., Ledokoly (Icebreakers), Leningrad, "Sudostroyeniye", 1972.

2. Popov, Yu. N., Faddayev, O. V., Kheysin, D. Ye., and Yakovlev, A. A., Prochnost' sudov plavayushchikh vo l'dakh (Strength of ships floating in ice), Leningrad, "Sudostroyeniye", 1967.

3. Trebovaniya k postroyke sudov ledovogo plavaniya i ikh klassifikatsiya (Requirements for the construction of ships intended for ice navigation and their classification), Leningrad, Izd. AANII, 1964.

THE STRENGTH OF ICEBREAKERS AND TRANSPORT VESSELS

(According to data from strain-gauge tests)

V. A. Likhomanov pages 100-110

Strain-gauge tests of the strength of the side framing and shell plating of ships, conducted by the Laboratory of the Ice Qualities of Ships since 1963, had as their purpose the estimation of the external forces acting on a hull during dynamic contacts of the side with ice, determination of the maximum stresses originating in shipboard structures in impacts against ice, and also the investigation of the operation of hull structures under the effect of ice loads.

In the process of the tests, a unified scheme of the arrangement of resistance strain gauges on the elements of the hull structures of transport vessels intended for ice navigation was developed, and in the processing of the results of the tests methods of mathematical statistics were applied for the first time. The purposes and the programs of the tests have expanded. Great attention has begun to be devoted to the investigation of the reaction of a ship's hull with the ice, as a function of the ice conditions of navigation. In this case, durations of contact of the side with the ice were determined, the length of the zone of the distribution of the load at the moment of impact against the ice, the distribution of the probability of the quantity of impact against the ice along the forward end of the ship, etc.

In the tests a regular strain-gauge apparatus was used, including loop oscillographs of type K-12-21 and 8-channel 8ANCh-7M amplifiers. As the master elements, electrical resistance strain-gauges of 100 and 200 ohms, with a base of 20 millimeters, were used.

The success of full-scale tests depends to a considerable degree upon the scheme of the arrangement of the frame gauges on the elements of the side framing. In the given tests, the strain pickups were arranged on the

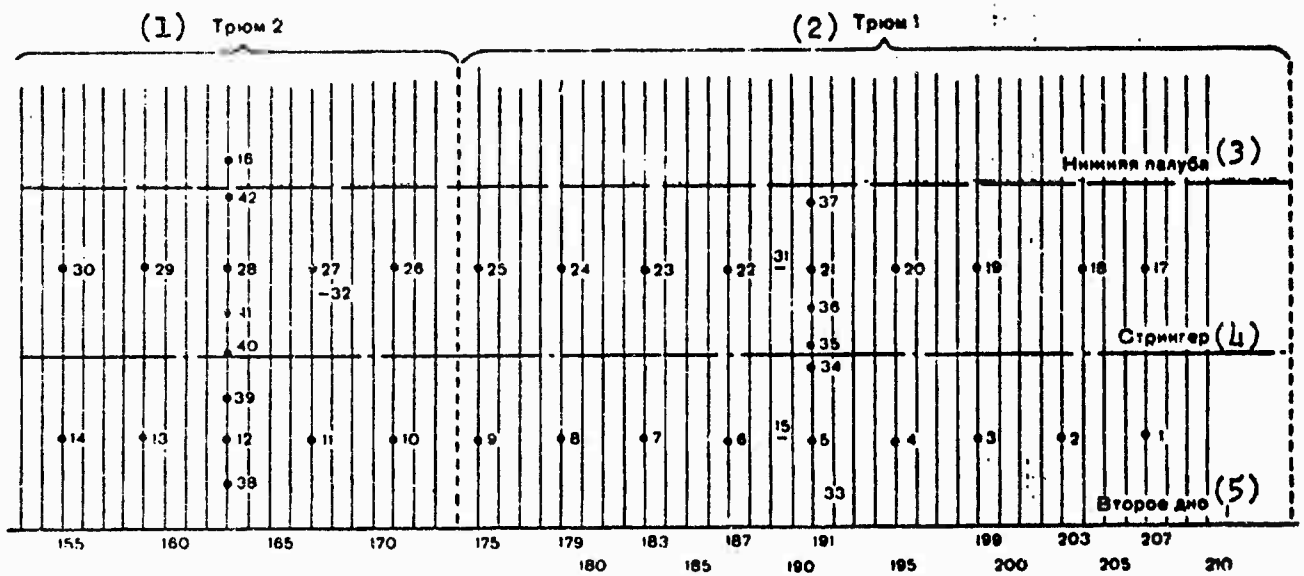

Figure 1. Diagram of the arrangement of strain-gauge pickup on the side framing and shell plating of the motorship "Olenegorsk". 1) No. 2 hold; 2) No. 1 hold; 3) lower deck; 4) stringer; 5) inner bottom.

side framing in a "cross": a horizontal line along the existing load line, and a vertical line along the molded depth along a frame (Figure 1).

The horizontal group of pickups usually consist of strain gauges located on the frame girders with an interval of two practical frame spacings, i.e., not more than 1.6 meter. Such a distance does not exceed the length of the zone of distribution of the ice load in dynamic contacts of the ship's side with the ice. Thus, the pickup of the horizontal line records each impact against the ice continuously over its entire extent.

The readings of the vertical group are used for the determination of the level of application of the ice load along the molded depth. The number and arrangement of the pickups on the frame are selected with such a calculation that it is possible to construct the curve of the distribution of the impact stresses along the height of the frame. Aside from the curves of the stresses determined for each specific case of loading, a curve is also constructed according to the average arithmetical values of stresses calculated for each pickup of the vertical group. Such a curve may be called the statistical curve of the stresses in the frame.

From an analysis of the readings of the pickup of the vertical groups it is apparent that the level of application of the ice load along the height of the side (molded depth) does not remain constant. With an increase in the thickness of the ice the region of application of the ice loads shifts downward from the existing waterline. Consequently, in order to bring the horizontal line of strain gauges closer to the region of maximum strains in the frames, it should be arranged somewhat below the existing load line (or ballast waterline). This requirement was fulfilled in the tests of the strength of the hulls of the motorship "Olenegorsk", the diesel-electric vessel "Navarin", the motorship "Barnaul", and others.

Sometimes the strain gauges are applied along the load line and the ballast waterline. If the region being monitored by the strain gauges extended to a considerable length, the vertical groups of pickups were arranged on two frames or more.

As experience in conducting full-scale tests demonstrated, the number of vertical lines should be increased to three-four groups, depending upon the length of the region being tested by strain gauges, and the variation of the angle of inclination of the frame to the vertical. At the same time, instead of two horizontal lines we may use one, arranging it 1.5--2 meters below the existing load line.

The diagram of the arrangement of the strain gauges in a "cross", apparently, is the most successful. It makes it possible, by means of a

small quantity of strain gauges, to obtain the greatest volume of information concerning the operation of the side covering and individual elements of it, in the effect of ice loads.

The scheme indicated for the arrangement of the strain gauges is applied only aboard transport vessels intended for ice navigation. In tests of the strength of the hulls of icebreakers, we cannot always use such a scheme, because of the side tanks and compartments, which hamper access to the side. Therefore, in tests of the strength of the hull of powerful Arctic and port icebreakers, in each case a separate scheme of the arrangement of the strain gauges was applied.

The general number of strain gauges aboard each ship is usually determined by the quantity of channels of the recording apparatus, synchronously recording the signals of the pickup. The time which the testing party has at its disposal for installation of the measuring circuit aboard the ship is also of great significance, especially aboard transport vessels, where installation operations can be conducted only in holds that are free of cargo. The installation of the pickups during cargo-handling operations in the hold is difficult. Aboard icebreakers the general quantity of strain gauges is regulated to a greater degree by the length of the sections of the side framing accessible for application of the pickups.

The strain gauges were attached until very recently to elements of the structure of the side framing by means of BF-2 or BF-4 cement. This operation was very laborious, since for acceleration of the process of polymerization of the cement, it was necessary to heat the places where the pickups were applied. Depending upon the thickness of the metal of the structure, the air temperature, and also the region where the strain gauge was arranged, the heating of each point in full-scale conditions lasted for three to four hours.

Aboard transport vessels the installation of a measuring circuit by the test party usually was performed in three to four days. In such a time period, we rarely succeeded in applying more than 25--30 pickups.

In the Laboratory of the Ice Qualities of Ships of the AANII, a new method of fastening the strain gauges to the side framing was developed. According to the new technology, the strain gauges are applied in laboratory conditions on a strip of steel foil with dimensions of 8 x 30 millimeters and a thickness of 0.15--0.2 millimeter. Aboard the ship, these strips are welded to the framing by contact point welding. The welding is accomplished around the perimeter of the plate, with a spacing of 1--1.5 millimeter. In this case, a special welding machine is used, which was fabricated in the work shops of the AANII according to drawings developed by the Central

Laboratory of Measuring Equipment (TsLIT) of the Izhorskiy Plant.

The new technology was successfully tested during the autumn-winter tests of 1970 aboard the diesel-electric vessel "Gizhiga". Only half as much time was expended on the installation of the strain gauges as usually was spent. Aside from this, the quality and reliability of the operation of the pickups was considerably improved. In the future in full-scale tests it is proposed to use only this method of fastening the strain gauges.

In estimating the strength of ships' hulls according to data from strain-gauge tests, it is necessary primarily to characterize the effect of ice loads on the framing of the hull, i.e., their duration, extent, etc.

An important characteristic of the dynamic contact of the side with the ice is the duration t of impact. The theoretical formula for the collision time in the impact of a ship against an ice floe with a curved edge has the form

$$t_{уд} = 1{,}61\,(A\sigma_c)^{-\frac{2}{5}} M_n^{\frac{2}{5}} v^{-\frac{1}{5}},$$

[$t_{уд} = t_{ud} = t_{impact}$] where A is a coefficient depending upon the shape of the ship's hull; σ_s [$\sigma_c = \sigma_s = \sigma_{warping}$] is the warping yield point of the ice; M_p is the given mass of the system of colliding bodies [$M_п = M_p = M_{given}$]; and v is the speed of the ship.

The processing of the results of tests conducted aboard various ships at different times demonstrated that on the average the duration of collision is quite accurately determined by the given formula. A comparison of the theoretical values of the collision time with experimental values obtained in tests of the icebreaker transport vessels of the "Amguyema" type are given below:

Duration of impact against ice (with an average speed of 6 knots):

with a curved edge (theoretical)..... 0.35

against fine broken ice of 8-10 balls (March 1970, diesel electric vessel "Vankarem", Sea of Okhotsk)..... 0.46

against solid sea ice, h = 40 centimeters, (November 1971, Kara Sea, diesel-electric vessel "Gizhiga")..... 0.51

against solid river fast ice, h = 40 centimeters (November 1971, river Yenisey, diesel-electric vessel "Gizhiga")..... 0.34

It was established that depending upon the ice conditions and the speed of the ship the duration of impact may amount to from 0.2 to 1 day or more. In motion in broken ice, the magnitude of c_{ud} decreases, and in solid ice (and especially when operating in short runs), it increases.

For estimation of the degree of the dynamic effect of the impact ice load, with relationship to hull structures of a ship, an investigation was made of the spectral characteristics of impact pulses according to the test data. It is known that in the spectrum of a short pulse of arbitrary shape frequencies satisfying the following condition predominate:

$$\omega < \omega_0 = \frac{2\pi}{t},$$

where t is the duration of impact.

Even for a pulse duration of t = 0.2 seconds, which is close to the minimum value, we obtain

$$\omega_0 = 31.4 \text{ radians per second} \simeq 5 \text{ gigahertz}.$$

The natural frequency of the first tone of the oscillations of the side framing structure usually considerably exceed the frequency ω_0. Therefore, for practical calculations we may assume that the ice load on the structures is statically applied.

The length of the zone of contact of the side of the ship with the ice in the impact was determined according to the oscillograms, by the synchronous pulse section method, at a fixed moment of time. In this case, the readings of the strain gauges of the horizontal lines were considered. It was established that the area of the application of the ice load is a limited quantity; it varies with respect to shape and dimensions as the edge of the ice is pressed down and broken. The zone of contact of the sides with the ice is extended several frame-spacings along the hull, and its length depends upon the lines of the ship at the place of impact against the ice, the speed, and the ice navigating conditions. Aside from this, the dependence of the length of the zone of contact upon the strength was found: with a decrease in the strength characteristics of the ice the length of the zone of contact increases.

For powerful icebreakers, moving in broken drifting ice, the length of the zone of contact is limited to 1.5--2.5 meters. In thick ice, when

breaking through ice fields and hummocks, the length of the zone of contact increases to 3 meters. In rare cases, the length of this zone may reach 5--6 meters. An increase in the length of the warping zone to 10--12 meters is noted only when icebreakers are wedged.

In transport vessels for ice navigation the length of the zone of contact is somewhat greater than in icebreakers. Usually the length of the zone of the distribution of the ice load is not less than three frame spacings, i.e., approximately 2 meters. In independent steaming of transport vessels in nearly solid and solid ice, and also when moving in a channel behind an icebreaker, the length of the zone of contract increases to 5--6 meters. The greatest length of the zone of contact with the ice for transport vessels was fixed in ice compression, when the load was applied statically. In this case, the length of the zone of contact increases to 10 meters or more.

Thus it was established that along the side the ice load is distributed in sections whose length is commensurable with the length of the overlapping. Therefore, for practical calculations of the strength of the side overlapping with various stringers on the ice load, the latter should be considered as distributed in part of the length of the stringer. In the calculations of the frame, the ice load should be considered as concentrated.

In order to estimate the work of the shell plating under the effect of the ice load, strain gauges were also cemented on the shell plating in the vicinity of the ice belt. In the tests of a number of ships, for determination of the relative deformations (strains) in longitudinal and transverse directions of the panel of the shell plating (within the limits of a frame spacing) the pickups were arranged in pairs at a right angle to each other. As we should expect, the deformations measured along the panel of the shell plating turned out to be small in comparison with the deformations in a transverse direction. This corresponds to the bending of the plates of the outer shell plating along a cylindrical form.

Since in the effect of an ice load the length of the zone of contact overlapped several frame spacings, the panel of the outer shell plating within the limits of one frame spacing may be considered as a plate rigidly fastened along the long sides of the support contour. With cylindrical bending of such a plate, the external pressure uniformly distributed within limits of the frame spacing s is determined by the equation

$$p = \frac{4h^2\sigma}{s^2},$$

where σ is the stress measured in the center of the span of the plate; and h is the thickness of the plate of shell plating.

According to this formula the external load acting on the shell plating at the moment of impact against the ice was calculated, for all transport vessels and icebreakers aboard which the tests were conducted.

During the tests of the motor ship "Olenegorsk" the maximum stresses fixed by the pickup in the center of the span of a panel of the outer shell plating reached 1300 kilograms per square centimeter. According to the calculation scheme accepted, the stresses in the support section of the panel in this case reached 2600 kilograms per square centimeter. The magnitude of the external load, corresponding to the maximum values of the stresses, amounted to 67 tons per square meter. The structural strength of the shell plating in this region of the hull was equal to 73 tons per square meter. Thus it was established that in those conditions of navigation in which the tests were conducted, ice loads acted on the shell plating of the ship approaching the calculated values, which made it possible to make the following conclusions concerning the strength of its shell plating.

One of the methods of estimating the strength of the side framing of a ship is a comparison of the maximum stresses measured by strain gauges in the process of tests with permissible stresses in hull structures. For a more detailed investigation of the strength, experimental data must be compared with calculated data, which makes it possible to determine the magnitude of the external load acting on the framing and to compare it with the structural strength of the side framing of the ship being tested.

As an example we will consider the results of tests of the hull of the motor ship "Olenegorsk", the side framing of which consists of the basic and intermediate frames of the same profile. Strain-gauge pickups were arranged along two horizontal and two vertical lines (see Figure 1).

According to the readings of the pickups of the vertical group, experimental curves of the distribution of normal stresses in a hold frame in the section between the lower deck and the inner bottom were constructed. Then the statistical curve of the stresses for a frame in this section was found, and according to it the place of application of the external load was determined.

In considering the features of the structure of the side overlapping between the lower deck and the inner bottom, the calculation of the structural strength of the overlapping (shell plating) was accomplished as the calculation of the individual frames, for the effect of a concentrated ice load. The

point of its application was assumed to be in the region of the maximum ordinate of the statistical curve of the stresses.

For estimation of the role of the stress-bearing stringer in providing ice strength of the side plating, the calculation was performed according to three schemes: a) without consideration of the effect of the stringer; b) with consideration of the stringer as an elastic intermediate support for the frame; and c) with the stringer as a rigid intermediate support.

The calculations demonstrated that a side stringer, operating as an intermediate elastic support, increases the structural strength of the plating by approximately 10%.

In Figure 2 an experimental curve of the distribution of normal stresses in a hold frame is compared with a theoretical curve constructed for the second case of calculations. Analysis of the experimental curve confirms our assumption that the ice load is close to a concentrated load and is applied in the span between the stringer and the lower deck, and the stringer operates as an intermediate elastic support for the frame.

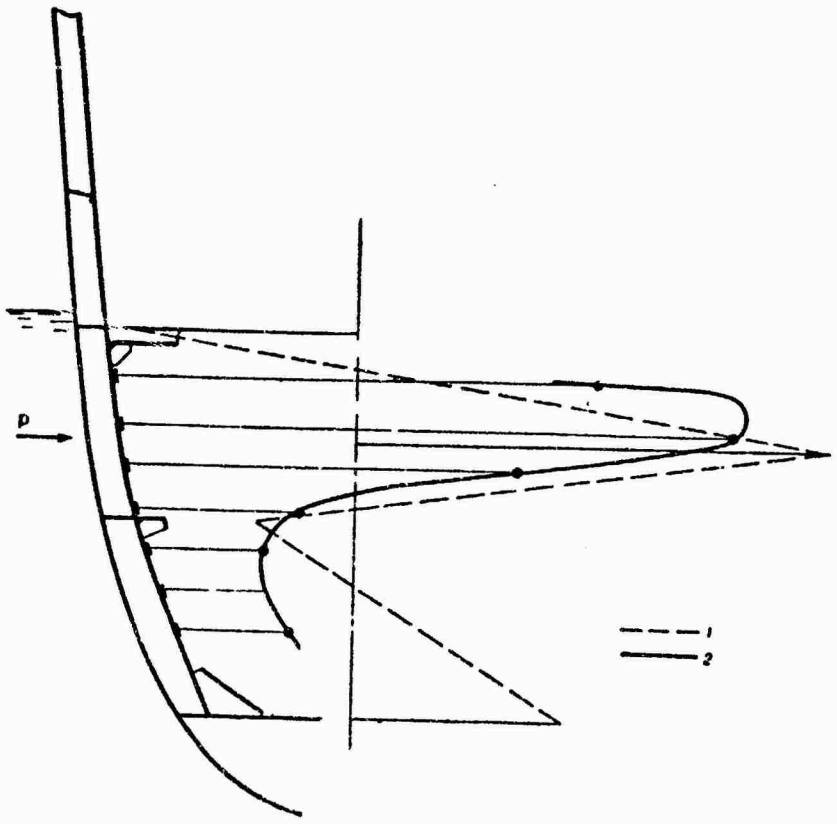

Figure 2. Theoretical (1) and experimental (2) curves of normal stresses in the hold branch of a frame:

Since the calculated curve of the stresses in the frame is similar to the experimental curves, we may with adequate accuracy restore the magnitude of the external ice load according to the readings of each strain gauge of the horizontal line. For this the stress measured by the strain gauge was compared on the appropriate scale with the ordinate calculated curve, constructed in fractions of the force P. Thus the magnitude of the external load P was determined for each specific case.

In a similar manner we may find the maximum external load, which corresponds to the maximum values of the stresses measured in the frames. During the tests of the motor ship "Olenegorsk" the greatest stress according to data from pickups of the horizontal group reach 2070 kilograms per square centimeter. Assuming that the load was applied in accordance with the statistical curve of stresses, we obtain the maximum value of the intensity of the ice load, q = 67 tons per meter. The structural strength of the side framing of the motor ship "Olenegorsk" in this region is equal to 68 tons per meter. Thus, the greatest stresses fixed in the process of the tests correspond to the limiting permissible ice loads for ships of the given type. From this example it is apparent that according to the readings of the strain gauges of the vertical groups the place of application of ice loads is determined.

Analysis of the statistical curves demonstrates that in the majority of cases the line of the arrangement of the strain gauges of the horizontal lines does not coincide with the maximum statistical curves of the stresses (Figure 3). Consequently, each pickup of the horizontal line on the average fixes the stresses constituting only a certain part of the maximum stresses. For example, at one of the stages of the tests of ships of the "Amguyema" type, the strain gauges of the horizontal groups on the average fixes approximately 70--80% of the maximum stresses in the frame. Consequently, by means of the readings of the pickups of the vertical groups processed statistically we may introduce quantitative corrections to the readings of the strain gauges of the horizontal groups.

During the processing of the results of the tests, the distribution of impacts in time was also investigated, the distribution function of the quantity of impact for unit of length of the bow end of the ship was determined, etc. It was established that for icebreakers an important characteristic is the quantity of impact falling in a given region of the bow end in a unit of time. The stastical processing conducted according to data from tests of powerful icebreakers in operation by short runs made it possible to find the law of distribution of this quantity. It turned out that the number of impact pulses acting on a given region of the hull in a unit of time is subordinate to Poisson's law. The number of impulses which a powerful icebreaker receives in the

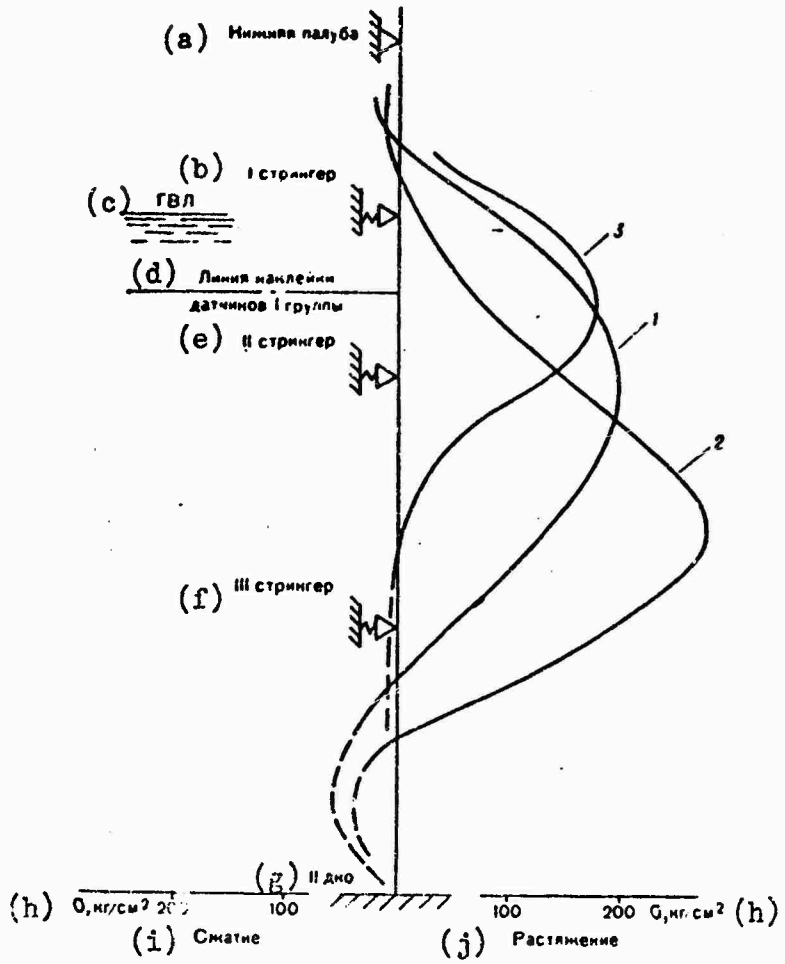

Figure 3. Statistical curves of stresses for broken ice with a thickness of 80--100 centimeters (1), 150--200 centimeters (2) and 60--80 centimeters (3). a) lower deck; b) first stringer; c) load line; d) line of application of pickups of group 1; e) second stringer; f) third stringer; g) inner bottom; h) σ, kilograms per square centimeter; i) compression; j) tension.

region of its ice belt during an Arctic navigation season amounts to approximately 5×10^5. Such a quantity of impact is great enough so that in the calculations we can consider the probability of the origin of fatigue phenomena in the material of the hull after several years of operation of the ship.

For transport vessels navigating in the ice mainly under the escort of icebreakers and in considerably easier conditions, such investigations were not conducted.

In order to characterize the stresses originating in the elements of the structure of the side framing and shell plating, from a probability standpoint, curves of the distribution of the values of the stresses were constructed. In the processing of experimental data the mathematical expectation was found for stresses $\underline{x}$ and their dispersion $\underline{s}$. These parameters are to some degree indices of the strength of the framing of the hull and the degree of difficulty of the ice situation.

The results of statistical processing of the stresses fixed by one of the strain gauges in the shell plating of a powerful icebreaker are given in Figure 4. The data obtained in work in severe ice conditions were subjected to processing. The averaging of the frequencies for each interval of stresses from 100 kilograms per square centimeter and higher was conducted in a tabular form. Small values of the stresses were not considered. The calculations demonstrated that the distributions of the amplitudes in all cases are described by Pearson type III curves. For example, according to data from measurements in the operation of an icebreaker off Graham Bell island, the probability of achieving stresses of $\sigma = x$ kilograms per square centimeter is calculated according to the formula

$$P(x) = 1{,}14e^{-\frac{x}{100}}.$$

The results of strain-gauge tests of many other transport vessels and icebreakers were subjected to analogous processing.

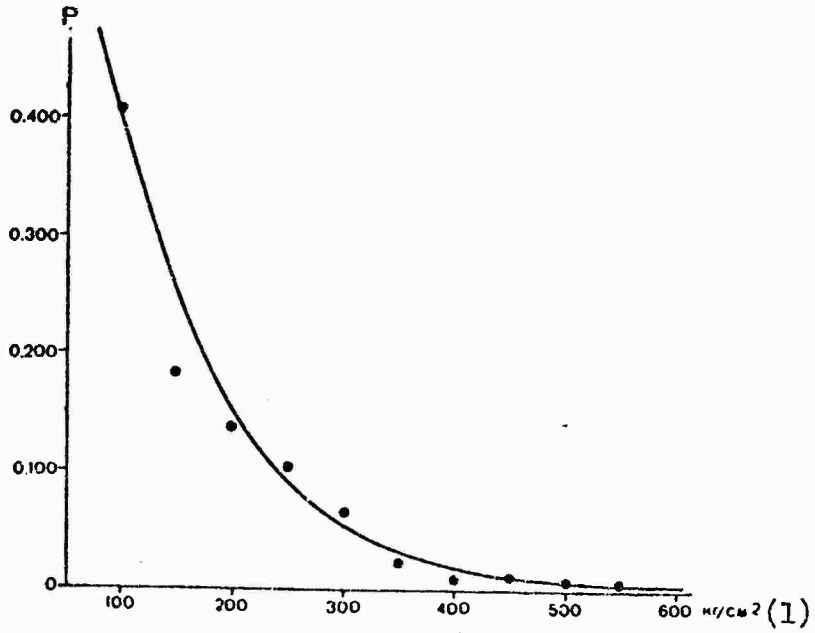

Figure 4. Theoretical curve of the distribution of stresses in shell plating (• indicates points obtained experimentally. 1) kilograms per square centimeter.

The probability of reaching the calculated stresses, as calculated by means of extrapolation of the distribution functions obtained, for transport vessels is much greater than for icebreakers. However, in practice cases of the reaction of icebreakers with ice are possible (impact against ground ice, reflected impact, etc.), in which stresses originate in the structures that considerably exceed the measured values. Therefore, it is not advisable to determine the calculated ice load on powerful Arctic icebreakers only on the basis of statistical processing of strain-gauge tests. These loads must be designated with a consideration of the requirements of preservation of strength of the icebreaker in any possible cases of reaction with ice, i.e., according to the extreme values of the loads.

BIBLIOGRAPHY

1. Davydov, V. V., Mattes, N. V., and Sivertsev, I. N., Uchebnyy spravochnik po prochnosti sudov vnutrennego plavaniya (Handbook on the strength of ships for inland navigation), Moscow, "Rechnoy transport", 1958.

2. Popov, Yu. N., Faddeyev, O. V., Kheysin, D. Ye., and Yakovlev, A. A., Prochnost' sudov plavayushchikh vo l'dakh (Strength of ships floating (navigating) in ice), Leningrad, "Sudostroyeniye", 1967.

3. Spravochnik po stroitel'noy mekhanike korablya (Handbook on the structural mechanics of ships), Leningrad, Sudpromgiz, 1958-1960.

STRAIN-GAUGE TESTS OF ICEBREAKING TRANSPORT VESSELS

V. A. Likhmanov and D. I. Solostyanskiy pages 111-117

Transport vessels of the "Amguyema" type have an ice class of UL (Arkt). They are intended to navigate in Arctic and freezing seas during the entire period of the navigation season under the escort of icebreakers. Aside from this, they can navigate independently in solid ice with a thickness of up to 0.5 meters and in large broken ice that covers most of the surface.

Ships of this type constitute the most numerous group of ships of the category UL (Arkt), and a considerable part of the cargo shipments in the most complex ice conditions falls to their share.

Full-scale tests of ships of the "Amguyema" type have been conducted since 1963. One of the tasks of such tests was the study of the strength of the hull. Investigations of the strength of the hull were conducted by means of electrical resistance strain gauges, which are fastened to the side framing and shell plating. The pickups are arranged basically along the actual load line and are cemented on the beams of the frame. The length of a region being tested by strain gauges on the average amounted to 15--20 meters (from the second to the fifth theoretical frame). In practice, aboard ships of this type the entire side part of the forward end was investigated, to the beginning of the cylindrical insert, with the exception of the bilge strake.

The tests were conducted at different times of year in regions with various ice conditions: in winter in the Sea of Okhotsk, in summer and autumn in young growing ice and old ice of the Arctic. Only in the very beginning period of the Arctic navigation season was strain-gauge testing of icebreaking transport vessels not conducted.

The tests were conducted in various ice situations: a) in level fields of ice with a thickness from 20 to 50 centimeters; b) in fine broken ice of various thickness, with a sea cover of 6--10 balls; c) in large broken ice

with a sea cover of 6--8 balls, with inclusion of fragments of fields with a thickness up to 3 meters.

In November 1970 ships of class UL (Arkt) were tested in level fast ice on the Yenisey. Such experiments in fresh-water ice were not previously conducted. In level solid ice the ships advanced independently, and in large broken ice and fine broken ice they proceeded astern of an icebreaker. In all the tests the ships were not taken out of operation, and continued to perform their basic functions. The full-scale data obtained were processed by methods of mathematical statistics.

As the statistical processing demonstrated, the duration t of impact impulses, depending upon ice conditions and the speed of the ship, varied from 0.1 to 1 second (in severe conditions it increased to 2 seconds or more). The average value of the time of collision (0.40--0.45 seconds) agrees well with the theoretical value. No effect of the lines of the bow on the magnitude of t was observed.

The variation of the length of the zone of contact in impacts of the hull against the ice is subordinate to the same quantitative relationships as for ships of other ice classes and icebreakers. The least length of the zone of contact (2--3 meters) was observed in motion in thin broken ice, and the greatest (5--6 meters or more) was fixed in operation in short runs in level fast ice with a thickness of about 1 meter.

The diversity of ice conditions in which the ships of the given type were tested made it possible to investigate the factors affecting the distribution of the quantity of impact along the bow end of the ship. For this, the quantity of impacts fixed by each strain gauge of the horizontal line as the ship navigated with a fixed speed was calculated. The impulses in which stresses of less than 50 kilograms per square centimeter originated were not considered.

From Figure 1 it is apparent that the distribution curves obtained according to data from the tests in various ice conditions have a similar nature: all of them have the maximum in the vicinity of the 21st to 27th frames, and further on the number of impacts sharply decreases, while at the beginning of the second hold; the 33rd to 35th frames) a certain increase in the quantity of impulses is again observed.

In observations of the breaking of the ice it was established that ships of the "Amguyema" type, moving in level solid ice with a thickness up to 30 centimeters, break 3-4 elongated ice sectors with the bow end. With an increase in the thickness of the ice, the quantity of sectors decreases to 2--3,

and their dimensions increase. The breaking of the next to the last sector occurs in the vicinity of the 23th to 27th frame, corresponding to the maximum of curves 1, 2, and 3 (see Figure 1). The last ice sector is broken at the beginning of the second hold, where an increase in the quantity of impulses is also observed (33rd to 37th frames). The boundary of the breaking of the sectors falls in the area between the 27th and 33rd frames, which also explains the decrease in the quantity of impacts in this region.

Curve 4 was constructed according to data from tests of a ship in fresh river fast ice, the features of the breaking of the ice there being as yet little studied. In this case, the maximum of the curve shifts somewhat towards the bow end, but, however, the shape of the curve is preserved. We should note that the quantity of impact pulses obtained in fresh-water ice is not great, and therefore curve 4 is less representative.

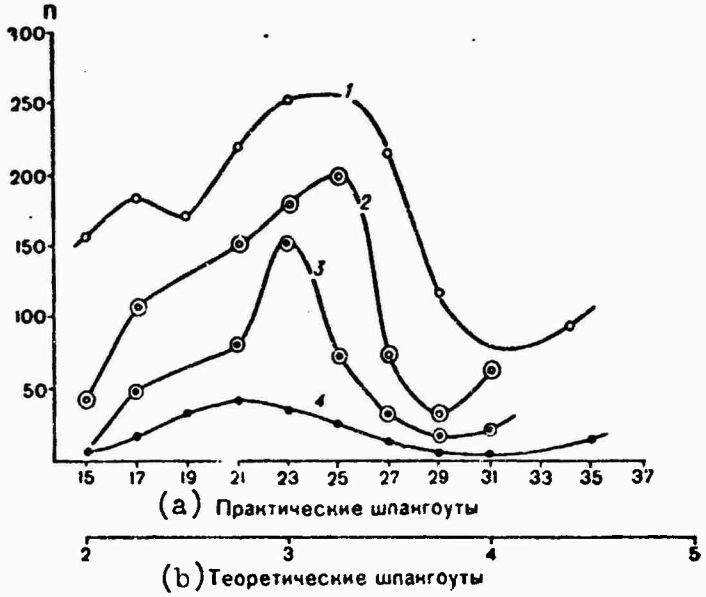

Figure 1. Distribution of the quantity of impact along the waterline: 1) large broken ice; 2) fields of level sea ice, h = 20--25 centimeters; 3) level sea ice, h = 40 centimeters; 4) level river fast ice, h = 40 centimeters.
a) practical frames; b) theoretical frames.

Curve 1 reflects the picture of the motion of the ship in large and fine broken ice, with a sea cover of 6--8 balls. The curves of the distribution of the quantity of impulses in motion in fine broken ice of a different coverage factor is analogous. The shape of curve 1 may be explained in the following manner. If we consider that the broken ice is uniformly arranged along the surface of the water, the quantity of impact per unit of length of the

hull for each point of the waterline will be proportional to tgα (α is the angle of inclination of the waterline to the center line of the ship). Then with a single impact of each ice floe, the curves of the distribution of the quantity of impulses along the bow end of the ship will decrease smoothly as the distance from the center line to the side increases.

During the motion of the ship in thin broken ice in dynamic contact with individual ice floes, at first part of the hull protrudes which directly adjoins the stem. As a result of the impact, part of the ice floes are thrown to a definite distance and some of them enter into contact with the side of the ship for a second time. Therefore, in the extent of the bow end, up to the beginning of the cylindrical insert, zones of increased frequency of impact are formed, corresponding to the regions of the 21st--27th and 33rd--37th frames for ships of the "Amguyema" type.

Analysis of the distribution of the probability of the number of impacts per unit of length of the load line in the forward part of the ship, according to data from each strain gauge of the horizontal line, demonstrates that in spite of the different ice conditions in each specific case of the tests and the different speeds of the ships, the probability distributions are the same in general nature (Figure 2).

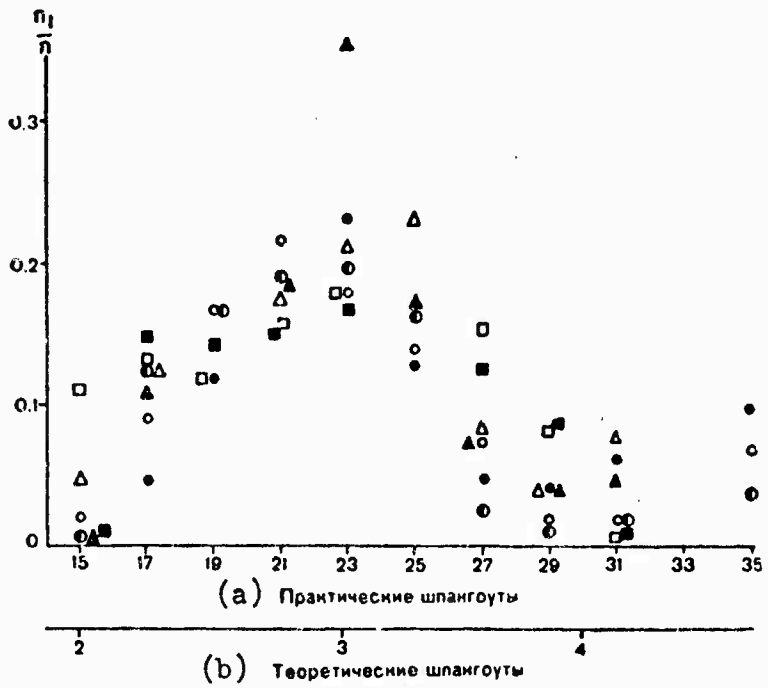

Figure 2. Distribution of the probability of the quantity of impacts, according to test data: o fields, h = 20--25 centimeters; ◐ fine broken ice, 6--8 balls; ● level fast ice 50 centimeters, h = 40 centimeters; △ fields, h = 40 centimeters; ▲ fresh-water fast ice, h = 40 centimeters; □ fine broken ice, 6--8 balls, h to 4 meters; ■ large broken ice, field fragments, h up to 2.5 meters.

Consequently, we may consider that the probability of a definite number of impacts falling into a given retion of the bow e..d of the hull depends upon the shape of the bow section. A comparison of the data obtained with results of strain-gauge tests of ships of other ice categories and types confirms this conclusion, since such a nature of the distribution curves was obtained only for ships of the "Amguyema" type.

The basic task of strain-gauge tests of strength was the determination of stresses in the elements of the structure of the side plating and the external loads causing these stresses at the moment of impact of the ship against the ice. For establishment of the connection of the magnitude of the stresses with the ice conditions, the data were processed by the method of mathematical statistics. The general level of the magnitude of the stresses was characterized by the magnitude of the mathematical expectation $\bar{x}$ of the stresses and their dispersion s. Along the length of the region being tested by strain gauges, curves of the distribution of these magnitudes for various ice conditions were constructed.

The results of the processing of experimental data demonstrated that the average values of the stresses are uniformly distributed along the water line. The nature of their distributions does not depend upon the ice conditions of navigation, which have an effect only on the magnitude of the average stresses. The greatest values of the average stresses in the hull were fixed during the motion of the ship with an average speed of 7 knots in large broken two-year ice with a thickness of 1.5--2 meters, and a sea coverage of 6--8 balls. The maximum stresses in the framing and shell plating were measured in these same ice conditions (2500 kilograms per square centimeter).

The external loads acting on the shell plating during an impact against the ice were determined with consideration of the assumption of the cylindrical shape of the venting of a panel of shell plating. In this case the external loads corresponding to the maximum measured stresses turned out to be close to the magnitude of the structural strength of the shell plating for the given retion of the hull.

Impact ice loads on the side framing of a ship were determined in accordance with the methodology explained in the article "The strength of icebreakers and transport vessels (according to data from strain-gauge tests)" in this collection. The side plating was calculated for two cases of the application of a load: along a side stringer and between the stringers. The stringers are considered as beams lying on a solid elastic base. The external load was applied in the region of the greatest ordinate of the statistical curve of stresses, constructed according to data from the vertical group of pickups.

Calculations according to data from strain gauges of the horizontal groups demonstrated that the maximum values of the external loads on the side framing during the tests amounted to about 60% of the structural strength of the framing. From Figure 3 it is apparent that the greatest external loads were fixed in the region of the 27th frame (the structural strength of this region is somewhat lower than at the beginning of the first hold).

The probability of maximum permissible stresses originating in the framing of the hull was estimated according to data from the strain gauges of the horizontal groups.

As is apparent from Figure 4, the probability of the appearance of stresses close to the maximum permissible is small. In this case the excess of the impact stresses over the level of 1000 kilograms per square meter is equally probable for those ice conditions in which the tests were conducted. In more complex ice conditions or in motion at high speeds in large broken thin ice, the probability of the origin of maximum permissible stresses increases.

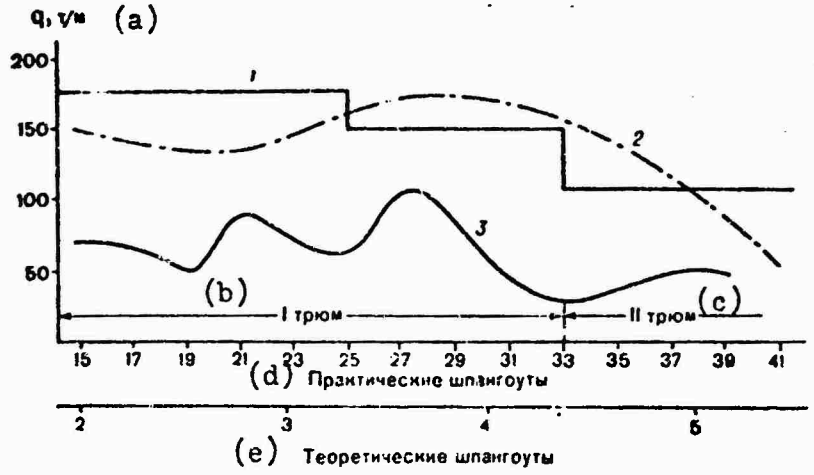

Figure 3. Comparison of the calculated ice load (2) and the structural strength of the ship (1) with the magnitude of the maximum experimental external load (3). a) q, tons per meter; b) No. 1 hold; c) No. 2 hold; d) practical frames; e) theoretical frames.

Aboard ships of the "Amguyema" type, investigations of elastic transverse oscillations of the hull originating in the motion of the ship in ice were conducted. By means of strain gauges cemented to the deck, the stresses of variable sign originating in the deck due to ice vibration were measured. The frequency and shape of the elastic vertical oscillations of the hull were also measured. The cause of vibration of the type indicated is found in impacts

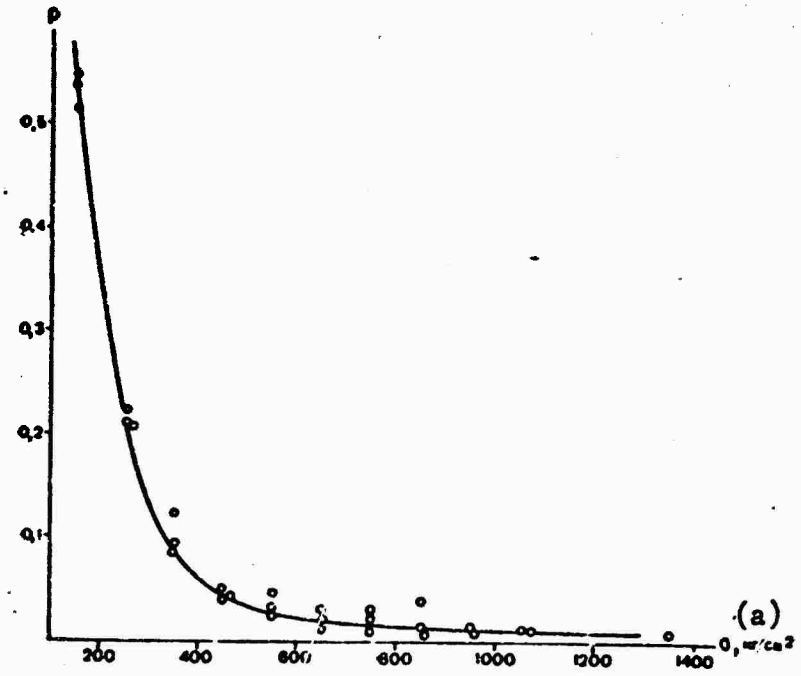

Figure 4. Statistical curve of the distribution of stresses in a frame. a) σ, kilograms per square centimeter.

against the ice of the part of the hull directly adjoining the stem. This was established by means of comparison of data from measurements of deck strain gauges with the readings of pickups of the horizontal groups on the framing.

Amplitudes of elastic oscillations increase with an increase in the speed of the ship. The stresses originating in the deck reach the greatest values in motion in thin broken ice. After the impact of the stem against an individually floating ice floe and the exit of the ship to clear water, the cyclic stresses exceeding 200 kilograms per square centimeter were fixed. There were no greater values of the stresses from ice vibration fixed during the test.

Thus, data from strain gauge tests make it possible to reach the following conclusions:

1. The strength of the hulls of icebreaking transport vessels of the "Amguyema" type corresponds to their ice category of UL (Arkt). These ships can navigate in Arctic and freezing non-Arctic seas in established and extended navigation seasons.

2. The probability of stresses exceeding those permissible originating in the hull increases during navigation in old drifting large broken ice, with a sea cover of 6--8 balls, at a speed of more than 6--8 knots, and also in thick fast ice in operation in short runs.

3. Independent navigation by continuous steaming in solid homogeneous ice at maximum speed of the propulsion plant is safe for the strength of the hull of ships of this class. Proceeding behind an icebreaker in any ice conditions also presents no hazard for these vessels. However, in steaming in a channel broken by an icebreaker in solid ice, we should avoid impacts against the edge of the channel and also reflected impacts.

4. The elastic oscillations of the hull originating in motion in ice may cause fatigue phenomena in the material of the deck and superstructures after several years of operation of the vessel.

ON THE DISTRIBUTION OF PROBABILITIES OF THE NUMBER OF IMPACTS OF A SHIP'S HULL AGAINST THE ICE

V. S. Kudishkin

pages 118-122

In the motion of a ship in solid ice, its bow end experiences the effect of ice loads in the form of impact pulses, originating at the moment that the ice is broken by individual sections of the hull. The total external ice load is a discrete sequence of impact pulses, distributed in a random manner along the length of the bow end. The quantity of impulses, their amplitudes, and also the nature of distribution of impulses along the length of the bow end at any fixed moment of time are determined by the random external factors caused by the breaking of the ice by the ship's hull.

For the study of the random process of the reaction of a ship's hull with the ice, an estimate of the statistical parameters of individual components of this process is necessary. Among them are the average values of the amplitudes of impulses and the statistical distribution of impulses along the length of the bow end of the ship. In this article the distribution of the number of pulses received by the bow end of a ship in a certain interval $\underline{t}$ of time is considered.

As full-scale tests demonstrated, the speed of a ship moving in solid homogeneous ice of uniform thickness varies but little in the entire interval of the time of motion of the ship. Thus, if as the event x_k ($k = 0, 1, 2\ldots$) we assume the number of pulses which the bow end receives in an interval of time (t_0, $t_0 + t$), the probability that in this interval precisely k-events will occur depends only upon the duration of the interval and does not depend upon the beginning of the reading of the time of motion of the ship, t_0. We will designate this probability as $p_k(t)$.

We will take an adequately large interval of the time of motion of the ship (-T, T) and divide this interval into finite non-intersecting intervals (t_0, t_1), (t_2, t_3), (t_4, t_5)... so that $t_0 < t_1 < t_2 < t_3 < \ldots < t_n$. It is clear

that the number of impulses received by the ship in one of these intervals does not depend upon the quantity of impulses obtained in other intervals. Consequently, the events $x_i(t_0, t_1)$, $x_j(t_2, t_3)$, $x_m(t_4, t_5)$ form a set of independent random quantities.

The results of strain-gauge tests demonstrated that the average duration of the pause between the two adjacent pulses amounts to approximately 1 second. Then the probability of receiving 2 pulses or more with an adequately small value of Δt may be considered to be negligible in comparison with the probability of receiving precisely one impulse, i. e.,

$$p_1(t + \Delta t) = \lambda \Delta t + o(\Delta t),$$

where λ is the average density of impulses (average quantity of impulses per unit of time), and $o(\Delta t)$ are the terms depending upon Δt in such a manner that

$$\lim_{\Delta t \to 0} \frac{o(\Delta t)}{\Delta t} = 0.$$

Consequently, we may make the conclusion that the distribution of the probabilities of receiving a definite number of impulses by the bow end of the ship corresponds to Poisson's law.

At a known average density λ of impulses, the probability that precisely n-impulses in a time t will fall to the bow end of the ship is determined according to the formula [1, 2]:

$$p_n(t) = \frac{(\lambda t)^n}{n!} e^{-\lambda t}.$$

We will find the number of impulses received by the bow end from the beginning of the counting to the moment t, as a random function X(t) of the argument t. This function can take only whole number values (n = 0, 1, 2...) and does not decrease with an increase of its argument. The increment of the function in the interval (t_i, t_j) is equal to the number of impulses that appeared in a given interval. If we assume that x(0) = 0, then in a fixed interval (0, t):X(t) = n. We will determine the distribution function for X(t)

$$F(x, t) = e^{-\lambda t} \sum_{n=0}^{x} \frac{(\lambda t)^n}{n!}.$$

The mathematical expectation and dispersion for X(t) are equal to each other

$$MX(t) = \lambda t = DX(t).$$

In Table 1 the empirical distribution of the number of impulses received by the bow end of a ship in motion in solid ice with a thickness of 35 centimeters at a speed of 5--6 knots in 3 seconds is given. In the table the probabilities for each value of the number of impulses are also indicated, calculated under the assumption that the random quantity under consideration precisely follows a Poisson law of distribution. The mathematical expectation of the parameter λ of this law was determined from an experiment. For estimation of the approximation of the theoretical distribution curve to the empirical curve, the corresponding distribution functions were constructed (Figure 1). As a criterion of agreement of these curves, the Pearson criterion was selected:

$$\chi^2 = \sum_{i=1}^{t} \frac{(m_i - np_i)^2}{np_i}.$$

The number of degrees of freedom of this distribution is equal to

$$r = k - c - 1,$$

where k is the number of intervals and c the number of connections imposed. The calculation of χ^2 is presented in Table 2. Because of the small number of tests in the intervals 11, 12, 13, 14, and 15 they are combined into one interval 11. We will select the level of significance for the criterion g = 5% and according to Table IV of the appendix of reference [1] at 9 degrees of freedom (the number of connections superimposed is t = 1) we find $\chi^2_{0.05} = 16.9$. The calculated value of $\chi^2 = 13.77$, i.e., $\chi^2 < \chi^2_g$.

Thus, at the selected level of significance the hypothesis that the number of impulses received by the bow end in the motion of the ship in solid ice is distributed according to a Poisson law does not contradict the observation. Some divergence between the theoretical and empirical distribution functions may be explained by the inadequate quantity of experimental material and the presence of a sensitivity threshold of the measuring apparatus used.

Table 1

Calculation of the Empirical and Theoretical Distribution Functions of the Number of Impacts of a Ship's Hull Against the Ice

(1) Число наблюдаемых импульсов x_i	(2) Число испытаний, в которых фиксировали наблюдаемые импульсы, m	(3) Частота $\omega_n(x) = \frac{m_i}{n}$	(4) Эмпирическая функция распределения $W(x) = \sum_{k=0}^{x} \omega(k)$	(5) Вероятность $P_n(x)$	Теоретическая функция распределения (6) $F(x)$
0	16	0,029	0,029	0,015	0,015
1	40	0,072	0,101	0,062	0,077
2	75	0,136	0,237	0,132	0,209
3	96	0,175	0,412	0,184	0,393
4	100	0,182	0,594	0,195	0,588
5	82	0,149	0,743	0,163	0,751
6	56	0,102	0,845	0,115	0,866
7	41	0,074	0,919	0,069	0,935
8	18	0,032	0,951	0,036	0,971
9	12	0,021	0,972	0,018	0,989
10	5	0,009	0,981	0,007	0,996
11	2	0,003	0,984	0,002	0,998
12	2	0,003	0,987	0,001	0,999
13	2	0,003	0,990	0,0003	0,999
14	1	0,001	0,991	0,0001	0,999
	$n = 548$	0,991		0,999	

$$\lambda t = \frac{2299}{548} = 4,195 \simeq 4,2$$

Key: 1) number of impulses observed, x_i; 2) number of tests in which the impulses observed were fixed, m; 3) frequency, $\omega_n(x) = (m_i/n)$; 4) empirical distribution function, $W(x) = \sum_{k=0}^{x} \omega(k)$; 5) probability $P_n(x)$; 6) theoretical distribution function $F(x)$.

Table 2

Calculation of χ^2

(1) № интервалов k	m_i	(2) Вероятность p_i	np_i	(3) Уклонение $m_i - np_i$	$(m_i - np_i)^2$	$\frac{(m_i - np_i)^2}{np_i}$
1	16	0,015	8	8	64	8
2	40	0,062	34	6	36	1,05
3	75	0,132	72	3	9	0,125
4	96	0,184	101	5	25	0,247
5	100	0,195	106	6	36	0,339
6	82	0,163	89	7	49	0,550
7	56	0,115	63	7	49	0,777
8	41	0,069	38	3	9	0,236
9	18	0,036	19	1	1	0,052
10	12	0,018	10	2	4	0,400
11	5	0,007	4			
12	2	0,002	1			
13 (11)	2 (12)	0,001	1 (8)	4	16	2
14	2	0,0003	1			
15	1	0,0001	1			
Σ			548			13,77

Key: 1) number of intervals k; 2) probability p_i; 3) deviation $m_i - np_i$.

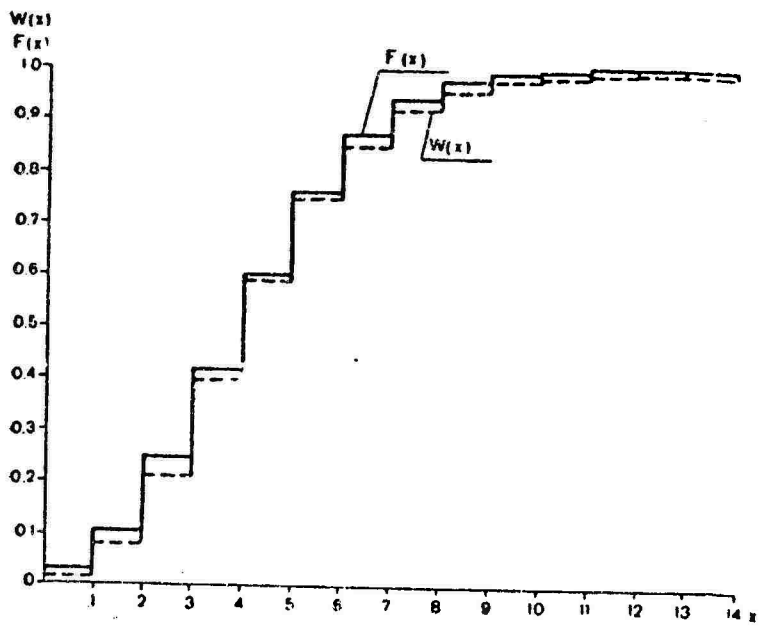

Figure 1. Empirical W(x) and theoretical F(x) distribution functions of the number of impulses received by the bow end of a ship during 3 seconds.

BIBLIOGRAPHY

1. Smirnov, N. V., and Dunin-Barkovskiy, N. V., Kurs teorii veroyatnostey i matematicheskoy statistiki dlya tekhnicheskikh prilozheniy (Course in the theory of probabilities and mathematical statistics for technical application), Moscow, "Nauka", 1965.

2. Gnedenko, B. V., Kurs teorii veroyatnostey (Course in the theory of probabilities), Moscow, Fizmatgiz, 1961.

EXCITATION OF VERTICAL ELASTIC OSCILLATIONS OF A SHIP'S HULL IN MOTION IN THE ICE

V. S. Kudishkin

pages 123-131

In conducting full-scale tests of icebreakers and ships for active ice navigation in the ice, a general vibration of the ship's hull was noted, differing from the vibration experienced when underway in clear water. The elastic oscillations originating in the motion of a ship in solid and broken ice have a random nature (Figures 1 and 2), and the average values of their amplitudes are several times higher than in clear water [1].

The problem of the origin of horizontal elastic oscillations of the hull in the effect of external ice defects symmetrical relative to the center line of the ship was considered in reference [3]. In this article the problem of the excitation of vertical elastic bending oscillations of the ship's hull is investigated.

Strain-gauge tests demonstrated that in motion in solid ice impact impulses of random magnitude (A_i) act on the bow end of the ship in random non-overlapping intervals of time $(t_0, t_1)(t_1, t_2)\ldots(t_{i-1}, t_i)$, falling in random regions of the side $(x_0, x_1)(x_1, x_2)\ldots(x_{i-1}, x_i)$. We will designate the vertical component of the impulse as a_i and assume that a_i form a set of random mutually independent quantities also independent of the coordinates of the points of application of the impulses (x_i) and upon the moment of their appearance (t_i). Let us assume that a_i have the identical probability density $f(a)$. We will designate the average density of the pulses (the number of pulses per unit of time) as λ.

As the basic characteristics of the forced elastic oscillations of the ship's hull we will assume the spectral density of the power of these oscillations G_{zz}. In this case we will consider the ship's hull as a mechanical system with constant distributed parameters, and we will present the external

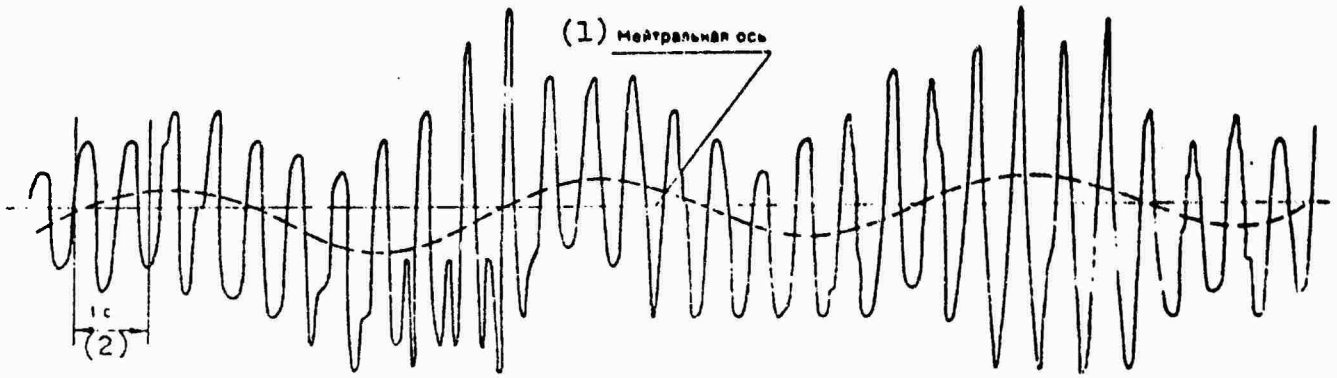

Figure 1. Vertical elastic oscillations of the hull of the diesel-electric vessel "Vankarem" in motion in broken ice. 1) neutral axis; 2) 1 second.

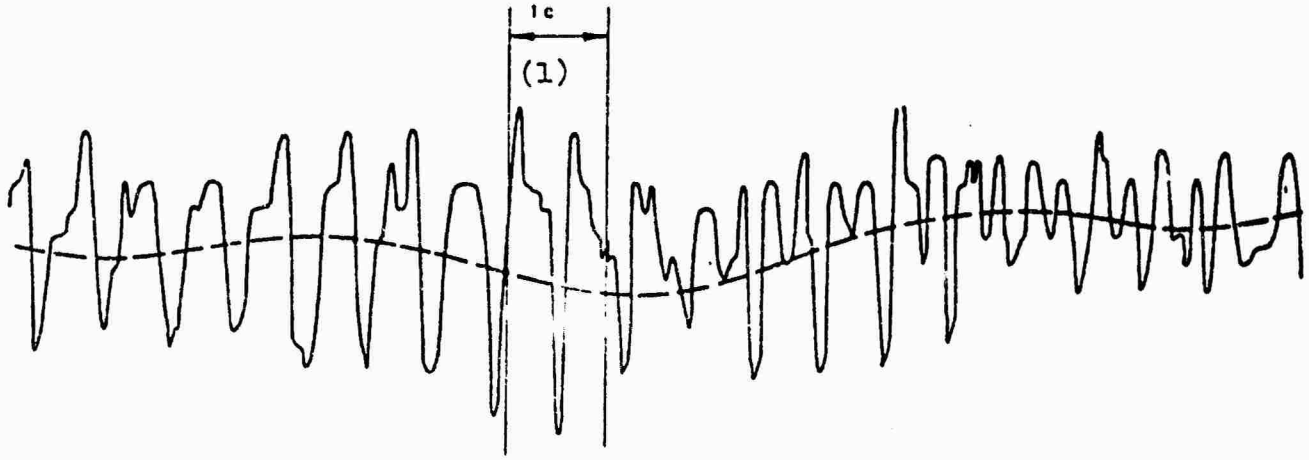

Figure 2. Ice vibration in the motion of a ship in solid ice. 1) 1 second.

ice forces in the form of a random sequence of a large number of impact impulses of random amplitude.

The differential equation of the forced vertical oscillations z(x, t) of the ship's hull, as beams of variable section with a length L, with a consideration of the forces of internal friction in the structure has the form [1]:

$$\left(1+\varepsilon\frac{\partial}{\partial t}\right)\frac{\partial^2}{\partial x^2}\left(EI\frac{\partial^2 z}{\partial x^2}\right)+m(x)\frac{\partial^2 z}{\partial t^2}=f(x,t), \tag{1}$$

where E is the modulus of elasticity; I(x) is the moment of inertia of the area of the cross sections of the beam; m(x) is the mass of the beam, distributed along its length; ε is the coefficient of internal friction; f(x, t) is a certain realization of the external effect, which may be written in the following manner [3]:

$$f(x,t)=\sum_{i=1}^{N}a_i\delta(x-x_i)\,\delta(t-t_i). \tag{2}$$

Where $(x-x_i)$ and $\delta(t-t_i)$ are Dirac delta-functions, equal to zero everywhere except point $x = x_i$ and $t = t_i$. Losses due to the forces of internal friction are small, and therefore the shapes of the free oscillations of the beam differ but little from the shapes of the free oscillations of the same beam without resistance. We will consider the frequencies ω_n and the shape v_n of the free non-attenuating oscillations of the hull as being known, where

$$\frac{d^2}{dx^2}\left(EI\frac{d^2v_n}{dx^2}\right)-\omega_n^2 m(x)\,v_n=0. \tag{3}$$

Then each item out of sum (2) may be expanded into a series according to the shapes of the free oscillations. Having divided the right-hand part of equation (1) by m(x) and having assumed that the series converges, we will obtain

$$\frac{\sum_{i=1}^{N}a_i\delta(x-x_i)\,\delta(t-t_i)}{m(x)}=\sum_{n=1}^{\infty}Q_n(t)\,v_n(x). \tag{4}$$

By using the properties of orthogonality of the shapes of the free oscillations and the property of convolution of the delta-function, we find

the coefficients of this series

$$Q_n(t) = \frac{\sum_{i=1}^{N} a_i \delta(t - t_i) v_n(x_i)}{\int_0^L m(x) v_n^2(x)\, dx}. \tag{5}$$

The general solution of heterogeneous equation (1) consists of the solution of the homogeneous equation without the right-hand part and a particular solution of the heterogeneous equation with the right-hand part, in the form of a sequence of random impulses. As a consequence of the steady-state nature of the problem, understood in the conventional sense, the solution of the homogeneous equation will not be considered. We will seek the solution of the heterogeneous equation in the form of the series

$$z(x, t) = \sum_{n=1}^{\infty} \varphi_n(t) v_n(x). \tag{6}$$

Having substituted expression (6) into formula (1), having divided both its parts by $m(x) \neq 0$, and considering condition (3) for determination of the unknown function $\varphi_n(t)$ we will obtain a linear heterogeneous second-order differential equation

$$\ddot{\varphi}_n + \varepsilon\omega_n^2\dot{\varphi}_n + \omega_n^2\varphi_n = a_n \sum_{i=1}^{N} a_i v_n(x_i)\, \delta(t - t_i), \quad (n = 1, 2\ldots), \tag{7}$$

where

$$a_n^{-1} = \int_0^L m(x)\, v_n^2(x)\, dx. \tag{8}$$

Thus, the initial equation (1) in partial derivatives is reduced to a counted set of linear equations (7) with one degree of freedom. The subscript n indicates the tone of the natural oscillations of the ship's hull.

We will designate the reaction of the beam, i. e., its bending at the moment t to the effect of a single pulse applied at the moment τ, as $h(t,\tau)$. We will consider the function $h(t,\tau)$ as equal to zero, when the absolute magnitude of the difference between t and τ exceeds a certain assigned number

$|t-\tau| > T_1$. We will fix the final large interval of time ($-T<t<T$), where $T \gg T_1$, and determine the event B_m as the appearance of precisely m-impulses in the interval under consideration. We will limit ourselves to values of t lying in the integrand ($-T+T_1<t<T-T_1$) so that we may ignore the effect of many impulse appearing outside the interval (-T, T).

The expression (7) has constant coefficients, so that $h(t, \tau)$ depends only upon the difference t and τ. Consequently, the solution of equation (7) may be presented in the form of a series

$$\varphi_n(t) = \alpha_n \sum_{i=1}^{\infty} a_i v_n(x_i) h(t, t_i). \tag{9}$$

By using the theorem of the conditional mathematical expectation of the quantity being sought in the hypothesis D_m, we will calculate the average value of the function $\varphi_n(t)$

$$M[\varphi_n(t)] = \sum_{m=0}^{\infty} P(B_m) M[\varphi_n(t) B_m]. \tag{10}$$

At the hypothesis B_m we have

$$M[\varphi_n(t) B_m] = \alpha_n \sum_{i=1}^{m} M[a_i v_n(x_i) h(t, t_i) B_m]. \tag{11}$$

Taking into consideration the fact that a_i, t_i, x_i are independent, and the moments of appearance of the impulses (t_i) are uniformly distributed in the interval (-T, T) and using the theorem of the mathematical expectation of the product of independent random quantities, we find

$$M[a_i v_n(x_i) h(t, t_i) B_m] = \frac{\bar{a} g_n}{2T} \int_{-\infty}^{t} h(t-\tau)\, d\tau. \tag{12}$$

Here

$$\bar{a} = \int_{-\infty}^{\infty} a f(a)\, da; \tag{13}$$

$$g_n = \int_S v_n(x)\, p(x)\, dx, \tag{14}$$

where $v(x)$ is the probability density of an impulse falling at this point. The upper limit of integral (12) was selected to be equal to t, since for systems that can be physically accomplished $h(t, \tau) \equiv 0$ at $t < \tau$. The lower limit of the integral was selected with consideration of the effect of the previous effect. The sum (11) contains m identical terms of the form of (12).

Then

$$M[\varphi_n(t) | B_m] = z_n g_n \frac{m\bar{a}}{2T} \int_{-\infty}^{t} h(t-\tau)\, d\tau. \tag{15}$$

The probability of the bow end of the ship receiving a definite number of impulses during the motion in solid ice is subordinate to a Poisson law of distribution[1], i. e.,

$$P(B_m) = \frac{(2\lambda T)^m}{m!} e^{-2\lambda T}. \tag{16}$$

Having substituted expressions (15) and (16) into formula (10), we obtain

$$M[\varphi_n(t)] = z_n g_n \sum_{m=0}^{\infty} \left[\frac{(2\lambda T)^m}{m!} e^{-2\lambda T} \frac{m\bar{a}}{2T} \int_{-\infty}^{t} h(t-\tau)\, d\tau \right]. \tag{17}$$

By performing the replacement of the variables, after the necessary calculations, we find

$$M[\varphi_n(t)] = z_n g_n (\lambda \bar{a}) \int_0^{\infty} h(\tau)\, d\tau. \tag{18}$$

The weight function $h(\tau)$ is determined as the solution of equation (7) with the right-hand part in the form of a single impulse function, satisfying the zero initial conditions

$$h_n(t) = \frac{e^{-\frac{\omega_n^2}{2} t}}{p_n} \sin p_n t, \tag{19}$$

1. See the article by V. S. Kudishkin, "On the distribution of probabilities of the number of impacts of a ship's hull against the ice," in this collection.

where

$$p_n = \omega_n \sqrt{1 - \frac{\varepsilon^2 \omega_n^4}{4}}. \tag{20}$$

Having substituted this expression into formula (18) we finally obtain

$$M[\varphi_n(t)] = \frac{a_n k_n}{\omega_n^2} (\bar{a}). \tag{21}$$

By using the theorem of the mathematical expectation of the sum, we find the average value of the bending of the beam

$$M[z(x, t)] = \sum_{n=1}^{\infty} M[\varphi_n(t)] v_n(x) = (\bar{a}) \sum_{n=1}^{\infty} \frac{a_n k_n}{\omega_n^2} v_n(x). \tag{22}$$

We determine the correlation function $K_{\varphi_n}(t_1, t_2)$ in the following manner:

$$K_{\varphi_n}(t_1, t_2) = M[\varphi_n(t_1) \varphi_n(t_2)] = \sum_{m=0}^{\infty} P(B_m) \times \tag{23}$$
$$\times M[\varphi_n(t_1) \varphi_n(t_2) B_m],$$

where

$$M[\varphi_n(t_1) \varphi_n(t_2) B_m] = x_n^2 \sum_{i, k=1}^{m} M[a_i a_k v_n(x_i) v_n(x_k) \times \tag{24}$$
$$\times h(t_1, t_i) h(t_2, t_k) / B_m].$$

At $i \neq k$ the random quantities $a_i v_n(x_i) h(t_1, t_i)$ and $a_k v_n(x_k) h(t_2, t_k)$ are statistically independent, and consequently,

$$M[a_i a_k v_n(x_i) v_n(x_k) h(t_1, t_i) h(t_2, t_k) B_m] =$$
$$= g_n^2 \frac{(\bar{a})^2}{4T^2} \int_{-\infty}^{t} \int_{-\infty}^{t} h(t_1 - \tau_1) h(t_2 - \tau_2) d\tau_1 d\tau_2 = \left[\frac{g_n \bar{a}}{2T} \int_0^{\infty} h(\tau) d\tau \right]^2. \tag{25}$$

At i = k we have

$$M\left[a_k^2 v_n^2(x_k)\, h(t_1, t_k)\, h(t_2, t_k)\right] = \frac{c_n \bar{a}^2}{2T} \int_0^\infty h(\tau)\, h(\tau + t)\, d\tau, \tag{26}$$

where

$$c_n = \int_0^L v_n^2(x)\, p(x)\, dx. \tag{27}$$

The sum (24) contains m^2-m terms of the form (25) that differ from zero and m terms of the form (26). Then

$$M\left[\varphi_n(t_1)\, \varphi_n(t_2)/B_m\right] = a_n^2 (m^2 - m)\left[\frac{g_n \bar{a}}{2T} \int_0^\infty h(\tau)\, d\tau\right]^2 + \frac{a_n^2 c_n m \bar{a}^2}{2T} \int_0^\infty h(\tau)\, h(\tau + t)\, dt. \tag{28}$$

Having substituted expressions (28) into formula (23) and having used expression (16) for $p(B_m)$, we obtain the following expression for the correlation function:

$$K_{\tau_n}(t) = a_n^2 g_n^2 \left[\lambda \bar{a} \int_0^\infty h(\tau)\, d\tau\right]^2 + a_n^2 c_n \lambda \bar{a}^2 \int_0^\infty h(\tau)\, h(\tau + t)\, d\tau. \tag{29}$$

Having substituted the value of the weight function h(t), according to formula (19), into this equation, we will have

$$K_{\tau_n}(t) = \frac{a_n^2}{\omega_n^2}\left[\frac{c_n \lambda \bar{a}^2}{2p_n} e^{-\frac{\varepsilon \omega_n^2}{2} t}\left(\frac{p_n}{\varepsilon \omega_n^2} \cos p_n t + \frac{1}{2} \sin p_n t\right) + \frac{g_n^2}{\omega_n^2} (\lambda \bar{a})^2\right]. \tag{30}$$

According to the known correlation function we may determine the spectral density of the power of the forced oscillations of the ship's hull:

$$G_{zz}(\omega) = \sum_{n=1}^{\infty} G_{\tau_n}(\omega), \tag{31}$$

where

$$G_{\varphi_n} = \frac{1}{\pi} \int_{-\infty}^{\infty} K_{\varphi_n}(\tau) e^{-i\omega\tau} d\tau. \tag{32}$$

By using formula (29), we obtain

$$G_{\varphi_n}(\omega) = \frac{\pi_n^2}{\pi} \int_{-\infty}^{\infty} \left[g_n i\bar{a} \int_0^{\infty} h(\tau)\, d\tau \right]^2 e^{-i\omega t}\, dt + \\ + \frac{\pi_n^2}{\pi} \int_{-\infty}^{\infty} \left[c_n i\bar{a}^2 \int_0^{\infty} h(t)\, h(t+\tau)\, dt \right] e^{-i\omega\tau} d\tau. \tag{33}$$

The first item of equation (33) contains a term with a delta-function, and the second may be simplified by replacement of the variables

$$G_{\varphi_n}(\omega) = \frac{2\pi_n^2 g_n^2}{\omega_n^4} (i\bar{a})^2 \delta(\omega) + \frac{a_n^2 c_n}{\pi} (i\bar{a})^2 |\Phi(i\omega)|^2, \tag{34}$$

where

$\Phi(i\omega) = \dfrac{1}{\omega_n^2 - \omega^2 + i\varepsilon\omega_n^2\omega}$ is the frequency charactistic of the linear system with the subscript n.

We finally find the spectral density of the power of the forced vertical bending oscillations of the ship's hull being sought:

$$G_{zz}(\omega) = 2(i\bar{a})^2 \delta(\omega) \sum_{n=0}^{\infty} \frac{a_n^2 g_n^2}{\omega_n^4} + \frac{\lambda\bar{a}^2}{\pi} \sum_{n=1}^{\infty} \frac{\pi_n^2 c_n}{\left(\omega_n^2 - \omega^2\right)^2 + \varepsilon^2\omega_n^4\omega^2}. \tag{35}$$

Thus, the spectral density of the power of the forced oscillations of the hull is continuous in the entire interval of the variation of frequencies with the exception of the beginning of the coordinates, where there is a characteristic corresponding to the constant component of the process. Since the coefficient ε of internal friction is small, the continuous part of the spectrum will have maximums near point $\omega = \omega_n$, i.e., on the natural frequencies of the free oscillations of the ship's hull.

The attenuation factor $\varepsilon\omega_n^2$ depends upon the frequency of the corresponding shape of the free oscillations and rapidly increases with an increase in the number n of the shape. Thus, the random external load considered

will basically excite an oscillation of the lower tones.

For an example, we will give data from measurements of the vertical elastic oscillations of the hull of the diesel-electric vessel "Vankarem". In motion in solid and broken ice (see Figure 1, 2), oscillations of the hull in ballast were recorded with a frequency of 1.2 oscillations per minute and loaded with a frequency of 94 oscillations per minute. The calculation of the vertical elastic oscillations demonstrated that the measured frequency is close to the first tone of the natural oscillations of the hull.

According to Todd's approximate formula

$$N = 94\,000 \sqrt{\frac{BH^3}{DL^3}},$$

where L = 123 meters; B = 18.54 meters; H = 11.6 meters; and D = 11,200 tons. Then

$$N = 94\,000 \sqrt{\frac{18.54 \cdot 11.6^3}{11\,200 \cdot 123^3}} = 104 \text{ oscillations per minute.}$$

Thus, we may make the following conclusions:

1. In the motion of a ship in solid ice, elastic vertical oscillations of the hull are excited--the ice vibration.

2. The presence of items containing harmonic terms cos $p_n t$ and sin $p_n t$ in the expression for the correlation function indicates the periodicity of these oscillations.

3. Stable vertical oscillations of the ship's hull correspond to the lower tones of its natural oscillations.

BIBLIOGRAPHY

1. Babayev, N. N., and Lentyakov, V. V., Nekotoryye voprosy obshchey vibratsii sudov (Some problems of the general vibration of ships), Leningrad, Sudpromgiz, 1961.

2. Lening, G. H., and Battin, R. G., Sluchaynyye protsessy v zadachakh avtomaticheskogo upravleniya (Random processes in problems of automatic control), (Russian translation), Moscow, Izd-vo inostr. lit-ry, 1958.

3. Kheysin, D. Ye., "General vibration of a ship's hull in motion in solid ice," Sudostroyeniye (Shipbuilding), 1970, No. 9.

ELASTIC OSCILLATIONS OF A SHIP'S HULL IN THE EFFECT OF RANDOM PULSED ICE LOADS

D. Ye. Kheysin

pages 132-136

During independent motion of ships in ice, frequently a general vibration of the hull is noticed, not associated with the operating regime of the propulsion plant. In this case, transverse vertical and horizontal bending oscillations of the hull, of lower tones, are recorded. The only cause of these oscillations is the effect of dynamic ice loads on the bow end of the ship.

Data from observations and strain-gauge tests demonstrate that the reaction of the ship with the ice may be considered as a random process, in which the impact impulses of random amplitude at random moments of time t_i act on various sections of the side with random coordinates x_j. In a steady-state regime of the motion of the ship in homogeneous ice, this process may be considered as steady-state and ergodic.

In calculations of the elastic oscillations the hull of a ship is usually considered as a non-prismatic elastic beam with a length L. The rigidity EI and the linear mass ρ are considered to be assigned functions of the coordinate x along the axis of the beam.

If a random dynamic load is acting on the beam, then the oscillations caused by it have a random nature. In reference [4], the pulsed external effect of a random ice load on the hull were represented by a set of delta-functions, randomly distributed in time. We will investigate this problem in more detail, with a consideration of the real shape of the impact pulses. As the basic characteristic in the description of the forced random oscillations we will accept the spectral density, since according to the spectrum we may determine the resonance zones, and, in the first approximation, the reactions of the structure [2].

The differential equation of small bending oscillations of a ship's hull w(x, t), with a consideration of a scattering of energy, has the form

$$\frac{\partial^2}{\partial x^2}\left[EI\frac{\partial^2}{\partial x^2}\left(w+a\frac{\partial w}{\partial t}\right)\right]+\rho\left(\frac{\partial^2 w}{\partial t^2}+b\frac{\partial w}{\partial t}\right)=F(x,t). \tag{1}$$

The coefficients a and b characterize the attenuation associated with the internal and external resistance. The external force F is a random impulsive function of the coordinate x and time t.

We will designate a set of realizations of the external disturbing force as $\{{}^kF(x, t)\}$, where any realization is determined in the section $0<x<L$. The k-th solution of differential equation (1) corresponds to each k-th realization of the external effects:

$${}^kw(x, t)\in\{{}^kw(x, t)\},$$

where $\{{}^kw(x, t)\}$ is a set of possible reactions of the beam, the probability characteristics of which are being sought.

If the external effect on the beam is steady-state, then its reactions will also be steady-state.

We will consider a quite large interval of time (-T, T). A typical realization of a random pulsed process for this interval has the form

$${}^kF(x, t)=\sum_{j=-N}^{N}{}^k\varphi_j(t)\,\delta(x-x_j). \tag{2}$$

Here ${}^k\varphi_j(t)$ is a function describing in time the j-th pulse of the k-th realization, equal identically to zero outside the interval $t_{2j}\leq t\leq t_{2j+1}$. The number of impulses falling in the interval under consideration for a steady-state regime is determined according to the formula $2N+1=2\lambda T$, where λ is the average density of impulses, i.e., their average number in a unit of time.

The shape of the pulses is assigned by a non-random function of time u(t), which is identically equal to zero outside the interval $0\leq t\leq 1$, so that

$${}^k\varphi_j(t)={}^ka_ju\left(\frac{t-t_{2j}}{{}^k\tau_j}\right),$$

where ${}^k\tau_j = t_{2j+1} - t_{2j}$ is the duration of the j-th impulse in the k-th realization, ${}^k a_j$ is the amplitude of the impulse.

The duration of the impact impulses, the magnitude of the pause between the successive impacts, the amplitudes of the impact impulses, and the coordinates of the points of their application will be considered to be statistically independent random quantities.

Let us assume that by one calculation method or another we have succeeded in determining the principal forms of the free non-attenuating oscillations of the beam, $b_n(x)$, and the corresponding natural frequencies ω_n, and

$$\frac{d^2}{dx^2}\left(EI\frac{d^2v_n}{dx^2}\right) - \omega_n^2 \rho v_n = 0. \tag{3}$$

Each item in sum (2) may be represented in the form of a series, with respect to the forms of the free oscillations. Having divided this sum by $\rho \neq 0$ and using the property of orthogonality of the forms of the free oscillations with a weight ρ, we obtain

$$\frac{{}^k a_j u_j(t)\,\delta(x-x_j)}{\rho(x)} = \sum_{n=1}^{\infty} \frac{{}^k a_j u_j(t)\, v_n(x_j)\, v_n(x)}{\int_0^L \rho(x)\, v_n^2(x)\, dx}. \tag{4}$$

We will omit the sum sign with respect to the subscript j here and further on. We will seek the solution to equation (1) in the form of the series

$$w(x, t) = \sum_{n=1}^{\infty} \varphi_n(t)\, v_n(x).$$

Having substituted this expression into equation (1), with a consideration of formulas (4) and (3), we obtain a linear second-order differential equation with a random right-hand part for the determination of $\varphi_n(t)$:

$$\ddot{\varphi}_n + (b + a\omega_n^2)\dot{\varphi}_n + \omega_n^2 \varphi_n = a_n {}^k a_j u_j(t)\, v_n(x_j), \tag{5}$$

where

$$a_n^{-1} = \int_0^L \rho(x)\, v_n^2(x)\, dx.$$

Thus, the problem is reduced to a unidimensional one, and it is equivalent to the problem of the effect of a discrete random signal to the input of a linear system with one degree of freedom. Each such system with the subscript n corresponds to the n-th form of the free oscillations of a beam. The initial set of impulses, the amplitudes of which are multiplied by the weight multiplier, depending upon the multiplier of the form of the oscillations under consideration, act on each unidimensional system.

According to the known ratio between the spectral densities of the input and output for linear systems, we obtain the following expression for the spectral density of the forced oscillations of a beam:

$$S_w(\omega) = \sum_{n=1}^{\infty} S_{F_n}(\omega) |Y_n(i\omega)|^2. \tag{6}$$

Here $Y_n(i\omega)$ is the frequency characteristic of a unidimensional linear system with the subscript n: $S_{F_n}(\omega)$ is the spectral density of the external effect for the n-th form.

In accordance with the general theory of the spectra of pulsed random processes, we find the spectral density of the aperiodic pulsed random process under consideration, with a zero average value [1]

$$S_{F_n}(\omega) = \frac{\lambda \sigma_{an}^2}{\pi} \int_0^{\infty} \xi^2 |g(\omega\xi)|^2 w_\tau(\xi)\, d\xi, \tag{7}$$

where σ^2_{an} is the dispersion of the amplitudes of the impact impulses; $w_\tau(\xi)$ is the distribution function of the duration of the impulses; $g(\omega\xi)$ is the Fourier spectrum of the form of a single impulse,

$$g(\omega\xi) = \int_0^1 u(t) e^{-i\omega\xi t}\, dt.$$

According to the determination of the dispersion,

$$\sigma^2_{an} = \sigma_n^2 E_k \{a_j^2 v_n^2(x_j)\}.$$

By using the theorem of the product of the mathematical expectations of independent random quantities, we obtain

$$\sigma^2_{an} = \sigma_n^2 E_k \{a_j^2\}\, E\{v_n^2(x_j)\}. \tag{8}$$

As a consequence of the statistical independence of the sequence of random amplitudes ${}^{k}a_j$, the result of averaging according to the k-realization does not depend upon the subscript j. For the other comultiplier from formula (8) we perform averaging along the entire length of the hull, assuming the known density of the probability of an impulse $p(x_j)$ falling at a point with the coordinate $x = x_j$. Then

$$\sigma^2_{an} = \bar{a}^2 a_n^2 \int_0^L p(x) v_n^2(x)\, dx.$$

We finally find the spectral density of the external effect, corresponding to the n-th form of the three oscillations of the beam

$$S_{F_n}(\omega) = \frac{\lambda \bar{a}^2 a_n^2}{\tau} \int_0^\infty \xi^2 |g(\omega\xi)|^2 w_\tau(\xi)\, d\xi \int_0^L v_n^2(x)\, p(x)\, dx. \tag{9}$$

We determine the frequency characteristics $Y_n(i\omega)$ according to the formula

$$Y_n(i\omega) = \frac{1}{\omega_n^2 - \omega^2 + i\omega\left(b + a\omega_n^2\right)}.$$

Having substituted this expression into equality (6) and having used equation (7), we find the spectral density of the forced oscillations of the beam

$$S_w(\omega) = \frac{\lambda \bar{a}^2}{\tau} \int_0^\infty \xi^2 |g(\omega\xi)|^2 w_\tau(\xi)\, d\xi \times$$

$$\times \sum_{n=1}^{\infty} \frac{a_n^2 \int_0^L v_n^2(x) p(x)\, dx}{\left(\omega^2 - \omega_n^2\right)^2 + \left(b + a\omega_n^2\right)^2 \omega^2}. \tag{10}$$

Investigations of the forced oscillations of the ship's hull under the effect of impact ice loads demonstrated that the distribution of impulses in time is subordinate to Poisson's law. The pauses between the successive impulses are distributed according to an exponential law

$$w_T(t) = T_1 e^{-\frac{t}{T_1}},$$

where T_1 is the average duration of the pause between impulses. Obviously, $T_1^{-1} \approx \lambda$.

Assuming that the duration of each pulse τ_0 is identical and considering that $\tau_0 << T_1$, from formula (7) we obtain [1]

$$S_{F_n}(\omega) = \frac{\lambda \bar{a}^2 \tau_0^2}{\pi} |g(\omega\tau_0)|^2 \chi_n^2 \int_0^L v_n^2(x) p(x) dx.$$

Thus, at $\tau_0 << T_1$ the continuous spectrum of the external effect coincides with the spectrum of a single impulse with an accuracy up to the constant multiplier. For the sequence of delta-functions we are dealing with "white noise". The formula for the spectral density for the forced oscillations of the beam in this case coincides with what was obtained in reference [4].

The resistance factors a and b are usually not great, so that the continuous spectram (10) has maximums near the points $\omega = \omega_n$, i.e., on the natural frequencies of the free oscillations. The attenuation factor $b + a\omega_n^2$ depends upon the frequency of the corresponding form of the free oscillations and increases with an increase in the form number n. Thus, the spectral density of the forced oscillations will rapidly decrease, beginning with a certain value of the frequency $\omega = \omega_m$.

At a short duration τ_0 of the impulses, regardless of their form, the spectral density remains constant up to frequencies comparable with respect to order of magnitude with τ_0^{-1} [3]. It is clear that in fulfillment of the condition $\tau_0^{-1} > \omega_m$ the approximation of the impulses by delta-functions, used in reference [4], does not lead to any significant errors. At comparatively small values of τ_0^{-1}, it is necessary to consider the actual form of the impact impulse.

The spectral density of a single impulse rapidly decreases for frequencies $\omega > \tau_0^{-1}$. Thus, the spectrum of the forced random oscillations of the ship's hull will rapidly decrease, both due to attenuation in the region of high frequencies, and as a consequence of the limited nature of the width of the spectrum of each impulse. If τ_0^{-1} with respect to order of magnitude is comparable with the lower natural frequencies of the free oscillations of the hull, it is basically the lower tones of the oscillations that will be excited.

BIBLIOGRAPHY

1. Levin, B. R., Teoreticheskiye osnovy statisticheskoy radiotekhniki (Theoretical bases of statistical radio engineering), Moscow, "Sovetskoye radio", 1969.

2. Morrow, C. T., "On the creation of structures and equipment for space purposes," in the collection: Sluchaynyye kolebaniye (Random oscillations), Moscow, "Mir", 1967.

3. Khar'kevich, A. A., Teoreticheskiye osnovy radiosvyazi (Theoretical bases of radio communications), Moscow, Gostekhizdat, 1957.

4. Kheysin, D. Ye., "Vibration of a ship's hull in motion in solid ice," Sudostroyeniye (Shipbuilding), 1970, No. 9.

STATIC BENDING OF BEAMS IN THE EFFECT OF RANDOM ICE LOADS

D. Ye. Kheysin

pages 137-147

The other dimensions of the girders of the side framing of the hulls of ships intended for ice navigation depend upon the magnitude of the external ice loads. In the calculations, the ice loads are considered to be applied statically, and the carrying capacity of the structures is determined only in the elastic zone.

Full-scale strain-gauge tests of the strength of the side structures of icebreakers and transport vessels demonstrated that ice loads are random in nature. This should be considered both in the determination of the calculated loads for individual elements of the framing and in the processing of experimental data.

Methods of calculating beams and beam system for the effect of random loads may be developed if the designs operating in the elastic zone are considered as linear systems with distributed parameters. The probability approach to the investigation of such systems is possible in two cases: in the first case, if for the problem under consideration we may construct a Green function, i.e., determine the lines of the effect; in the second place, if the random distrubance may be represented in the form of superposition of non-random functions with random amplitudes [4]. In the calculation of beams in the elastic zone these requirements can practically always be accomplished.

The external effects causing the bending of beams are usually reduced to a system of transverse and longitudinal stresses and bending moments. The random nature of the external effects in the static calculations should be considered by investigating them as random quantities or random functions of three-dimensional coordinates. In a general case, the external effects may be statistically independent. In a linear statement of the problem this makes it possible to investigate each type of load individually, using the principal of superposition.

We will consider the static bending of a long beam under the effect of a random transverse load q(x). The bending of such a beam satisfies the differential equation

$$\frac{d^2}{dx^2}\left(EI\frac{d^2x}{dx^2}\right) = q(x) \tag{1}$$

and the boundary conditions at its end. In equation (1) the magnitude of EI is variable in a general case of rigidity of the beam.

We will define two types of transverse loads on a beam: continuous and discrete. In the first case, a distributed load q(x) acts on the beam, which is a quite smooth random function of the coordinate x. In the second case, static concentrated forces Q_j, applied at points with random coordinates $x = x_j$ act from time to time on the beam. The forces Q_j and the coordinates x_j form system of statistically independent random quantities.

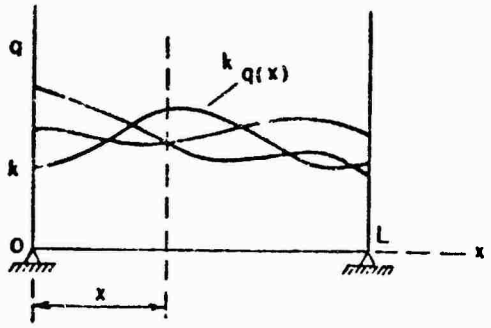

Figure 1. Explanation of the calculation of beams for the effect of continuous random loads.

We will investigate a case of a continuously distributed load. We will designate the set of possible realizations of the external load as $\{{}^k q(x)\}$. Several such realizations are shown in Figure 1. The average value of the external load as a function of the coordinate x is obtained by having averaged the realizations throughout the set

$$E_k\{{}^k q(x)\} = \bar{q}(x).$$

We may always decenter the random external load q(x). As a consequence of the linear nature of the problem, in the future we will consider only the decentered external effects with a 0 mathematical expectation. Then the solutions will be found with an accuracy up to a determined component, corresponding to the average value of the external load.

We will represent the continuous centered random function q(x) as a superposition of a counted set of clementary components with random amplitudes [1]:

$$q(x) = \sum_{n=1}^{\infty} V_n v_n(x), \tag{2}$$

where V_n are random quantities with zero average values; $v_n(x)$ are the fundamental (natural) functions of the problem, forming a complete orthogonal system of the functions.

We will determine the correlation function of the external load

$$K_q(x, \xi) = \sum_{i,j=1}^{\infty} E\{V_i V_j\} v_i(x) v_j(\xi). \tag{3}$$

At i = j

$$E\{V_i^2\} = K_{ii} = D_i,$$

where D_i is the dispersion of the random quantity V_i.

At i ≠ j

$$E\{V_i V_j\} = K_{ij},$$

where K_{ij} is the correlation moment of the random quantities V_i and V_j.

Thus, we find the correlation function of the external effect

$$K_q(x, \xi) = \sum_{i=1}^{\infty} v_i(x) v_i(\xi) D_i + \sum_{i \neq j}^{\infty} v_i(x) v_j(\xi) K_{ij} \tag{4}$$

and the dispersion

$$D_q(x) = \sum_{i=1}^{\infty} |v_i(x)|^2 D_i + \sum_{i \neq j}^{\infty} v_i(x) v_j(x) K_{ij}. \tag{5}$$

If the three-dimensional correlation function of the external effect $K_q(x, \xi)$ is assigned, the elements of the correlation matrix $\|K_{ij}\|$ may be determined from expression (3), using the condition of orthogonality of the fundamental functions. Having multiplied both parts of expression (3) by

$v_m(x)$ and $v_n(x)$ and having twice integrated throughout the entire length L of the beam, we obtain

$$K_{mn} = \int_0^L \int_0^L K_q(x, \xi) v_m(x) v_n(\xi) \, dx \, d\xi. \tag{6}$$

If all the coefficients V_n of expansion (2) are uncorrelated, then $K_{mn} = 0$ at $m \neq n$. Then we are dealing with a canonical expansion and formulas (4) and (5) are simplified.

As is known [3], the solution of the static problem of bending of a beam with the right-hand part q(x) may be presented in the form of a series according to the natural functions (eigenfunctions),

$$w(x) = \sum_{n=1}^{\infty} \frac{v_n(x)}{\lambda_n} \int_0^L q(\xi) v_n(\xi) \, d\xi, \tag{7}$$

where λ_n is an eigenvalue corresponding to the n-th eigenfunction of the problem.

According to the determination, for the correlation function of the bucklings,

$$K_w(x, \xi) = \sum_{m, n=1}^{\infty} \frac{v_m(x) v_n(\xi)}{\lambda_m \lambda_n} \int_0^L \int_0^L K_q(x, \xi) v_m(x) v_n(\xi) \, dx \, d\xi.$$

Considering expressions (3) and (6), we finally obtain the correlation function of thebucklings of the beam

$$K_w(x, \xi) = \sum_{m, n=1}^{\infty} \frac{v_m(x) v_n(\xi)}{\lambda_m \lambda_n} K_{mn}. \tag{8}$$

The dispersion may be found according to the following formula:

$$D_w(x) = \sum_{m, n=1}^{\infty} \frac{v_m(x) v_n(x)}{\lambda_m \lambda_n} K_{mn}. \tag{9}$$

It is not difficult to determine the correlation functions and dispersions for the other elements for the bending of the beam, such as, for example, for the correlation function of the bending moment

$$K_{\mathfrak{M}}(x, \xi) = E^2 I(x) I(\xi) \sum_{m, n=1}^{\infty} \frac{v_m''(x) v_n''(\xi)}{\lambda_m \lambda_n} K_{mn}.$$

Thus, with the known three-dimensional correlation function of the external effect, the solution of the problem of the static bending of a beam under the effect of a random external load is performed according to the following scheme.

It is primarily the eigenfunctions and eigenvalues of the problem that are found. Then according to the average value of the external effect the average value of the bending of the beam is determined. Finally, according to the given correlation function of a decentered external effect, the elements of the correlation matrix are calculated and the correlation functions and dispersions of the buckling and other elements of the bending of the beam are determined.

Actually, the statistical characteristics of the external effect are frequently unknown and we can obtain only an indirect concept of them according to the results of measurements performed in real structures. In this case, the reverse problem arises--to find the characteristics of the external effect q(x) according to a known reaction of an elastic system w(x). If the Green function G(x, ξ) is known, it is necessary to solve a first-order Fredholm integral equation with a symmetrical kernel

$$w(x) = \int_0^l G(x, \xi) q(\xi) d\xi.$$

If the orthostandardized system of eigenfunctions $v_n(x)$ is determined, then, by using the theorem of expansion [3], we obtain

$$q(x) = \sum_{n=1}^{\infty} \lambda_n v_n(x) \int_0^l v_n(\xi) w(\xi) d\xi + \varphi(x), \tag{10}$$

where $\varphi(x)$ is an arbitrary function, orthogonal to all the eigenfunctions $v_n(x)$. For a complete orthostandardized sequence of functions $v_n(x)$ the arbitrary function $\varphi(x) \equiv 0$ and the solution of (10) are the sole ones [2].

Then

$$K_q(x, x') = \sum_{m, n=1}^{\infty} \lambda_m \lambda_n v_m(x) v_n(x') \int_0^L \int_0^L v_m(\xi) v_n(\eta) K_w(\xi, \eta) d\xi d\eta, \qquad (11)$$

where $K_w(\xi, \eta) = E\{w(\xi)w(\eta)\}$ is the correlation function of the beam reaction (in the given case of buckling), which may be calculated according to the results of the experiments. Actually, the measurements are conducted in a finite set of points, so that the complexity lies in approximating the correlation function $K_w(\xi, \eta)$ according to a discrete series.

Expression (11) may be simplified by means of expansion of the buckling of the beam into a series according to the eigenfunctions

$$w(x) = \sum_{j=1}^{\infty} c_j v_j(x). \qquad (12)$$

Having substituted this expression into formula (11), and considering the conditions of orthogonality of the eigenfunctions, we find

$$K_q(x, x') = \sum_{m, n=1}^{\infty} \lambda_m \lambda_n v_m(x) v_n(x') E\{c_m c_n\}. \qquad (13)$$

This equation may be considered as a conversion of formula (8). By performing the measurements at s points with coordinates x_i ($i = 1, 2, \ldots s$), we obtain a system of algebraic equations

$$w(x_i) = \sum_{j=1}^{s} c_j v_j(x_i), \; i = 1, 2 \ldots s.$$

Having solved this system, we determined, in approximation, the first coefficients of expansion (12). Having substituted the expansion factors c_i calculated by such a manner (from the experiments) into formula (13) and performing the appropriate averaging, we obtain approximate expression for $K_q(x, x')$. We will not go into the details of the proof of the convergence of the process.

We will shift further to discrete random loads, characteristic for the process of the reaction of a ship's hull with the ice, when local ice loads of an impulsive nature act on the hull structures.

We will consider the simplest case of a single-span prismatic beam with a rigidity EI = const. At different times, transverse concentrated static forces Q_j act on the beam, applied at points with random coordinates $x = x_j$ (Figure 2). The random quantities Q_j and x_j are statistically independent, and the density of the probability of the distribution of amplitudes $g_Q(Q)$ and the probability density of $p_x(x_j)$ falling at a point with the coordinate $x = x_j$ are considered to be assigned. The calculation of the average values and dispersion of the elements of the bending of the beam are of practical interest, i. e., the bucklings, bending moments, etc.

For the mathematical expectation the following principle is proper, which is valid in any arrangement of the supports of the beam:

The mathematical expectation of the bending element of the beam in the effect of a randomly applied concentrated load on it is equal to the value of the corresponding bending element in the effect of a non-random load on the beam, distributed with an intensity $q(x) = \overline{Q} p_x(x)$, where $\overline{Q}$ is the mathematical expectation of the amplitude of the random load, $p_x(x)$ is the probability density of the load falling at that point.

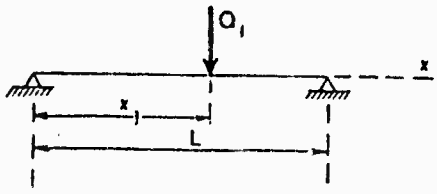

Figure 2. Effect of the concentrated force on the beam.

We will designate the set of possible values of the load as $\left\{{}^{k}Q_j\right\}$. By averaging according to the k-realizations and considering the statistical independence of Q_j, we obtain

$$E_k\{{}^{k}Q_j\} = \overline{Q} = \int_{-\infty}^{+\infty} Q g_Q(Q)\, dQ.$$

We will give the proof of the principle advanced for buckling of the beam. Buckling under the effect of the concentrated force ${}^{k}Q_j$, applied at point $x = x_j$, is determined according to the formula

$${}^{k}w_{Q_j}(x) = {}^{k}Q_j \gamma(x, x_j), \tag{14}$$

where $\gamma(x, x_j)$ is the buckling of the beam, caused by the unit force applied at point $x = x_j$ (the line of effect).

By calculating the mathematical expectations for both parts of equality (14) and using the theorem of the mathematical expectation of the product of statistically independent quantities, we obtain

$$E_k\{{}^k w_{Q_j}(x)\} = \overline{w_Q(x)} = \bar{Q}\int_0^L \bar{\gamma}(x, \xi)\, p_x(\xi)\, d\xi. \tag{15}$$

The buckling of the beam under the effect of the distributed load q(x) may be found according to the formula [5]:

$$w_q(x) = \int_0^L \gamma(x, \xi)\, q(\xi)\, d\xi. \tag{16}$$

The right-hand parts of expression (15) and (16) coincide if we assume that $\bar{Q}\, p_x(x) = q(x)$, which it was also required to prove. The corresponding proof may be given for any element of the bending of the beam. Consequently, the determination of the average values of the elements of the bending of beams in the effect of discrete random loads is reduced to the calculation of the beams for the effect of non-random loads, distributed in accordance with the density of the probability of $p_x(x)$ falling at that point. A similar situation occurs for any linearly deformed elastic system.

We will find the dispersion of the bucklings of the beam. According to the determination of the dispersion

$$\sigma_w^2 = \overline{w_Q^2(x)} - (\overline{w_Q(x)})^2,$$

where

$$\overline{w_Q^2(x)} = \overline{Q^2}\int_0^L \gamma^2(x, \xi)\, p_x(\xi)\, d\xi. \tag{17}$$

By using formulas (15) and (17), we obtain

$$\sigma_w^2 = \overline{Q^2}\,[\bar{\gamma}^2 - (\bar{\gamma})^2] + (\bar{\gamma})^2 \sigma_Q^2. \tag{18}$$

where

$$\overline{\gamma^2} = \int_0^L \gamma^2(x, \xi)\, p_x(\xi)\, d\xi; \quad \overline{\gamma} = \int_0^L \gamma(x, \xi)\, p_x(\xi)\, d\xi. \tag{19}$$

In formula (18) the average value and dispersion of the external loads are considered to be assigned. Full-scale strain-gauge tests of ships demonstrated that the distribution of the amplitudes of external ice loads on the framing is close to a Rayleigh distribution. In this case the mathematical expectation and dispersion are associated by the following dependence:

$$\bar{Q} = \sigma_Q \sqrt{\frac{\pi}{2}},$$

and instead of formula (18) we may write

$$\sigma_w^2 = \bar{Q}^2 \left[\overline{\gamma^2} \frac{2 + \pi}{\pi} - (\bar{\gamma})^2 \right]. \tag{20}$$

The dispersion of the other elements of the bending are determined in an analogous manner. In particular, for the bending moments we may use formulas (18), and (19), substituting into them the quantity EI γ'' instead of the buckling γ.

As an example we will consider a single-span freely resting beam, assuming the probability of an external force striking it is identical throughout the entire length of the beam. The average value of the bending moment is found according to the formula for a beam loaded with a uniform load, q = ($\bar{Q}$/L) i.e.,

$$\overline{\mathfrak{M}(x)} = -\frac{\bar{Q}L}{2}\left(\frac{x}{L} - \frac{x^2}{L^2}\right),$$

and we will determine the dispersion according to the following equation

$$\sigma_{\mathfrak{M}}^2 = \frac{x^2}{3}\left(1 - \frac{x}{L}\right)^2 \left(\sigma_Q^2 + \frac{1}{4}\bar{Q}^2\right).$$

If the amplitudes of the external force is constant, Ω = const, and only the point of application of the force is random, then $\sigma_{\Omega} = 0$ and the dispersion of the bending moment is

$$\sigma^2_{\mathfrak{M}} = \frac{x^2}{12}\left(1 - \frac{x}{L}\right)^2 \bar{\Omega}^2.$$

The dimensionless curves of the bending moments $\bar{\mathfrak{M}}/\Omega L$ and the mean square deviation $\sigma_{\mathfrak{M}}$ for this case are given in Figure 3.

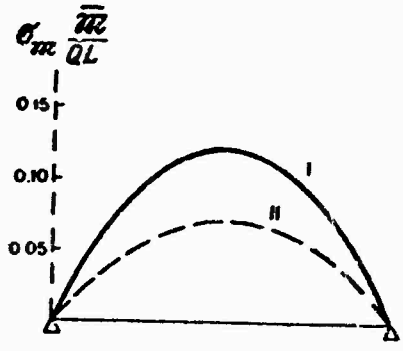

Figure 3. Dimensionless curves of the average bending moments (I) and the mean square deviations (II) for a freely resting beam.

The dependences obtained in this article may be used not only for a single-span beams but also in the calculation of multi-span beams and beam systems. For example, the probability method was applied in the processing of data from strain-gauge tests of the side framing of a powerful icebreaker.

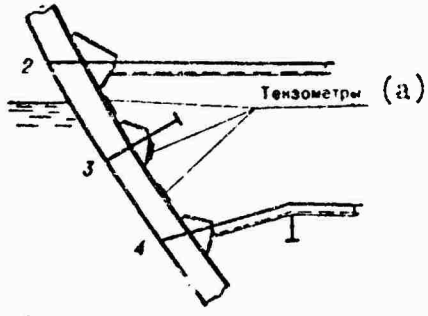

Figure 4. Diagram of the arrangement of strain-gauges on the side framing of a powerful icebreaker. a) strain gauges.

Strain-gauge stress pickups were cemented on the shelves of the frames near the existing waterline (Figure) for estimation of the nature of distribution of the ice load along the molded depth in this region. The calculation scheme for the frame is shown in Figure 5. In the processing of experimental data, the readings of the strain gauges in the middle of spans 2--3 and 3--4 were compared. In all the oscillograms, without exception, the readings of these strain gauges are opposite in sign, i.e., if the shelf of the frame in the section 2--3 is extended, then in the section 3--4 it is compressed, and vice versa. This corresponds to the ice load applied in the limits of one span.

In the processing of experimental data, 113 oscillograms were selected, with impulses corresponding to the impact in span 3--4. For each impulse, the ratios of the stresses σ_1 in the center of the span experiencing the impact to the stresses σ_2 in the adjacent unloaded span were calculated. Since the moments of inertia and the moments of resistance of the frame in spane 2--3 and 3--4 are identical, we may assume the ratio σ_1/σ_2 is equal to the ratio of the span bending moments m_{3-4}/m_{2-3}. A histogram of the experimental values of this ratio is given in Figure 6.

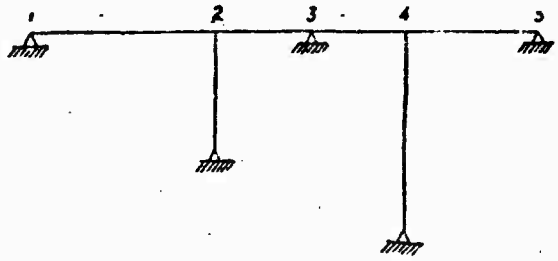

Figure 5. Diagram of the calculation of the frame.

Later the statistical characteristics of the selection were calculated, and its representativeness was proven. In this case the average value of the ratio m_{3-4}/m_{2-3} turned out to be equal to 4.0, and the mean square deviation $\sigma_m = 1.17$.

For the analysis of the results obtained, theoretical calculations were also performed for a load uniformly distributed in the span 3--4, distributed throughout the triangle, and the concentrated load applied at various points along the length of the section. For all these cases the ratio η_{3-4}/η_{2-3} was determined (Figure 7). In a case of a uniformly distributed load, this ratio is equal to 4.0, which coincides with the average measured value. This makes it possible to affirm that the probability of the effect of the ice load along the molded depth within limits along section 3--4 is identical.

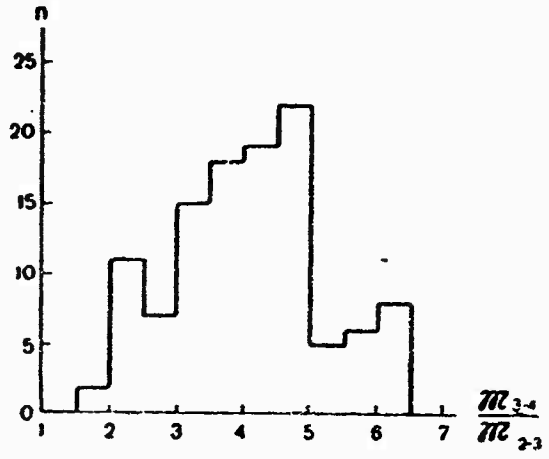

Figure 6. Histogram of the ratios of the span moments m_{3-4}/m_{2-3}, n is the number of measurements.

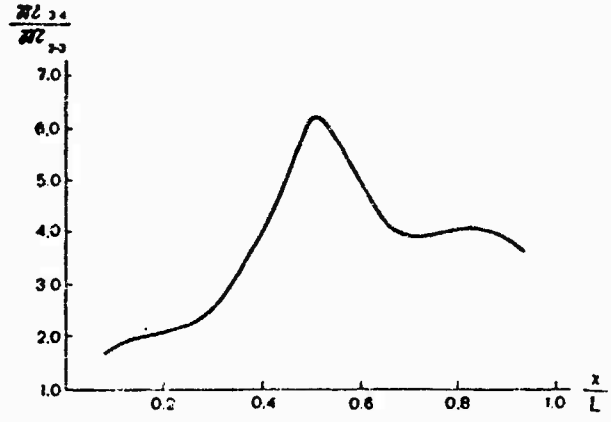

Figure 7. Dependence of the ratio m_{3-4}/m_{2-3} upon the place of application of the concentrated force in span 3--4.

It is apparent that the calculation of the side framing for the effect of distributed ice loads is equivalent to the calculation with respect to average values. The calculation for the effect of concentrated forces corresponds to the extreme measured values of the ratio m_{3-4}/m_{2-3} (see the histogram in Figure 6 and the curve in Figure 7). Indicentally, the probability of these values is already not so small and for the interval 5.5--6.5 amounts to P = 0.1. Consequently, in the given case the calculation of the side framing for the effect of concentrated loads is better justified.

BIBLIOGRAPHY

1. Venttsel', Ye. S., Teoriya veroyatnostey (Theory of probabilities), Moscow, "Nauka", 1969.

2. Korn, G., and Korn, T., Spravochnik po matematike (Handbook on mathematics), Moscow, "Nauka", 1968.

3. Courant, R., and Hilbert, D., Metody matematicheskoy fiziki (Methods of mathematical physics) (Russian translation), volume I, Moscow - Leningrad, Gostekhizdat, 1934.

4. Sveshnikov, A. A., Prikladnyye metody teorii sluchaynykh funktsii (Applied methods of the theory of random functions), Moscow, "Nauka", 1968.

5. Spravochnik po stroitel'noy mekhanike korablya (Handbook on the structural mechanics of a ship), volume 1, Leningrad, Sudpromgiz, 1958.

DETERMINATION OF THE PLIABILITY FACTORS OF THE ELASTIC COVERINGS OF FRAMES IN THE EFFECT OF AN ICE LOAD

V. A. Likhomanov, and O. V. Faddeyev pages 148-153

With respect to their nature, ice loads are local, and, as a rule, they are applied in the region of the existing waterline. The width of the zone of contact of the ship's side with the ice in this case is usually not great in comparison with the length of the frame. Therefore, the ice load may be considered as concentrated and applied within the limits of one span. In such a case, the frame may be considered as a single-span elastic beam, fastened at the ends. If there are no stringers in the composition of the side plating, the pliability factors of the elastic covering (fastening) of the ends of this beam may be easily calculated, by using the method of successive balancing of the unit [1, 2].

In the presence of stringers, the determination of the pliability factors of the fastenings is essentially complicated. Usually in such cases these factors are designated in approximation or a calculation is made of the entire framework of the frame, which has led to cumbersome calculations.

In this article a simplified method of calculating the pliability factors is discussed. The effect of cross connections on the bending of the frames will be considered by the introduction of a correction factor φ, which is the ratio of the angle of rotation of the support section in elastic fastening to the angle of rotation of the support section of a freely resting beam in the effect of the single moment

$$\varphi = \frac{v'_{упр.з}}{v'_{св.оп}}.$$

[$v_{упр.з} = v_{upr.z} = v_{\text{elastic fastening}}$; $v_{св.оп} = v_{sv.op} = v_{\text{freely resting}}$]

In the derivation of the calculation dependences we will assume that the cross connections are located at equal distances from each other and from the deck.

We will consider the continuous beam represented in Figure 1. The external load is applied in the span 1--2. For disclosure of the static indefiniteness of this beam, it is feasible to use the theorem of three moments. The equations of these moments for the hold branch of the frame (span 2--4) have the form:

$$\begin{cases} \mathfrak{N}_0\mathfrak{M} = -\frac{\mathfrak{M}l_0}{2\cdot 3El_0} - \frac{M_0 l_0}{2\cdot 6El_0} + \frac{2f_A}{l_0}, \\ \frac{\mathfrak{M}l_0}{2\cdot 6El_0} + \frac{M_0 l_0}{2\cdot 3El_0} + \frac{2f_A}{l_0} = -\frac{M_0 l_0}{2\cdot 3El_0} + \frac{Ml_0}{2\cdot 6El_0} - \frac{2f_A}{l_0}, \end{cases}$$

where f_A is the sag of the elastic support (stringer) under the effect of the reaction R.

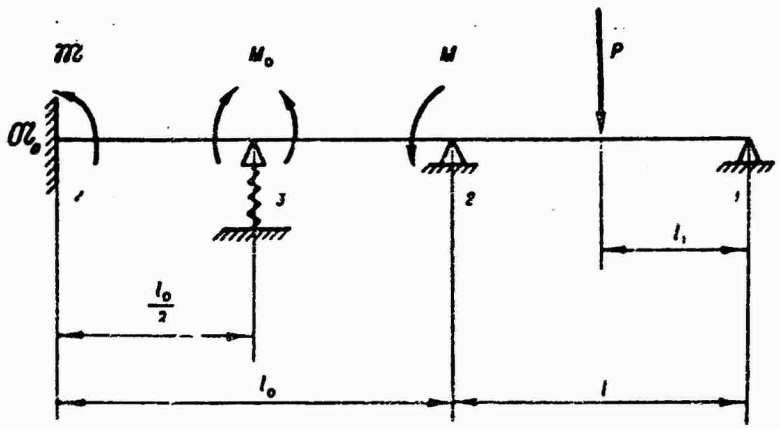

Figure 1. Calculation scheme with one stringer: 1) upper deck; 2) lower deck; 3) stringer; 4) inner bottom; $2l_0$ pliability factor of the elastic fastening.

After conversions, we obtain

$$\begin{aligned} \mathfrak{M}\left(2 + \frac{12El_0}{l_0}\mathfrak{N}_0\right) + M_0 - \frac{24El_0}{l_0^2} f_A = 0, \\ \mathfrak{M} + 4M_0 + \frac{48Ei_0}{l_0^2} f_A = M. \end{aligned} \qquad (1)$$

The sag of the stringer is determined according to the formula

$$f_A = AR = \frac{A}{l_0}(4M_0 - 2\mathfrak{M} + 2M), \qquad (2)$$

where A is the pliability factor of the elastic support

$$A = \frac{L^4}{\mu^4}\frac{1}{sEI};$$

L is the span of the stringer; s is the frame spacing (frame distance); EI is the rigidity of the stringer; and μ is a characteristic number depending only upon the support fastenings of the stringer.

Having substituted the value of f_A into equations (1) and having designated the following symbols

$$B_1 = \frac{48EI_0}{l_0^3}A,$$

$$C_1 = \frac{48EI_0}{l_0}\mathfrak{N}_0,$$

we will have

$$\begin{cases} \mathfrak{M}\left(2 + B_1 + \frac{C_1}{4}\right) + M_0(1 - 2B_1) = MB_1, \\ \mathfrak{M}(1 - 2B_1) + 4M_0(1 + B_1) = M(1 - 2B_1). \end{cases}$$

By solving this system of equations, we find

$$\mathfrak{M} = \frac{8B_1 - 1}{7 + 16B_1 + C_1(1 + B_1)}M, \qquad (3)$$

$$M_0 = \frac{(1 - 2B_1)\left(2 + \frac{C_1}{4}\right)}{7 + 16B_1 + C_1(1 + B_1)}M.$$

The angle of rotation of the hold frame at the lower deck, with consideration of expressions (2) and (3), is determined according to the formula

$$v' = -\frac{Ml_0}{3EI_0}\frac{1}{4}\frac{12 + 48B_1 + \frac{C_1}{4}(7 + 16B_1)}{7 + 16B_1 + C_1(1 + B_1)} = -\frac{Ml_0}{3EI_0}\varphi_1.$$

Thus, the correction factor φ in the installation of one stringer and elastic fastening of the lower end of the frame will be equal to

$$\varphi_I = \frac{1}{4}\,\frac{12 + 48B_1 + \frac{C_1}{4}(7 + 16B_1)}{7 + 16B_1 + C_1(1 + B_1)}. \qquad (4)$$

Similarly, with two stringers

$$\varphi_{II} = \frac{1}{6}\,\frac{45 + 864B_2 + 2187B_2^2 + \frac{C_2}{3}(26 + 372B_2 + 486B_2^2)}{26 + 372B_2 + 486B_2^2 + \frac{C_2}{3}(15 + 141B_2 + 81B_2^2)}, \qquad (5)$$

where

$$B_2 = \frac{54EI_0}{l_0^3}A,$$

$$C_2 = \frac{54EI_0}{l_0}\mathfrak{A}_0.$$

With three stringers

$$\varphi_{III} = \frac{1}{8}\,\frac{168 + 5904B_3 + 45\,312B_3^2 + 49\,152B_3^3 + \frac{C_3}{4}(97 + 2784B_2 +}{97 + 2784B_3 + 14\,944B_3^2 + 8192B_3^3 + \frac{C_3}{4}(56 + 1248B_3 +}$$

$$\frac{+ 14\,944B_3^2 + 8192B_3^3)}{+ 4352B_2^2 + 1024B_3^3}, \qquad (6)$$

where

$$B_3 = \frac{96EI_0}{l_0^3}A;$$

$$C_3 = \frac{96EI_0}{l_0}\mathfrak{A}_0.$$

In Table 1 the values of φ are given, as calculated for a different number of stringers (n = I, II, III) and different variations of the fastening of the hold branch of the frame at the inner bottom: 1) $\mathfrak{A}_0 = l_0/2EI_0$ (the support pair coefficient $\varkappa = 0.5$); 2) $\mathfrak{A}_0 = \infty$; 3) $\mathfrak{A}_0 = 0$. According to the

values of φ found the curves were constructed (Figure 2), from which it is apparent that the greatest effect of the cross connections on the bending of the frames is noted at $B_n < 5$. This must be considered in the calculations of the strength of the hull structures.

Table 1

Values of the Coefficient φ

B	(1) Один стрингер			(2) Два стрингера			(3) Три стрингера		
	φ_I^x	φ_I^∞	φ_I^0	φ_{II}^x	φ_{II}^∞	φ_{II}^0	φ_{III}^x	φ_{III}^∞	φ_{III}^0
0	0,436	0,438	0,429	0,289	0,289	0,288	0,217	0,217	0,217
0,5	0,617	0,625	0,600	0,514	0,518	0,511	0,412	0,412	0,412
1,0	0,697	0,719	0,652	0,606	0,614	0,584	0,486	0,487	0,483
2,0	0,770	0,812	0,692	0,698	0,721	0,649	0,575	0,582	0,560
3,0	0,804	0,859	0,709	0,745	0,782	0,674	0,632	0,640	0,602
4,0	0,825	0,887	0,718	0,775	0,819	0,697	0,671	0,690	0,616
5,0	0,838	0,906	0,724	0,794	0,848	0,701	0,700	0,725	0,638
6,0	0,847	0,920	0,728	0,809	0,867	0,708	0,723	0,754	0,647
7,0	0,853	0,929	0,731	0,820	0,883	0,714	0,741	0,777	0,661
8,0	0,859	0,937	0,733	0,829	0,895	0,718	0,755	0,795	0,671
9,0	0,863	0,944	0,735	0,835	0,906	0,719	0,767	0,811	0,679
10,0	0,866	0,949	0,737	0,842	0,913	0,724	0,778	0,825	0,686

Key: 1) one stringer; 2) two stringers; 3) three stringers.

Calculation of the strength of the frames according to the proposed methodology is performed in the following manner:

1. Expressions are compiled for the angles of rotation of the loaded span of the frame to the left and to the right of the rigid supports.

2. The angles of rotation of the beam to the left and to the right of the support are equalized. From the solution of the equation obtained, the magnitude of the corresponding support moment is found.

3. The values of B_n and C_n are determined.

4. The numerical values of the support moments are found and the other elements of the bending are determined.

Example. Determine the strength of the tweendeck branch of the frame represented in Figure 1. The frame is rigidly fastened at the inner bottom ($\alpha_0 = 0$): $l = 2.80$ meters; $l_1 = l/2 = 1.40$ meters; $l_0 = 3.80$ meters; $s = 0.3$ meter; $i = 7330$ cm^4; $i_0 = 5905$ cm^4; $w = 616$ cm^3; $w_0 = 338$ cm^4;

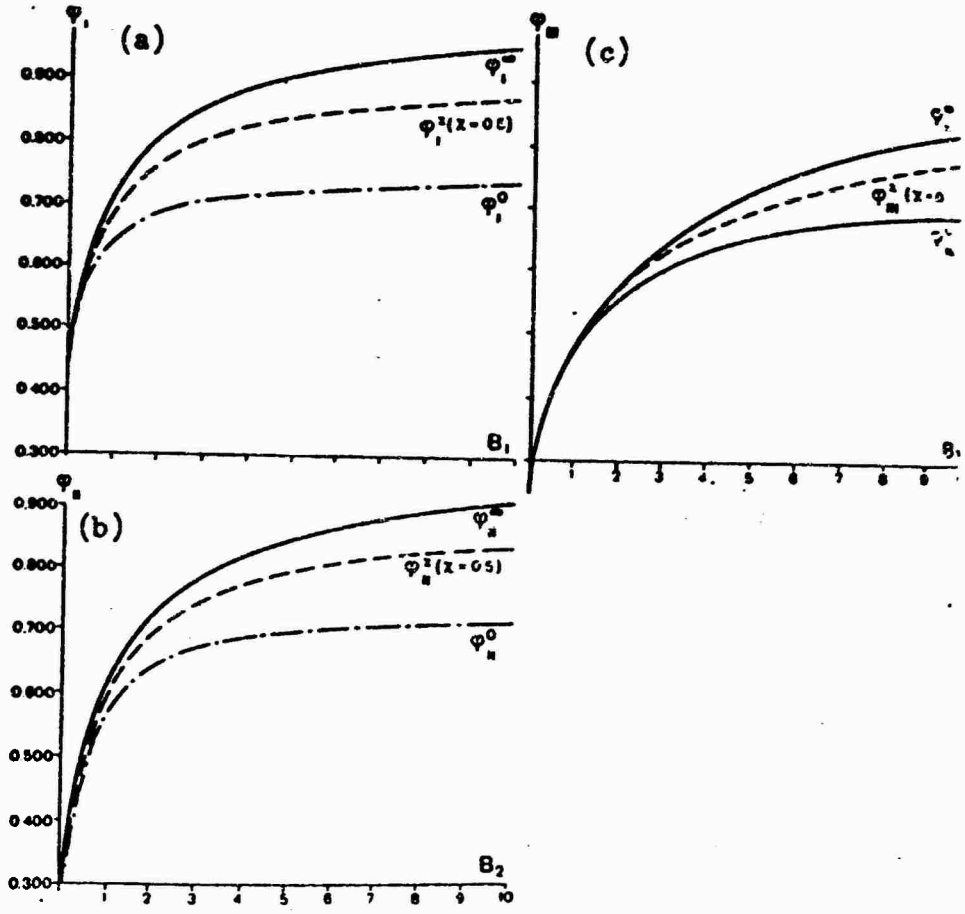

Figure 2. Values of the Coefficient φ at 1(a), 2 (b) and 3 (c) cross connections.

L = 2.40 meter; I = 42,450 cm^4; $\sigma_{dop} = \sigma_t = 2400$ kg/cm^2; $\chi = 0.5$; $\mu = 3.577$ (for the stringer) [$\sigma_{доп} = \sigma_{dop} = \sigma_{additional}$; $\sigma_T = \sigma_t = \sigma_{yield}$].

Solution. We find the support moment M acting on section 2. For this we compile an expression for the angles of rotation of the frame to the left and to the right of support 2.

The angle of rotation to the right of the support is

$$v'(P, M) = \frac{Pl^2}{16Ei} - \frac{Ml}{3Ei}.$$

The angle of rotation to the left of the support is

$$v'_{l_0}(M) = \varphi_1 \frac{Ml_0}{3Ei_0} = \frac{Ml_0}{3Ei_0} \frac{3(1+4B_1)}{7+16B_1}.$$

Having equalized the angles of rotation to the left and to the right of the support, and having designated $a = (l/l_0)(i_0/i)$, we obtain

$$M = \frac{3}{16} Pl \frac{a(7 + 16B_1)}{3(1 + 4B_1) + a(7 + 16B_1)}.$$

We calculate the values of a and B_1:

$$a = \frac{2,8}{3,8} \frac{7330}{5905} = 0,914,$$

$$B_1 = 48 \frac{EI_0}{l_0^3} A = \frac{48}{\mu^4} \frac{L}{s} \left(\frac{L}{l_0}\right)^3 \frac{I_0}{I} = \frac{48}{3,577^4} \frac{2,4}{0,3} \left(\frac{2,4}{3,8}\right)^3 \frac{5905}{42\,450} = 0,0817.$$

Then

$$M = \frac{3}{16} Pl \frac{0,914(7 + 16 \cdot 0,0817)}{3(1 + 4 \cdot 0,0817) + 0,914(7 + 16 \cdot 0,0817)} = 0,123Pl.$$

The greatest bending moment in the tweendeck branch of the frame is

$$M_{max} = \frac{Pl}{4} - \frac{M}{2} = 0,250Pl - 0,062Pl = 0,188Pl.$$

The structural strength of the tweendeck branch of the frame is

$$q = \frac{\sigma_T w}{0,188ls} = \frac{2400 \cdot 616}{0,188 \cdot 2,8 \cdot 0,3 \cdot 10^5} = 93,5 \text{ T/m}.$$

BIBLIOGRAPHY

1. Korotkin, Ya. I., Lokshin, A. V., and Sivers, N. L., Izgib i ustoychivost' sterzhney i sterzhnevykh sistem (Bending and stability of rods and rod systems), Moscow - Leningrad, Mashgiz, 1953.

2. Popov, Yu. N., Faddeyev, O. V., Kheysin, D. Ye., and Yakovlev, A. A., Prochnost' sudov, plavayushchikh vo l'dakh (Strength of ships navigating in ice), Leningrad, "Sudostroyeniye", 1967.

ON THE CALCULATION OF THE SIDE SHELL PLATING FOR THE EFFECT OF AN ICE LOAD

D. I. Solostyanskiy

pages 154-170

Full-scale tests of ships in the ice [3, 5] demonstrated that the ice load on the shell plating is local, limited along the length of the plate, and uniform within the limits of one frame spacing.

Since the length of a plate in the vicinity of the ice belt, as a rule, is several times greater than its width, the calculation is reduced to the calculation of a thin plate of infinite length for a local load.

In the article solutions of this problem are given for a local load, distributed along the length of the plate according to a triangle law and a parabolic law. The numerical values of the bucklings and bending moments are given in the table, together with the corresponding values for a uniformly distributed load [4].

In the second part of the article, the bending of an infinite plate loaded by a local load in an elastic-plastic zone is considered. Curves of the limiting loads are constructed for the elastic-plastic bending of a plate of infinite length, and also curves of the ratios of the limiting loads for elastic and elastic-plastic bending.

1. Elastic Bending

The bending of a thin plate of infinite length in an elastic zone is described by a biharmonic differential equation

$$D\nabla^2\nabla^2 w = p(x, y), \tag{1}$$

where p(x, y) is the law of distribution of the external load normal to the plane of the plate; $(E\delta^3/12(1-\mu^2))$ is the cylindrical rigidity of the plate;

δ and w are the thickness and the buckling of the plate, respectively; Ξ is Young's modulus; and μ is the Poisson ratio.

If we assume that the beginning of the coordinates is at the center of the zone of application of the load, and the coordinate axes are matched with the axes of symmetry of the plate (Figure 1), the solution of equation (1) may be presented in the form of the sum of two Fourier integrals:

$$w = \frac{2}{\pi D}\left(\int_0^\infty U_1(\alpha, y)\cos\alpha x\, d\alpha + \int_0^\infty U_2(\alpha, y)\sin\alpha x\, d\alpha\right), \qquad (2)$$

determining the symmetrical and anti-symmetrical components of the buckling.

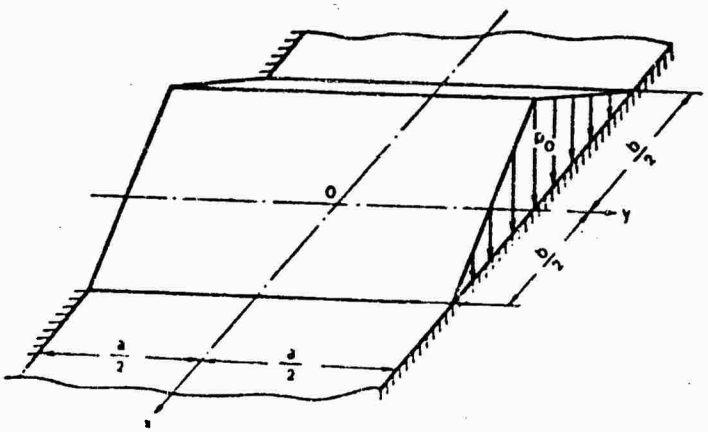

Figure 1. Infinite plate, which is loaded by a local load, distributed according to a triangle law.

For calculations of the ice strength of the shell plating, three types of local load are of interest:

1. Distributed throughout a triangle (Figure 1)

$$p(x, y) = p_0\left(1 - \frac{2|x|}{b}\right)$$

in an impact against the angle of the ice edge;

2. Distributed according to a parabolic law

$$p(x, y) = p_0\left[1 - \left(\frac{2x}{b}\right)^2\right]$$

in an impact against a curved edge, and

3. A uniformly distributed load

$$p(x, y) = p_0 = \text{const}$$

at $-\frac{b}{2} \leqslant x \leqslant \frac{b}{2}$, , corresponding to uniform compression.

If $x < -(b/2)$ and $(b/2) < x$, then $p(x, y) = 0$.

In the cases under consideration the load is symmetrical relative to the axis oy and is constant along this axis. Consequently, in expression (2) the anti-symmetrical term tends toward zero

and the external load may be represented by the integral

$$p(x, y) = \frac{2}{\pi} \int_0^{\infty} Q(\alpha, y) \cos \alpha x \, d\alpha, \tag{3}$$

where

$$Q(\alpha, y) = \int_0^{\infty} p(\xi, y) \cos \alpha \xi \, d\xi. \tag{4}$$

Having substituted the expressions for the load and the buckling, (3) and (2), into differential equation (1), we obtain an equation in partial derivatives

$$\frac{\partial^4 U_1(\alpha, y)}{\partial y^4} - 2\alpha \frac{\partial^2 U_1(\alpha, y)}{\partial y^2} + \alpha^4 U_1(\alpha, y) = Q(\alpha, y). \tag{5}$$

Since there are no derivatives of the function U_1 with respect to the variable α in the left-hand part, equation (5) may be integrated as an ordinary differential equation

$$U_1(\alpha, y) = (A + By) \operatorname{sh} \alpha y + (C + Dy) \operatorname{ch} \alpha y + \Phi(\alpha, y), \tag{6}$$

where the integration constants A, B, C and D are functions of the parameter α and are determined by the boundary conditions at the edge, $y = \pm(b/2)$, and the particular solution $\Phi(\alpha, y)$ entirely depends upon the form of the local load. Since the latter is constant along the axis oy, the particular solution is equal to

$$\Phi(\alpha, y) = \Phi(\alpha) = \frac{\int_0^{b/2} p(\xi) \cos \alpha \xi \, d\xi}{\alpha^4}. \tag{7}$$

Because of the symmetry of the plate and the identical fastening of the edges on the frames, the constants, in odd functions, in solution (6), tend toward zero:

$$A = D = 0.$$

The constants at even functions B and C are determined by the conditions of the fastening of the edges for a freely resting plate

$$\left.\begin{aligned} w &= 0, \\ \frac{\partial^2 w}{\partial y^2} &= 0, \end{aligned}\right\}_{y=\frac{a}{2}} \tag{8}$$

and for a rigidly fastened plate

$$\left.\begin{aligned} w &= 0, \\ \frac{\partial w}{\partial y} &= 0, \end{aligned}\right\}_{y=\frac{a}{2}}. \tag{9}$$

Conditions (8) and (9) are valid at any values of x and the parameter only in a case if, when y = (a/2),

$$U_1(\alpha, y) = \frac{\partial^2 U_1(\alpha, y)}{\partial y^2} = 0$$

and

$$U_1(\alpha, y) = \frac{\partial U_1(\alpha, y)}{\partial y} = 0$$

respectively.

Having calculated the derivative functions $U_1(\alpha, y)$ with a consideration of expression (7), for the freely supported edges

$$\begin{cases} B\frac{a}{2}\operatorname{sh}\frac{\alpha a}{2} + C\operatorname{ch}\frac{\alpha a}{2} = -\Phi(\alpha), \\ B\left(2\operatorname{ch}\frac{\alpha a}{2} + \frac{\alpha a}{2}\operatorname{sh}\frac{\alpha a}{2}\right) + C\alpha\operatorname{ch}\frac{\alpha a}{2} = 0 \end{cases}$$

and for the rigidly fastened edges

$$\begin{cases} B\frac{\alpha a}{2}\operatorname{sh}\frac{\alpha a}{2} + C\operatorname{ch}\frac{\alpha a}{2} = -\Phi(\alpha), \\ B\left(\operatorname{sh}\frac{\alpha a}{2} + \frac{\alpha a}{2}\operatorname{ch}\frac{\alpha a}{2}\right) + C\alpha\operatorname{sh}\frac{\alpha a}{2} = 0. \end{cases}$$

We will find the values of the arbitrary constants B and C:

for a freely supported plate

$$\left.\begin{aligned} B &= \frac{a}{2\operatorname{ch} u}\Phi(\alpha), \\ C &= -\frac{2\operatorname{ch} u + u\operatorname{sh} u}{2\operatorname{ch}^2 u}\Phi(\alpha), \end{aligned}\right\} \tag{10}$$

for a rigidly fastened plate

$$\left.\begin{aligned} B &= \frac{a\operatorname{sh} u}{\operatorname{sh} u\operatorname{ch} u + u}\Phi(\alpha), \\ C &= -\frac{u\operatorname{ch} u + \operatorname{sh} u}{\operatorname{sh} u\operatorname{ch} u + u}\Phi(\alpha), \end{aligned}\right\} \tag{11}$$

where

$$u = \frac{\alpha a}{2}.$$

By using expressions (6), (7), (10) and (11), we obtain the general expression for the elastic surface of an infinite plate, loaded by a local load

$$w = \frac{2}{\pi D}\int_0^\infty \Phi(\alpha)\left[1 + \frac{\alpha y\operatorname{sh}\alpha y\operatorname{ch} u - (2\operatorname{ch} u + u\operatorname{sh} u)\operatorname{ch}\alpha y}{2\operatorname{ch}^2 u}\right]\cos\alpha x\, d\alpha \tag{12}$$

at free resting of the edges, and

$$w = \frac{2}{\pi D}\int_0^\infty \Phi(\alpha)\left[1 + \frac{\alpha y\operatorname{sh}\alpha y\operatorname{sh} u - (\operatorname{sh} u + u\operatorname{ch} u)\operatorname{ch}\alpha y}{\operatorname{sh} u\operatorname{ch} u + u}\right]\cos\alpha x\, d\alpha \tag{13}$$

with rigid fastening of the edges.

The other elements of the bending are determined according to the general formulas of the theory of bending of plates by differentiation of expressions (12) and (13) with respect to x and y under the integral sign.

Formulas for maximum buckling and bending moment at the center of the plate under the load, and also for the moment in the fastening, as a

Table 1

Principal Elements of the Bending of a Freely Supported Infinite Plate Loaded with a Local Load

	(1) Вид местной
	(2) равномерная
(5) Нагрузка p в функции параметра ξ	p_0
(6) Частное решение $\Phi(x, y) = \Phi(x) = \dfrac{\int_0^{b/2} p \cos \alpha\xi \, d\xi}{\alpha^4}$	$\dfrac{p_0}{\alpha^5} \sin u \dfrac{b}{a}$
(7) Общее выражение прогиба $w(x, y)$	$\dfrac{2p_0}{\pi D} \int_0^\infty \dfrac{\sin u \frac{b}{a}}{\alpha^5} \left[1 + \right.$ $\left. + \dfrac{\alpha y \operatorname{sh} \alpha y \operatorname{ch} u - (2 \operatorname{ch} u + u \operatorname{sh} u) \operatorname{ch} \alpha y}{2 \operatorname{ch}^2 u}\right] \times$ $\times \cos \alpha x \, d\alpha$
(8) Максимальный прогиб w_0 при $y = 0; \quad x = 0$	$\dfrac{p_0 a^4}{8\pi D} \int_0^\infty \dfrac{1}{u^5} \left(1 - \dfrac{2 \operatorname{ch} u + u \operatorname{sh} u}{2 \operatorname{ch}^2 u}\right) \times$ $\times \sin u \dfrac{b}{a} \, du$
(9) Максимальный изгибающий момент посредине пластины M_{0x} при $y = 0; \quad x = 0$	$\dfrac{p_0 a^2}{2\pi} \left\{ \int_0^\infty \dfrac{1}{u^2} \dfrac{\operatorname{th} u}{2 \operatorname{ch} u} \sin u \dfrac{b}{a} \, du + \right.$ $+ \mu \int_0^\infty \dfrac{1}{u^3} \left(1 - \dfrac{2 \operatorname{ch} u + u \operatorname{sh} u}{2 \operatorname{ch}^2 u}\right) \times$ $\left. \times \sin u \dfrac{b}{a} \, du \right\}$

Table 1 (continued)

Principal Elements of the Bending of a Freely Supported Infinite Plate Loaded with a Local Load (continued)

нагрузки (1)	
(3) треугольная	(4) параболическая
$p_0\left(1-\frac{\lvert 2\xi\rvert}{b}\right)$	$p_0\left[1-\left(\frac{2\xi}{b}\right)^2\right]$
$\frac{2p_0}{b\alpha^2}\left(1-\cos u\,\frac{b}{a}\right)$	$\frac{4p_0}{b\alpha^2}\left(\frac{\sin u\,\frac{b}{a}}{u\,\frac{b}{a}}-\cos u\,\frac{b}{a}\right)$
$\frac{4p_0}{\pi D}\int_0^\infty \frac{1-\cos u\,\frac{b}{a}}{b\alpha^6}\left[1+\right.$ $\left.+\frac{\alpha y\,\mathrm{sh}\,\alpha y\,\mathrm{ch}\,u-(2\,\mathrm{ch}\,u+u\,\mathrm{sh}\,u)\,\mathrm{ch}\,\alpha y}{2\,\mathrm{ch}^2 u}\right]\times$ $\times\cos\alpha x\,d\alpha$	$\frac{8p_0}{\pi D}\int_0^\infty \frac{1}{b\alpha^6}\left(\frac{\sin u\,\frac{b}{a}}{u\,\frac{b}{a}}-\cos u\,\frac{b}{a}\right)\left[1+\right.$ $\left.+\frac{\alpha y\,\mathrm{sh}\,\alpha y\,\mathrm{ch}\,u-(2\,\mathrm{ch}\,u+u\,\mathrm{sh}\,u)\,\mathrm{ch}\,\alpha y}{2\,\mathrm{ch}^2 u}\right]\times$ $\times\cos\alpha x\,d\alpha$
$\frac{p_0a^4}{8\pi D}\left(\frac{a}{b}\right)\int_0^\infty \frac{1}{u^6}\left(1-\frac{2\,\mathrm{ch}\,u+u\,\mathrm{sh}\,u}{2\,\mathrm{ch}^2 u}\right)\times$ $\times\left(1-\cos u\,\frac{b}{a}\right)du$	$\frac{p_0a^4}{4\pi D}\,\frac{a}{b}\int_0^\infty \frac{1}{u^6}\left(1-\frac{2\,\mathrm{ch}\,u+u\,\mathrm{sh}\,u}{2\,\mathrm{ch}^2 u}\right)\times$ $\times\left(\frac{\sin u\,\frac{b}{a}}{u\,\frac{b}{a}}-\cos u\,\frac{b}{a}\right)du$
$\frac{p_0a^2}{2\pi}\,\frac{a}{b}\left\{\int_0^\infty \frac{1}{u^3}\,\frac{\mathrm{th}\,u}{2\,\mathrm{ch}\,u}\times\right.$ $\times\left(1-\cos u\,\frac{b}{a}\right)du+\mu\int_0^\infty \frac{1}{u^4}\times$ $\times\left(1-\frac{2\,\mathrm{ch}\,u+u\,\mathrm{sh}\,u}{2\,\mathrm{ch}^2 u}\right)\times$ $\left.\times\left(1-\cos u\,\frac{b}{a}\right)du\right\}$	$\frac{p_0a^2}{\pi}\,\frac{a}{b}\left\{\int_0^\infty \frac{1}{u^3}\,\frac{\mathrm{th}\,u}{2\,\mathrm{ch}\,u}\times\right.$ $\times\left(\frac{\sin u\,\frac{b}{a}}{u\,\frac{b}{a}}-\cos u\,\frac{b}{a}\right)du+$ $+\mu\int_0^\infty \frac{1}{u^4}\left(1-\frac{2\,\mathrm{ch}\,u+u\,\mathrm{sh}\,u}{2\,\mathrm{ch}^2 u}\right)\times$ $\left.\times\left(\frac{\sin u\,\frac{b}{a}}{u\,\frac{b}{a}}-\cos u\,\frac{b}{a}\right)du\right\}$

Key: 1) form of local load; 2) uniform; 3) triangular; 4) parabolic; 5) load p as a function of the parameter ξ; 6) particular solution; 7) general expression of buckling w(x, y); 8) maximum buckling w_0 at y=0; x=0; 9) maximum bending moment in center of plate M_{0x} at y=0; x=0.

Table 2

Principal Element of the Bending of a Rigidly Fastened Infinite Plate, Loaded with a Local Load

	(1) Вид местной (2) равномерная
(5) Нагрузка p в функции параметра ξ	p_0
(6) Частное решение $\Phi(\alpha, y) = \Phi(\alpha) = \frac{\int_0^{b/2} p \cos \alpha \xi \, d\xi}{\alpha^4}$	$\frac{p_0}{\alpha^5} \sin u \frac{b}{a}$
(7) Общее выражение прогиба $w(x, y)$	$\frac{2p_0}{\pi D} \int_0^\infty \frac{\sin u \frac{b}{a}}{\alpha^5} \left[1 + \frac{\alpha y \operatorname{sh} \alpha y \operatorname{sh} u - (\operatorname{sh} u + u \operatorname{ch} u) \operatorname{ch} \alpha y}{\operatorname{sh} u \operatorname{ch} u + u}\right] \times \cos \alpha x \, d\alpha$
(8) Максимальный прогиб w_0 при $y = 0;\ x = 0$	$\frac{p_0 a^4}{8\pi D} \int_0^\infty \frac{1}{u^5} \left(1 - \frac{u \operatorname{ch} u + \operatorname{sh} u}{\operatorname{sh} u \operatorname{ch} u + u}\right) \times \sin u \frac{b}{a} \, du$
(9) Максимальный изгибающий момент посредине пластины M_{0x} при $y = 0;\ x = 0$	$\frac{p_0 a^2}{2\pi} \left\{ \int_0^\infty \frac{1}{u^3} \frac{u \operatorname{ch} u - \operatorname{sh} u}{\operatorname{sh} u \operatorname{ch} u + u} \sin u \frac{b}{a} \, du + \mu \int_0^\infty \frac{1}{u^3} \left[1 - \frac{u \operatorname{ch} u + \operatorname{sh} u}{\operatorname{sh} u \operatorname{ch} u + u}\right] \times \sin u \frac{b}{a} \, du \right\}$
(10) Максимальный изгибающий момент в заделке M_x при $y = \frac{a}{2};\ x = 0$	$-\frac{p_0 a^2}{2\pi} \int_0^\infty \frac{1}{u^3} \frac{\operatorname{sh} u \operatorname{ch} u - u}{\operatorname{sh} u \operatorname{ch} u + u} \sin u \frac{b}{a} \, du$

Table 2 (continued)

Principal Element of the Bending of a Rigidly Fastened Infinite Plate, Loaded with a Local Load (continued)

нагрузки		
	(3) треугольная	(4) параболическая
p	$p_0\left(1-\frac{\lvert 2\xi\rvert}{b}\right)$	$p_0\left[1-\left(\frac{2\xi}{b}\right)^2\right]$
w(0, 0)	$\frac{2p_0}{b\alpha^6}\left(1-\cos u\frac{b}{a}\right)$	$\frac{4p_0}{b\alpha^6}\left(\frac{\sin u\frac{b}{a}}{u\frac{b}{a}}-\cos u\frac{b}{a}\right)$
w(x, y)	$\frac{4p_0}{\pi D}\int_0^\infty \frac{1}{b\alpha^6}\left(1-\cos u\frac{b}{a}\right)\left[1+\right.$ $\left.+\frac{\alpha y\,\mathrm{sh}\,\alpha y\,\mathrm{sh}\,u-(\mathrm{sh}\,u+u\,\mathrm{ch}\,u)\,\mathrm{ch}\,\alpha y}{\mathrm{sh}\,u\,\mathrm{ch}\,u+u}\right]\times$ $\times\cos\alpha x\,d\alpha$	$\frac{8p_0}{\pi D}\int_0^\infty \frac{1}{b\alpha^6}\left(\frac{\sin u\frac{b}{a}}{u\frac{b}{a}}-\cos u\frac{b}{a}\right)\times$ $\times\left[1+\frac{\alpha y\,\mathrm{sh}\,\alpha y\,\mathrm{sh}\,u}{\mathrm{sh}\,u\,\mathrm{ch}\,u+u}-\right.$ $\left.-\frac{(\mathrm{sh}\,u+u\,\mathrm{ch}\,u)\,\mathrm{ch}\,\alpha y}{\mathrm{sh}\,u\,\mathrm{ch}\,u+u}\right]\cos\alpha x\,d\alpha$
M_{0x}	$\frac{p_0a^4}{8\pi D}\frac{a}{b}\int_0^\infty \frac{1}{u^6}\left(1-\frac{u\,\mathrm{ch}\,u+\mathrm{sh}\,u}{\mathrm{sh}\,u\,\mathrm{ch}\,u+u}\right)\times$ $\times\left(1-\cos u\frac{b}{a}\right)du$	$\frac{p_0a^4}{4\pi D}\frac{a}{b}\int_0^\infty \frac{1}{u^6}\left(1-\frac{u\,\mathrm{ch}\,u+\mathrm{sh}\,u}{\mathrm{sh}\,u\,\mathrm{ch}\,u+u}\right)\times$ $\times\left(\frac{\sin u\frac{b}{a}}{u\frac{b}{a}}-\cos u\frac{b}{a}\right)du$
M_x	$\frac{p_0a^2}{2\pi}\frac{a}{b}\left\{\int_0^\infty \frac{1}{u^4}\frac{u\,\mathrm{ch}\,u+\mathrm{sh}\,u}{\mathrm{sh}\,u\,\mathrm{ch}\,u+u}\times\right.$ $\times\left(1-\cos u\frac{b}{a}\right)du+$ $+\mu\int_0^\infty \frac{1}{u^4}\left[1-\frac{u\,\mathrm{ch}\,u+\mathrm{sh}\,u}{\mathrm{sh}\,u\,\mathrm{ch}\,u+u}\right]\times$ $\left.\times\left(1-\cos u\frac{b}{a}\right)du\right\}$	$\frac{p_0a^2}{\pi}\frac{a}{b}\left\{\int_0^\infty \frac{1}{u^4}\frac{u\,\mathrm{ch}\,u-\mathrm{sh}\,u}{\mathrm{sh}\,u\,\mathrm{ch}\,u+u}\times\right.$ $\times\left(\frac{\sin u\frac{b}{a}}{u\frac{b}{a}}-\cos u\frac{b}{a}\right)du+$ $+\mu\int_0^\infty \frac{1}{u^4}\left(1-\frac{u\,\mathrm{ch}\,u+\mathrm{sh}\,u}{\mathrm{sh}\,u\,\mathrm{ch}\,u+u}\right)\times$ $\left.\times\left(\frac{\sin u\frac{b}{a}}{u\frac{b}{a}}-\cos u\frac{b}{a}\right)du\right\}$
M_y	$-\frac{p_0a^2}{2\pi}\frac{a}{b}\int_0^\infty \frac{1}{u^4}\frac{\mathrm{sh}\,u\,\mathrm{ch}\,u-u}{\mathrm{sh}\,u\,\mathrm{ch}\,u+u}\times$ $\times\left(1-\cos u\frac{b}{a}\right)du$	$-\frac{p_0a^2}{\pi}\frac{a}{b}\int_0^\infty \frac{1}{u^4}\frac{\mathrm{sh}\,u\,\mathrm{ch}\,u-u}{\mathrm{sh}\,u\,\mathrm{ch}\,u+u}\times$ $\times\left(\frac{\sin u\frac{b}{a}}{u\frac{b}{a}}-\cos u\frac{b}{a}\right)du$

Key: 1) form of local load; 2) uniform; 3) triangular; 4) parabolic; 5) load p as a function of the parameter ξ; 6) particular solution; 7) general expression of buckling w(x, y); 8) maximum buckling w_0 at y=0; x=0; 9) maximum bending moment in center of the plate M_{0x} at y=0; x=0; 10) maximum bending moment in the fastening M_x at y=(a/2); x=0.

function of the nature of the distribution of the local load, are given in Tables 1 and 2.

The improper integrals entering into the expressions for the maximum buckling and bending moments were calculated by means of the "Ural-2" EVM (electronic computer). The numerical values are presented in Tables 3 and 4 in the form of dimensionless coefficients, which are the ratio of the buckling and the moments of an infinite plate under the effect of a local load to the corresponding elements of the bending of a strip beam, loaded by a uniformly distributed load with an intensity t_0.

Table 3

Maximum Buckling and Bending Moments in the Center of a Freely Supported Plate of Infinite Length, Loaded by a Local Load

$\frac{b}{a}$	$k_1 = w_0 \frac{384D}{5p_0a^4}$			$k_2 = M_{0x} \frac{8}{p_0a^2}$			$k_3 = M_{0y} \frac{8}{p_0a^2}$		
	(1) Тип нагрузки								
	(2) равномерная	(3) треугольная	(4) параболическая	(2) равномерная	(3) треугольная	(4) параболическая	(2) равномерная	(3) треугольная	(4) параболическая
0,2	0,146	0,077	0,103	0,183	0,070	0,123	0,157	0,077	0,110
0,4	0,281	0,152	0,202	0,342	0,132	0,233	0,255	0,133	0,188
0,6	0,401	0,222	0,294	0,476	0,186	0,351	0,312	0,173	0,243
0,8	0,502	0,287	0,377	0,588	0,235	0,418	0,342	0,200	0,280
1,0	0,587	0,346	0,452	0,680	0,276	0,492	0,355	0,219	0,304
1,2	0,655	0,400	0,517	0,754	0,311	0,558	0,359	0,231	0,320
1,4	0,710	0,444	0,572	0,814	0,340	0,610	0,357	0,237	0,328
1,6	0,753	0,484	0,619	0,861	0,362	0,654	0,352	0,240	0,332
1,8	0,786	0,519	0,657	0,899	0,382	0,691	0,346	0,241	0,333
2,0	0,811	0,550	0,690	0,931	0,399	0,723	0,338	0,241	0,332
2,2	0,832	0,577	0,720	0,953	0,413	0,749	0,334	0,239	0,329
2,4		0,601	0,743		0,424	0,770		0,236	0,326
2,6		0,622	0,763		0,434	0,787		0,233	0,322
2,8		0,639	0,779		0,439	0,801		0,230	0,318
3,0		0,655	0,793		0,446	0,813		0,227	0,314
3,2		0,668	0,802		0,450	0,823		0,223	0,311

Key: 1) type of load; 2) uniform; 3) triangular; 4) parabolic.

In order to shift from the load distributed in a limited section of the plate to the load q distributed throughout the line, it is sufficient to shift to the limits in the expressions for the elements of the bending of the plates, having directed $b \to 0$, $p_0 \to \infty$. We will assume that the total magnitude of the load for all three cases is identical ($Q = p_0ab$), and then the intensity of a linearly distributed load remains finite and tends to the following values for uniform, triangular, and parabolic loads, respectively:

$$q = p_0b; \quad q = \frac{1}{2}p_0b \; ; \quad q = \frac{2}{3}p_0b$$

Table 4

Maximum Buckling and Bending Moments in Fastening and in the Center of a Rigidly Fastened Plate of Infinite Length, Loaded by a Local Load

$\frac{b}{a}$	$k_1 = w_0 \frac{384D}{p_0 a^4}$			$k_2 = M_x \frac{12}{p_0 a^2}$			$k_3 = M_{0x} \frac{24}{p_0 a^2}$			$k_4 = M_{0y} \frac{24}{p_0 a^2}$		
	(1) Тип нагрузки											
	(2) равномерная	(3) треугольная	(4) параболическая	(2) равномерная	(3) треугольная	(4) параболическая	(2) равномерная	(3) треугольная	(4) параболическая	(2) равномерная	(3) треугольная	(4) параболическая
0,2	0,260	0,130	0,173	0,338	0,178	0,233	0,301	0,156	0,206	0,303	0,167	0,217
0,4	0,484	0,251	0,332	0,578	0,321	0,417	0,519	0,289	0,377	0,437	0,274	0,345
0,6	0,662	0,358	0,469	0,744	0,435	0,558	0,706	0,398	0,517	0,482	0,338	0,414
0,8	0,790	0,448	0,580	0,854	0,527	0,665	0,826	0,492	0,628	0,472	0,373	0,442
1,0	0,872	0,525	0,671	0,923	0,599	0,746	0,905	0,567	0,713	0,443	0,390	0,448
1,2	0,938	0,588	0,741	0,965	0,657	0,807	0,954	0,627	0,778	0,410	0,396	0,442
1,4	0,976	0,636	0,792	0,990	0,699	0,847	0,983	0,672	0,824	0,380	0,394	0,427
1,6	0,992	0,674	0,829	0,996	0,731	0,875	0,994	0,707	0,856	0,355	0,389	0,410
1,8	1,0	0,705	0,856	1,0	0,758	0,895	1,0	0,735	0,880		0,386	0,394
2,0	1,0	0,730	0,877	1,0	0,778	0,910	1,0	0,758	0,897		0,375	0,379
2,2	1,0	0,750	0,891	1,0	0,794	0,918	1,0	0,774	0,907		0,370	0,365
2,4	1,0	0,766	0,900	1,0	0,806	0,923	1,0	0,789	0,914		0,362	0,354
2,6	1,0	0,779	0,906	1,0	0,816	0,926	1,0	0,800	0,918		0,356	0,344
2,8	1,0	0,788	0,908	1,0	0,823	0,926	1,0	0,809	0,919		0,350	0,335
3,0	1,0	0,797	0,910	1,0	0,829	0,926	1,0	0,816	0,920		0,345	0,327

Key: 1) type of load; 2) uniform; 3) triangular; 4) parabolic.

The elements of the bending for all three variations will have identical limits, namely:

1) With freely supported edges, the value of the maximum buckling is determined by the formula

$$w_0 = \frac{qa^3}{8\pi D}\int_0^\infty \frac{1}{u^5}\left(1 - \frac{2\operatorname{ch} u + u \operatorname{sh} u}{2\operatorname{ch}^2 u}\right) du,$$

and the maximum bending moment of the center of the plate

$$M_{0x} = \frac{qa}{2\pi}\left\{\frac{1}{2}\int_0^\infty \frac{1}{u}\frac{\operatorname{th} u}{\operatorname{ch} u}\, du + \mu\int_0^\infty \frac{1}{u^2}\left(1 - \frac{2\operatorname{ch} u + u \operatorname{sh} u}{2\operatorname{ch}^2 u}\right) du\right\},$$

2) With rigidly fastened edges the maximum buckling is

$$w_0 = \frac{qa^3}{8\pi D}\int_0^\infty \frac{1}{u^5}\left(1 - \frac{u \operatorname{ch} u + \operatorname{sh} u}{\operatorname{sh} u \operatorname{ch} u + u}\right) du,$$

the bending moment at the center is

$$M_{0x} = \frac{qa}{2\pi}\left\{\int_0^\infty \frac{1}{u^2}\frac{u \operatorname{ch} u - \operatorname{sh} u}{\operatorname{sh} u \operatorname{ch} u + u}\, du + \mu\int_0^\infty \frac{1}{u^2}\left(1 - \frac{u \operatorname{ch} u + \operatorname{sh} u}{\operatorname{sh} u \operatorname{ch} u + u}\right) du\right\}$$

and the bending moment in the fastening is

$$M_x = \frac{qa}{2\pi}\int_0^\infty \frac{1}{u^2}\frac{\operatorname{sh} u \operatorname{ch} u - u}{\operatorname{sh} u \operatorname{ch} u + u}\, du.$$

Example. Determine the limiting load and maximum buckling of the outer shell plating of the ice belt of the bow end of the icebreaker "Semyon Chelyuskin". To find the intensity of the ice load acting on a plate and its buckling, according to the stresses measured in the shell plating in strain-gauge tests of the icebreaker, if the distance between the frames a=300 millimeters, the yield point (ultimate strength) of the steel is σ_t = 4000 kg/cm^2, the thickness of the shell plating δ = 16 millimeters, and the maximum stresses measured in the center of the span of the shell plating between the frames is σ_{0x} = 1600 kg/cm^2.

We will assume the length of the distribution of the load is equal to 0.5 meter on the basis of an analysis of the curves of the bending stresses measured in a frame to which the plate under consideration adjoins [3], and we will assume the nature of the distribution of the ice load is parabolic (Figure 2).

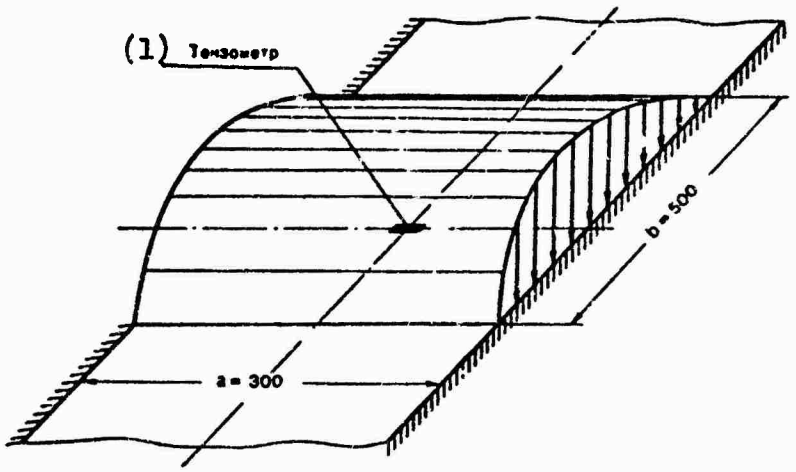

Figure 2. Diagram of the calculation of the side shell plating of an ice-breaker for an ice load. 1) strain gauge.

For a plate with rigidly fastened edges at (b/a) = (500/300) = 1.67, according to Table 4, the buckling factors and the moments in the fastening and in the center of the plate amount to

$$k_4 = 0{,}84; \quad k_5 = 0{,}88; \quad k_6 = 0{,}865.$$

We find the stresses of the transverse bending in the center of the plate according to the formula:

$$\sigma_{0x} = k_6 \frac{p_0 a^2 6}{2\delta^2},$$

from whence the maximum intensity of the ice load corresponding to the measured stresses is equal to

$$p_0 = \frac{4\sigma_{0x}\delta^2}{k_6 a^2} = \frac{4 \cdot 1600 \cdot 16^2 \cdot 10}{0{,}865 \cdot 300^2} = 210 \ \text{T/m}^2.$$

In this case, we find the buckling under the strain gauge according to the formula

$$w_0 = \frac{p_0 a^4}{384D} k_4 = \frac{210 \cdot 300^4 \cdot 12(1-0{,}3^2)}{10 \cdot 384 \cdot 2{,}1 \cdot 10^6 \cdot 16^3} 0{,}84 = 0{,}47 \text{ mm}.$$

The limiting pressure of the ice corresponding to the achievement of the yield point in the extreme fibers of the support sections of the plate amounts to

$$p_{0\,пр} = \frac{2\sigma_т \delta^2}{k_5 a^2} = \frac{2 \cdot 4000 \cdot 16^2 \cdot 10}{0{,}88 \cdot 300^2} = 258 \text{ T/m}^2,$$

which corresponds to the maximum buckling

$$w_{0\,max} = \frac{258 \cdot 300^4 \cdot 12(1-0{,}3^2)}{10 \cdot 384} 0{,}84 = 0{,}58 \text{ mm}.$$

2. Elastic-Plastic Bending

Experience in the operation of ships in the ice and analysis of ice damages [1, 7] demonstrates that with adequate plasticity of the material and an absence of cold brittleness, the carrying capacity of the shell plating is not exhausted by its elastic bending. Thus, during tests of a ship of the UL class in the Arctic, the motor ship "Ivan Moskvin", the shell plating continued to operate even after the failure of the frames and the partial separation of them from the shell plating. The residual deformations of the shell plating observed in this case were not great and sometimes were the ordinary corrugation characteristic for ships strengthened for ice navigation with a comparatively thin shell plating.

In considering the bending of the shell plating in the elastic-plastic zone as a limiting state for the sections of the plate loaded by a local load, we will assume that a cylindrical yield hinge originates, with the formation of a two-faceted angle on it [2].

The plastic deformations originating in this case are considered to be small, although considerably exceeding the corresponding elastic deformation. This assumption is necessary so that the equations of the deformations remain linear. It is valid if the bucklings of the plate remain small in comparison with its thickness.

The moment in the yield hinge, having reached a limiting value, is preserved at a constant figure

$$m_t = \frac{1}{4}\sigma_t h^2. \qquad (14)$$

We will find the magnitude of the limiting load if we equalize the work of the external load to the work of the limiting moments m_t on the two-faceted discontinuity angle in the hinges.

For a uniform pressure p in a section with a length b a form of failure of the plate close to the so-called "envelope", Figure 3 [2, 6], corresponds to the physical sense. An angle of 45° corresponds to the minimum work of the internal forces.

The picture of the formation of cylindrical hinges in a freely supported plate differs from the picture in a rigidly fastened plate (see Figure 3) only in the absence of yield hinges along the edges. Therefore, in the future both cases of the fastening of the edges are considered together.

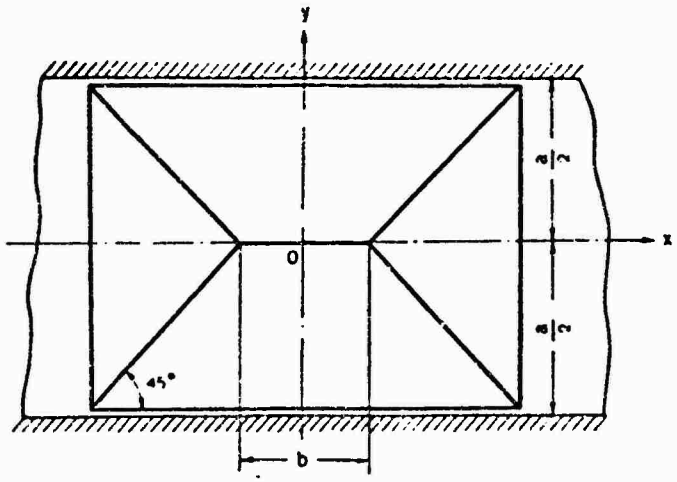

Figure 3. Formation of cylindrical yield hinges in an infinite plate loaded by a uniformly distributed local load.

Having assumed the buckling in the center of the plate to be equal to one, we will compile an expression for the work of the external load:

$$A = \tfrac{1}{2}bap. \qquad (15)$$

The work of the limiting moments originating in cylindrical hinges is determined by the following sum (we may ignore the elastic forces in comparison with the work of the limiting moment):

$$A = m_1 \sum_i \theta_i l_i, \tag{16}$$

where l_i is the length of the i-th cylindrical hinge; θ_i is the magnitude of the i-th two-faceted angle.

In the deformation of a plate according to the form indicated in Figure 3, the work of the external forces, according to equation (16), with a consideration of formula (14), is determined in the following manner (the angles θ are replaced by $\sin \theta_i$, in view of their smallness):

in a case of freely supported edges

$$A = \sigma_T \delta^2 \left(3 + \frac{b}{a}\right) \tag{17}$$

and in a case of rigidly fastened edges

$$A = 2\sigma_T \delta^2 \left(2 + \frac{b}{a}\right). \tag{18}$$

Having equalized expression (17) and (18) to formula (15), we find the following values of the limiting uniformly distributed local load for an infinite plate in bending in an elastic-plastic zone:

for a freely supported plate

$$p_{np} = \frac{\sigma_T \delta^2}{ab}\left(2\frac{b}{a} + 6\right), \tag{19}$$

[$p_{пр} = p_{pr} = p_{limiting}$] and for a rigidly fastened plate

$$p_{np} = \frac{\sigma_T \delta^2}{ab}\left(4\frac{b}{a} + 8\right). \tag{20}$$

If the length of the distribution of the local load b in formulas (19) and (20) tends toward infinity we obtain the well-known values of the limiting load for a strip beam, operating in an elastic-plastic zone, with the formation of one or three yield hinges (depending upon the fastening of the edges):

with freely supported edges

$$\lim_{b\to\infty} p_{np} = 2\frac{\sigma_t \delta^2}{a^2},$$

and with rigidly fastened edges

$$\lim_{b\to\infty} p_{np} = 4\frac{\sigma_t \delta^2}{a^2}.$$

For the finite values of the ratio (b/a), curves of the limiting loads are constructed, with a consideration of elastic-plastic bending of the plate (Figure 4).

The curves of the loads, for convenience, are presented in the dimensionless form, and this makes it possible to use them with any yield point of the material of the plate, and also with any thickness of the shell plating of the ice belts that is encountered in practice.

As the curves indicate, with an increase in the length b, the values of the limiting loads approach the real load asymptotically for a uniformly loaded strip beam, i.e., as in a case of elastic bending (see Tables 3 and 4).

The limiting load, distributed along the line, may be obtained if the length b of the distribution tends toward zero. From formulas (19) and (20) it is apparent that p_{pr} in this case increases infinitely. However, the limiting linearly distributed load q_{pr} remains finite, tending toward the magnitude $p_{pr}b$, and taking the following values:

for a freely supported plate

$$q_{np} = \lim_{b\to 0} p_{np} b = 6\frac{\sigma_t \delta^2}{a},$$

and for a rigidly fastened plate

$$q_{np} = \lim_{b\to 0} p_{np} b = 8\frac{\sigma_t \delta^2}{a}.$$

Considering the rapid growth of p_{pr} at small values of the ratio b/a in practical calculations, especially when (b/a) < 1, it is convenient to use the curves (Figure 5).

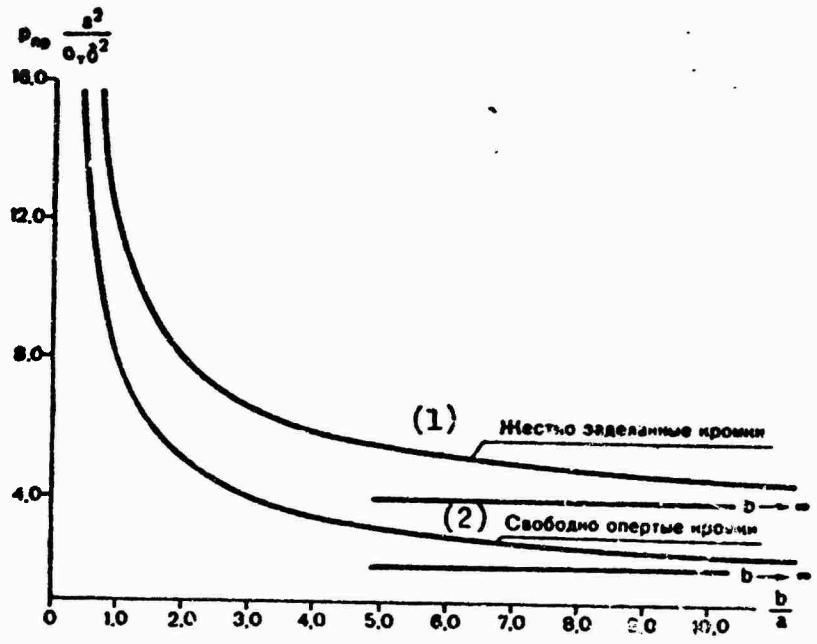

Figure 4. Limiting local loads for plates of infinite lengths in an elastic-plastic zone. 1) rigidly fastened edges; 2) freely supported edges.

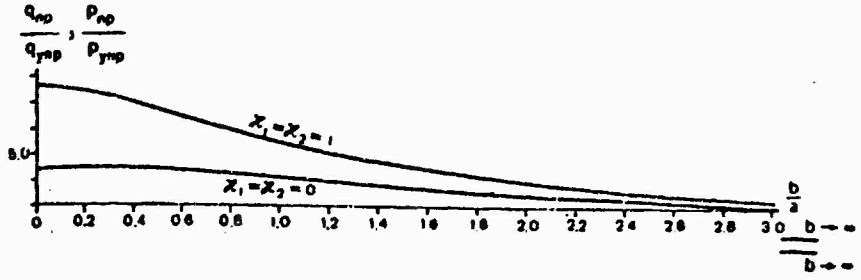

Figure 5. Ratio of limiting loads in elastic and elastic-plastic zone for plates of infinite length, loaded by a local uniformly distributed load.

The limiting load p_{upr} and q_{upr} [$p_{упр} = p_{upr} = p_{elastic}$] for elastic bending of the plate, used in the construction of the curves in Figure 5, were calculated according to the bending moments in the section $y = \pm(a/2)$ of a rigidly fastened infinite plate ($\chi_1 = \chi_2 = 1$) and according to the moment in the center of the span of a freely supported plate ($\chi_1 = \chi_2 = 0$), with consideration of the coefficients k_2 and k_5 (see Tables 3 and 4) for a uniformly distributed load.

Example. Determine the structural strength of the shell plating of the motor ship "Estoniya" in the midship section in the operation of the plate in an elastic-plastic zone if the yield point of the material of the shell plating is

2400 kg/cm^2, the frame spacing a = 700 mm; and the shell plating thickness δ = 19 mm.

For the midship section of the ship, the condition of ice compression is the calculation condition, when the ice load has a great length along the ship. Nevertheless, full-scale strain-gauge tests demonstrated that the compression occurs very irregularly, and, consequently, with a large frame spacing the edges of the plate may be considered as freely supported. We will assume that the length b of the distribution of the load along the frame is 800 millimeters. Then the calculated bending moment is equal to

$$M_{0x} = \frac{p_0 a^2}{8} k_2,$$

where k_2 = 0.732 is determined according to Table 3 $\left(\frac{b}{a} = \frac{800}{700} = 1{,}14\right)$. We find the limiting load in the operation of the plate in an elastic zone according to the equation

$$\frac{p_{упр} a^2}{8} k_2 = \sigma_т \frac{\delta^2}{6} = 2400 \frac{19^2}{6},$$

from whence

$$p_{упр} = \frac{2400 \cdot 19^2 \cdot 8 \cdot 10}{700^2 \cdot 6 \cdot 0{,}732} = 32 \ \text{т/м}^2.$$

According to Figure 5, for (b/a) = 1.14 the ratio (p_{pr}/p_{upr}) = 4.0, and the limiting load in the operation of the plate in an elastic-plastic zone amounts to

$$p_{пр} = 4 \cdot 32 = 128 \ \text{т/м}^2.$$

BIBLIOGRAPHY

1. Popov, Yu. N., Faddeyev, O. V., Kheysin, D. Ye., and Yakovlev, A. A., Prochnost' sudov,plavayushchikh vo l'dakh (Strength of ships navigating in ice), Leningrad, "Sudostroyeniye", 1967.

2. Rzhanitsyn, A. R., Raschet sooruzheniy s uchetom plasticheskikh svoystv materialov (Calculation of structures with consideration of the plastic properties of materials), Moscow, Gosstroyizdat, 1954.

3. Solostyanskiy, D. I., "Full-scale tests of the strength of an icebreaker of the 'Dobrynya Nikitich' type," Tr. NTO Sudproma (Transactions of the Scientific and Technical Society of the Shipbuilding Industry), No. 131, Leningrad "Sudostroyeniye", 1969.

4. Kheysin, D. Ye., "Bending of a rigid plate of an infinite length under the effect of a local load," Sudostroyeniye (Shipbuilding), 1962, No. 4.

5. Kheysin, D. Ye., and Solostyanskiy, D. I. "Strain-gauge tests of the ice strength of transport vessels and icebreakers," Tr. NTO-Sudproma, No. 74, Leningrad, "Sudostroyeniye," 1966.

6. Drucker, D. C., "Plastic Design Methods-Advantages and Limitations," SNAME, Transactions, volume 65, New York, 1957, pp. 172-190.

7. Johansson, B. M., "On the ice-strengthening of ship hulls," International Shipbuilding Progress," vol. 14, N 154, Rotterdam.

SOME FEATURES OF THE DESIGNING OF TRANSPORT VESSELS FOR ICE NAVIGATION

D. D. Maksutov

pages 171-178

In this article certain problems of the designing of transport vessels for ice navigation are considered, a knowledge of which is necessary for the solution of one of the basic problems--provision of accident-free navigation of these vessels with economically efficient speeds in the ice.

It is known that the speed of a ship in the ice depends mainly upon the correspondence of the capacity of the propulsion plant and the ice strength of the forward part of the hull. The capacity of the propulsion plant of transport vessels is usually determined from the condition of providing a given speed in clear water. But in the designing of ships intended for navigating in ice it is necessary that this capacity correspond to the ice strength of the hull, i.e., so that in the use of full capacity navigation in definite ice conditions is accident-free. However, in existing practice of the designing of transport vessels for ice navigation, the requirement indicated is not always observed.

As a result ships that are close to each other with respect to tactical and technical data, having the UL classification of the USSR Registry, but designed by different design organizations, may differ with respect to their ice qualities. This circumstance limits the possibility of the effective use of these ships in ice conditions.

Transport vessels of higher ice categories are intended basically for independent navigation in broken and solid ice behind an icebreaker. Therefore, in calculations of the strength of the forward part of their hulls, we should consider the possibility of an impact of a ship against floating ice floes, or against the edge of a channel. Ice conditions (dimensions of ice floes and the degree to which they cover the sea) must be stipulated preliminarily.

Aside from this, the structural strength of the ship[1] must be determined, especially that of its bow end.

We will introduce two concepts of the speed of a ship in the ice:

the maximum speed achievable--the speed which the ship can develop in definite ice conditions in the use of the full power of the propulsion plant (with given hull lines);

the maximum permissible speed--the speed which is determined by the structural strength of the ship's hull, basically its bow section (upon condition of accident-free collision of the ship with ice).

These two speeds must be in a definite correspondence, and for safe operation of the ship in the ice it is desirable that the permissible speed somewhat exceed the speed that is achievable. In this case, we may use the full power of the propulsion plant without a risk of receiving dangerous ice damage. Thus, if we know these two speeds, it is not difficult to establish the necessary ratio between the capacity of the propulsion plant of the ship and the structural strength of the bow end of its hull.

In the motion of the ship into the ice, each section of its hull takes up an ice load, the magnitude of which is stipulated basically by the shape of the hull (especially its bow section), the speed of the ship, the physico-mechanical properties of the ice, and the ice navigation conditions. This load depends upon the geometrical parameters of the ship's side, and in particular upon the mutual ratio of the angles α and β at the point of impact (α is the angle between the tangential to the waterline at the point of impact and the center line; β is the angle between the tangential to the frame at the point of impact and the plant of the buttocks).

In order to determine the maximum permissible speed of the ship into the ice, we will make use of a formula for the intensity of the calculated ice load in the impact of a ship against the ice floe [2]

$$q_s = 0{,}084 \left(\frac{D_1}{C' + C'' \frac{D_1}{D_2}} \right)^{1/3} \frac{v_s^{4/3} l_1^{4/3} \gamma_c^{2/3}}{\sin^{2/3} \beta \cos^{2/3} \beta}, \qquad (1)$$

1. By the structural strength of the ship we mean the carrying capacity of the shell platings or of individual structures, which is determined with a consideration of the actual dimensions of the elements of the framing and shell plating when stresses equal to the yield point of the material are reached in them.

[$q_H = q_n = q_{load}$] where D_1 is the weight (displacement) of the ship, in tons; D_2 is the weight of the ice floe, in tons; v_s is the speed of the ship, in knots; σ_s is the temporary resistance of the ice to warping, tons per square meter [$\sigma_c = \sigma_s = \sigma_{warping}$]; $l_1 = 0.01$ m; $m = 1.6 \cos\beta + 0.11$ is a coefficient depending upon the angle β [2]; C' and C'' are coefficients depending upon the angle β and the relative coordinate of the point of impact x/L [2].

Then we find the structural strength q_{str} of the hull [$q_{ctr} = q_{str} = q_{structural}$] in the vicinity of each theoretical frame and construct its curve along the length of the bow end of the ship:

$$v_s = \left(\frac{q_{ctr}}{0{,}084}\right)^{0.4} \frac{\sin^{0.6}\beta \cos^{0.4}\beta}{l_1^{0.2} \sigma_c^{0.4}} \sqrt{\frac{C' + C'' \frac{D_1}{D_2}}{D_1}}. \qquad (2)$$

Having substituted the various values of D_2 and σ_s into expression (2), we find the speed as a function of the ice navigation conditions. The least of the speeds obtained in such a manner will be the maximum permissible speed of the ship in the given ice condition, determined by the values of D_2 and σ_s.

At $D_2 = \infty$ (in a case of collision of the ship with a solid ice field), formula (2) is somewhat simplified. The speed v_s, calculated at $D_2 = \infty$, is the limiting safe speed, with which the ship can strike against the edge of an infinite ice field, without receiving dangerous damages in this case.

We may find the maximum achievable speed according to the formula [1]

$$R_{ice} = k_1 \gamma_1 \sqrt{rh} \left(\frac{B}{2}\right)^2 \left(1 + 2 f_T \alpha_n \frac{L}{B}\right) + k_2 \gamma_1 rhB (f_T + \alpha_n \operatorname{tg} \alpha^\circ) \times$$
$$\times F_n + k_3 rh \gamma_1 L \operatorname{tg}^2 \alpha^\circ F_n^2, \qquad (3)$$

where $R_{ch.l}$ [$R_{ice} = R_{ch.l} = R_{net.ice}$] is the net ice resistance, in kilograms; γ_1 is the density of the ice, in kilograms per cubic meter [$\gamma_1 = \gamma_1 = \gamma_{ice}$]; B is the beam of the ship, in meters; f_t is the friction factor of the ice against the side of the ship [$f_T = f_t = f_{friction}$]; α_n is the coefficient of fineness of the bow branch of the waterline [$\alpha_n = \alpha_n = \alpha_{bow}$]; α° is the angle of entry of the waterline; F_n is the relative speed; L is the length of the ship, in meters;

h is the thickness of the ice floe, in meters; r is the length of the ice floe, in meters (the averaged horizontal dimension of the ice floe); $k_1 k_2 k_3$ are dimensionless coefficients calculated according to the curves of reference [1].

The ice conditions in this formula are characterized by the parameter rh. Since a definite value of the weight D_2 of the ice floe corresponds to each value of rh, depending upon their thickness and length, it is not difficult to find their weight according to the thickness of the ice floes (Table 1).

Table 1

Dependence of the Weight of Ice Floes upon their Thickness h and Horizontal Dimensions r

(1) h, м	(2) rh, м²	(3) D_2, т	(1) h, м	(2) rh, м²	(3) D_2, т
0,5	2,75	10	1,5	33,6	500
0,5	3,86	10	1,5	58,4	1000
1,0	9,0	50	2,0	68,0	2000
1,0	12,0	100	2,0	100,0	3000

Key: 1) h, meters; 2) rh, square meters; 3) D_2, tons.

Thus, we may construct a curve of the dependence of the achievable speed upon the ice conditions characterized in the given case by the weight D_2 of the ice floes. In comparing the curves $v_{dop} = f(D_2)$ and $v_{dost} = (D_2)$ [$v_{доп} = v_{dop} = v_{permissible}$; $v_{дост} = v_{dost} = v_{achievable}$], we determine the maximum safe speed with which the ship can proceed in broken ice of definite characteristics, developing its full power. If the curve of the achievable speed is arranged below the curve of the permissible speed, the ship may use its power fully for movement in broken ice without any apprehension of receiving ice damage. Otherwise, the strength of the ship will not make it possible for it to develop speeds above the permissible values and, consequently, in these conditions the ship will not be able to use the full power of its propulsion plant.

For convenience in the construction of the graph, on the abscissa axis, instead of the absolute value of D_2 it is more feasible to plot the values of $\lg D_2$.

It is desirable that the curves v_{dost} and v_{dop} be arranged on the graph as close as possible to each other, but, however, as was already indicated, to provide for navigation safety of the ship it is necessary that the permissible

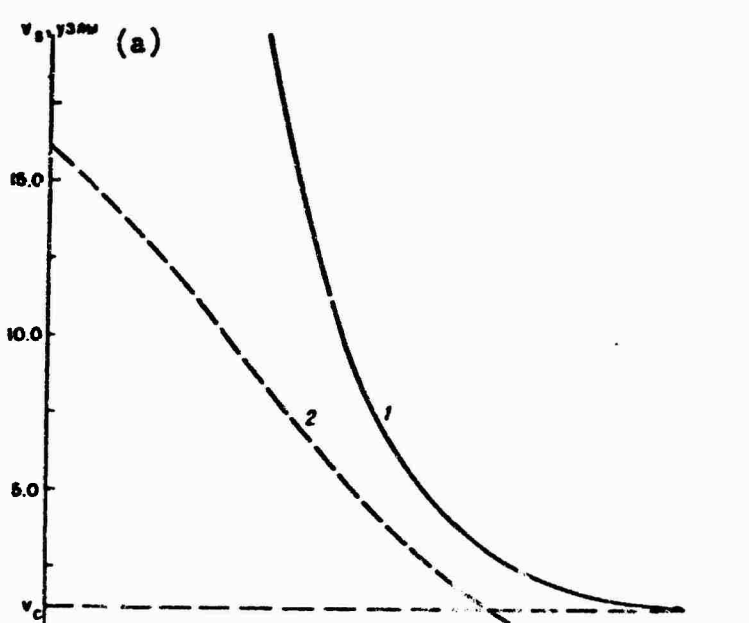

Figure 1. Dependence of the permissible (1) and achievable (2) speeds upon ice conditions for a ship of category UL with an efficient ratio of the strength of the hull and the capacity of the propulsion plant.

speed of the ship somewhat exceed the achievable speed (Figure 1). It is known that the least probability of receiving damage from the impact of the bow end against the ice threatens a ship in proceeding in broken ice with a sea cover of 9--10 balls, regardless of the dimensions of the ice floes. In this case, the achievable speed of the ship is so small that a collision of the hull with ice floes, as a rule, rarely leads to any damage to it.

The motion of a ship in thin broken ice with a sea cover of up to 6 balls is most hazardous, if there are large spaces of clear water and the speed of the ship approaches the maximum speed in clear water. In such a case impact of the ship against an ice floe may lead to serious damages. Therefore, in practice it is necessary to take into consideration the conditions in which a collision of a ship with an ice floe may occur.

The method explained for calculation and comparison of the permissible and achievable speeds can be feasibly used in the process of the designing of ships for ice navigation for a uniform distribution of the ice loads along the length of the bow end, and also to establish the optimum ratio between the strength of the ship's hull and the capacity of its propulsion plant.

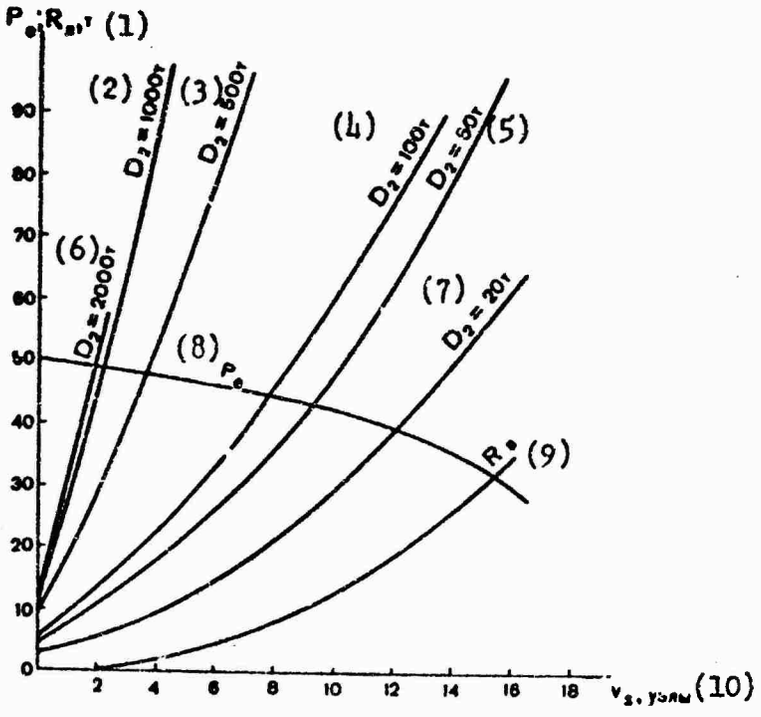

Figure 2. Curve of the ice navigating capability of a ship: P_e is the thrust of the screw propeller (in the given case at the maximum capacity of the propulsion plant); D_2 is the weight of the ice floes; R_v is the resistance of the water [$R_в = R_v = R_{water}$]. 1) P_e; R_1, tons; 2) D_2 = = 1000 tons, 3) D_2 = 500 tons; 4) D_2 = 100 tons; 5) D_2 = 50 tons; 6) D_2 = 2000 tons; 7) D_2 = 20 tons; 8) P_e; 9) R_v; 10) v_s, knots.

If in the designing of the ship definite ice conditions and speed are assigned, for the determination of the necessary capacity of the propulsion plant we may use the curves of ice navigating capability (Figure 2). On them the curves of the ice resistance $R_1 = f(v, D_2)$ are plotted, calculated according to the methodology in reference [1], and the curves of the thrust of the screw propeller, $P_e = \varphi(v, N_p)$ for different values of the capacity N_p. According to the curves we may determine both the necessary capacity, depending upon the ice conditions and the speed, and also the speed, according to the given capacity and ice condition.

In the given case according to the curves of the ice navigating capability the maximum achievable speed is found. The value of this speed is substituted into formula (1), and then the intensity of the ice load q_n is determined. According to the results of the calculation, a curve of the distribution of the ice load along the length of the bow end of the ship is constructed, as a function of definite ice conditions and the speed achievable. Then the extremes are ascertained and if necessary the theoretical design is corrected

at those places where the curve $q_n = f(D_2, v_{dost})$ has a clearly expressed maximum. In this case, the navigating capability of the ship in clear water is not decreased. However, we usually succeed in smoothing the "maximum" on the curve of q_n by means of varying the angles of inclination of the frames to the vertical and the angles between the tangential to the waterline and the center line, i. e., by selection of the most faborable combination of these angles in the vicinity of the extreme points on the curve. For the corrected design, the final ice load is calculated, a curve of its distribution along the length of the ship is constructed, and the calculated load is found by means of straightening the curves of the ice load in individual sections. The calculated load obtained by such a method also will determine the structural strength q_{str} of the hull.

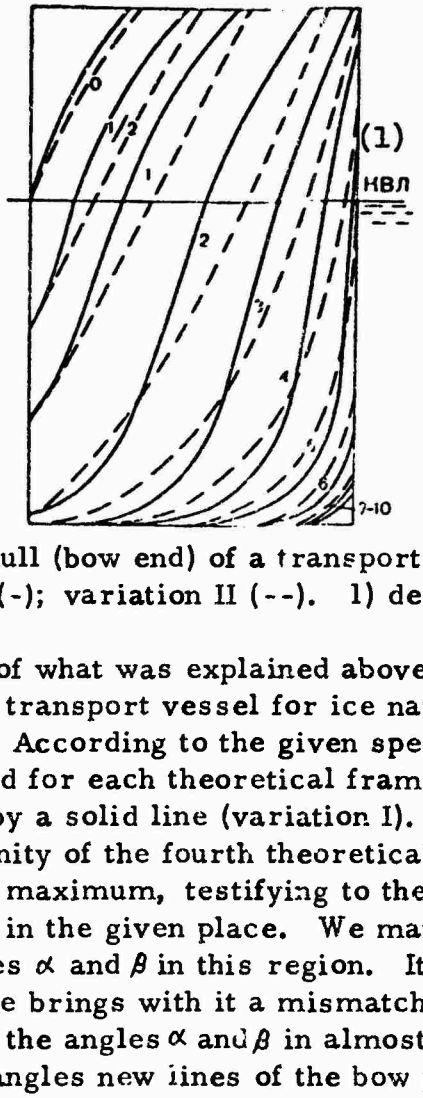

Figure 3. Design of a hull (bow end) of a transport vessel intended for ice navigation: variation I (-); variation II (--). 1) design waterline.

For illustration of what was explained above, we will give an example. A design of the hull of a transport vessel for ice navigation was developed (Figure 3, solid lines). According to the given speed of ice conditions, the ice load q_n is determined for each theoretical frame. The curve of the load q_n is given in Figure 4 by a solid line (variation I). From Figure 4 it is apparent that in the vicinity of the fourth theoretical frame the load curve has a clearly expressed maximum, testifying to the unsuccessful selection of the shape of the lines in the given place. We may make the curve smoother, having changed the angles α and β in this region. It is known that the revision of the design in one place brings with it a mismatch, and consequently it is required that we change the angles α and β in almost all the bow frames. After the change of the angles new lines of the bow part of the hull are obtained (Figure 3, dashed line), and in this case all the basic elements of the design remained unchanged. Then the ice load q_n was again determined for each

theoretical frame and its curve constructed (Figure 4, dashed line, variation II). The new curve is a smooth curve and has no extreme points. This testifies to the fact that the correction of the design was successfully performed. The values of q_n according to variation II are assumed as the initial data for the designation of the calculated load. In this case, the curve of the calculated load may be selected in the form of a broken stepped line (Figure 4, dash-dot line).

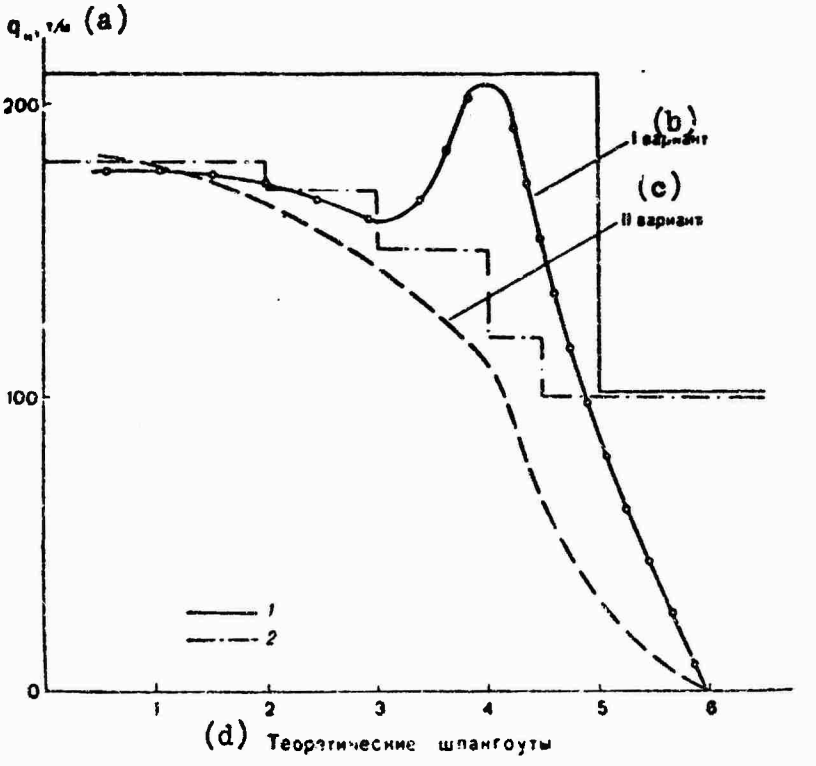

Figure 4. Curves of the distribution of ice loads q_n along the length of the bow part of the ship: 1) load accepted for calculation of the strength of the hull framing (variation I); 2) the same (variation II). a) q_n, tons per meter; b) variation I; c) variation II; d) theoretical frames.

If we accept variation I of the curve q_n and do not correct the design, we would have to determine the calculated load according to the maximum magnitude of q_n. The explicitly exaggerated value of the ice load in the given case would bring with it an increase in the weight of the framing in this region. Thus, a rational selection of the shape of the hull lines of the ship will make it possible to decrease the calculated ice loads essentially, which will lead to a decrease in the weight of the ice reinforcement and, accordingly, to a saving of steel.

By applying the method explained in the designing of transport vessels intended for navigation in ice, we may considerably improve their ice qualities, and, consequently, also the efficiency of operation due to a decrease in the accident rate and an increase in the speed in the channel behind powerful ice-breakers.

BIBLIOGRAPHY

1. Kashtelyan, V. I., Pozdnyak, I. I., and Ryvlin, A. Ya., Soprotivleniye l'da dvizheniyu sudna (Resistance of the ice to the motion of a ship), Leningrad, "Sudostroyeniye", 1968.

2. Popov, Yu. N., Faddeyev, O. V., Kheysin, D. Ye., and Yakovlev, A. A., Prochnost' sudov plavayushchikh vo l'dakh (Strength of ships navigating in ice), Leningrad, "Sudostroyeniye", 1967.

ON A SCIENTIFIC-RESEARCH VESSEL FOR THE ARCTIC AND ANTARCTIC

D. D. Maksutov, Yu. N. Popov, and O. V. Faddeyev pages 179-185

The Program of the Soviet Antarctic Expedition provides for a broad complex of oceanographic, geophysical, hydrographic, and aerometerological investigations in the waters of the Southern Ocean, washing the shores of Antarctica.

Relief of workers who wintered in the area, delivery of cargoes, and performance of scientific research off the shores of Antarctica must be performed in the short navigation season (January-March) in exceptionally complex meterological conditions and a difficult ice situation.

For 18 years cargo and workers who were to spend the winter in Antarctica were delivered by the diesel-electric vessel "Ob'" (sometimes together with other ships not equipped for active ice navigation). However, the limited possibilities of berthing participants in the expedition on board it, the inadequate volume of refrigerator spaces, the small and inconvenient areas for the performance of a full complex of scientific research are hampering the performance of the expanding scientific works of the Soviet Antarctic Expedition more and more.

For the fulfillment of these problems, it is desirable to have a special ship for active ice navigation, making it possible to perform an expanded complex of scientific-research work on the seas of the Arctic and Antarctic, to provide for the delivery and return to the Motherland of the personnel of the Soviet Antarctic Expedition, to transport the expedition's cargoes and foodstuffs to the Antarctic. In order to reduce expenditures on the designing and construction of such a vessel, as a prototype we may use a transport vessel intended for active ice navigation of the same type as the diesel-electric vessel "Amguyema", in this case having preserved its principal dimensions, hull shape, and the basic outfitting of the main power plant.

The principal dimensions of the new ship are the same as in ships of the "Amguyema" type:

Length, overall	133.8 meters
Length, along design waterline (at draft of 7.5 meters)	123.0 meters
Beam, overall	18.8 meters
Molded depth	11.6 meters
Draft, maximum (with cargo and full supplies)	8.79 meters
Displacement, full (at draft of 8.79 meters)	13,645 tons

The shape of the hull lines is:

Angle of inclination of the stem to the horizontal	29°
Inclination of the bow frames from the center line in the vicinity of the design waterline	50°
Inclination of side to the vertical in the vicinity of the midships section	6.5°
Angle of entry of the design waterline	23.5°
Coefficient of fineness (at draft of 7.5 meters)	0.665

Experience in the operation of ships in the Arctic has demonstrated that the shape and strength of the hull of ships of the "Amguyema" type, in combination with a diesel-electric power plant with a capacity of 7200 horsepower provides for high ice qualities in navigation in the ice and good seagoing qualities in clear water.

In the use of the total capacity of the main propulsion plant the ship can break through level solid ice with a thickness of up to 50 centimeters at a speed of 3--4 knots. The maximum speed of this ship, with a full load, amounts to about 15 knots. The calculated range at full supplies of fuel (2370 tons) with a speed of 15 knots may reach approximately 20,000 miles, and with a speed of 13.5 knots, 22,000 miles.

The machinery plant of the ship is diesel-electric (single-shaft), and includes four main diesels with a capacity of 1800 horsepower each and for direct-current generators with a capacity of 1250 kilowatts at 810 rpm. The two-armature direct concurrent electric propulsion motor, with a voltage of 1000 volts in each armature, develops a capacity of 6400 horsepower at 115/170 rpm. The steel screw propeller has four removeable blades.

The shipboard electric-power station consists of five diesel generators of type DGR 300/500-1, with a capacity of 300 kilowatts (alternating three-phase current generators, with a voltage of 380 volts, motors of type 6ChN25/34 with a capacity of 450 horsepower at 500 rpm).

The ship is unsinkable at all the operating variations of the load, even if any two adjacent main watertight compartments are simultaneously flooded.

On board the ship it is necessary to provide for berthing 205 persons, including: 78 crew; 31 permanent marine expedition; and 96 expedition being transported. It is proposed to berth the crew in single-bunk and two-bunk staterooms, and the expedition personnel in two-bunk and four-bunk staterooms. The living compartments of the crew will be arranged separately from the staterooms of the expedition personnel (in the midship part of the ship on the upper deck, the superstructure deck, and the bridges). The participants in the expeditions are berthed in staterooms in the forward and after parts of the upper deck and the superstructure deck, and also in the forward part of the lower deck. All the staterooms have good natural illumination and air-conditioning systems.

The cargo spaces of the ship must be calculated for the transportation of 2100 tons of general cargo (specific stowage factor 2.0 cubic meters per ton) and approximately 380 tons of foodstuffs, including about 180 tons of products requiring refrigeration.

The necessity of the delivery of fresh food products to Antarctica requires the outfitting of special refrigeration rooms on board the ship, with a separate compressor plant, and also storerooms for dry provisions and canned foods.

In the after part of the ship a platform will be located for a helicopter of type V-2 and a complex of spaces associated with its servicing.

In the development of the design, special attention should be devoted to the problem of the most efficient arrangement of the laboratories, scientific equipment, and various spaces intended for the performance of observations and research work: proximity to working places which are located on the open part of the deck, convenient entries for the transportation of apparatus and instruments, good lighting, ventilation, and arrangement in blocks (by types of observation).

For the performance of a complex of scientific research work on board the ship it is necessary to provide the following laboratories:

An oceanographic complex block (hydrological, hydrochemical, bottom sediment, and hydrobiological laboratories, a space for scuba divers, storerooms for the storage of oceanographic equipment, and a bathymetric laboratory);

The aerometerological complex block (by aerological, meterological, and actinometric, synoptic and radiosynoptic laboratories, the "meteorite" radar set, a compartment for the processing of radiosond balloons, and storerooms for the storage of balloons and radiosonds);

A geophysical complex block (geomagnetic and gravimetric laboratories);

A photolaboratory;

A compartment for office work; and

A hydrographic deck house, combined with the chart house.

All the laboratories will be equipped with the necessary apparatus, and with special tables and shelves. The bulkheads provided between the laboratories are of light demountable construction, which will make it possible, if there is a change in the profile of the investigation, to perform the replanning of the compartments.

The hydrological laboratories intended for the study of the thermal regime, currents, and oscillations of the level of the sea. It must consist of three compartments: the apparatus room (in the stern end of the ship), the bathometer room and a workshop (in the bow end on the superstructure deck).

In the apparatus room a GM-32 recording radio wave graph apparatus is installed, a GM-33 radio current gauge, and a GM-15 electromagnetic current gauge, and also repeaters from the log and gyrocompass.

In the workshop shelves are installed for the storage of the mechanisms of the BPV-2 letter-printing rotaters. Together with the workshop the bathometer room is located.

The hydrochemical laboratory is intended for the performance of complex analysis of sea waters, and it is located on the superstructure deck on the port side toward the bow. The laboratory is equipped with special tables, shelves, and exhaust hoods, a refrigerator, etc.

The preliminary processing of bottom samples and the analysis of material will be performed in the bottom sediment laboratory (at the stern, on the superstructure deck). The equipment of the laboratory consists of a drying chamber, a laboratory table, a refrigerator cabinet, a cabinet for storage and drying of bottom sediment samples, and also a special apparatus which will be installed by the contractor on board the finished ship.

The hydrobiological laboratory is intended for preliminary processing of samples, and it is located on the superstructure deck in the after part of the ship The laboratory will be equipped with a special aquarium suspended in gimbals, a laboratory table, refrigerator, and cabinet.

The compartment for the scuba divers is colocated with the ship's divers' gear locker. It is equipped with an electrical compressor, a filter for purification of the air, a table for disassembly and repair of aqualungs, and shelves for storing them. It is located on the lower deck, on the starboard side.

The laboratory of meteorology and actinometry is intended for the recording and processing of data from meterological and actinometric observations, and consists of two adjacent compartments. It is located on the deck of the first bridge. In a large compartment, control panels will be installed for the two shipboard GM-6 hydrometerological stations, and a control panel for the pulsed light IVO-1 altimeter for determining the lower boundary of clouds. For the recording of meterological and actinometric elements, EPP-09 electronic potentiometers and EMP-209M recording bridges are installed. In this same place, repeaters from the log and gyrocompass are also installed. In a smaller compartment spaces are provided for apparatus making it possible to receive data from artificial satellites of the Earth and a universal automatic station. Outside the laboratory, on the open part of the bridges, mast, and also on a special boom in the forward part of the ship, places are provided for the fastening of pickups and meterological instruments.

The synoptic laboratory is intended for the study of the physical processes in the atmosphere, determining the weather conditions and the changes of the weather, and for the compilation of weather forecasts in the region where the ship is navigating. The laboratory consists of two adjacent compartments: the synoptic laboratory itself and the radiosynoptic laboratory, located in the midship part of the ship on the superstructure deck. The synoptic laboratory is equipped with the necessary apparatus, meterological instruments, and special tables. P-53 teletypes will be installed in the radio synoptic laboratory, as well as FAK-P phototelegraphic (facsimile) apparatus, and various radio receiving apparatus.

The laboratory of the "Meteorit" radar set is intended to hold the apparatus for the "Meteorit" radar set, providing for tracking and observation of radiosondes, and it is located on the deck of the first bridge in the midship superstructure. The stabilization apparatus and the power supply are located on the decks lying below, in the appropriate compartments. The antenna of the radar set is installed on a stabilized platform, which provides for normal operation of the receiving apparatus at any angles of list of the ship.

The aerological laboratory is intended for the processing of information received from radiosondes, and also for the preparation and checking of radiosondes before launching, and it is located together with the laboratory of the "Meteorit " radar set. It is equipped with monitoring and measuring radio receiving apparatus, a "Vega" counter, a pressure chamber, etc. Places are also provided in the laboratory for installation of additional apparatus.

In the after part of the ship, on each side, special aerological stalls are provided for holding radiosondes before launching. There is also a special compartment here for the processing of radiosonde balloons with plasticizers, and it is located in the after part of the ship on the upper deck. A compartment is also provided there for storing the balloons. For filling the balloons, there are supplies of helium kept on board the ship (1500 cubic meters), and a special system for feeding gas to the launching site of the radiosondes which is located on the superstructure deck at the stern. The balloons can be filled inside a portable wind shield.

The geomagnetic laboratory is intended for the study of the magnetic field of the Earth, its distribution in space and variation in time, depending upon the latitude and longitude of the observation position. It is located on the superstructure deck in the after part of the ship, on the starboard side. A place and fastening for the installation of the magnetometer is provided in the laboratory.

The gravimetric laboratory is intended to hold apparatus making it possible to study the gravitational forces of the Earth, and it is located on the upper deck in the midship part of the ship. In the laboratory places are provided for the installation of gravimeters, gyrostabilizing platforms, and a pendulum instrument. We should note that for the laboratories of the geophysical complex a number of other instruments are being developed. Repeaters for the log and gyrocompass, and a radio receiver for receiving precision time signals, will be installed in stationary positions.

It is proposed to combine the hydrographic deck house with the chart house, and in it the apparatus providing for the performance of marine and hydrographic operations will be placed. Instruments will be installed there for the determination of the course, speed, distance run, and depth. Part of the special apparatus installed in the chart room is common for the use of the navigator and hydrographer. For depth-measuring operations, the installation of two PEL-3 fathometers and two NEL-6 deep-water fathometers is provided. In the deck house a place is also provided for an electronic computer. For navigational purposes, a NEL-10 fathometer will be installed.

A compartment will be outfitted on board the ship for office (Cameral) processing of materials and graphic work, with the necessary equipment, and also a photo laboratory.

The program of oceanological investigations provides for the installation of buoy stations at great depth aboard such ships. For this, in the forward end of the ship on the superstructure deck a special winch of type LES-29 with a traction force of 2500 tons will be installed, with a drum holding 7650 meters of cable with a diameter of 6.8--11.5 millimeters. By means of this winch, buoy stations may be placed at depths up to 6000 meters. The storage of four sets of buoy ropes is provided on electric reels. The launching of buoys into the water and lifting them from the water will be performed by the cargo booms. The transportation of storage of buoys, spar buoys, and anchors is provided for in No. 1 tweendeck. For the performance of various oceanological operations, the following winches are installed on the ship's deck:

in the forward part of the ship, along both sides: two cable winches of type LEROK-1.2; two cable winches of type LERK-1.

in the after part of the ship, along both sides, are located: two cable winches of type LEROK-1.2; two cable winches of type LOKS1-1.

Deep-water trawling, according to the program of the hydrobiologist, is provided for by nets of the "Dzhedi" type, by means of a winch for the placement of buoy stations, with the cable led through a strengthened cathead.

All the shipboard devices must be designed with consideration of the specifics of the operation of the ship in conditions of the Arctic and Antarctic.

The lifeboats used are of the enclosed type, with the following capacities: two of 50 persons each (with a motor and radio set), and two of 69 persons capacity each (with a manually operated drive), and are installed on each side. Aside from this, there is stowage for twelve life rafts, with a total capacity of 120 persons. Thus, in the boats on one side 119 persons can be placed, and accordingly, on two sides 238 persons. Consequently, on board the ship an additional 33 persons can also be berthed (the personnel complement of the ship is 205 persons) on sofas and folding bunks. For shipboard needs, a working launch is provided, stowed in the after part of the ship on superstructure deck.

The cargo gear must provide for normal unloading of the expedition cargo when the ship is anchored in a roadstead. The ship must be equipped with cargo booms having a lift capacity of 5--10 tons (8 units) and two heavy-lift booms, with a lift capacity of 40 tons each.

Thus, the new scientific research vessel, outfitted with its special equipment, will make it possible to expand research operations in the seas of the Arctic and Antarctic considerably, and also provide for the delivery of the greater part of the expeditionary personnel and the necessary cargoes to Antarctica. The set of communal, medical, and sanitary-hygenic compartments provided on board the new ship, the special domestic systems (air conditioning, air refrigeration, and modern equipment and finishing of the living compartment) will create good conditions for the life and work of the personnel and the participants in the expedition.

EXPERIMENTAL STUDY OF THE FRICTION OF ICE

A. Ya. Ryvlin pages 186-199

The forces of friction play an essential part among the components of ice resistance in the operation of a ship in various ice conditions. This, therefore, is precisely why a large part of modern devices intended for improving the ice navigating capability of ships (hydraulic washing and hydrodynamic systems, shaking devices, pneumatic washing systems, devices for heating the side in the vicinity of the ice waterline, and others) are directed toward decreasing the forces of friction of the ship's shell plating against the ice cover. Without having studied the nature and the quantitative relationship of external friction, we cannot model the process of the motion of the ship in the ice. From the standpoint of the nature and mechanism of external friction, until recent times a number of contradictory hypotheses have existed. This is explained by the complexity of the processes originating during the sliding of two solid bodies. According to contemporary concepts, friction has a double molecular-mechanical nature. It is caused by volumetric deformation of the material and the overcoming of intermolecular bonds, originating between the contact sections of rubbing surfaces [5].

Some times an incorrect explanation is given to the slipperiness (lubricity) [6], which has been affirmed since the time of the British physicist Reynolds, who assumed that it depends upon the capability of the ice to decrease its melting point under pressure (the so-called regelation--an anomalous property of water, bismuth, and antimony, distinguishing them from other substances). However, the assumption that the pressure in the zones of contact between the ice and some other body (such as, for example, the runners of a sled or sleigh) may serve as the cause of a decrease of the melting point by 10--20 degrees, as a result of which even below freezing an interbedding of water may form, is easily refuted.

The true nature of the slipperiness of ice was explained for the first time by K. B. Veynberg [2]: the melting of the ice in the friction of other

bodies against it occurs as a consequence of the liberation of heat originating in the zones of actual contact (practically instantaneously), as a result of the transformation of the work of the forces of friction into heat. Thus, in zones of actual contact the ice melts and lubricating layers appear.

S. S. Budnevich and B. V. Deryagin proved that the friction of ice is subordinate to boundary friction laws (the force of friction does not depend upon speed and is proportional to the load). At low temperatures, and also at low pressures and slide speeds, sometimes "dry" friction in a pure form is observed [1], which differs sharply from friction with self-lubrication in the numerical values of the friction factors.

According to the hypothesis of B. V. Deryagin, the mechanism of boundary lubrication with water is based on the presence of definite slip planes inside the lubricating layer [4]. The special arrangement of the molecules, preserved after the melting of the ice, which, as is well known, has a crystalline structure, facilitates the formation of these planes. The absence of such slip planes in comparatively fixed layers of water, apparently, also explains the poor slippage in cases when friction occurs along a surface covered with water or at a positive temperature. At a low temperature the slippage deteriorates somewhat due to the decrease in the area in the zones of actual contact, in which the lubricating layer appears. At a very low temperature, the lubricating layer is not formed at all and the friction factor reaches a maximum value; it is equal to the dry friction factor of ice.

As the investigations of S. S. Budnovich demonstrate, on the friction surface there are always irregularities, in comparison with which the radius of the effect of the molecular forces of attraction is small. Aside from this, the true area of contact is not great and it is difficult to determine it. Therefore, for the friction of the ice we may assume the Coulombe-Amonton law [1]. This principle refers to the greatest degree to the slippage of ice floes along a ship's shell plating, in which contact of bodies of large dimensions occurs.

For the solution of practical problems associated with the navigation of ships in ice, it is necessary primarily to know the numerical magnitude of the friction factors of the ice, and also the nature of their dependence upon external factors, which determine the process of the reaction of the hull with the ice. For the modeling of the motion of the ship in the ice it is necessary to have analogous information concerning the friction of laboratory ice.

Materials concerning the friction factors of ice against steel and ice against ice are encountered in the works of Soviet and foreign authors:

R. I. Runeberg, V. I. Arnol'd-Alyab'yev, S. S. Budnevich, I. N. Yevanel'yev, V. V. Veynberg, F. P. Bouden, S. D. Niven, Ya. Ye. Yanson, S. L. Landtman, V. R. Milano, R. M. White, and others. However, available data cannot be used directly for the solution of the practical problems indicated, since the greater part of them was obtained in a laboratory from small specimens. This decreases the accuracy of the calculations, since the problem of the scale effect in the determination of friction factors by means of tests of specimens remains unclear. There are serious grounds to assume that friction factors in full-scale conditions may differ considerably from those in laboratory conditions [7, 8].

For the study of the external friction of ice, a methodology making it possible to bring the test conditions (the dimensions of the rubbing surfaces, their state and other external conditions: coefficient of mutual overlapping, slip velocity, specific pressure, total temperature, and temperature gradient) to the real conditions was used.

The static and dynamic friction factors of the ice were determined by means of the method which has been given the name of Coulombe tribometer. This method is simple and reliable. The use of the method indicated is associated with the necessity of towing the specimens along a horizontal working surface. In this case the friction factors are calculated as the ratio of the towing force S to the weight P_o [$P_o = P_o = P_{specimen}$] and the load P_{gr} [$P_{гр} = P_{gr} = P_{load}$] located on it ($f_{st}$ [$f_{ст} = f_{st} = f_{towing}$] at the initial moment of motion in the towing of the object from its place, and f_{din} [$f_{дин} = f_{din} = f_{dynamic}$] in uniform motion of the specimen along the working surface)[1] i.e.,

$$f_{ст} = \frac{S_{ст}}{P_o + P_{гр}},$$

$$f_{дин} = \frac{S_{дин}}{P_o + P_{гр}}.$$

Tests with full-scale ice during a number of years have been performed in the fresh water area of the Gor'kovskaya experimental test station (near Leningrad) and in the Arctic on the ice of Tiksi Bay. In the development of the methodology of the tests and their performance, aside from the author, junior scientific worker Ye. Petrov and tool engineer G. V. Parkhomov participated. The results of the tests, run on fresh-water ice, were published earlier [9].

1. Due to the technical complexity the area of the zones of actual contact was not determined.

An ice cover served as the working surface for tests in full-scale (natural) conditions. The dimensions of the ice test area amounted to about 8x80 meters. It was located on sections of the ice cover having different roughness, degree of disintegration, and snow cover. Ice specimens were prepared from natural ice. Their base was given a cylindrical or octagonal shape, with a diameter from 70 to 134 centimeters.

A steel specimen was made of sheet steel in the form of a tank of cylindrical shape with a diameter of 70 centimeters and a height of 15 centimeters. The lower side of the tank, which served as the working base of the specimen, with respect to the degree of roughness approximately corresponded to the outer shell plating of an icebreaker in the vicinity of the ice belt. The tank was filled with a fluid which could be heated by an electrical heating element plate inside the tank.

In order to create adequate specific pressure on the plane of friction, the specimens were loaded from above by ice blocks and cast-iron or concrete loads of a given weight (Figure 1). The total maximum weight of the specimen reached 920 kilograms, which, in conversion to the area of its base, corresponded to a specific pressure of 230 grams per square centimeter. A vibrator was placed on top of the specimen, and this vibrator consisted of an electric motor with a load eccentrically arranged on its shaft. The vibrator stand was firmly fastened to the specimen by screw shaft (Figure 2).

The towing of the full-scale specimens was performed by means of a tractor or cross-country vehicle. The system of blocks fastened on the ice made it possible to perform back-and-forth towing of the specimen, preserving the horizontal position of the towing table, which excluded the additional force pressing the specimen against the working surface or separating the specimen from it.

Measurements of the traction force were performed by a ring strain-gauge dynamometer, which was included in the cable directly before the specimen. The traction force measured in such a manner turned out to be equal to the friction force. Consideration of losses due to friction in the blocks and due to the natural oscillations of the cable in this case was not required. The dynamometer had a high class of accuracy, its readings were fixed on oscillograph paper, which made it possible to record the variation of the force in time. On the same paper the towing speed was simultaneously recorded, for the recording of which a special pickup was installed on the specimen. Its working link was moved along a wire stretched along the direction of the towing of the specimen.

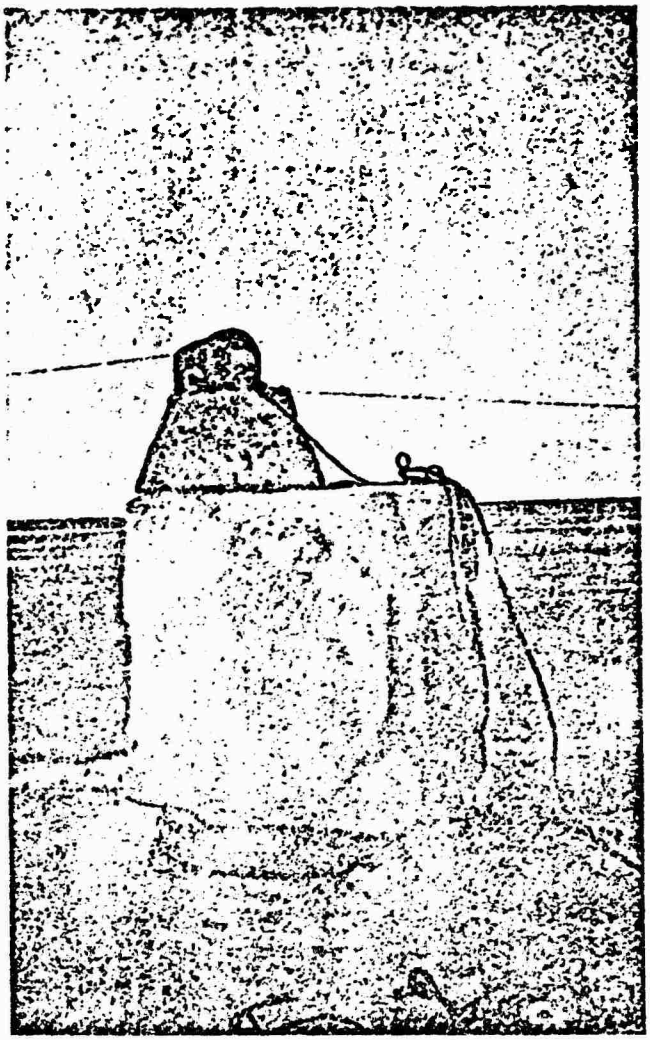

Figure 1. Specimen for full-scale tests.

In the oscillograms the static friction force corresponded to the maximum deviation of the beam at the moment of towing of the specimen. The dynamic friction was found by means of averaging the readings of the dynamometer in the section where the motion of the specimen was uniform, i.e., at the speed v = const. The friction factors were calculated as the averages according to data from 7--10 measurements.

As is well known, in the process of full-scale experiments it is difficult to achieve reproducability of the external conditions. In order to avoid errors requiring the introduction of correlation factors, the compari-

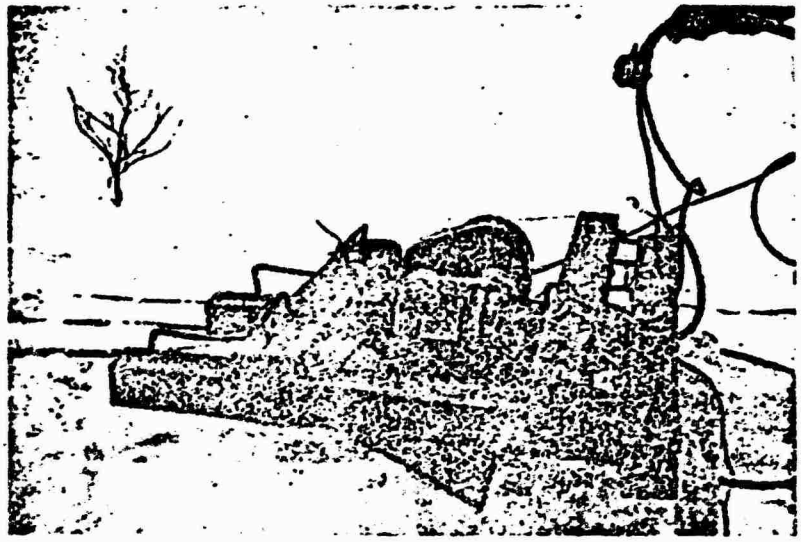

Figure 2. Vibrator--instrument for measuring speed--and loads mounted on a full-scale specimen.

son of experiments is widely used: alternately in the course of a comparatively short segment of time runs were made, in which only one given parameter was subjected to change; the stability of the other conditions of the experiment was subjected to careful control.

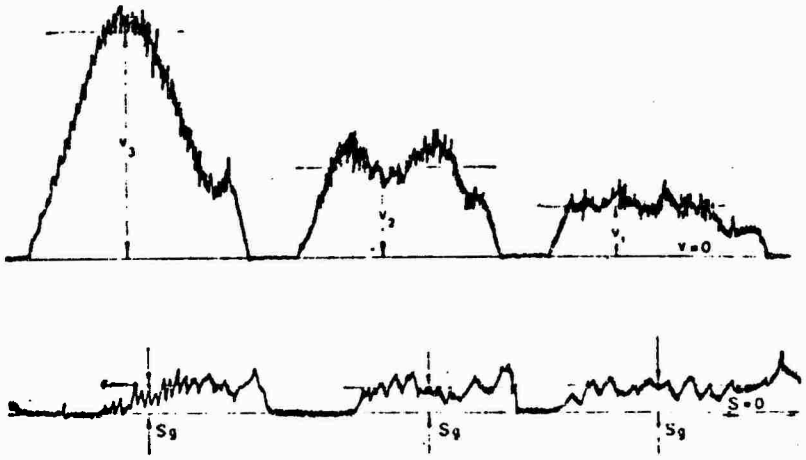

Figure 3. Recording of friction parameters in variable slip velocity (v_1, v_2, and v_3).

The experiments with respect to the study of the friction of ice along painted wood and along steel were performed by the author in the Ice-Thermic Laboratory of the All-Union Scientific Research Institute of Hydraulic

Engineering imeni Vedeneyev, and the determination of the friction factors of paraffin[1] in the Laboratory of Theoretical Naval Architecture imeni Krylov of the Leningrad Shipbuilding Institute. All the laboratory specimens had a cylindrical shape with a base diameter of about 100 millimeters. The specific pressure on the friction plane varied from 6.85 to 155 grams per square centimeter. The ice specimens were tested at 0°, and the paraffin specimens at 15°. The working surface, with a length of 1.1 meter and a width of 0.4 meter, was equipped with flanges making it possible to flood it with water. The friction factors were calculated according to data from 10--20 measurements.

We will consider the detailed effect of external factors on the friction of ice.

The slip velocities of specimens in the process of the experiments varied from 0.2 to 5.0 meters per second, which embraces practically the entire range of speeds of ships in ice. As an analysis of the test materials demonstrated, the variations of the speed have no essential effect from the magnitude of the dynamic friction factor of steel against ice (Table 1 and Figure 3).

Table 1

Effect of Slip Velocity on the Dynamic Friction Factor

(1) Удельное давление, г/см² (2)	Скорость буксировки, м/с	$f_{дин}$ (3)	Удельное давление, г/см² (1)	Скорость буксировки, м/с (2)	$f_{дин}$ (3)
68	0,5	0,092	110	1,25	0,085
68	1,2	0,13	110	4,5	0,115
68	5,0	0,11			

(4) Примечания. 1. Опыты проводились при температуре 0,8°. 2. Образцом служила сталь гладкая, рабочей поверхностью — лед пресный сухой с зернистой поверхностью.

Key: 1) specific pressure, grams per square centimeter; 2) towing speed, meters per second; 3) dynamic friction factor; 4) Notes: 1. The experiments were conducted at a temperature of 0.8°. 2. Smooth steel served as the specimen, and dry fresh-water ice with a grainy surface as the working surface.

1. In certain test basins paraffin replaces fine broken ice.

This conclusion refers to an equal degree to the friction of steel and ice specimens, both along a dry ice surface and along a surface covered with a layer of water. It is valid for fresh-water and sea ice in the entire range of specific pressures and temperatures (from 2.5 to -30°) investigated.

The specific pressure on the friction plane (referred to the total area of the base of the specimen) varied from 55 to 230 grams per square centimeter. The experiments demonstrated that both static and dynamic friction factors of steel against ice are practically independent of this parameter if its magnitude exceeds 100 grams per square centimeter (Table 2).

Table 2

Effect of the Specific Pressure on Friction Factors

(1) Удельное давление, г/см²	(2) $f_{ст}$	(3) $f_{дин}$	(1) Удельное давление, г/см²	(2) $f_{ст}$	(3) $f_{дин}$
68	0,35	0,130	140	0,21	0,077
80	0,38	0,125	190	0,30	0,070
110	0,22	0,100	230	0,28	0,068
115	0,30	0,067			

(4) Примечания. 1. Испытания проводились при температуре 1,2°. 2. Скорость буксировки составляла 1,0—1,5 м/с. 3. Образцом служила сталь гладкая, рабочей поверхностью — лед пресный сухой с зернистой поверхностью.

Key: 1) specific pressure, grams per square centimeter; 2) static friction factor; 3) dynamic friction factor; 4) Notes: 1. The tests were conducted at a temperature of 1.2°. 2. The towing speed was 1.0--1.5 meters per second. 3. Smooth steel served as the specimen, and dry fresh-water ice with a grainy surface as the working surface.

The temperature of the medium (air) varied in the process of the tests, conducted at various periods of the year, from 2.5 to -30°, i.e., in practically the entire range of temperatures encountered in the navigation of ships in ice (Figure 4, a). At low temperatures the experiments were conducted in the autumn-winter at Tiksi, and at positive periods of the same place in the summer season, and in the autumn and winter near Leningrad. The scattering of the points in Figure 4, a, is explained by errors of measurements and the instability of the external conditions.

The experiments demonstrated that the static friction factor increases somewhat with a decrease in temperature, and the dynamic friction factor is

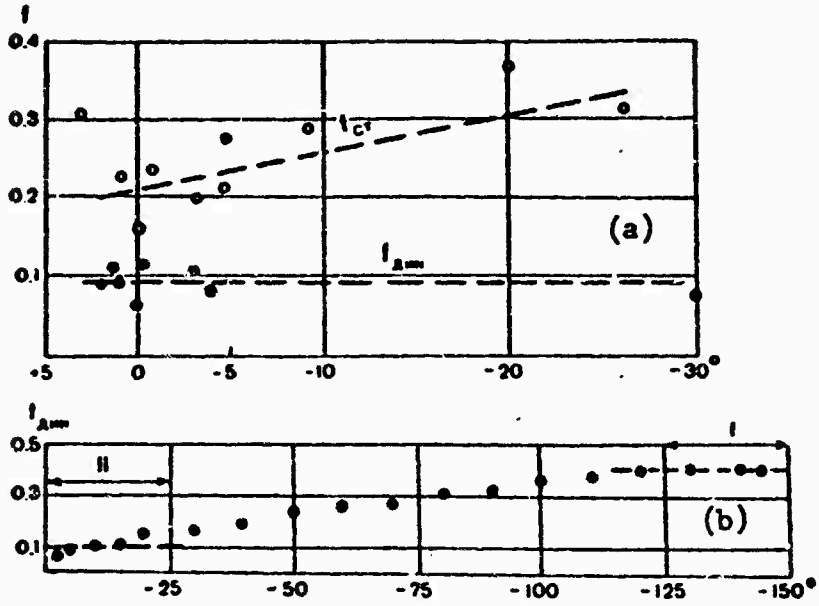

Figure 4. Dependence of the friction factor of steel against ice upon the air temperature: a) according to the author's data; b) according to S. S. Budnevich's data; I) region of dry friction; II) region of temperatures investigated.

practically independent of it. This conclusion, which seems unusual at the first glance, is explained by the narrow temperature range in which the experiments were conducted, and also by errors of measurement. In any case, we may definitely affirm that in the range considered the dependence of f_{din} upon temperature is weakly expressed, which agrees with the results of the investigations of S. S. Budnevich in a broader range of temperatures: from 0 to -150° (Figure 5, b).

The freezing of a steel specimen to an ice surface at a negative temperature has an essential effect on the magnitude of the static friction factor (Table 3). At first with an increase in the freezing time from 0.1--0.5 to 5--10 minutes (depending upon the temperature) it increases, reaching a maximum magnitude, and with a further increase remains constant. Experiments in the investigation of bodies freezing to the ice were performed on a dry ice cover.

Table 3

Effect of the Freezing of a Steel Specimen to Ice on the Static Friction factor

(1) Характер рабочей поверхности	Температура, °С (2)	Время примерзания, мин (3)	$f_{ст}$ (4)
		(6)	
(5) Лед морской с ровной зернистой поверхностью	—2	20 и более	0,4
	—2	10	0,33
	—2	5	0,30
	—2	0,2—0,5	0,25
(7) Лед морской с ровной поверхностью	—28	(8) 2 и более	0,53
	—28	1—2	0,43
	—28	0,1—0,5	0,39
(9) Лед пресный с сухой зернистой поверхностью	—5	10	0,78
	—5	5	0,54
	—5	1—2	0,44
	—5	0,1—0,5	0,29

Key: 1) Nature of working surface; 2) temperature, degrees Centigrade; 3) freezing time, minutes; 4) static friction factor; 5) sea ice with level grainy surface; 6) 20 or more; 7) sea ice with level surface; 8) two or more; 9) fresh-water ice with a dry grainy surface.

The heating of a steel specimen by means of an electrical heating element is of interest in the estimation of the efficiency of heating the sides of an icebreaker to improve its ice navigating capability. The experiments were comparative in nature: in identical conditions the towing of the specimen was performed alternately with heating and without heating. The results of one series of such experiments are given in Table 4.

Table 4

Effect of the Heating of the Specimen on the Static Friction Factor

(1) Температура образца, °С	(2) Время примерзания, мин	(3) $f_{ст}$
	(4) Без обогрева	
—3,0	10,0	0,78
—3,0	5,0	0,54
—3,0	1—2	0,44
	(5) С обогревом	
4,0	1—10	0,27
5,0	1—10	0,19
6,0	1—10	0,16
7,0	1—10	0,22
8,0	1—10	0,12

(6) Примечания 1. Испытания проводились при температуре воздуха —5°. 2. Рабочей поверхностью служил лед пресный с сухой, слегка шероховатой поверхностью.

Key: 1) temperature of specimen, degrees Centigrade; 2) freezing time, minutes; 3) static friction factor; 4) without heating; 5) with heating; 6) Notes:

1. The tests were conducted at an air temperature of -5°. 2. Fresh-water ice with a dry, slightly rough surface served as the working surface.

In the heating of a steel specimen to a positive temperature, freezing seas and the static friction factor decreased considerably. In heating, the dynamic friction factor remained practically unchanged.

The problem of the effect of the state of the surface of the ice cover on friction is of undoubted interest. In the process of the experiment, we succeeded in investigating the basic factors characterizing this state: roughness, degree of disintegration of the surface of the ice cover, originating in melting, and the presence of water and a snow cover on the surface.

The roughness of the ice surface[1] varied within limits which are characteristic for the ice cover of fresh-water and sea ice of natural formation. The results of certain experiments are given in Table 5.

Table 5

Effect of the Roughness of an Ice Cover on the Friction Factors

(1) Место и месяц испытаний	(2) Температура воздуха, °С	(3) Состояние поверхности льда	(4) $f_{ст}$	(5) $f_{дин}$
(6) Тикси, май	0	(7) Гладкая	0,15	0,06
	0	(8) Шероховатая ($h_б \approx 0,5$ мм)	0,20	0,08
(9) Тикси, ноябрь	—20	(7) Гладкая	0,32	0,08
	—26	(10) Шероховатая ($h_б \approx 0,8$ мм)	0,39	0,07
(11) Горьковская, март	—8	(7) Гладкая	0,29	0,07
	—8	(12) Шероховатая ($h_б \approx 1,0$ мм)	0,26	0,10

(13) Примечание. $h_б$ — высота бугорков шероховатости.

Key: 1) Place and month of test; 2) air temperature, decrees Centigrade; 3) state of the ice surface; 4) static friction factor; 5) dynamic friction factor; 6) Tiksi, May; 7) smooth; 8) rough ($h_b \approx$ 0.5 millimeter); 9) Tiksi, November; 10) rough ($h_b \approx$ 0.8 millimeter); 11) Gor'kovskaya, March; 12) rough ($h_b \approx$ 1.0 millimeter); 13) Note: h_b is the height of the protuberances

1. We are speaking of a roughness that is incommensurably less than the dimensions of the specimen.

of roughness [$h_б = h_b = h_{protuberance}$].

As is apparent from Table 5, the variation of the roughness of the surface of the ice cover within the limits considered has no essential effect on the friction factors. This conclusion logically agrees with the contemporary concepts of the mechanism of the friction of ice, based on the hypothesis of the discrete nature of the actual contact of the rubbing surfaces.

The degree of disintegration of the surface of the sea ice under the effect of solar radiation is partially manifested in the fact that a destruction layer resembling firn with respect to external appearance is formed on its surface. Such a change in the surface of the ice cover leads to a noticeable increase in the static friction factor and an insignificant change in the dynamic factor (Table 6).

During first autumn or late spring frosts, when the destruction layer of ice freezes, forming a hard crust, the friction factors become equal to the friction factors of ordinary rough ice (Table 7).

Table 6

Effect of the Degree of Destruction of the Ice Surface on Friction Factors

(1) Место и месяц испытаний	(2) Состояние поверхности льда	(3) $f_{ст}$	(4) $f_{дин}$
(5) Тикси, май	(6) Шероховатая жесткая ($h_0 = 0$ см)	0,15	0,07
	(7) Деструкционный слой глубиной ($h_0 = 2$—3 см)	0,26	0,11
(8) Тикси, июнь	(9) Деструкционный слой глубиной ($h_0 = 3$—5 см)	0,24	0,12
	(10) Деструкционный слой глубиной ($h_0 = 6$—8 см)	0,49	0,13

(11) Примечание. Испытания проводились при температуре 0°.

Key: 1) place and month of test; 2) state of ice surface; 3) static friction factor; 4) dynamic friction factor; 5) Tiksi, May; 6) rough, hard (h_o = 0 centimeter); 7) destruction layer with depth (h_o = 2--3 centimeters); 8) Tiksi, June; 9) destruction layer with depth (h_o = 3--5 centimeters; 10) destruction layer with depth (h_o = 6--8 centimeters); 11) Note: tests conducted at temperature of 0°.

Table 7

Effect of the Freezing of the Destruction Layer of Ice on Friction Factors (Tiksi, May)

(1) Температура, °С	(2) Состояние поверхности льда	(3) $f_{ст}$	(4) $f_{дин}$
0	(5) Деструкционный слой (h = = 2—3 см)	0,26	0,11
—2	(6) То же, при заморозках до —3°	0,19	0,09

Key: 1) temperature, degrees Centigrade; 2) state of ice surface; 3) static friction factor; 4) dynamic friction factor; 5) destruction layer (h = 2--3 centimeters); 6) the same, in first autumn or late spring frosts to -3°.

The snow cover on the surface of the ice essentially affects the friction factors (Table 8). In the slippage of the specimen along the surface of the ice covered with freshly fallen snow, a ridge (tongue) of displaced snow is formed before the specimen. With a height of snow cover of up to 10--15 centimeters or more the specimen slides along the snow with its entire plane, without touching the ice, and with a lesser height partially along the snow and partially along the ice.

Table 8

Effect of Freshly Fallen Snow on Friction Factors

(1) Место и месяц испытаний	Температура, °С (2)	(3) Состояние поверхности льда	(4) $f_{ст}$	(5) $f_{дин}$
(6) Тикси, май	0	(7) Шероховатая без снега	0,16	0,07
	0	(8) Свежий снег ($h_{сн}$ = 0,5 см)	0,17	0,08
	—3	(9) Свежий снег ($h_{сн}$ = 2 см)	0,27	0,14
(10) Тикси, июнь	0	(11) Свежий снег ($h_{сн}$ = 15 см)	0,92	0,26

Key: 1) Place and month of test; 2) temperature, degrees Centigrade; 3) state of ice surface; 4) static friction factor; 5) dynamic friction factor; 6) Tiksi, May; 7) rough, without snow; 8) fresh snow (h_{sn} = 0.5 centimeter) [$h_{сн}$ = h_{sn} = h_{snow}]; 9) fresh snow (h_{sn} = 2 centimeters); 10) Tiksi, June; 11) fresh snow (h_{sn} = 15 centimeters).

In the sliding of the specimen along the surface of the ice covered with dry grainy snow, the plastic displacement of the snow is different in nature: the snow is partially pushed to the sides and to a greater degree rises above the specimen. In this case the friction factors also increase, although not so sharply as in the presence of fresh snow (Table 9).

Table 9

Effect of Granular Snow on Friction Factors (Tiksi, November)

(1) Температура, °С	(2) Состояние поверхности льда	(3) $f_{ст}$	(4) $f_{дин}$
—28 (5)	Шероховатая сухая без снега	0,32	0,07
—2 (6)	Плотный сухой крупинчатый снег (h = 10—20 см)	0,42	0,13

Key: 1) temperature, degrees Centigrade; 2) state of ice surface; 3) static friction factor; 4) dynamic friction factor; 5) rough and dry, without snow; 6) dense dry granular snow (h = 10--20 centimeters).

Water covering the surface of the ice has no noticeable effect on the friction factors (Table 10).

Table 10

Effect of Water on Friction Factors

(1) Место испытаний	(2) Температура, °С	(3) Состояние поверхности льда	(4) $f_{ст}$	(5) $f_{дин}$
(6) Горьковская	0,8 (7)	Зернистая сухая	0,21	0,08
	1,5 (8)	Зернистая влажная	0,30	0,07
	0,2 (9)	Зернистая, покрытая водой ($h_в$ = 3 см)	0,40	0,10
(10) Тикси	0 (7)	Зернистая сухая	0,26	0,11
	0 (11)	Зернистая, покрытая водой ($h_в$ = 15 см)	0,21	0,11

Key: 1) location of tests; 2) temperature, degrees Centigrade; 3) state of surface of ice; 4) static friction factor; 5) dynamic friction factor; 6) Gor'kovskaya; 7) grainy and dry; 8) grainy and moist; 9) grainy, covered with water (h_v = 3 centimeters) [$h_в = h_v = h_{water}$]; 10) Tiksi; 11) grainy, covered with water (h_v = 15 centimeters).

In the given case the presence of water does not facilitate a decrease in the friction factors, and sometimes even somewhat increases them, since it only removes the heat formed in friction in zones of actual contact, without changing the slide conditions (as was already noted, only the water which is formed in zones of actual contact in the melting of the ice improves the friction characteristics of the ice: such water has a special molecular structure).

The solidity of the ice has no essential effect on the friction factors which are practically identical for sea ice and fresh-water ice. We may be convinced of this, having analyzed the data of Tables 1--11.

Table 11

Effect of Mutual Arrangement and Direction of the Metals of the Axes of the Crystals of Ice Specimens on the Friction Factor (Tiksi, May)

(1) Направление буксировки	(2) $f_{ст}$	(3) $f_{дин}$
⊥	0,50	0,08
∥	0,70	0,08
=	0,51	0,08

(4) Примечание. Поверхность образца гладкая, рабочая поверхность зернистая влажная.

Key: 1) Direction of towing; 2) static friction factor; 3) dynamic friction factor; 4) note: surface of specimen is smooth, working surface is grainy and wet.

The mutual arrangement of the axes of the crystals and the direction of the towing of the ice also has no noticeable effect on the magnitude of the dynamic friction factor (f_{st} decreases somewhat in sliding along the axes of the crystals). This is confirmed by the results of tests of specimens of sea ice, the crystals of which add a columnar nature and were arranged vertically (Table 11). Alternately, the lower or upper edge of the specimen (⊥) served as the working space of the specimen in towing, and also the side edges, and in the latter case the direction of towing either coincided with the direction of the axes of the crystals (=) or made an angle of 90° with them (∥).

The average numerical values of the dynamic friction factor of the ice against the ice and the steel against the ice approximately coincides, while the static friction factor of the ice against the ice is approximately twice as

great as the static friction factor of the steel against the ice.

The effect of vibration on the friction factors was studied to ascertain the mechanism of the effect and to estimate the possibility of the use of shaking devices aboard icebreakers. The tests of the specimens were comparative in nature: in identical conditions, alternately, runs of a steel specimen were made with the effect of vibration on it, and without it. The vibrator consisted of an electric motor with a capacity of 1 kilowatt, operating at 1410 revolutions per minute, and a weight eccentrically fastened on its shaft (this load weighed 50--15 grams, and lay 6--8 centimeters from the axis of rotation). The results of the tests (Table 12) made it possible to establish the fact that vibration essentially decreases the static friction factor of steel against ice (by approximately a factor of 1.5--2.0), and the dynamic factor remains practically unchanged[1]. The most intensive change in the static friction factor is noted at negative temperatures, since in vibration freezing to the ice is entirely eliminated. The decrease in the magnitude of f_{st} of ice at positive temperatures is caused by the resonant drop of the force of friction, which is theoretically validated in reference [3].

Table 12

Effect of Vibration on Friction Factors (Gor'kovskaya, March)

(1) Вид испытаний	(2) Состояние поверхности	(3) Время примерзания, мин	(4) $f_{ст}$	(5) $f_{дин}$
	(6) Температура 0,8°			
(7) Без вибрации	(8) Зернистая влажная	—	0,32	0,08
(9) С вибрацией	То же (10)	—	0,22	0,07
	(11) Температура —5,0°			
(7) Без вибрации	(12) Гладкая сухая	10	0,78	Не определялся (13)
		5	0,54	
		1	0,44	
(9) С вибрацией	То же (10)	10	0,31	То же (10)
		5	0,30	"
		1	0,24	"

1. The static friction factor of the ice is more subject to changes under the effect of various external factors (temperature, heating, vibration, etc.), while f_{din} is practically independent of them. Therefore, for approximate practical calculations it is advisable to use the mean static values of the dynamic friction factor (in particular the average value of the dynamic friction factor of steel against ice in the absence of a snow cover may be assumed to be equal to 0.1).

Key to Table 12: 1) form of tests; 2) state of surface; 3) freezing time; 4) static friction factor; 5) dynamic friction factor; 6) temperature 0.8°; 7) without vibration; 8) grainy, wet; 9) with vibration; 10) the same; 11) temperature -5.0°; 12) smooth and dry; 13) not determined.

Laboratory investigations of the friction of ice were performed in a more limited volume. The specimens were prepared from salt water. Polished and rusty steel served as the working surface, and also wood coated with paint, which was applied on treated filler. The possibility of covering the working surface with a layer of water was provided. The tests were conducted at a temperature of 0 degrees and a specific pressure of 155 grams per square centimeter.

The experiments demonstrated that the average value of the friction factor of ice against rusty steel (by dry ice and ice covered with water) is close to that obtained in full-scale conditions ($f_{st} \approx 0.15$). The friction factors of ice against polished steel and painted wood are considerably less: $f_{st} \approx 0.04$; $f_{din} \approx 0.02$.

The average value of the friction factors of paraffin against paraffin and paraffin against painted wood (dry and covered with water), obtained by laboratory methods, amount to: $f_{st} = 0.19$; $f_{din} = 0.10$.

Thus, in the use of wooden models covered with ordinary paint for tests in model ice of natural composition, the modeling conditions are not observed (no identity of friction factors of the model and natural ice). In the future it will be necessary to create special friction coatings for models.

BIBLIOGRAPHY

1. Budnevich, S. S., and Deryagin, B. V., "On the sliding of solid bodies along ice," ZhTF (Journal of theoretical physics), Volume XXII, No. 12, 1952.

2. Veynberg, V. B., Led (Ice), Moscow, Gostekhizdat, 1940.

3. Grigor'yeva, S. R., and Tolstoy, D. M., "On the resonant drop of the force of friction," Dokl. AN SSSR (Bulletin of the USSR Academy of Science), volume 167, No. 3, 1960.

4. Deryagin, B. V., Chto takoye treniye? (What is friction?), Moscow, Izd-vo AN SSSR, 1963.

5. Kragel'skiy, I. V., Treniye i iznos (Friction and wear), Moscow, "Mashinostroyeniye", 1968.

6. Kuznetsov, V. D., Fizika tverdogo tela (Solid physics), volume 1, Gostekhizdat, 1937.

7. Lavrov, V. V., Deformatsiya i prochnost' l'da (Deformation and strength of ice), Leningrad, Gidrometeoizdat, 1969.

8. Nogid, L. M., "Modelling the motion of a ship in a solid ice field and in broken ice," Tr. LKI (Transactions of Leningrad Shipbuilding Institute), No. XXVIII, 1959.

9. Ryvlin, A. Ya., and Petrov, Ye. Yu., "On the problem of the experimental determination of the friction factors of ice in natural conditions," in the collection: Problemy Arktiki i Antarktiki (Problems of the Arctic and Antarctic), volume 21, Leningrad, Gidrometeoizdat, 1965.

IMPROVEMENT OF THE METHOD OF PREPARATION OF MODEL ICE

I. I. Poznyak pages 200-209

In the ice basin of the Arctic and Antarctic Scientific Research Institute, as a model of the ice cover, polycrystalline weakened ice of natural composition is used. The decrease in the strength of the ice is accomplished by the introduction of impurities into its crystalline lattice and by the creation of considerable intercrystal layers. In practice, this is achieved by means of dissolving common salt NaCl in the water from which the ice is frozen.

The homogeneity of the ice and its polycrystalline structure is caused by the introduction of a large quantity of fine particles of ice, which are the centers of crystallization, into the upper super cooled layer of water. Therefore, the growth of the ice at all points of the ice cover begins almost simultaneously. The crystallization nuclei are formed in the spraying of water over the basin at an air temperature of (-10)--(-12°). The water temperature in the basin is brought to the crystallization temperature, depending upon the quantity of dissolved salt.

Such a method of preparation of the ice cover in the ice basin, making it possible to grow ice with given strength characteristics many times, satisfies the following ratios of the theory of the modelling of the motion of a ship in the ice:

$$\frac{h_н}{h_м} = \frac{(\sigma_р)_н}{(\sigma_р)_м} = \frac{E_н}{E_м} = \lambda,$$

$$f_н = f_м; \quad \nu_н = \nu_м; \quad \rho_н = \rho_м,$$

where h is the thickness of the ice cover [$h_н = h_n = h_{natural}$; $h_м = h_m = h_{model}$]; σ_r is the ultimate bending strength of the ice [$\sigma_р = \sigma_r$]; E is the modulus of elasticity of the ice; f is the friction factor; ν is the Poisson ratio; ρ is the density of the ice; and λ is the modulus of similarity.

The subscript "n" signifies natural ice, and "m" the model.

The theory of the modelling of the motion of a ship in ice and the method of preparation of the model of the ice cover are explained in detail in reference [1]. In certain cases, for observation of modelling conditions it is necessary to prepare an ice cover of relatively small strength. The maintenance of the constancy of the strength characteristics of such ice (from experiment to experiment) requires great practice on the part of the experimenter.

Considerably weakened ice has a comparatively high plasticity, which may cause excess bendings of the ice plate in failure and a certain disruption of the similarity of the geometry of the breaking of ice by the model in comparison with natural ice. In order to test models of supericebreakers in the ice basin of the AANII, ice of considerable thickness and with a great weakening of the strength characteristics is necessary. The methodology of the preparation of the model of the ice cover indicated in this case must be improved.

This article is devoted to the development of a practical method for the preparation of model ice with low strength characteristics, low plasticity, and increased elastic properties.

We will consider the features of the crystalline structure of laboratory ice and its strength properties. Model ice is heterogeneous in thickness: the stronger, upper part has a smooth surface, and the less strong, lower part a rough surface with a characteristic figure. This is caused by its crystalline structure and by the effect of the temperature gradient. V. V. Lavrov [2] considers that such a heterogeneity may be explained by the pecularity of the growth of ice in a solution of NaCl. In growing ice to a given thickness, the upper layers succeed to a considerable degree to free themselves both of the ions of Na^+ and Cl^- and also upon other foreign impurities, which as the ice grows are displaced to the lower boundary. Each elementary layer of the ice cover passes through such a stage of formation. As a result, the ice crystals in the lower layers have a lesser strength bond than in the upper layers, since they are separated from each other to a greater degree by the intercrystalline layers, containing brine as well as the foreign impurities.

In order to determine the ultimate bending strength σ_r of the model ice, in the ice basin specimens cut through the entire thickness of the ice field were tested as a beam on two supports, with the application of a failure force in the center of the span. As a consequence of the heterogeneity of the ice in thickness the magnitude of σ_r depends upon the direction of the effect of the breaking force. If in the bending of the specimen a stretching of the upper layers occurs, the temporary resistance to bending (we will designate it as $\sigma^{в}_r$ [$\sigma^{в}_r = \sigma^{в}_r = \sigma^{upper}_r$]) turns out to be greater than in a case when a stretching of the lower fibers, $\sigma^{н}_r$ [$\sigma^{н}_r = \sigma^{н}_r = \sigma^{upper}_r$] occurs.

In the entire range of values of σ_r (in the ice basin tests of models of various scales were conducted) the ratio $K = (\sigma^v_r / \sigma^n_r) = 2$. The quantity K can be called the homogeneity factor of the ice. The minimum values of the ultimate bending strength of the ice, which have been obtained up to the present time, at an ice thickness of 25--30 millimeters, amounted to : σ^v_r = = 0.34 kilograms per square centimeter, σ^n_r = 0.16 kilograms per square centimeter.

For polycrystalline ice, frozen from fresh water with the introduction of crystallization nuclei, the ice homogeneity factor K is close to one. In ice frozen from salt water, when the air temperature in the process of its growth was reduced from -10 to -15°, the coefficient K increased to 1.2--1.3. These experiments demonstrated that the strength heterogeneity of the model ice is determined to a considerable degree by the irregularity of the distribution of the foreign impurities and brine throughout its thickness.

For estimation of the elastic and plastic properties of model ice of various strengths, tests were made of specimens of ice for bending, with a load reaching 90% of σ_r, and with subsequent relief of the load. In this case, the buckling f of the specimen and the magnitude of the residual buckling Δf was determined, and according to them the work expended on the deformation of ice in elastic and elastic-plastic bending was estimated. It was established that the plastic properties of ice increase with an increase in the salinity of the water from which it is frozen. Ice prepared from water of high salinity should be considered as an elastic-plastic material.

Thus, according to the existing methodology, the ultimate bending strength of the model ice is determined by the salinity and temperature of the water from which it is frozen, by the air temperature at which it is formed and increases by the uniformity, by the quantity, and also by the dimensions of the crystallization nuclei introduced into the supercooled surface of the water. According to data from experiments, the dependence of the ultimate bending strength of such ice upon the salinity of the water from which it is frozen[1], has the form $\sigma_r = f(S)$, see Figure 1.

In the motion of a ship in a solid ice cover, the breaking of the ice is basically caused by the effect of the tensile stresses originating in its bending. Therefore, in Figure 1 the curves of $\sigma^v_r = f(s)$ are given for all the values of the ultimate strength of the ice, when the breaking force is applied from above downward. The ultimate strength of the ice also depends upon the thickness of the ice plate if it is frozen from water of constant salinity, i.e., $\sigma_r = f(h)$ at S = const. It is natural to assume that further weakening of the ice may be

1. The ice was frozen at an air temperature of (-10) -- (-12°).

achieved with an increase in the salinity of the water, and also with a decrease in the air temperature, since it determines the rate of growth of the ice and the quantity of impurities and brine in its intercrystalline space. However, weakening of the strength of the ice with an increase in the salinity of the water will, apparently, be of little effectiveness (see Figure 1). In the zone of high salinities (S = 25--30 0/00) a large increase in salinity corresponds to an insignificant decrease in the strength of the ice.

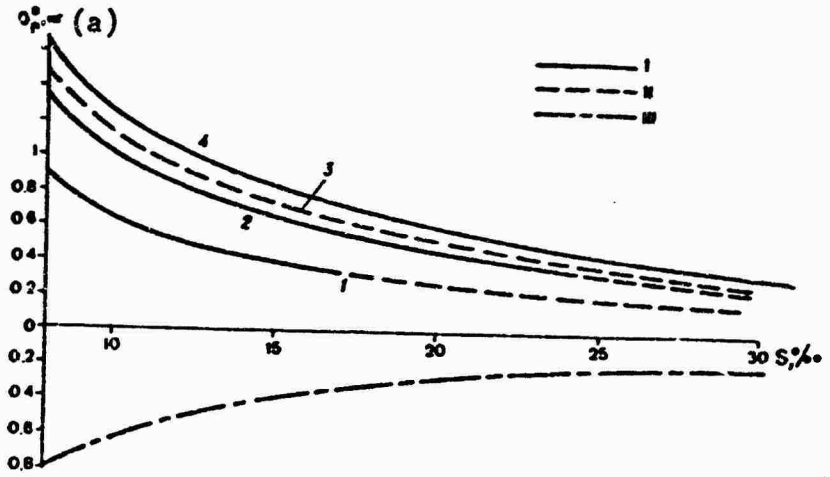

Figure 1. Dependence of σ^{v}_{r} upon the salinity of the water with an ice thickness of 10 millimeters (1), 15 millimeters (2), 20--22 millimeters (3) and 25--30 millimeters (4). I) according to experimental data; II) according to extrapolation data; III) presumed curve (in spraying of the surface of the ice with a NaCl solution, ice thickness 25--30 millimeters). a) σ^{v}_{r}, kilograms.

As we have already noted, it is very difficult to prepare ice from water with a salinity of 25--30 0/00 with constant strength and structural characteristics, in spite of the fact that all the initial data of the freezing regime of the ice are identical and are entirely observed. If we grow ice directly after the solution of salt in the water (~30 0/00), then for a long time it is not possible to introduce crystallization nuclei uniformly into the entire surface of the water. In individual sections, a concentration of crystallization nuclei is observed: the thin film of the ice cover that has formed is placed in motion, in places its exfoliation occurs, and in certain cases ice caps are formed. In time the intensity of this phenomenon decreases.

The ice grows in two layers (ratio of layers 1/3) with a clearly expressed discontinuity. The strength bond between the crystals in the lower layer is inadequate, and with even a small force they are easily separated from each other and from the interface (discontinuity). The upper layer is monolithic,

considerably stronger than the lower layer, and consists of fine crystallites. Such ice cannot be used for testing model ships, since the dimensions of the crystals on its lower surface are 2--2.5 times greater than in single-layer ice, which is usually prepared in the ice basin for an experiment. In time the dimensions of these crystals decrease and the interface between the layers disappears.

The causes of such phenomena are still little studied, but we may assume that in this case the following play an essential role: the "aging" of the NaCl brine, disruption of the thermodynamic regime, the presence of electrical fields at the ice--water interface, the rate of the diffusion processes in the NaCl brine that is heterogeneous in density.

As experiments demonstrate, only after thirty-five--forty days do we succeed in freezing an ice cover that is a recurrence of a previous ice cover with respect to strength and structural characteristics. In the growing of ice from water of high salinity, even insignificant deviations from the given temperature regimes of the water and air, and also the process of the introduction of crystallization nuclei, are felt on its quality.

An increase in the rate of growth of ice with a decrease in the air temperature leads to an increase in the intercrystalline space of the foreign impurities and the brine, which decreases the strength of the ice cover. This method of reducing the strength of the ice was proposed by us earlier and was used in the development of a methodology for the preparation of a model of an ice cover. In practice, in conditions of an ice basin we may decrease the air temperature to -18°. The ice frozen at such a temperature from water with a salinity of 30 0/00 (thickness 30 millimeters) is 23% weaker than ice prepared at a temperature of -12°, and in this case the heterogeneity factor increases from 2 to 2.3--2.4.

The decrease in the strength of the ice due to an increase in the salinity of the water and decrease in the air temperature leads to the fact that its elastic properties decrease, and the plasticity increases.

In the derivation of criteria of similarity determining the motion of the ship in solid ice, the assumption was made that the deformation of the ice is subordinate to Hooke's law up to the moment of failure. The ice cover of seas and inland water areas has both elastic and plastic properties. Therefore, it is more correct to consider it as elastic-plastic material. What additional relationships must be observed in the modelling of ice in this case?

It is known that the equations of dynamic equilibrium of a deformed body have the following form (Cauchy equations):

$$\left.\begin{aligned}
\frac{\partial \sigma_x}{\partial x}+\frac{\partial \tau_{xy}}{\partial y}+\frac{\partial \tau_{xz}}{\partial z}-\rho\frac{\partial^2 u_x}{\partial t^2}&=X,\\
\frac{\partial \tau_{yx}}{\partial x}+\frac{\partial \sigma_y}{\partial y}+\frac{\partial \tau_{yz}}{\partial z}-\rho\frac{\partial^2 u_y}{\partial t^2}&=Y,\\
\frac{\partial \tau_{zx}}{\partial x}+\frac{\partial \tau_{zy}}{\partial y}+\frac{\partial \sigma_z}{\partial z}-\rho\frac{\partial^2 u_z}{\partial t^2}&=Z,
\end{aligned}\right\} \qquad (1)$$

where σ, τ are stresses; u is the displacement vector; X, Y, Z are the components of the mass (volumetric) forces; and ρ is the density of the material.

Individual terms of system of equations (1) may be written in the following manner:

$$\frac{K}{L^3},\ \frac{\rho L}{t^2}.$$

where K has the dimensionality of the force.

As a criterion of similarity, here the ratio of the first complex to the second one is assumed [3]

$$\frac{Kt^2}{\rho L^4}=\frac{K}{\rho v^2 L^2}=\text{const.} \qquad (2)$$

Equations (1) describe the state of a deformed solid medium, and in their derivation no assumptions concerning the elasticity of deformation were made. Thus, the criterion of similarity (2) will refer both to elastic and to elastic-plastic bodies in a dynamic loading regime.

In a case of elastic deformations, it is necessary to satisfy two more criteria of similarity, which are obtained by working from Hooke's law. In a general form for a isotropic elastic body this law, expressing the connection between the stresses and deformations (strain), is written thus:

$$\left.\begin{aligned}
\sigma_x&=\frac{E}{2(1+\nu)}\left[u_{xx}+\frac{\nu}{1-2\nu}\theta\right],\\
\sigma_y&=\frac{E}{2(1+\nu)}\left[u_{yy}+\frac{\nu}{1-2\nu}\theta\right],\\
\sigma_z&=\frac{E}{2(1+\nu)}\left[u_{zz}+\frac{\nu}{1-2\nu}\theta\right],\\
\tau_{xy}&=\frac{E}{2(1+\nu)}u_{xy};\quad \tau_{yz}=\frac{E}{2(1+\nu)}u_{yz};\\
\tau_{xz}&=\frac{E}{2(1+\nu)}u_{xz},
\end{aligned}\right\} \qquad (3)$$

where E is the modulus of elasticity of the material; ν is Poisson's ratio; u_{ij} are deformation components;

$$\theta = u_{xx} + u_{yy} + u_{zz}.$$

As criteria of similarity here we may define two dimensionless quantities ν and (k/EL^2).

The criterion of similarity

$$\frac{K}{EL^2} = \text{const} \tag{4}$$

refers to small deformations of an elastic body.

In expressions (2) and (4) we obtain the ratio

$$\frac{\rho v^2}{E} = Ch = \text{const},$$

called the Cauchy number (criterion) of similarity.

The Cauchy criterion from the physical standpoint determines the constancy of the ratio of the external forces of a dynamic nature to the restoring forces of elasticity at the corresponding points of the model and in full scale. In modelling of the dynamic effect of the elastic forces as criteria of similarity we should assume the following dimensionless ratios:

$$\nu,\ Ch = \frac{\rho v^2}{E} \text{ и } \frac{K}{EL^2}. \tag{5}$$

In the ice basin as the model of the ice a polycrystalline weakened ice of natural composition is used, and therefore the Poisson ratios for the models and the full-scale ice may be considered as practically identical and the first of criteria (5) is satisfied.

In order for the forces of elasticity at the corresponding points of the model and the full-scale ice be referred to each other as λ^3 (the modelling of the motion of the ship in ice is accomplished according to criteria of gravitational similarity) should satisfy the ratio $(E_n/E_m) = \lambda$, which is derived from the third criterion of (5),

$$\frac{K_н}{E_н L_н^2} = \frac{K_м}{E_м L_м^2},\ \frac{E_н}{E_м} = \lambda. \tag{6}$$

Considering conditions (6), the Cauchy modelling criterion will be automatically satisfied if the ratio of the speeds of the full-scale vessel and the model satisfy the condition of gravitational similarity $(v_n/v_m) = \sqrt{\lambda}$.

Consequently if the Poisson ratios γ and the density ρ of the full-scale and model ice are equal, and the moduli of elasticity refer as a modulus of similarity λ , then the combined modelling of forces of a weight nature, forces of inertia, and forces of elasticity according to criteria of gravitational similarity is possible.

As follows from contemporary investigations [4], the elastic-plastic behavior of ice in comparatively slow loading is described by a model of a viscous-elastic Maxwell body. The equation connecting the stresses with the strains in this body may be written in the following form:

$$\left(\frac{1}{\tau_M} + \frac{\partial}{\partial t}\right)\sigma_{ik} = K\left(\frac{1}{\tau_M} + \frac{\partial}{\partial t}\right)u_{ll}\delta_{ik} + 2G\frac{\partial}{\partial t}\left(\dot{u}_{ik} - \frac{1}{3}u_{ll}\delta_{ik}\right). \tag{7}$$

where τ_m is the Maxwellian relaxation time of the stresses

$$\tau_M = \frac{\eta_M}{G}; \tag{8}$$

η_m is the coefficient of internal friction (viscosity); G is the modulus of shear, and K is the coefficient of volumetric compression,

$$G = \frac{E}{2(1+\nu)}; \quad K = \frac{E}{3(1-2\nu)}. \tag{9}$$

Equation (7) corresponds to small relative rates of deformation, u_{ik}. In rapidly changing dynamic loads, which occurs in the effect of the hull of the model or an icebreaker on an ice cover, we should use a Vogt model for an elastic-plastic behavior of ice

$$\sigma_{ik} = Ku_{ll}\delta_{ik} + 2G\left(1 + \tau_\Phi\frac{\partial}{\partial t}\right)\left(u_{ik} - \frac{1}{3}u_{ll}\delta_{ik}\right), \tag{10}$$

where $\tau_\Phi = (\eta\Phi/G)$ is the deformation relaxation time; $\eta\Phi$ is the coefficient of viscosity in shear.

From equations (7) and (10) as criteria of similarity we should assume three dimensionless ratios

$$\nu;\ \frac{K}{EL^3};\ \frac{\tau_M}{t}\ \text{or}\ \frac{\tau_\Phi}{t}.$$

Thus, for modelling the elastic-plastic behavior of ice observation of four criteria of similarity is required:

$$\nu;\ \frac{K}{EL^3};\ \frac{\rho v^2}{E};\ \frac{\tau_M}{t}\left(\frac{\tau_\Phi}{t}\right). \tag{11}$$

Three criteria from expression (11) are the same as for the elastic behavior of ice; the latter considers its classic properties.

Then

$$\frac{(\tau_M)_н}{(\tau_M)_м} = \frac{t_н}{t_м} = \frac{v_н}{v_м} = \sqrt{\lambda}, \tag{12}$$

i.e., the ratio of the relaxation time of model ice according to the Vogt and Maxwell laws, must equal the ratio of the velocities of the model and the full-scale body.

By considering equations (8) and (9), we obtain ν = const

$$\frac{(\eta_M)_н}{(\eta_M)_м} = \frac{(\eta_\Phi)_н}{(\eta_\Phi)_м} = \frac{t_н E_н}{t_м E_м} = \lambda^{3/2}. \tag{13}$$

Consequently, if the Poisson ratios for the model and full-scale ice are identical, the moduli of elasticity refer as λ, and the viscosity coefficients (coefficients of internal friction) as $\lambda^{3/2}$, then the combined modelling of mass forces, forces of inertia, forces of elasticity and plastic properties of ice according to criteria of gravitational similarity is possible.

From the theoretical standpoint, modelling of plastic properties of ice is possible. However, the plastic properties of full-scale and laboratory ice are still inadequately studied and no methodology has been developed for the preparation of fields of ice making it possible to satisfy the ratio (13) in laboratory conditions.

The weakening of the strength of the ice due to a further increase in the salinity of the water from which it is frozen, and also due to a decrease in the air temperature, is of little effect. Indicentally, in this case the operating conditions of the experimenters and the apparatus deteriorates.

It is well known that one of the methods of expediting the melting of the ice is its reaction with various layers. This has led to the thought of creating an effect on the surface of an already formed ice cover with a concentrated solution of the same salt, NaCl, which is added to the water for weakening it.

The experiments performed confirmed the possibility of practically eliminating the strength heterogeneity of an ice cover throughout its thickness and thus decreasing the ultimate strength σ^{v}_{r} of the ice. Thus, in the effect of a solution on the surface of ice with a thickness of 27 millimeters, prepared from water with a salinity of 27 0/00, in 18 minutes σ^{v}_{r} decreased by a factor of $\sim$2.

In the given case the weakening of the ice occurred due to the decrease in the strength bond between the crystals. In the application of a solution of NaCl salt on the surface of the ice cover, the melting of the crystallites of ice began, and then the brine penetrated into the capillaries and the intercrystalline spaces, the dimensions of which increased as a consequence of the fusion of their walls.

Thus, the addition to the methodology of the preparation of model ice makes it possible to: 1) obtain ice of low strength (in practice its strength may be decreased by approximately a factor of 2), see curves III and 4 in Figure 1; 2) obtain a given strength of the ice from water that has only half the salinity, which increases the elastic properties and decreases the plastic properties of the ice; 3) to decrease the anisotropy of the ice throughout its thickness to a considerable degree, which, apparently, will decrease the excess buckling of the ice in its failure; such ice will correspond to a greater degree to the modelling conditions, since in the derivation of criteria of similarity it is assumed that the ice cover is isotropic throughout its thickness.

An analogous effect was obtained by B. V. Lavrov, when he irradiated the surface of a plate of ice by the light from an electric lamp of 500 watts capacity at a distance of 4 centimeters. The thermal energy, absorbed mainly in the intercrystalline layers, weakened the bonds between the crystals and decreased the strength of the ice from σ^{v}_{r} 1.0 to σ^{v}_{r} 0.5 kilograms per square centimeter. But this method could not find practical application in the ice basin because of the large area of the water mirror (26 square meters), and besides the strength of the upper layer of ice again increases after a short interval of time, as soon as irradiation ceases.

The process of spraying the surface of the ice with a concentrated brine of NaCl is easily accomplished. For this the same sprayer is used by means of which the crystallization nuclei are introduced, but instead of water its tank is filled with a solution of NaCl of the same or a different concentration (Table 1).

Table 1

Concentrations of Solutions of NaCl for Spraying the Surface of the Ice

(1) Удельный вес при +15° С	(2) Содержание соли		Температура замерзания (°С)
	(3) в растворе	(4) на 100 частей воды	(5)
1,16	21,2	26,9	—18,2
1,17	22,4	29,0	—20,2
1,175	23,1	30,1	—21,2

Key: 1) density at +15° Centigrade; 2) salt content; 3) in solution; 4) per hundred parts of water; 5) freezing temperature (°C).

In conclusion we may note that the proposed improvement in the method of preparing laboratory ice increases the quality of laboratory experiments with respect to the modelling of the motion of a ship in a solid ice cover to a considerable degree.

BIBLIOGRAPHY

1. Kashtelyan, V. I., Poznyak, I. I., and Ryvlin, A. Ya., Soprotivleniye l'da dvizheniyu sudna (Resistance of ice to the motion of a ship), Leningrad, "Sudostroyeniye", 1968.

2. Lavrov, V. V., Deformatsiya i prochnost' l'da (Deformation and strength of ice), Leningrad, Gidrometeoizdat, 1969.

3. Nogid, L. M., "Modelling the motion of a ship in solid and broken ice," Tr. LKI (Transactions of the Leningrad Shipbuilding Institute), No. XXVIII, 1959.

4. Kheysin, D. Ye., "On the problem of elastic-plastic bending of an ice cover," Tr. AANII (Transactions of the Arctic and Antarctic Scientific Research Institute), volume 267, Leningrad, Gidrometeoizdat, 1964.

A REMOTE SENSOR FOR MEASURING THE SPEED OF SHIP MODELS IN ICE

V. I. Lobos and V. N. Lipatov pages 210-214

In the process of model tests of ships in an experimental ice station, it is necessary to measure the speed of the model. Usually the speed of translational motion may be determined by differentiating the measured track or integrating the acceleration of this motion. Quite simple methods of differentiation of the track exists, by means of various types of converters of physical quantities into electrical signals: induction, capacitants, photoelectronics, and other devices [1, 2].

The speed v is converted by these devices into the corresponding magnitudes of current $I = \varphi_1(v)$, voltage $u = \varphi_2(v)$ or frequency $f = \varphi_3(v)$ of an electrical signal. In the given case, the features of the design of the towing device of the experimental ice basin made it possible to apply a photoelectronic converter, which converted the angular velocity of rotation of a special disc installed on the axis of the drive wheel of the towing device into a discrete electrical signal with a sequence frequency depending linearly upon the speed. The sequence frequency of the pulses is associated with the speed of the model in the basin by the dependence

$$f = K_1 K_2 v,$$

where f is the sequence frequency of the electrical signals; v is the velocity of the translational motion of the model; K_1 is the conversion factor of the linear velocity into angular velocity; K_2 is the conversion factor of the angular velocity into the sequence frequency of the electrical signals.

The application of a linear conversion system simplifies the reading and calibration of the data.

The methodology of the measurement of the speed according to the variation of the frequency of the signal made it possible to reduce the effect of external destabilizing factors (temperature, variation of power supply, humidity, induction, etc.) to the minimum. The speed sensor developed in the AANII has three blocks: 1) a portable pickup (converter) for the velocity; 2) a transistorized frequency meter; 3) an EPP-09 recording instrument.

The measurement and recording of the speed is accomplished in the following manner: the ship model being tested is placed in motion by a special towing device, on the shaft of the drive wheel of which a disc with a geared rim is placed, entering into the composition of the velocity pickup unit.

The velocity pickup (Figure 1) is a contactless optical-electronic photodiode modulator. It consists of a L-1 light source, an optical device shaping a narrow light line, a D-1 photodiode and a transistorized keying circuit T-1. The geared rim of the disc is placed in the path of the light beam between the M-1 optical system and the photodiode. In the rotation of the disc, the gears of the rim periodically interrupt the continuous light flux, as a result of which short light pulses are formed, which, falling on the photodiode, cause the corresponding pulses of current in the circuit of the base of transistor T-1. Electrical pulses are taken from the collector of transistor T-1, and their sequence frequency and duration depend upon the speed of rotation of the discs, and, in the final analysis, upon the speed of the model in the basin. These pulses are fed along a cable to the input of the frequency meter (see Figure 1).

The frequency meter serves for conversion of the periodic sequence of the electrical pulses arriving at its input, to direct voltage (current), the magnitude of which is proportional to the sequence frequency of these pulses. The frequency of the signal is measured by means of a capacitor shaper, transmitting to the indicator a definite quantity of electricity for each period of the frequency being measured. The average value of the current I from the pulses arriving is found according to the formula

$$I = Qf,$$

where f is the frequency being measured; and Q is the quantity of electricity arriving at the indicator from the shaper.

The quantity of electricity in a pulse of the capacitor shaper is equal to the charge Q of the capacitor with capacitance C from the power source with a voltage u, i.e.,

$$Q = Cu.$$

Then the average current of the shaper pulses may be expressed by the equation

$$I = Cuf.$$

The capacitor frequency meters are linear systems and have a uniform scale.

The frequency meter includes the following units: 1) a two-cascade amplifier-limiter; 2) a shaping cascade; 3) a measuring circuit.

The amplifier-limiter creates pulses with quite a high steepness of the front of the signal being amplified, and thus provides for reliability of the operation of the shaping cascade in the low-frequency operating range. Aside from this, the limitation of the input signal excludes the possibility of parasitic amplitude modulation of this signal. The amplifier is assembled from two transistors, T-2 and T-3, according to a conventional circuit with a common emitter.

The square pulses taken from the collector load are differentiated by the T-4, R-13 circuit, limited from above by the D-3 diode, and are fed to the input of the shaping cascade.

The shaping cascade is a single flipflop oscillator with emitter connection, which is assembled from two transistors, T-4 and T-5. In the initial stage the T-4 triode is blocked and the triode T-5 is saturated.

The blocking of the T-4 triode is provided by the voltage of the divider R-14, R-15, which sends a potential that is less (with respect to modulus) than the potential of the emitters to the base of the T-4 triode, and also by the appropriate selection of the magnitude of the resistance in the circuit of the emitters R-18 (of the order of 1--5 kiloohoms). When a starting pulse of negative polarity is fed to the base of T-4, the single flipflop oscillator, under the effect of the internal processes, is reversed and makes the transition to the second state of unstable equilibrium, when T-4 is open and T-5 is closed. The duration of this state depends mainly upon the magnitude of the resistance R-19 and the capacity of the capacitor C-5 under which the devices again returns to the initial stable state. Thus, a pulse of negative polarity is formed at the collector of transistor T-5. This pulse is fed through the buffer cascade T-6 to the measuring circuit of the instrument.

The measuring circuit consists of charge capacitors, an integrating circuit, and the EPP-09 recording instrument.

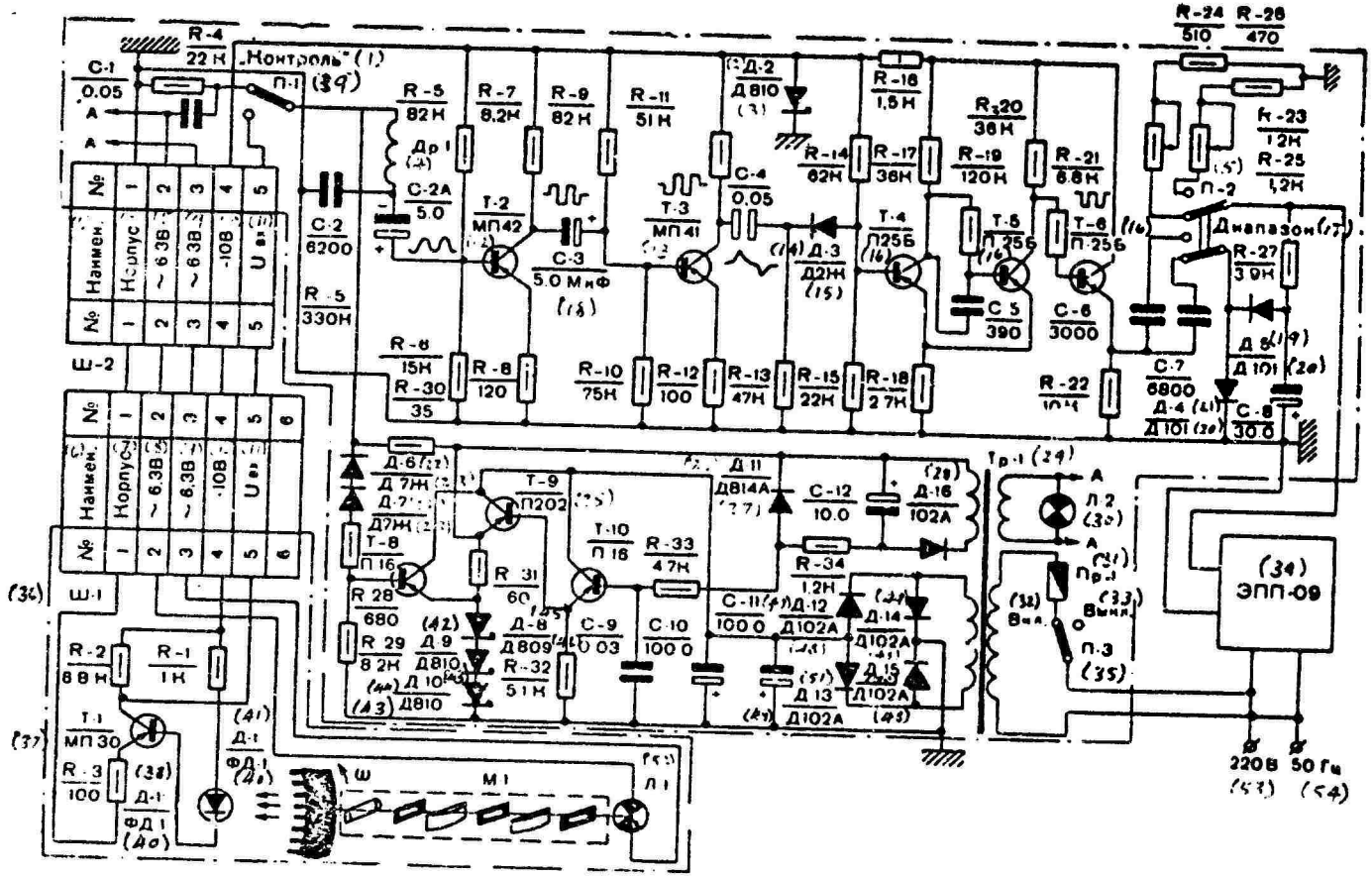

Figure 1. Simplified diagram of the speed-measuring sensor. 1) "Monitor"; 2) D-2; 3) D810; 4) Dr-1; 5) P-2; 6) designation; 7) hull; 8) ~6.3 volts; 9) ~6.3 volts; 10) -10 volts; 11) $U_{ex} = U_{vykh} = U_{input}$; 12) MP42; 13) MP41; 14) D-3; 15) D2Zh; 16) P25B; 17) range; 18) 5.0 microfarads; 19) D-5; 20) D101; 21) D-4; 22) D-6; 23) D7Zh; 24) D-7; 25) P202; 26) D-11; 27) D814A; 28) D-16; 29) Tr-1; 30) L-2; 31) Pr-1; 32) on switch; 33) off switch; 34) EPP-09; 35) P-3; 36) Sh-1; 37) MP30; 38) D-1; 39) P-1; 40) FD-1; 41) D-1; 42) D-9; 43) D810; 44) D-10; 45) D-8; 46) D809; 47) D-12; 48) D102A; 49) A-14; 50) D-15; 51) D-13; 52) L-1; 53) 220 volts; 54) 50 hertz.

At the moment of the arrival of the negative pulse at the measuring circuit, triode T-6 is entirely unblocked and a charging of the capacitor T-6 (C-7) occurs via the input circuit of the EPP-09, the divider of resistances R-24 (R-26), R-23 (R-25), R-27, tne diode D-5, the capacitants C-6 (C-7), the internal resistance of the saturated transistor T-6, and the negative side of the power supply. Upon the completion of the pulse, the triode T-6 is locked and the capacitor C-6 (C-7) is discharged through the diode D-6 and the resistors R-22.

The capacitor C-8 serves for shunting the input circuit of the EPP-09 according to the alternating components of the signal being measured.

By means of variable resistors R-23 and R-25 the calibration of the instrument is performed in each measuring range. The transition from one range to another is accomplished by switching over the tumbler switch T-2.

In the system automatic monitoring of the efficiency of the instrument in the process of its operation is provided. For this, network alternating voltage with a frequency of 50 hertz is fed to the input of the frequency meter via the changeover switch C-1.

The power supply of the frequency meter and the speed pickup is provided from a semiconductor stabilizer of the compensation type with silicon stabilitrons, sources of the reference voltage. A stabilizer of this type is characterized by the fact that the voltage at its output remains practically constant in changes of the input voltage or the load current as a result of the reverse effect of these changes on the regulating element of the device. Such a stabilizer contains measuring, amplifying, and regulating elements. In the circuit the regulating element is assembled from a transistor T-9 of type T-202, and the amplifying elements from transistors T-8, T-10, of type P-16. In the measuring element as a standard voltage source stabilitron D-8--D809, D-9--D810 are used. The calibration of the instrument was performed by the experimental-analytical method, with consideration of the assigned values of the speeds being measured and the known geometrical dimensions of the interrupter disc and the drivewheel of the towing device of the model. The instrument has two ranges of speeds being measured: the first range amounts to 0.04--0.5 meter per second; and the second 0.04--1.0 meter per second.

The calibration curve (Figure 2) is linear in nature.

The total error of measurement of the remote sensor does not exceed ±2%.

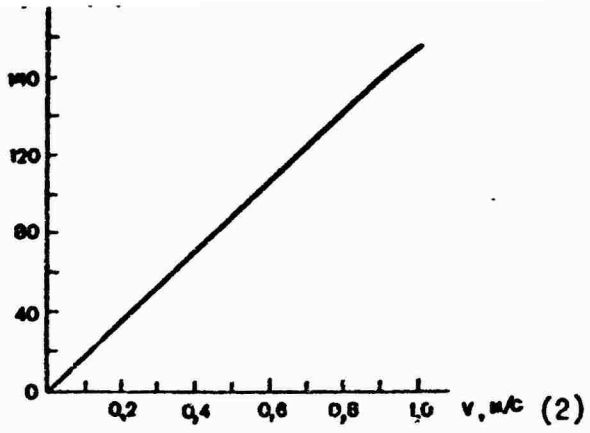

Figure 2. Calibration curve. 1) f, hertz; 2) v, meter per second.

BIBLIOGRAPHY

1. Turchin, A. M., Elektricheskiye izmereniya neelektricheskikh velichih (Electrical measurements of non-electrical quantities), Moscow, "Energiya", 1966.

2. Eksperimental'naya gidromekhanika sudna (Experimental hydromechanics of the ship), Tr. NTO SUDPROMA (Transactions of the Scientific and Engineering Society of the Shipbuilding Industry), No. 56, 1964.

MEASUREMENT OF THE THRUST OF SCREW PROPELLERS BY A TENSOMETER THRUST GAUGE

V. N. Lipatov and V. I. Lobos pages 215-220

For investigation of the basic propulsive characteristics of the propulsion complex of an icebreaker, data concerning the magnitude of the average and momentary thrust of the screw propellers are necessary, both in clear water and in motion in ice. In the AANII an experimental specimen of tensometer thrust gauge has been developed and fabricated, which in 1968--1970 was tested on board powerful icebreakers in the Arctic. The thrust operating principle is based on the measurement of elastic deformations of the casing of the thrust bearing. The installation of the instrument does not require any design changes of the shafting. As the tests demonstrated, the instrument makes it possible to measure the averaged and momentary thrusts with a high degree of accuracy.

The calibration of the instrument was accomplished when moored to a dock by means of the comparison of the readings of the instrument with the thrust characteristics of the screw propellers, and in this case it was assumed that the traction and thrust in this regime are equal.[1] The dependence obtained between the readings of the instrument and the thrust $P = T = f(b)$ turned out to be linear (Figure 1). The experimental points of[2] obtained during the measurement by the instrument have an insignificant scattering relative to the thrust characteristics of the propeller $P = f(n)$, which testifies to the stable operation of the thrust gauge.

1. For the screw propeller of a powerful icebreaker this difference amounts to $\approx 5\%$.

2. The identically designated groups of points refer to one cycle of dock trials.

An oscillogram of the variation of the thrust of the midship screw of the icebreaker in clear water (Figure 2, a) and an oscillogram of the recordings of the momentary thrust P of the starboard side screw in the motion of the icebreaker in the ice (Figure 2, b) graphically illustrate the pulsating nature of the variation of the thrust force. In the oscillogram (Figure 2, b) the simultaneous recording of the averaged thrust P' was performed by means of another system. The magnitudes of the averaged thrust obtained in these recordings practically coincide. In the statistical processing of the data from the recording of the thrust in dock trials, the dependence of the relative magnitude of the pulsations of the thrust, $2\Delta P_1/P_{max}$, (the period of which is commensurable with the period of one revolution of the screw) and the total variation of the thrust, $2\Delta P/P_{max}$, upon the number of revolutions of the screw propeller was obtained.

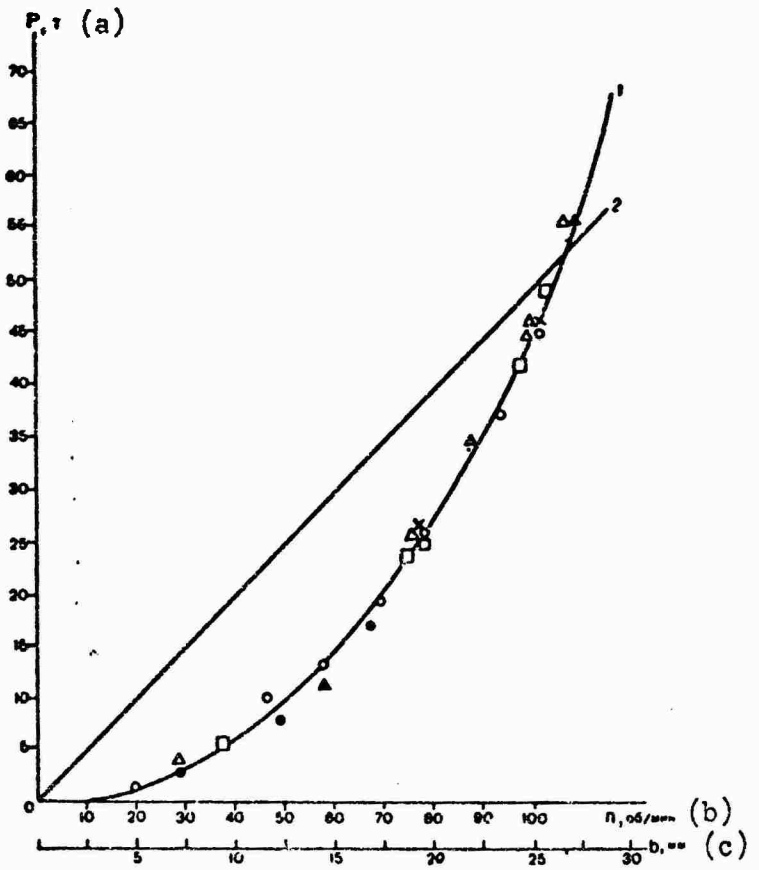

Figure 1. Dependence of the thrust P upon the revolutions n of the screw and the readings b of the instrument at P = f(n) (1) and P = f(b) (2). a) P, tons; b) n, revolutions per minute; c) b, millimeters.

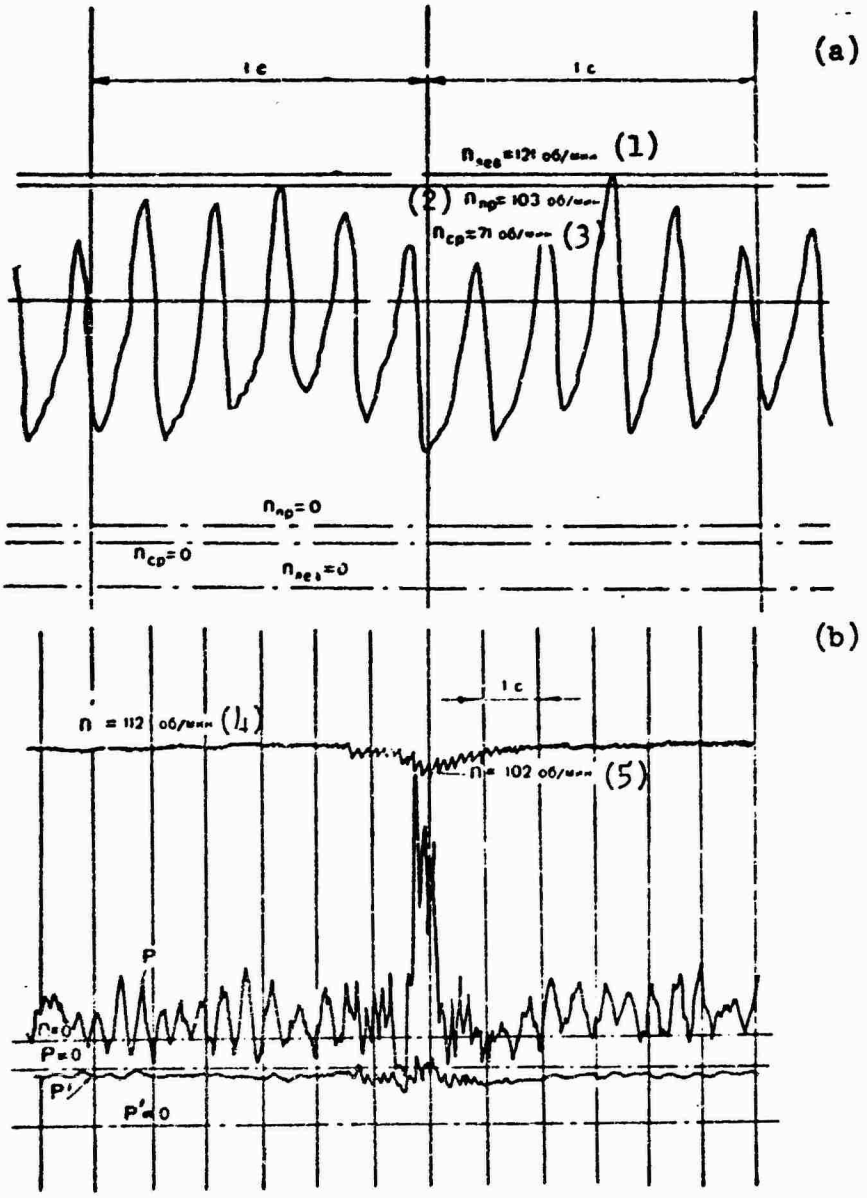

Figure 2. Oscillogram of the variation of the thrust of the center screw of an icebreaker in clear water (a) and in the reaction of the side screw with ice (b). 1) n_{lev} = 121 revolutions per minute [$n_{lev} = n_{port}$]; 2) n_{pr} = 103 revolutions per minute [$n_{pr} = n_{starboard}$]; 3) n_{sr} = 71 revolutions per minute [$n_{cp} = n_{sr} = n_{center}$]; 4) n = 112 revolutions per minute; 5) n = 102 revolutions per minute.

As is apparent from Figure 3, the absolute magnitude of the amplitudes of the thrust pulsation increases with an increase in the number of revolutions and an increase in the value of the center thrust. The divergence of curves 1 and 2 is explained by the damping effect of the oscillatory flow-propeller system, which is manifested more strongly at light loadings of the propeller. As a result of the processing of the oscillograms of full-scale measurements of the thrust in a quasi-steady-state operating regime of the propeller (the ship was moving with a uniform speed in clear water), the differential law of distribution of the thrust variation $\omega(P)$ was established (curve 1, Figure 4). It is characteristic that curve 1 is asymmetrical relative to its most probable experimental value, to which the magnitude of thrust P = 12 tons corresponds. In Figure 4, for comparison, curve 2 [1] of the four-bladed screw of a tanker is given, which with respect to its nature is analogous to curve 1.

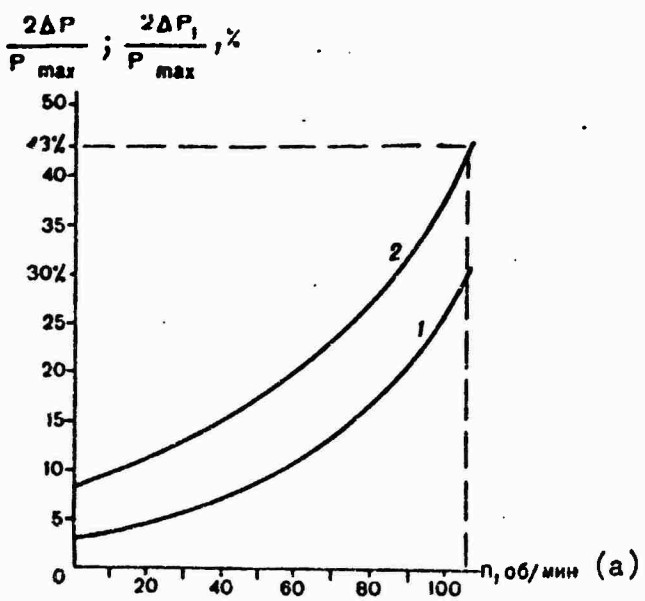

Figure 3. Pulsation (1) and variation of thrust (2) in dock trial. a) n, revolutions per minute.

By means of the experimental dependences $\omega(P)$, $2\Delta P/P_{max}$, and $2\Delta P/P_{max}$, the values of the thrust pulsations are determined in the maximum load of the side screw of an icebreaker. The maximum amplitudes of the pulsation turned out to be 26% higher, and the minimum 16% lower, than the average magnitude of the thrust. Analogous values of the amplitudes of pulsation without consideration of the damping effect of the system (19% and 11%) differ only insignificantly from the nature of the pulsations of the four-bladed screw of a single-screw tanker.

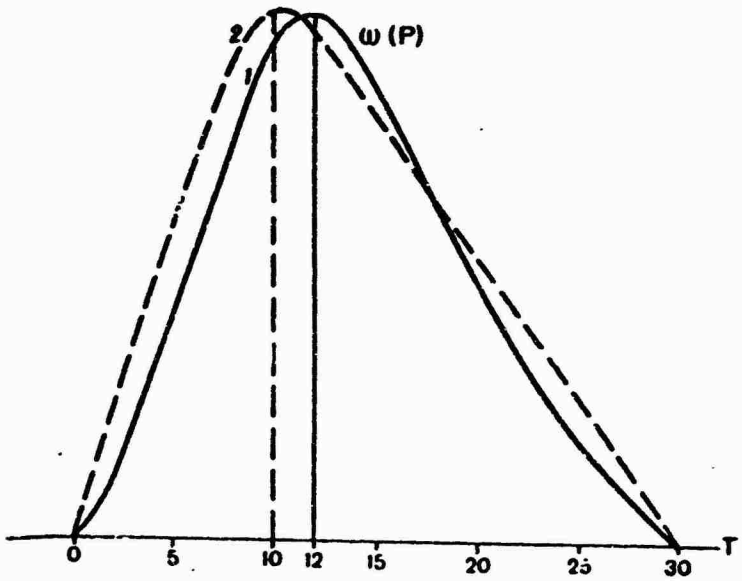

Figure 4. Differential law of distribution of thrust in clear water for the side screw of an icebreaker (1), and for the screw propeller of a tanker (2).

The dependences obtained as a result of the full-scale experiment, and characterizing the variation of the momentary and average thrust in the motion of an icebreaker in the ice, and also in the reaction of the screw with the ice (see Figure 2), agree well with the theoretical prerequisite. Thus, the notation of the momentary thrust in the oscillograms reflect the pulsation of the thrust forces, caused, apparently, by the hydrodynamic imbalance of the screw propeller and the skew of the flow. We may expect that the pulsations caused by the irregularity of the velocity field in the propeller disc, was manifested more noticeably at light loads of the propeller and in shifting of the rudder, and also in transitionsl regimes when the revolutions of the propeller were changed.

The period of variation of the thrust from hydrodynamic imbalance and the skew of the flow in the propeller disc, T_0, which was determined according to the oscillograms, turned out to be somewhat less than a period corresponding to one revolution of the propeller, which, most probably, may be explained by the circular displacement of the flow.

The period of variation in the reaction of the blades with the ice in partial wedging of the screw and in clear water always corresponds to the number of its revolutions. The time in which stabilization of the flow occurs with a change in the revolutions of the screw depends upon the mass of the water placed in motion with a definite speed, and this usually amounts to

several seconds. The pulsation of the thrust caused by the irregularity of the flow (the period $T_0/4$), apparently, integrates with the pulsation caused by the hydrodynamic imbalance and the skew of the flow in the propeller disc. In shifting of the rudder, passage of ice near the screw, and variation of the revolutions, a pulsation component of the thrust is briefly observed, with a period corresponding to the reaction of the blades of the screw with the medium, which probably is explained by the variation of the nature of the field in the propeller disc. The magnitude of this pulsation ($\approx$ 10% of the averaged thrust) is approximately a third of the pulsation, which, in our opinion, is caused by the hydrodynamic imbalance and the skew of the flow in the propeller disc.

The relative magnitude of the total thrust pulsation of the center screw of the icebreaker amounts to $\approx$ 10%. The frequency of pulsation of the thrust of the center screw is basically determined by the irregularity of the flow in the propeller disc, and its period corresponds to the reaction time of the blades with the medium (see Figure 2, a).

In the reaction of the blades with the ice or in partial wedging of the propeller, the magnitude of the momentary thrust may increase several times over (see Figure 2, b,) although the average thrust at first decreases due to the drop in revolutions. Analogous results were obtained during measurements of the thrust and its pulsation aboard American icebreakers of the "Wind" type [2].

Analysis of a large number of oscillograms testifies to the fact that the instrument reacts well to changes in the periodic forces, caused by such factors as the dynamic imbalance of the propeller, the skew and irregularity of the flow, and also by ice floes striking the blade.

Thus, the proposed tensometer thrust gauge may be used for measurement of the average and momentary thrust of screw propellers when ships are navigating in ice, for the determination of the reaction factors of the hull in the study of the vibration of the ships, and also for the solution of other practical and scientific problems.

BIBLIOGRAPHY

1. Katsman, F. M., and Kudrevatyy, G. M., Konstruirovaniye vinto-rulevogo kompleksa morskikh sudov (Designing of the propulsion and steering complex of seagoing vessels), Leningrad, "Sudpromgiz", 1963.
2. Edwards, R. J., "The development of Arctic sea transportation," Marketing and Transportation Situation, Washington, 1970, volume 4, No. 5.

A HIGHLY SENSITIVE AMPLIFIER FOR FULL-SCALE MEASUREMENTS OF THE THRUST OF PROPELLERS

V. I. Lobos and V. N. Lipatov pages 221-224

On the basis of information obtained during full-scale tests of a tensometer thrust gauge assembled from vacuum tubes in 1968-1969 aboard powerful icebreakers, at the Laboratory of Ice Qualities of Ships of the Arctic and Antarctic Institute a highly sensitive semiconductor direct-current amplifier (UPT) with conversion was developed. It is intended for measuring and recording weak signals of direct and pulsating currents, taken from the lattice of a measuring tensometer bridge [1, 2, 3] on the tape of the N370 automatic recording device (of a loop oscillograph).

The amplifier (Figure 1) consists of a modulator for the input signal, an alternating current preamplifier, a power amplifier, a detector and an indicator. The modulation of the direct-current input signal is accomplished by a Vp-1 electromechanical oscillator converter of VPG-62. The oscillator converter operates on a frequency of 400 hertz. The application of a VPG-62 mechanical converter as a modulator made it possible to expand the frequency range of the conversion of the input signals from 0 to 40 hertz, which is of important significance in investigations of the variation of the thrust magnitude during one revolution of the screw. The entire amplifier is assembled from eleven transistors. The alternating-current preamplifier consists of three amplification cascades, assembled according to one and the same circuit from transistors T-1--T-6. To decrease the level of the natural noises the first cascade T-1, T-2 is assembled from P28 and MP39B low-noise transistors. The cascade is permeated by a voltage of -8 volts from the D-1--D808 stabilized diode. The last two amplifying cascades T-3, T-4 and T-5, T-6 are assembled from P106 silicon transistors and are supplied with increased voltage -22 volts, from a stabilized D-2--D816A diode. In these three cascades, to increase the stability of amplification, increase the input and decrease the output resistances, and decrease the non-linear distortions, a multi-loop negative feedback (OOS) is used.

Each cell of the preamplifier is a two-cascade amplifier with indirect connection. The first transistors of cascade T-1 (T-3, T-5) are connected in a circuit with a common emitter (OE), the second transistor T-2 (T-4, T-6) according to a circuit with a common collector (OK). Direct-current OS is introduced from the emitter of transistor T-2 via the resistance R-7 to the base T-1, and thus the correct selection of the working point T-1 is provided, and stabilization of the power-supply regime and the amplification factor of the cascade in a wide range of temperatures is performed. The amplification factor of the cascade K-1 amounts to 30--50. For a more rigid stabilization of the amplifier via resistances R-8, R-22 deep inter-cascade OOS are accomplished. The application of emmitter receivers in each cascade makes it possible to decouple the cascades from each other with a high amplification factor, and the correct selection of the separating capacitors C-1, C-3, C-4 allows to weaken considerably the effect of induction of the fifty-hertz network frequency, and also to decrease the transmission of low-frequency components of the spectrum of the internal noises of the transistors.

From the emitter of transistor T-6 via the capacitor C-5 the signal is fed to the input of the final power amplifier. The circuit contains three cascades: the first cascade is assembled from transistor T-7, a P116, operating in a regime of class A, and the second is a phase-inverter cascade assembled from two transistors, T-8--T116 and T-9--P103 and the third is a power cascade, assembled from transistors T-10, T-11--P601. The latter is assembled according to the circuit of an asymmetrical two-cycle amplifier, having capacitive coupling with the load. The output cascade T-8--T-11 operate in a regime of class AB. The rest current of transistors T-10, T-11 depends upon the bias at the bases of transistors T-8, T-9, which is determined by the resistance of the diode D-3 in the straight direction. For balancing the circuit of these cascades it is necessary that the following equality be fulfilled:

$$\beta_{T\text{-}8}\beta_{T\text{-}10} = \beta_{T\text{-}9}\beta_{T\text{-}11},$$

where β is the amplification factor of the transistor with respect to current.

The final balancing of the output transistors is accomplished by the appropriate selection of the magnitude of resistance R-24. By means of this same resistance OOS with respect to current is realized between the output and the input of the final amplifier. The final amplifier also uses alternating-current OOS, via the capacitor C-9 and the resistors R-23 and R-27. The depth of OOS within small limits is regulated by the variable resistance R-27, which makes it possible to establish the needed measurements scale in the calibration of the instrument. In the amplifier a monitoring regime is pro-

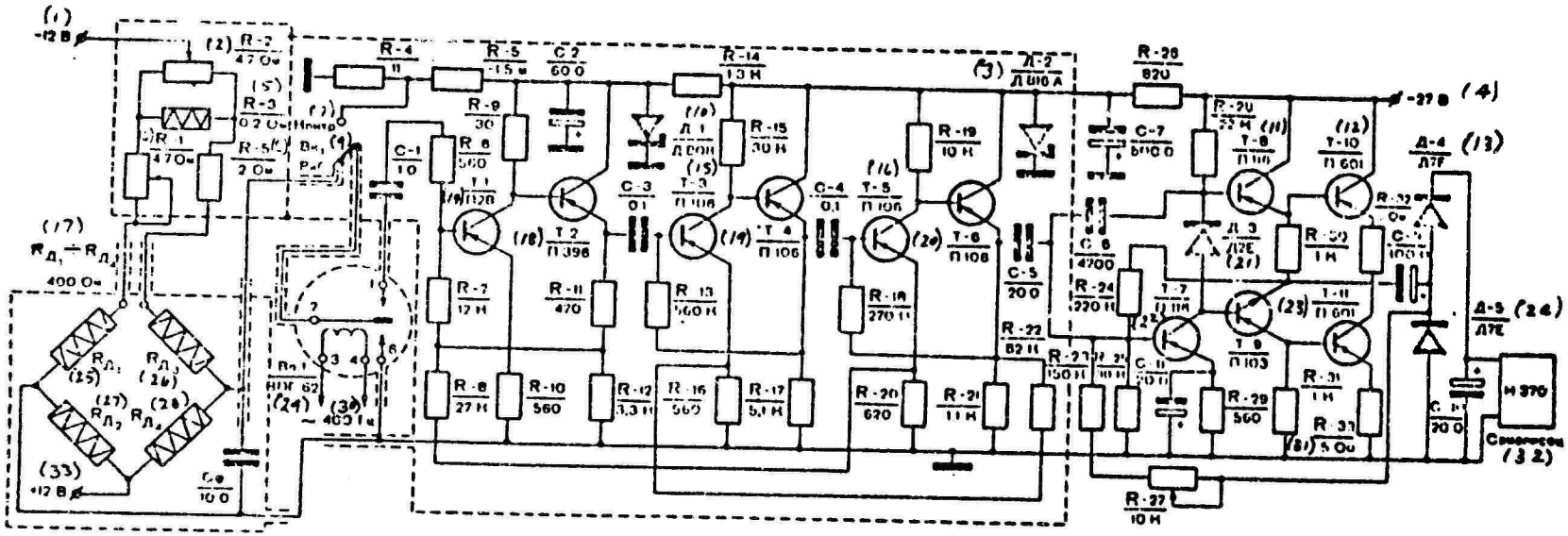

Figure 1. Simplified diagram of the UPG. 1) -12 volts; 2) R-2/47 ohms; 3) D-2/D812A; 4) -27 volts; 5) R-3/0.2 ohm; 6) R-1/4.7 ohms; 7) monitor; 8) R-5/2 ohms; 9) Vk_1, operation; 10) D-1/D808; 11) T-8/P116; 12) T-10/P601; 13) D-4/D7Ye; 14) T-1/P28; 15) T-3/P106; 16) T-5/P106; 17) R_{D_1}--R_{D_4}, 400 ohms; 18) T-2/P396; 19) T-4/P106; 20) T-6/P106; 21) D-3/D2Ye; 22) T-7/P116; 23) T-11/P601; 24) D-5/D7Ye; 25) R_{D_1}; 26) R_{D_3}; 27) R_{D_2}; 28) R_{D_4}; 29) Vp 1/VPG 62; 30) 400 hertz; 31) R-33/5 ohms; 32) N370 automatic recorder; 33) +12 volts.

vided, which is accomplished by the tumbler switch Vk_1. The amplified variable signal with a frequency of 400 hertz is fed via the divider capacitor C-9 to the diode detector D-4, D-5.

The constant component of the signal detected is recorded on the N370 automatic recorder, which was used on a scale of 5 volts. The amplifier is supplied from a stabilized voltage source, -27 volts.

The technical characteristics of the amplifier are as follows:

1. The amplification factor of the instrument, with consideration of OOS, is equal to 2×10^5.
2. The relative instability of the amplification factor does not exceed 0.1% at 10° Centigrade.
3. The effective value of the voltage of the internal noises, reduced to the input with a short-circuited input of the alternating-current amplifier, does not amount to more than 5 microvolts.
4. The level of induction from the BPG-62 electromechanical converter amounts to $\approx 1\%$ of the maximum magnitude of the signal being recorded.
5. The frequency range of the input signal is from 0 to 40 hertz.
6. The maximum output signal of the amplifier is 7 volts.
7. The output resistance of the amplifier is less than 3 ohms.
8. The modulation frequency is 400 hertz.
9. The input resistance of the amplifier is more than 2 kiloohms.
10. The current consumed from the power source does not exceed 50 milliamperes.

The full-scale tests of the instrument were conducted aboard a powerful icebreaker in the summer of 1970. The thrust was measured in the thrust bearing of the starboard side screw. The tensometer pickup R_{D_1}--R_{D_4} (see Figure 1) according to a complete four-arm bridge circuit were made fast to the upper lid of the thrust bearing with BF-2 cement. Each arm of the bridge consisted of two tensometers with a resistance of 200 ohms. All the arms of the bridge were active. The balancing of the bridge was accomplished by two potentiometers, R-1 (roughly) and R-2 (accurately).

The measuring bridge was supplied from an individual stabilized source of 12-volt direct voltage.

As was ascertained in the process of the test, for complete polymerization of BF-2 cement not less than 6--8 days is required. With observation of this condition, a considerable zero drift of the instrument is observed. The calibration of the instrument was accomplished when moored to the dock, with the operation of the propeller when the hull of the icebreaker was wedged

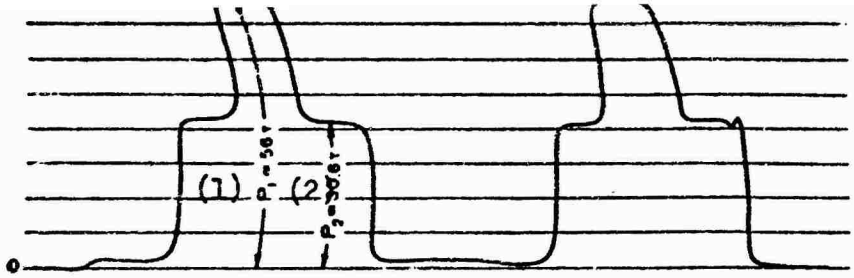

Figure 2. Diagram of the measurements of the average values of the thrust of the screw propeller of a powerful icebreaker when moored to the dock.

in the ice. The results of measurements of the thrust by the given instrument (Figure 2) and the thrust gauge assembled from vacuum tubes practically coincide.

Preliminary full-scale tests demonstrated that the technical characteristics of the semiconductor amplifier make it possible to use it in a tensometer thrust gauge for measurement of the thrust of the screws of icebreakers with an adequate degree of accuracy.

BIBLIOGRAPHY

1. Belen'kiy, B. I., and Mints, M. B., Vysokochuvstivitel'nyye UPT s preobrazovaniyem (Highly sensitive direct-current amplifiers with conversion), Moscow, "Energiya", 1970.

2. Lipatov, V. N., and Lobos, V. I., "Measurement of the thrust of screw propellers by a tensometer thrust gauge," (in this collection).

3. Raschet skhem na tranzistorakh (Calculation of transistorized circuits), translation from the English, Moscow, "Energiya", 1969.

EFFECT OF THE FORM OF THE STATIC CHARACTERISTICS OF A PROPELLER INSTALLATION ON THE MANEUVERING QUALITIES OF AN ICEBREAKER

V. Ya. Yagodkin

pages 225-232

Conditions of navigation in ice impose special requirements upon the equipment of the propulsion plant of icebreakers. The correct selection of the static characteristics of propeller installations increases the operating reliability of icebreakers and icebreaking transport vessels to a considerable degree.

The static characteristics of the propeller installation include in themselves both the characteristics of the variation of the moment of resistance to the rotation of the screw propeller, depending upon its speed at various operating regimes, $M_s = f(n_v)$ [$M_c = M_s = M_{resistance}$; $n_s = n_v = n_{propeller}$], and the mechanical characteristics of the propeller device in the same regimes, $n_g = f(M_g)$. Their intersections determine the points of steady-state (static) operating regimes of the propeller installation.

For transport vessels, the characteristics are usually selected according to the two points corresponding to full power when moored (at dock trials) and when underway in free water. In the selection of the static characteristics of icebreakers, it is necessary to consider the specifics of their operation [2, 3], that is, in the calculation of the moment of resistance of the propeller we should consider the additional moment which must be applied to the screw propeller to break the ice that has gotten under its blades.

In order to estimate the effect of the form of the characteristics of the propeller installation on the maneuvering qualities of an icebreaker, we will consider the reversing regime. The reversing of an icebreaker may be subdivided into the following stages: 1) reversing of the screw propeller; 2) braking of the icebreaker; and 3) acceleration of the icebreaker in the reverse direction (going astern).

At high initial speeds of the icebreaker in free water, the period of the reversing of the screw propeller is brief in comparison with the reversing of the icebreaker. The propeller begins to rotate in the reverse direction and picks up full revolutions going astern in a time during which the translational speed of the ship in the initial direction is decreased only insignificantly (altogether by a few percent). Consequently, the operating regime of the propeller and the entire propeller installation in reversing characteristics lying above those obtained during dock trials (Figure 1) is determined by the stopping time of the icebreakers, which in reversings is usually several tens of times greater than the time of the transitional process in the propeller installation. Therefore, we may consider the operation of the propeller installation in the reversing characteristics as a quasi-static regime.

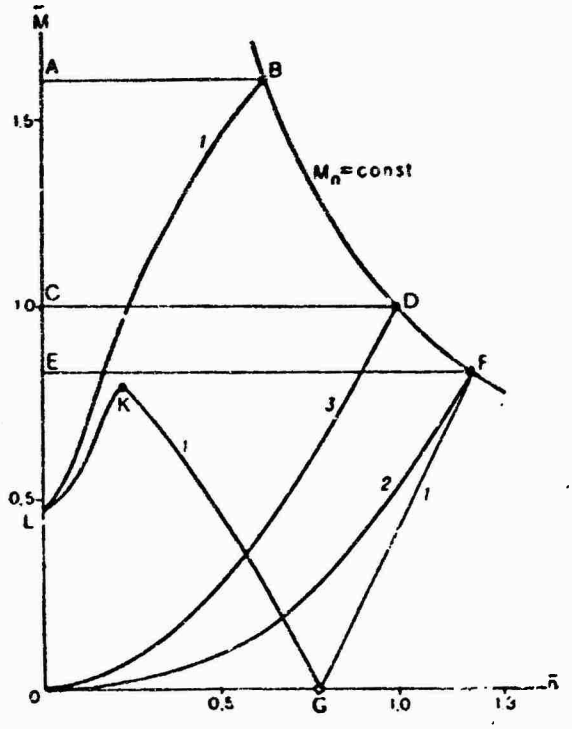

Figure 1. Static characteristics of a propeller installation: 1) reversing characteristics (with constant speed of the icebreaker); 2) characteristics of the steaming of the ship in free water; 3) dock-trial characteristics.

The decrease in the braking and acceleration time is especially important for icebreakers and ships intended for active ice navigation in operation by impacts with short runs.

If we consider that the speed of the icebreaker during the reversing of the screw propeller is constant, which is valid for clear water, the curves of the moments of resistance to the rotation of the screw propeller in reversing (reversing characteristics) will be characterized by considerable negative moments of resistance in the section GKL (see Figure 1) and by increased moments of resistance in comparison with the dock-trial characteristics after the beginning of the operation of the propeller when going astern (section BL). For convenience, the reversing characteristics are usually placed in one quadrant (see Figure 1, curve 1). In reversing an icebreaker, the operating regime of the drive of the screw propeller may correspond to any point of the curve 1.

To decrease the reversing time, it is necessary to achieve complete use of the equipment constituting the drive of the screw propeller in the entire range of the variation of the characteristics of the propeller in the reversing of the icebreaker.

The steady-state operating regime of any propeller installation is determined by the points of intersection of the characteristics of the propeller and the mechanical characteristics of the propeller device (propulsion engine) at a given position of the levers of the control station.

For estimation of the effects of various mechanical characteristics of the propeller installation on the maneuvering qualities of an icebreaker, we will perform a comparative calculation of the reversing of an icebreaker at three initial characteristics (see Figure 1): 1) at a constant moment on the propeller (characteristic EF), which tentatively corresponds to the operation of the diesel directly on the screw propeller; 2) at a constant power on the propeller shaft in the range of the dock-trial characteristics--underway characteristics in free water (curve CDF); 3) at a constant speed on the propeller shaft in the entire working range (curve BDF).

The comparative calculation was performed according to the Lipets-Lebedev method [1] in relative units. This method makes it possible to obtain the dependences $v_s = f(s)$ and $t = \varphi(s)$ if the variation of the accelerating forces from the speed is known.

For an icebreaker this force is equal to

$$T - R_1 = f(v), \tag{1}$$

where v_s is the speed of the icebreaker; s is the track passed over by the icebreaker; t is time; T is traction (thrust); and R_1 is the resistance to the motion of the icebreaker [$R_{\text{л}} = R_1 = R_{\text{icebreaker}}$]. The equation of motion

of an icebreaker with a displacement Δ has the form

$$T - R_a = \frac{\Delta}{g}\frac{dv}{dt}. \tag{2}$$

We will present (2) in the form

$$\frac{T - R_a}{\Delta} g = \frac{dv}{dt} \tag{3}$$

Considering v in units, Δ in tons, and T and R_1 in kilograms, we will write the previous equation in the following manner:

$$\frac{dv_s}{dt} = F\xi, \tag{4}$$

where $F(T-R_1)/1000$ is the relative accelerating force, in kilograms per ton; $\xi = (g3600^2/1852 = 68.7 \times 10^3$ miles per hour^2, is the acceleration in the effect of a force of 1 kilogram on a mass of 1 ton.

The accelerating forces in the operation of the propeller installation (propulsion plant) at various mechanical characteristics is not difficult to find.

It is known that for the screw propeller

$$T = k_1 \rho n^2 D^4, \tag{5}$$

$$M = k_2 \rho n^2 D^5, \tag{6}$$

where ρ is the density of the water; n is the speed of rotation of the propeller; D is the diameter of the propeller; k_1 and k_2 are the thrust coefficient and the moment coefficient, depending upon the relative advance λ_p of the propeller.

From formulas (5) and (6) it follows that

$$T = M \frac{k_1}{k_2}\frac{1}{D}. \tag{7}$$

It is convenient to perform the calculations in relative units, having assumed as the basic quantities the parameters of the propulsion plant, operating with a nominal capacity when moored (in dock trials). The ratio k_1/k_2 for each value of λ_p is found according to the curves of the effect of the propeller, and then we construct the dependence $k_1/k_2 = f(\lambda_p)$. Having substituted the values of k_1/k_2, M and D-1 into formula (7), we construct the dependence of the thrust of the propeller upon the relative advance. Then the thrust T_1; T_2; and T_3 for all three regimes are determined according to the points of intersection of the mechanical characteristics with the characteristics of the propeller.

If we know the speed of the ship

$$v_s = \frac{\lambda_p}{1-w} nD \tag{8}$$

(w is the running flow factor) and the ratio between λ_p and n for the propeller thrusts $T_{1;\ 2;\ 3}$, we find the dependence

$$T = f(v_s).$$

It is convenient to perform the calculations in a tabular form. As a result, we obtain the dependences of the thrust forces T_1; T_2; T_3 upon the speed of the ship (Figure 2). In this same drawing the dependence of the resistance R_1 to the motion of the icebreaker in clear water upon the speed $\overline{v}_s$, expressed in relative units, is given.

The algebraic difference of the ordinates $\overline{T}$ and $\overline{R}_1$, i.e., $\overline{T} - \overline{R}_1 = \overline{F}$ determines the force in braking the icebreaker within limits of speeds $\overline{v}_s = 1.0 \text{--} 0$ and in acceleration of the icebreaker in the reverse direction within limits $\overline{v}_s = 0 \text{--} -1.0$. In finding the relative magnitude $\overline{F}$ we construct a diagram of the reversing of the icebreaker along the track s passed over and according to time t.

The comparison of the time and the track passover in braking and acceleration of the ship with various static characteristics of an electrical propulsion plant demonstrates the advantages of one form or other of mechanical characteristics.

The method of constructing the curve $\overline{v}_s = f(\overline{s})$ is based on the equality of the angles α and β (Figure 3) at the identical speeds, since

$$\operatorname{tg}\alpha = \operatorname{tg}\beta = \frac{dv_s}{dt}\frac{1}{v_s}. \tag{9}$$

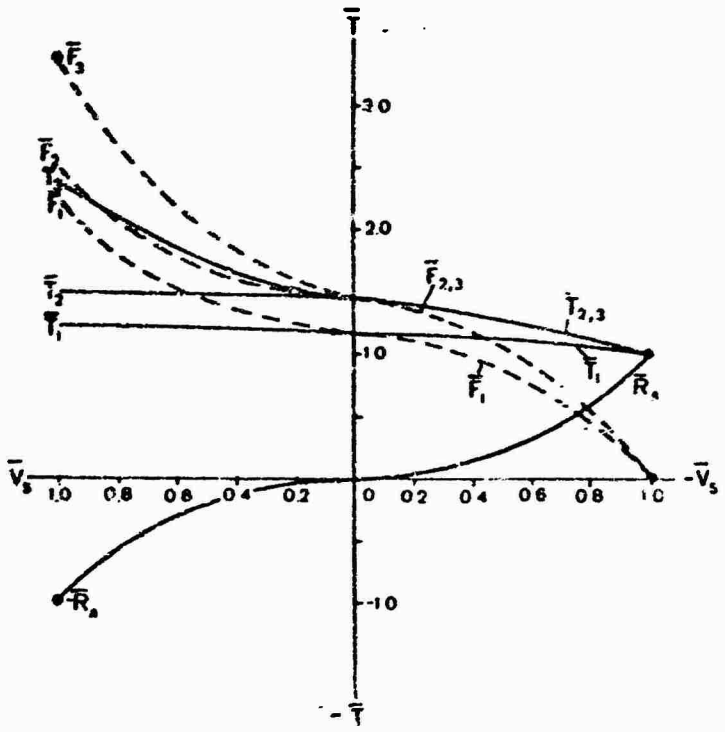

Figure 2. Dependence of the force expended in braking and acceleration of the ship in a reversing regime upon various mechanical characteristics of the propulsion plant.

For the construction of the dependence $\bar{v}_s = f(\bar{s})$, it is necessary to divide the speed interval $\bar{v}_s$ from 0 to 1.0 into an arbitrary number of sections, and the greater the number of sections taken, the more accurate the construction will be. The curve $\bar{F} = f(\bar{v}_s)$ is replaced by a stepped line and within the limits of each section the accelerating force F is a constant quantity, each equal to its average value. The points of the average value $\bar{F}$ (such as, for example, point b, Figure 3) connect the straight lines with the beginning of the coordinate, and in this case the angles will be proportional to the force $\bar{F}$. Further construction of the function $\bar{v}_s = f(\bar{s})$ is clear from Figure 3.

For construction of the dependence $\bar{T} = f(\bar{s})$ we draw beams from point 0' to the points of the average values of the speed $\bar{v}_s$ in the sections accepted. Then, beginning at the point 0' we draw perpendiculars to these beams. The curve $\bar{T} = f(\bar{s})$ will be located between the corresponding sections of the curve $\bar{v}_s = f(\bar{s})$.

For each mechanical characteristic of the propulsion plant, its own reversing diagram is constructed. According to the data obtained from the

diagrams $\bar{v}_s = f(\bar{s})$ and $\bar{v}_s = f(\bar{t})$, we may estimate the reversing time and the track passed over by the icebreaker in braking and acceleration for any initial values of v_s and T, and in reversings from any positions of the levers of the control station.

A comparison of the time and the track passed over in reversing of the propulsion plant, having different static characteristics, makes it possible to estimate the effects of the full power of the propulsion engine on the maneuvering qualities of the ship.

For an example, the reversing of an electrical propulsion plant for a ship intended for active ice navigation of the same type as the diesel-electric vessel "Lena" was calculated for three different mechanical characteristics (see Figure 1). On the basis of the comparative calculations, curves $\bar{v}_s = f(\bar{t})$ and $\bar{v}_s = f(\bar{s})$ in reversing were constructed. The calculation demonstrated that at a constant moment of rotation on the propeller shaft (the characteristic EF, Figure 1), the braking time in clear water increases by approximately 46% and the track passed over by the ship in braking by approximately 47% more than in operation at a constant power on the propeller shaft (the characteristic BDF, Figure 1). The total reversing time in this case increases by approximately 71%.

From a comparison of the time and track in braking, according to the characteristics CDF and BDF (see Figure 1), it is apparent that the use of full power of the primary engine in the entire range of variation of the characteristics of the screw (BDF) decreases the braking time by approximately 24% and the path passed over by the ship in this time by approximately 22%. The total reversing time of the ship in this case decreases by more than 24%.

Consequently, in the designing of propulsion plants of icebreakers and ships for active ice navigation, we should strive to select such characteristics which would make it possible to use the capacity of the mechanical plant entirely in the entire range of variation of the characteristics of the screw propeller. This makes it possible to decrease the time expended on braking and acceleration of the icebreaker.

A decrease in the time required for stopping and starting up again is essentiall important for icebreakers in operation with impact with short runs. In this case the icebreakers must operate in reversing regimes continuously: they must back down along the channel that has been broken and build up speed for the impact against the ice, i.e., each cycle of motion of the icebreaker in these cases is characterized by two accelerations and one braking. A decrease in the braking and acceleration time of the icebreaker will decrease the period between two impacts against the ice accordingly, and, consequently, increase the efficiency of its operation. A reduction in

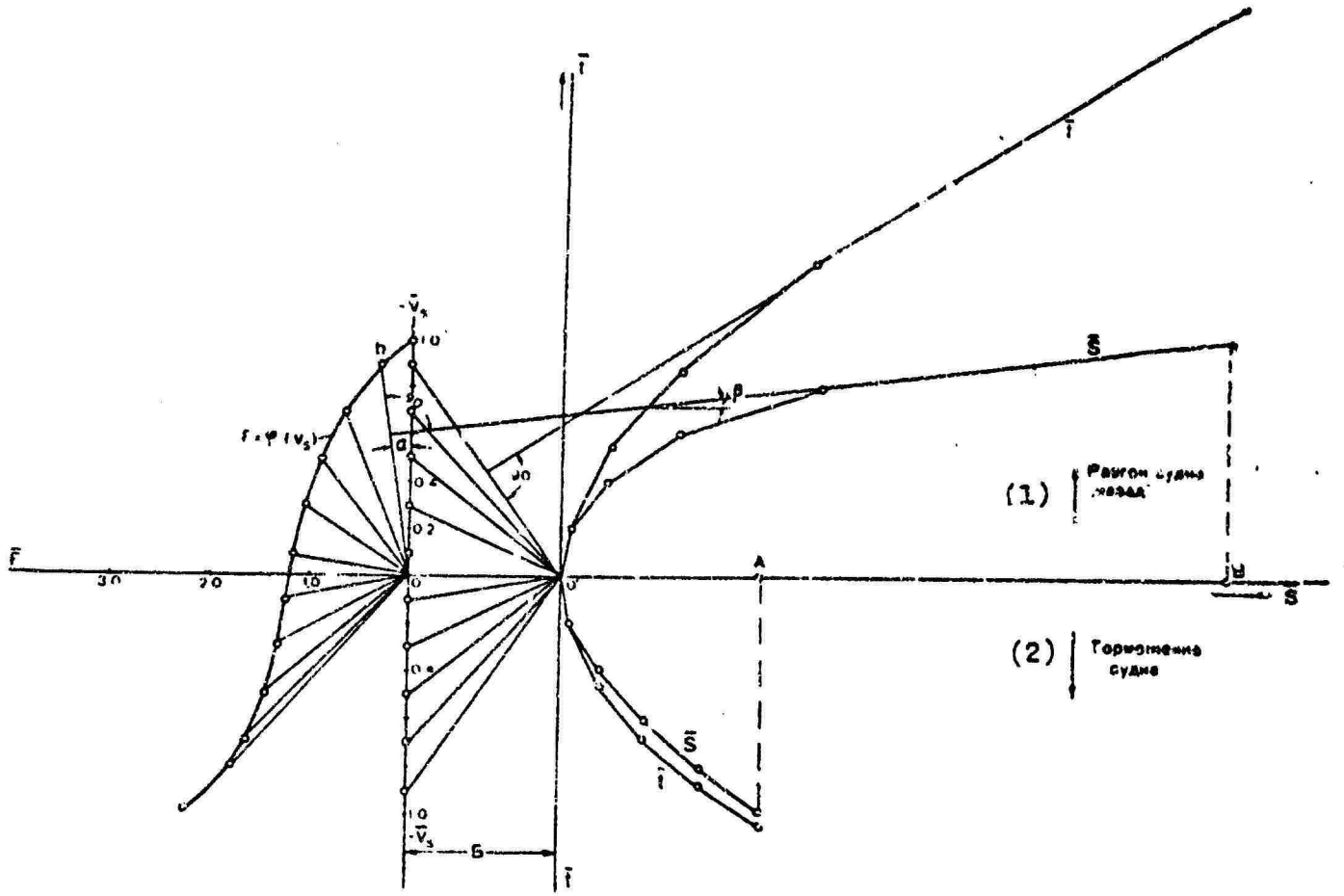

Figure 3. Diagram of reversing. 1) acceleration of the ship "astern"; 2) braking of the ship.

the braking time is important for an icebreaker also in breaking out ships that have gotten stuck in the ice. In these conditions, the icebreaker must run almost firmly against the ship being broken out, and, to avoid collision, must have the capability of stopping rapidly.

Increased efficiency of the drive of the screw propellers will make it possible to reduce time required for breaking out ships and forcing through ice bridges, which as a result will expedite the escorting of a convoy in the ice, and consequently increase the efficiency of the use of an icebreaker.

BIBLIOGRAPHY

1. Kudryavtsev, A. P., Turboperedachi dlya sudov (Turbine transmissions for ships), Kiev, Oborongiz, 1959.

2. Khaykin, A. B., and Yagodkin, V. Ya., "Calculation of the static characteristics of the GEU (main propulsion plant) of icebreaking vessels," Sudostroyeniye (Shipbuilding), 1966, No. 1.

3. Yagodkin, V. Ya., "Analytical determination of the moment of resistance to the rotation of a screw propeller in its reaction with ice," in the collection Problemy Arktiki i Antarktiki (Problems of the Arctic and Antarctic), No. 13, Leningrad, "Morskoy transport", 1963.

COLOPHON

Trudy AANII
(Transactions of the Arctic and Antarctic Scientific Research Institute),
Volume 309

Ledovyye kachestva sudov

Senior editors: D. Ye. Kheysin and Yu. N. Popov

Editor: L. I. Romanova

Technical Editor: I. K. Pelipenko

Copy Editor: I. A. Krayneva and T. N. Chernenko

Setup in press 15 March 1972. Signed to press 8 February 1973.

M-11068 Paper 60x90 1/116, typography No. 1.
Printed signatures 15.125 (including one insert) Uch. izd. 1.15.35.

Printing 650 copies Index OL-167 Order 1312

Price 1 ruble 18 kopecks.

Gidrometeoizdat, Leningrad, 199053, 2-ya liniya (second line), 23

Leningradskaya tipografiya (Leningrad typography) No. 12 imeni M. I. Lokhankov

"Soyuzpoligrafprom" of the State Committee of the Council of Ministers of the USSR for matters of Publishing Houses, Polygraphy and Books Trade

Leningrad, 196120, UL Pravda, 15.

ABSTRACTS

UDC 629.124.791.07

"Methods of estimating the ice navigating capability of a ship in solid ice," Kashtelyan, V. I., Trudy AANII (Transactions of the Arctic and Antarctic Scientific Research Institute), volume 309, pages 5-17.

An analysis of existing methods of estimation of the ice navigating capability in solid ice when steaming continuously and when an icebreaker is operating in short runs is given. In the solutions of problems associated with the designing of icebreakers, and also the planning of their operation in ice, it is recommended that a semi-empirical method of calculating the ice resistance, developed at the AANII, be used. Devices for measuring the icebreaking capability of the ship when steaming continuously and operating in short runs are considered.

One illustration, one table, twelve bibliographic entries.

UDC 629.124.791:551.467

"On the ice navigation speed of ships in extremely solid ice," Kheysin, D. Ye., Trudy AANII, volume 309, pages 18-26.

The stability of the motion of a ship in solid ice with a thickness close to the limiting thickness is investigated. The probability of stopping for given intervals of time is estimated. An estimate is given of the dispersion of the force of the ice resistance according to a three-point static scheme of icebreaking. Dimensionless parameters are introduced that make it possible to compare the ice navigation speed (ice navigating capability) of ships of the same type.

Three illustrations, two tables, thirteen bibliographic entries.

UDC 629.124.791:551.467

"Resistance to the motion of transport vessels in solid ice," Maksutov, T. D., Trudy AANII, volume 309, pages 27-34.

The derivation of a formula for estimation of the resistance of solid ice to the motion of icebreaking transport vessels is given. The derivation of the formula is based on the results of model and full-scale experiments on a number of ships intended for active ice navigation. In the graphs given in the article the close similarity of the values of the ice resistance of two icebreaking transport vessels with different lines, obtained according to a formula proposed by the author and according to data from full-scale tests, is illustrated. An estimate is also given of the effect of the lines of the forward end of the ship's hull on its ice resistance.

Three illustrations, four bibliographic entries.

UDC 629.12.011:551.467

"Use of probability methods in estimating the maneuvering qualities of ships in ice," Kheysin, D. Ye., Trudy AANII, volume 309, pages 35-49.

The process of the reaction of a ship's hull with the ice is considered as a discrete random sequence of statistically independent impact pulses, acting in the zone of contact with the ice. The probability model accepted is used in the analysis in the stability of motion in a ship along a straight course in the ice. An estimate of the dispersion of the deviation from the course is made, and the average number of yawings per unit of time is determined. The probability approach is used for the investigation of the scattering of coasting runs of the ship in randomly heterogeneous ice. In this case, the probability of the deviation of the length of a coasting run from its average value is determined.

Four illustrations, eleven bibliographic entries.

UDC 629.124.791.07

"Investigation of the inertial characteristics of unsteady-state motion of an icebreaker in ice," Ryvlin, A. Ya., and Tegkayeva, T. Kh., Trudy AANII, volume 309, pages 50-56.

Methods are given for calculation of the inertial characteristics (length and time of runs) in unsteady-state operating regimes of an icebreaker in ice: acceleration, stopping, reversing, and motion in the ice from start-

ing up. On the basis of calculations, curves were constructed of the dependence of the inertial characteristics upon a number of the parameters of the ship and the ice: displacement, initial speed, thickness of the ice, form of the ice cover, degree of ice cover, and compression.

Four illustrations, one table, two bibliographic entries.

UDC 629.124.791

"Wedging of icebreakers in ice," Popov, Yu N., and Kashtelyan, V. I., Trudy AANII, volume 309, pages 57-72.

For the first time in a systematized form problems associated with the wedging of an icebreaker in the ice are discussed. The basic attention is devoted to an estimate of the efficiency of various methods of freeing it from wedging.

Five illustrations, eight bibliographic entries.

UDC 629.123.07(99)

"Features of the operation of icebreaking transport vessels in the Antarctic," Maksutov, D. D., Trudy AANII, volume 309, pages 73-78.

Brief information is given concerning the features of the ice regime of the Antarctic seas. The ice conditions for navigation of ships in the vicinity of the Soviet Antarctic stations are noted, with an indication of the features of the approach to the shore, methods of mooring the ships, and unloading cargoes. The essential differences of the operation of ships in the Antarctic from customary Arctic conditions cause the necessity for a thorough study of the features of the ice regime of the seas of the Southern Ocean and the operating conditions of icebreaking transport vessels there.

One illustration, four bibliographic entries.

UDC 629.124.791.07

"Effect of the lines of an icebreaker on the magnitude of ice loads," Popov, Yu. N., Tegkayeva, T. Kh., and Faddeyev, O. V., Trudy AANII, volume 309, pages 79-87.

The effect of the hull lines of an icebreaker on the magnitude of ice loads is analyzed. Formulas and curves are given which illustrate the dependence of the magnitude of the ice loads on the side framing and the

external shell plating upon the angle β of inclination of the frames, the coefficient α_n of fineness of the forward part of the waterline, and the ratio L/B of the length of the hull to the beam.

Four illustrations, one table, two bibliographic entries.

UDC 629.124.791.07

"Determination of the ice loads on an icebreaker's hull with consideration of reflected impact," Popov, Yu. N., Tegkayeva, T. Kh., and Faddeyev, O. V., Trudy AANII, volume 309, pages 88-99.

A calculation formulas is given for determination of the given velocity of a "reflected" impact, with consideration of all the velocity components of a ship originating as a result of the first (direct) impact. Formulas are given for the determination of the ice loads on the side framing and the external shell plating in a reflected impact.

Five illustrations, five tables, three bibliographic entries.

UDC 629.124.791.07

"The strength of icebreakers and transport vessels (according to data from strain-gauge tests)," Likhomanov, V. A., Trudy AANII, volume 309, pages 100-110.

The determination of the magnitude of the dynamic stresses and investigation of the reaction of a ship's hull with the ice, depending upon the ice conditions, made it possible to investigate the duration of the impact, the length of the distribution zone, the region of application of the load with respect to the depth and the length of the hull. By means of the arrangement of strain gauges in a "cross" it was established that the ice load is a concentrated force and is statically applied. The construction of the statistical curves of the distribution of stresses in a frame makes it possible to select a calculation scheme for the comparison of the results of tests of the strength and the theoretical calculated strength of a ship of a given type.

Four illustrations.

UDC 629.123.791.07(98)

"Strain-gauge tests of icebreaking transport vessels," Likhomanov, V. A., and Solostyanskiy, D. I., Trudy AANII, volume 309, pages 111-117.

The results of full-scale tests of ships of the "Amguyema" type in the ice of the Arctic and freezing non-Arctic seas are analyzed and generalized.

Four illustrations.

UDC 629.12.011:551.467

"On the distribution of probabilities of the number of impacts of a ship's hull against the ice," Kudishkin, V. S., Trudy AANII, volume 309, pages 118-122.

The problem of the correspondence of the distribution of probabilities of obtaining a definite number of impulses at the bow end of a ship in motion in the ice to Poisson's law is considered.

An empirical curve of the distribution functions is given, and a theoretical curve is calculated. There correspondence according to the Pearson criterion is determined.

One illustration, two tables, two bibliographic entries.

UDC 629.12.011:551.467

"Excitation of vertical elastic oscillations of a ship's hull in motion in the ice," Kudishkin, V. S., Trudy AANII, volume 309, pages 123-131.

A mathematical model of the origin of vertical elastic oscillations of a ship's hull in motion in the ice is proposed. In this case, the external ice forces are presented in the form of a random sequence of a large number of impact impulses of random amplitude. As a basic characteristic of the force elastic oscillation, the spectral density of the power of these oscillations is accepted.

Formulas are obtained for the correlation function and the spectral density of the power of the forced vertical bending oscillations of the ship's hull. An example of the experimental recording of these oscillations is given.

Two illustrations, three bibliographic entries.

UDC 629.12.011:624.046

"Elastic oscillations of a ship's hull in the effect of random pulsed ice loads," Kheysin, D. Ye., Trudy AANII, volume 309, pages 132-136.

Forced oscillations of a ship's hull as a non-prismatic elastic beam are investigated, the oscillations being caused by random ice loads. The scattering of the energy of the bending oscillations associated with the internal and external resistance is considered. The reaction of the hull with the ice is considered as a steady-state random process. The spectral density of the forced random oscillations of the hull is determined.

Four bibliographic entries.

UDC 629.12.011:624.046

"Static bending of beams in the effect of random ice loads," Kheysin, D. Ye., Trudy AANII, volume 309, pages 137-147.

The static bending of beams in the effect of random loads in two types is considered: random loads distributed along the length of the beam and discrete loads. According to a given correlation matrix of the external effect, the correlation functions of bucklings and bending moments are determined. The reverse problem is also solved--according to the known reactions of the beam the characteristics of the external effect are found. As an example, the results of the processing of data from strain-gauge tests of the side framing of an icebreaker are given.

Seven illustrations, five bibliographic entries.

UDC 629.12.011.72

"Determination of the pliability factors of the elastic coverings (fastenings) of frames in the effect of an ice load," Likhomanov, V. A., and Faddeyev, O. V., Trudy AANII, volume 309, pages 148-153.

A simplified method of determining the pliability factors of the elastic fastening of frames in the presence of cross connections is proposed. Calculation formulas and curves are given for a case of the installation of one, two, or three stringers. An example of the calculation of a frame by means of the proposed curves is given.

Two illustrations, one table, two bibliographic entries.

UDC 629.12.011:624.046

"On the calculation of the side shell plating for the effect of an ice load," Solostyanskiy, D. I., Trudy AANII, volume 309, pages 154-170.

The bending of a thin infinite band under the effect of a local load is considered, and its carrying capacity in the elastic and elastic-plastic zones is determined.

Five illustrations, four tables, seven bibliographic entries.

UDC 629.124.791.001.2

"Some features of the designing of transport vessels for ice navigation," Maksutov, D. D., Trudy AANII, volume 309, pages 171-178.

For purposes of providing accident-free navigation of transport vessels in ice, a method is proposed for determination of the permissible speed of the ship in broken ice of various characteristics. The essential effect of the lines of the forward end of the ship on its strength in an impact against an ice floe or against the edge of the channel is noted. A method is proposed for correction of the theoretical design of the forward end of the ship to obtain the minimum possible value of ice loads on the ship's hull in impacts against the ice.

Four illustrations, one table, two bibliographic entries.

UDC 629.123(98)(99)

"On a scientific-research vessel for the Arctic and Antarctic," Maksutov, D. D., Popov, Yu. N., and Faddeyev, O. V., Trudy AANII, volume 309, pages 179-185.

Data are given, and the general characteristics also, of a new scientific-research vessel intended for performing a complex of scientific-research work in the seas of the Arctic and Antarctic, and also for the transportation of scientific workers who will spend the winter, expedition cargoes, and foodstuffs to the Antarctic.

UDC 551.322

"Experimental study of the friction of ice," Ryvlin, A. Ya., Trudy AANII, volume 309, pages 186-199.

The results of full-scale and laboratory experimental investigations of the friction of ice are given, the experiments being performed in a freshwater and sea ice cover. The average statistical magnitudes of the static and dynamic friction factors of the ice against steel and of ice against ice are determined, at various external conditions, an analysis is given of the

dependence of these coefficients upon such factors as the slip velocity, specific pressure, temperature, salinity of the ice, roughness, and degree of snow cover of its surface, and others. The magnitudes of the friction factors may be used for consideration of the friction of a ship's shell plating against the ice and for other engineering calculations.

Four illustrations, twelve tables, nine bibliographic entries.

UDC 551.321.8

"Improvement of the method of preparation of model ice," Poznyak, I. I., Trudy AANII, volume 309, pages 200-209.

A method is proposed for preparation of a model of ice with a decreased strength, low plasticity, and increased elastic properties. The possibility of the modelling of the plastic properties of ice according to criteria of gravitational similarity is theoretically validated.

One illustration, one table, four bibliographic entries.

UDC 629.1.053:629.123.001.57

"A remote sensor for measuring the speed of ship models in ice," Lobos, V. I., and Lipatov, V. N., Trudy AANII, volume 309, pages 210-214.

The features of the measurement of the speed of models in an experimental ice basin are considered, and a description is given of a similar device operating on the frequency principle, with a photodiode modulator, as used in the basin of the AANII.

Two illustrations, two bibliographic entries.

UDC 629.1.037:629.124.791

"Measurement of the thrust of screw propellers by a tensometer thrust gauge," Lipatov, V. N., and Lobos, V. I., Trudy AANII, volume 309, pages 215-220.

The results of the measurement of the thrust of the screw propellers of powerful icebreakers by a tensometer thrust gauge in dock-trial regimes with the reaction of the propeller with ice and in clear water are given; the magnitude of the pulsation and the law of the variation of the thrust as a function of the revolutions of the propeller are determined, on the basis of oscillograms of full-scale tests; the features of the variation of the thrust of the side and center screws of the icebreakers are considered.

Four illustrations, two bibliographic entries.

UDC 621.375.4:629.1.037

"A highly sensitive amplifier for full-scale measurements of the thrust of propellers," Lobos, V. I., and Lipatov, V. N., Trudy AANII, volume 309, pages 221-224.

The circuit and features of a semiconductor direct-current amplifier with conversion are considered, the device having adequate sensitivity and stability for its use in the composition of a tensometer thrust gauge in full-scale measurements of the thrusts of screw propellers, and the results of the calibration of such a thrust gauge aboard a powerful icebreaker are given.

Two illustrations, three bibliographic entries.

UDC 629.124.791.07

"Effect of the form of static characteristics of a propeller installation on the maneuvering qualities of an icebreaker," Yagodkin, V. Ye., Trudy AANII, volume 309, pages 225-232.

In the article the possibilities of improving the maneuvering qualities of ships for ice navigation are considered with a change in the static characteristics of the propulsion engine. The solution of the equation of motion of the ship is performed by the graphoanalytic method.

Three illustrations, three bibliographic entries.

2498

CSO: 9244/0392-W -END-